Durham E-Theses

The role of emerin and LEM domain proteins in nuclear envelope assembly and cytoskeleton organisation

Salpingidou, Georgia

How to cite:

Salpingidou, Georgia (2005) *The role of emerin and LEM domain proteins in nuclear envelope assembly and cytoskeleton organisation*, Durham theses, Durham University. Available at Durham E-Theses Online: http://etheses.dur.ac.uk/2203/

Use policy

The full-text may be used and/or reproduced, and given to third parties in any format or medium, without prior permission or charge, for personal research or study, educational, or not-for-profit purposes provided that:

- a full bibliographic reference is made to the original source
- a link is made to the metadata record in Durham E-Theses
- the full-text is not changed in any way

The full-text must not be sold in any format or medium without the formal permission of the copyright holders.

Please consult the full Durham E-Theses policy for further details.

Academic Support Office, Durham University, University Office, Old Elvet, Durham DH1 3HP
e-mail: e-theses.admin@dur.ac.uk Tel: +44 0191 334 6107
http://etheses.dur.ac.uk

The role of emerin and LEM domain proteins in nuclear envelope assembly and cytoskeleton organisation

by

Georgia Salpingidou

A copyright of this thesis rests with the author. No quotation from it should be published without his prior written consent and information derived from it should be acknowledged.

A thesis submitted at the University of Durham for the degree of Doctor of Philosophy

School of Biological and Biomedical Sciences

University of Durham

August 2005

1 5 MAR 2006

DECLARATIONS

I declare that the experiments described in this thesis were carried out by myself in the School of Biological and Biomedical Sciences, University of Durham, under the supervision of Prof. Chris J. Hutchison. This thesis has been composed by myself and is a record of work that has not been submitted previously for a higher degree. All references have been consulted by myself unless stated otherwise.

Salpingidou

Georgia Salpingidou

I certify that the work reported in this thesis has been performed by Georgia Salpingidou, who, during the period of study, has fulfilled the conditions of the Ordinance and Regulations governing the Degree of Doctor of Philosophy.

Chris J. Hutchison

The copyright of this thesis rests with the author. No quotation from it should be published in any format, including electronics and the internet, without the author's prior consent. All information derived from this thesis must be acknowledged appropriately.

ACKNOWLEDGEMENTS

I would like hereby to take the opportunity to thank a number of people whose help is invaluable to me:

My parents, Domna and Vassili, and my brother Christo for all their love and support throughout the years, being it emotional or financial; for all those welcoming breaks at home every Christmas and summertime and for all the supplies of my favourite pita and sweets to keep me going when back in Durham.

My supervisor Prof. Chris Hutchison for giving me the opportunity to do this PhD, for all his help and advice throughout my studies, and for all the support during the writing up.

Special thanks to my second supervisor Dr. Martin Goldberg for always listening so patiently and for his *Xenopus* expertise; to our technician Mrs Pamela Ritchie for dealing so patiently with all the requests and problems and for looking so well after the frogs; to previous and current members of the lab: Dr Ewa Markiewicz, Dr. Mauricio Alvarez-Reyes, Dr. Rekha Rao, Naomi Willis, Vanja Pekovic, Dr. Fida Casans, Tom Cox and Fahad Al-Zoghaibi..

Also special thanks to all the people who contributed to this work by providing their reagents or their knowledge: Dr. Ryszard Rzepecki, for his help at the very first steps of my PhD; Prof. Carl Smythe for his help to purify the emerin peptides; Prof. Ian Mattaj for providing the Nup107 antibody; Dr. Tony O'Sullivan for all his help with the LAP12 antibody; Prof. Patrick Hussey for the β-tubulin antibody, Simon Dimmock for his help in the yeast-two-hybrid experiments; Dr. Bill Simon, Dr. David Dixon and Joanne Robson for their great help with the 2-D gels and the proteomics work, and Mrs. Christine Richardson for her time with me at the confocal microscope.

At last but not least I would like to say a big thank you to my boyfriend Kosta (also known as Tinito) who gave up his laid back life in Mexico to stay with me in England, and who, after four years of complaining about the weather, still hasn't left!
I would have probably never made it without him.

ABSTRACT

The nuclear envelope (NE) plays a fundamental role in the cell by separating nuclear from cytoplasmic activities, and mutations in NE proteins have been associated with a diverse array of diseases. In the present study the *Xenopus* cell-free system was used to investigate the function of the inner nuclear membrane protein, emerin, which is associated with the Emery-Dreifuss muscular dystrophy (X-EDMD).

Initially, the order and dynamics of NE assembly in *Xenopus* egg extracts have been investigated. Using a panel of antibodies it was shown that NE assembly proceeds by the ordered recruitment of two membrane populations, Nuclear Envelope Precursor vesicles -A and –B (NEP-A and NEP-B), to chromatin. As shown by immunofluorescence NEP-B vesicles, together with nucleoporins (Nups), appear first around chromatin at about ten minutes after initiation of NE assembly while NEP-A vesicles appear at a later stage, at about twenty minutes. To investigate the role of different emerin domains in this process, four human emerin peptides consisting of amino acids (aa) 1-70, 1-176, 1-220 and 73-180 were added individually to *Xenopus* nuclear assembly reactions at different concentrations and the effect on nuclear vesicle recruitment and NPC formation was monitored. Immunofluorescence analysis showed that peptides containing the LEM domain of emerin interfere with a correct NE assembly by inhibiting chromatin decondensation and recruitment of membranes to chromatin. This inhibitory effect was shown to be exerted mainly on NEP-A membranes and on Nup62 and Nup153. By the use of two antibodies, raised against the LEM domain of human emerin and LAP2β, two proteins of 30 and 36 kD, respectively, were identified in *Xenopus*. Both proteins were shown to reside in the NEP-A membrane population providing an explanation for the preferential inhibition of NEP-A recruitment to chromatin by exogenously added LEM domain containing emerin peptides.

To further investigate whether the domain specific inhibitory effects of emerin on nuclear assembly correlate with specific interacting proteins, co-precipitation experiments were performed to identify emerin binding proteins in the *Xenopus* cytosol. From these experiments β-tubulin was identified as a protein able to interact with emerin peptides 1-70 and 73-180. Staining of X-EDMD cells, which lack emerin, with a β-tubulin antibody revealed no alterations in the organisation of the microtubule (MT) network. The most prominent effect of emerin mutations regarding MTs was the position of the Microtubule Organising Centre (MTOC) relative to the NE. Staining for the centrosomal protein pericentrin revealed a mis-localisation of the MTOC away from the NE in X-EDMD cell lines at distances at least double compared to control cells.

CONTENTS

LIST OF FIGURES

LIST OF TABLES

ABBREVIATIONS

1-D	1-dimensional
2-D	2-dimensional
aa	amino acid
AD-	autosomal dominant
Ade	adenine
ADP	adenosine diphosphate
AR-	autosomal recessive
ATP	adenosine triphosphate
BIA	biomolecular interaction analysis
BLAST	basic local alignment search tool
BMP	bone morphogenetic protein
bp	base pairs
BRB	blot rinse buffer
BSA	bovine serum albumin
cDNA	complementary DNA
CFP	cyan fluorescent protein
CHO	chinese hamster ovary
CMT2	Charcot-Marie-Tooth type 2
CPK	creatine phosphokinase
DAPI	4',6-diamidine-2-phenylindole dihydrochloride
DCM-CD	dilated cardiomyopathy with conduction system disease
d.f.	degrees of freedom
DMEM	Dulbecco's modified Eagle's medium
DMSO	dimethyl sulphoxide

DNA	deoxyribonucleic acid
ECL	enhanced chemiluminescence
EDMD	Emery-Dreifuss muscular dystrophy
EDTA	ethylenediaminetetra acetic acid
EGFP	enhanced green fluorescent protein
EGS	ethylene glycol bis-(succinic acid N-hydroxysuccinimide ester)
EGTA	1,2,-di(2-aminoethoxy)ethane-NNN'N'-tetra-acetic acid
ER	endoplasmic reticulum
FEISEM	field emission in-lens scanning electron microscopy
FG	phenylalanine-glycine
FITC	fluorescein isothiocyanate
FLIP	fluorescence loss in photobleaching
FPLD	familial partial lipodystrophy
FRAP	fluorescence recovery after photobleaching
FRET	fluorescence resonance energy transfer
GCL	germ cell less
GFP	green fluorescent protein
gr	gram
GTP	guanosine triphosphate
HCL	hydrochloric acid
HDF	human dermal fibroblast
HEPES	N-2-hydroxyethylpiperazine- N'-2-ethane-sulphonic acid
HGPS	Hutchinson-Gilford progeria syndrome
His	histidine
HP1	heterochromatin protein 1

HRP	horse radish peroxidase
HSP	heat shock protein
I	isoleucine
IFs	intermediate filaments
ICMTs	isoprenylcysteine carboxymethyltransferases
IMAC	immobilised metal affinity chromatography
INM	inner nuclear membrane
IPTG	isopropyl-β-thiogalactosidase
K	lysine
kb	kilobases
kD	kilodalton
KSCN	potassium thiocyanate
L or Leu	leucine
LAPs	lamina associated polypeptides
LB	Luria-Bertani medium
LBR	lamin B receptor
LGMD-1B	Limb-girdle muscular dystrophy 1B
LSS	low speed supernatant
µg	microgram
µl	microlitre
µm	micron (micrometre)
µM	micromolar
M	methionine
MAD	mandibuloacral dysplasia
MALDI-TOF	matrix-assisted laser desorption and ionisation time-of-flight

MEB	modified extraction buffer
min	minutes
mM	millimolar
MP	membrane precursor
Mr	relative molecular weight
mRNA	messenger RNA
MS	mass spectrometry
MT	microtubule
MTOC	microtubule organising centre
N	asparagine
NaCI	sodium chloride
NaN_3	sodium azide
NCBI	National Centre for Biotechnology Information
NE	nuclear envelope
NEBD	nuclear envelope breakdown
NES	nuclear export signal
NHS	N-hydroxysuccinimide
Ni-NTA	nickel-nitrilotriacetic acid
NLS	nuclear localisation signal
nm	nanometre
NMR	nuclear magnetic resonance
NPC	nuclear pore complex
Nup	nucleoporin
ONM	outer nuclear membrane
PAGE	polyacrylamide gel electrophoresis

PBS	phosphate buffered saline
PC	phopshocreatine
PCR	polymerase chain reaction
PMF	peptide mass fingerprinting
PMSF	phenylmethylsulfonyl fluoride
PMSG	pregnant mares'serum gonadotropin
Q	glutamine
R	arginine
RNA	ribonucleic acid
RNAi	RNA intereference
rpm	revolutions per minute
RT	room temperature
S or Ser	serine
sec	seconds
SDS	sodium dodecyl sulphate
SEM	standard error of the mean
SNIB	sperm nuclear isolation buffer
STDV	standard deviation
T or Thr	threonine
TBS	Tris buffered saline
TEMED	N ,N ,N' ,N' –tetramethylethylenediamine
TM	transmembrane
TRITC	tetramethyl rhodamine isothiocyanate
Trp	tryptophan
UV	ultraviolet

V	valine
v/v	volume for volume
w/v	weight for volume
WS	Werner syndrome
XLK	*Xenopus* kidney cells
XTC	*Xenopus* tadpole cells
Y	tyrosine
YFP	yellow fluorescent protein

CHAPTER 1

GENERAL INTRODUCTION

1.1 The nucleus

All life is organised in cells, which can be classified in two major groups: prokaryotic and eukaryotic. Eukaryotic cells are characterised by a much higher degree of complexity and the main feature that distinguishes them from prokaryotic cells is the existence of the nucleus, an organelle that encloses almost all of the cellular DNA. Although many hypotheses have been formulated as to the origin of the eukaryotic nucleus (Forterre, 1995; Moreira and Lopez-Garcia, 1998; Sogin, 1991; Takemura, 2001; Vellai *et al.*, 1998; Zillig *et al.*, 1988) it most probably evolved through a symbiotic mechanism between an archaebacterium and a eubacterium (Margulis *et al.*, 2000) 1.8 to 2.7 billion years ago (Hedges *et al.*, 2001). The evolution of the nucleus offered very important advantages to eukaryotes by protecting their DNA from shear forces in the cytoplasm and by allowing for more protein variety through splicing by separating temporally and spatially transcription from translation.

The nucleus is a highly compartmentalised organelle. It is surrounded by a nuclear envelope, which is underlined by a network of proteins called lamins. It contains chromatin, which is highly arranged and forms distinct entities within the nucleus (Comings, 1980) and several other nuclear compartments like the nucleolus (Raska *et al.*, 2004), the Cajal or coiled bodies (Matera, 2003), the Gemini of coiled bodies or gems (Matera, 1998), the Promyelocytic Leukaemia Oncoprotein (PML) bodies (Dellaire and Bazett-Jones, 2004), the Perinucleolar compartment (PNC) and Sam68 nuclear bodies (SNB) (Huang, 2000), the clastosomes (Lafarga *et al.*, 2002) and the paraspeckles (Fox *et al.*, 2002). All of these nuclear bodies together with the

chromatin and proteins are also highly dynamic and it is these dynamic properties of the nucleus that are crucial for its accurate functioning (Belmont, 2003).

1.2 The Nuclear Envelope (NE)

What makes the nucleus a distinct cellular compartment is the presence of the nuclear envelope (NE), mention of which had been made by Brown as early as 1833 (as cited in Franke *et al.*, 1981). It consists of two concentric membranes, an inner and an outer nuclear membrane, which are separated by a lumenal space and connected at the pore membrane where the nuclear pore complexes (NPCs) reside. Underlying the NE is a meshwork of intermediate filaments called the lamina (Figure 1.1).

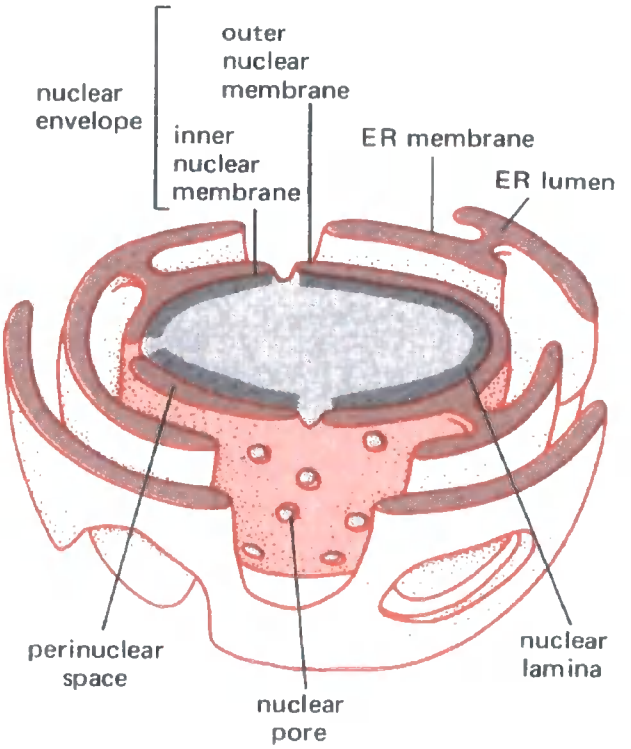

Figure 1.1: A three-dimensional drawing of the NE surrounding the nucleus (reproduced from Alberts *et al.*, 1989).

By surrounding the nucleus, the NE forms the interface between the nucleoplasm and the cytoplasm but it also facilitates the communication between these two compartments via the NPCs. It is also involved in several other important processes like in maintaining nuclear shape, in DNA replication, protein synthesis and processing.

1.2.1 The Outer Nuclear Membrane (ONM)

The ONM is the outer part of the NE that is in contact with the cytoplasm. It is in direct continuation with the rough Endoplasmic Reticulum (ER) and, like the ER, its surface is studded with ribosomes. Early studies showed that the ONM exhibits a high degree of similarity to ER membranes as far as the lipid pattern, protein and enzyme composition and patterns of glycoproteins is concerned (Franke *et al.*, 1981). However, although morphologically very similar, some degree of specialisation still exists as shown by comparison of the protein composition of the ONM and rough ER in rat liver nuclei, where proteins uniquely contained in the ONM fraction were identified (Richardson and Maddy, 1980).

Due to the presence of functional ribosomes on its surface the ONM is capable of protein synthesis and processing (Puddington *et al.*, 1985). The synthesised proteins can then be transferred to the lumenal space, which is in continuation with ER lumen. Apart from protein synthesis the ONM is also implicated in the biogenesis of cytoplasmic membranes (Kessel *et al.*, 1986; Pathak *et al.*, 1986).

1.2.2 The nuclear envelope lumen

The NE lumen or perinuclear space is a 150 Å wide aqueous domain separating the inner from the outer nuclear membrane and is in continuity with the ER lumen (Wischnitzer, 1958). Apart from accommodating the lumenal domains of integral membrane proteins it can mediate signal transduction events in and out of the nucleus. Its ability to act as a Ca^{2+}-storing compartment has implicated the lumen in important processes like membrane fusion and protein transport. Indeed, release of lumenal Ca^{2+} from mitotic NE vesicles was shown to be necessary for vesicle fusion during NE assembly (Sullivan *et al.*, 1993) and depletion of Ca^{2+} stores from the ER and NE lumen was shown to inhibit protein import in the nucleus by affecting NPC components (Greber and Gerace, 1995).

1.2.3 The Inner Nuclear Membrane (INM)

The INM is the part of the NE that faces the nucleoplasm and, although it is connected with the ONM at the pore membrane where the NPCs reside, it contains a unique set of proteins not found in the ONM or the ER (Chu *et al.*, 1998; Georgatos, 2001; Worman and Courvalin, 2000). Most of these so called INM proteins are type II integral membrane proteins with an N-terminus facing the nucleoplasm and a C-terminus located in the NE lumen (Hartmann *et al.*, 1989). The best characterised INM proteins so far are the Lamina Associated Polypeptides (LAPs) 1 and 2, the lamin B receptor (LBR), emerin and MAN1. However, reports on several other INM proteins exist. A recent study using subtractive proteomics identified 67 new potential NE proteins (Schirmer *et al.*, 2003). Currently known INM proteins are shown in

Figure 1.2 and are discussed below with the exception of emerin which will be discussed at a later stage.

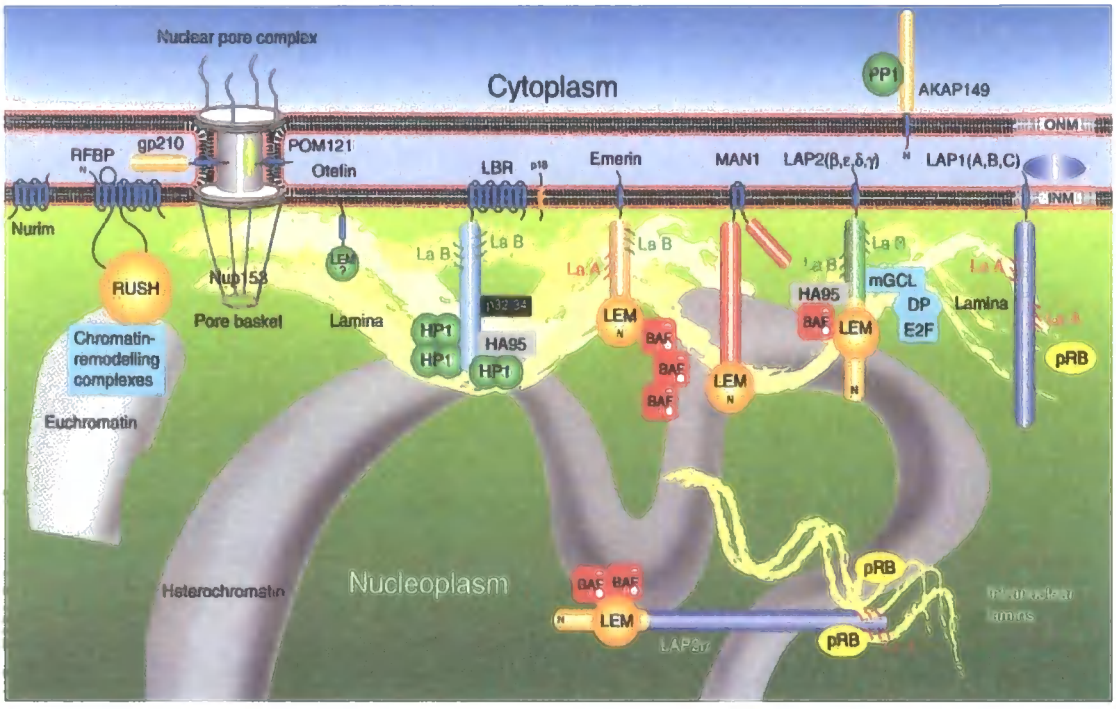

Figure 1.2: Diagrammatic presentation of the nuclear envelope and nuclear membrane proteins (reproduced after Foisner, 2001).

The inner, outer and pore nuclear membranes with residing proteins are depicted. The complex interactions at the nuclear periphery including membrane proteins, chromatin, lamins and other proteins are also shown.

1.2.3.1 The LAP family

The Lamina Associated Polypeptides are type II integral membrane proteins divided into LAP1 and LAP2 proteins. The LAP1 family includes three isoforms, LAP1A, LAP1B and LAP1C, which are alternatively spliced products of the same gene and were identified in the INM of rat liver nuclei as proteins of 75, 68 and 55 kD,

respectively (Senior and Gerace, 1988). As their name implies LAPs are able to bind lamins. LAPs 1A and 1B were shown to specifically bind lamins A, C and B1 by *in vitro* studies (Foisner and Gerace, 1993). Although a direct association of LAP1C with lamins was not shown, LAP1C could still interact with lamin B as part of complex that includes other proteins like LBR and p18 (Simos *et al.*, 1996). In any case, LAP1 complexes with lamins seem to be distinct and separate from complexes of LAP2 with lamins (Maison *et al.*, 1997). LAP1 isoforms are differentially expressed during development. LAP1C is expressed in all cells, whereas LAP1A and –B are expressed in differentiated cells only (Martin *et al.*, 1995). Their differential expression implies that LAP1A and -1B could be important in promoting nuclear stability in differentiated cells. Other proposed functions include targeting of lamins and membrane vesicles to chromosomes at the end of mitosis and attachment of lamins or other proteins in the nuclear envelope during interphase (Martin *et al.*, 1995).

LAP2 proteins, originally called thymopoietins, were described as three polypeptides of 75, 51 and 39 kD, highly expressed in the thymus with important functions in T-cell development and differentiation (Harris *et al.*, 1994). Further investigation revealed that the thymopoietins were alternatively spliced products of the same gene and that TMPO β was the human homologue of the rat LAP2 sequence (Harris *et al.*, 1995). To date three isoforms have been described in humans, LAP2α, β and γ, and seven isoforms in mice, LAP2 α, β, β', γ, δ, ε and ζ. All of them share a common N-terminal region consisting of 187 amino acids, which mediates binding to chromatin and a variable C-terminus, which mediates binding to lamins. All isoforms span the INM once, near their C-terminus, with the exception of LAP2α and ζ, which lack a

transmembrane domain resulting in a nucleoplasmic distribution (Dechat *et al.*, 2000). Several *in vitro* and *in vivo* studies confirm the association of LAPs2 with lamins. While LAP2α, the non-membrane bound isoform, is able to interact with lamin A/C via its unique C-terminus (Dechat *et al.*, 2000), LAP2β forms complexes with lamin B and is also able to bind chromosomes via its first N-terminal 85 amino acids (Furukawa *et al.*, 1998). Except lamins, BAF is another LAP2 interacting protein, first identified in a yeast-two hybrid screen (Furukawa, 1999). Interaction with BAF is mediated by the LEM domain and preferably involves BAF in a complex with DNA rather than itself (Shumaker *et al.*, 2001).

Their ability to interact with both, lamins and chromatin, makes LAPs very important molecules in nuclear structure and function. Apart from connecting chromatin to the NE they have been implicated in nuclear assembly and growth at the end of mitosis and cell cycle progression into S phase and apoptosis (Gant *et al.*, 1999; Vlcek *et al.*, 2002; Yang *et al.*, 1997) while their reported interactions with the retinoblastoma protein (Markiewicz *et al.*, 2002) and the germ-cell-less protein (Nili *et al.*, 2001) implicates them in transcriptional gene regulation.

1.2.3.2 LBR

LBR was first identified as a NE protein in avian cells (Worman *et al.*, 1988). Sequencing of the mammalian homologue (Ye and Worman, 1994) revealed that LBR has eight transmembrane domains and unlike most INM proteins it has both, the N- and C-terminus, facing the nucleoplasm. LBR was shown to interact directly with lamin B (Ye and Worman, 1994) and HP1, a chromatin associated protein (Ye and

Worman, 1996) although later studies suggest that the LBR-HP1 interaction actually occurs via histones H3/H4 (Polioudaki *et al.*, 2001). In the NE, LBR is part of a complex, which apart from lamins includes a specific LBR kinase (Simos and Georgatos, 1992) and p18, a protein that was shown to reside in both the inner and outer nuclear membrane (Simos *et al.*, 1996). By interacting with lamin B and HP1 it is believed that LBR functions in attaching the lamina and chromatin to the INM. It is also suggested that LBR is involved in targeting mitotic vesicles to chromatin during NE assembly (Chaudhary and Courvalin, 1993).

1.2.3.3 MAN1

The 'MAN antigens' were first described as antigens recognised by autoantibodies present in the serum of patients with collagenosis (Paulin-Levasseur *et al.*, 1996). One of these antigens was later identified as MAN1, a 82.3 kD INM protein with two transmembrane domains that shares the LEM domain, a conserved domain of approximately 40 residues, with emerin and LAP2 (Lin *et al.*, 2000). MAN1 together with SANE, another LEM domain containing protein (Raju *et al.*, 2003), are thought to be involved in the Bone Morphogenetic Protein (BMP) signalling by interacting with Smad proteins (Lin *et al.*, 2005; Osada *et al.*, 2003; Pan *et al.*, 2005).

1.2.3.4 Spectrin-repeat (SR) proteins

SR-containing proteins are structurally characterised by an actin-binding N-terminal domain, a rod domain that contains multiple spectrin repeats and a C-terminus that often has a transmembrane domain. The SR containing proteins associated with the

nucleus that have been characterised so far are called nesprins-1 and -2. Nesprins (Nuclear Envelope Spectrin Repeat) were first identified in a study searching for differentiation markers in vascular smooth muscle cells (Zhang *et al.*, 2001). They were shown to localise at the NE where they co-localised with other NE proteins like emerin and LAP1. The same proteins were identified in two other independent studies. A yeast two-hybrid screen with a muscle specific tyrosine kinase as bait identified these proteins as new components of the postsynaptic apparatus and named them Syne-1 and -2 (Synaptic Nuclear Envelope protein) (Apel *et al.*, 2000) while a BLAST search for proteins homologous to the spectrin repeats of *Drosophila* protein *kakapo* identified the same proteins in the NE of skeletal, smooth and cardiac muscle cells and therefore named them Myne-1 and-2 (Myocyte Nuclear Envelope) (Mislow *et al.*, 2002). However, later studies showed that the originally described nesprin-1 and -2 are actually shorter, N-terminal truncated versions of much bigger proteins that consist of 8797 and 6884 amino acids, respectively, and are also known as enaptin and NUANCE (Padmakumar *et al.*, 2004; Zhang *et al.*, 2002; Zhen *et al.*, 2002).

Despite the confusion in the terminology it is clear that these gigantic proteins are involved in very important cellular functions. They are capable of interacting with the actin cytoskeleton via their N-terminal domain while their transmembrane domain near the C-terminus allows them to attach to the NE where they interact with other INM proteins like emerin and lamin A (Mislow *et al.*, 2002). By connecting these two compartments SR proteins are thought to be involved in the maintenance of the nuclear structural integrity, in nuclear anchorage and migration, spatial orientation of nuclear contents and regulation of nuclear signalling (Hutchison, 2002). A further finding that nesprin-1 in addition to the NE is also localised at the Z-lines of

sarcomeres of cardiac and skeletal muscle implies an involvement in muscular dystrophies affecting skeletal and cardiac muscle (Zhang *et al.*, 2002).

1.2.3.5 SUN domain proteins

A number of INM proteins containing the SUN domain have been identified so far and include UNC-84, Sun2 and matefin.

UNC-84 is a *C. elegans* protein that has one transmembrane domain and a C-terminal domain that is shared with the *S. pombe* protein Sad1 and is therefore called SUN domain (Sad1, UNC-84 homology) (Malone *et al.*, 1999). It is localised at the inner nuclear envelope in a lamin-dependent manner (Lee *et al.*, 2002). The SUN domain of UNC-84 extends into the NE lumen where it is able to interact with another NE protein called Syne-1. Since Syne-1 is also able to bind actin it is proposed that UNC-84 is part of a protein complex that connects the nucleus to the actin cytoskeleton controlling processes like nuclear migration and anchorage (Starr and Han, 2003). UNC-84 is also able to bind, via its SUN domain, another INM protein called UNC-83, which also helps in transferring forces between the cytoskeleton and the nucleus probably by connecting the nucleus to microtubules (Starr *et al.*, 2001).

Sun2 is an 85 kD protein, which has a SUN domain localised in the NE lumen, one transmembrane domain and a nucleoplasmic domain able to stabilise the protein in the NE probably by interacting with the lamina (Hodzic *et al.*, 2004). As for UNC-84, Sun2 could be part of a complex that relays and/or regulates the traction forces necessary to anchor or move the nucleus.

Matefin was identified in *C. elegans* during a screen for SUN domain containing proteins. It has a molecular weight of 55 kD, two transmembrane domains and is localised at the NE of all embryonic cells and germ cells of late embryos, larvae and adults. It can bind to the *C. elegans* lamin, Ce-lamin, but does not require lamin for its NE localisation (Fridkin *et al.*, 2004).

1.2.3.6 Nurim

Nurim was identified when a visual screen of a GFP-fusion library was performed in mammalian cells (Rolls *et al.*, 1999). It is a 29 kD protein with multiple transmembrane domains and it differs structurally from other INM proteins in that it lacks a long N-terminal domain, and its N- and C- termini reside both on the nucleoplasmic side of the membrane. Also, unlike other INM proteins, it is not extractable with detergent and high salt showing a very tight association with the NE. It is probably targeted to the NE by binding to another membrane protein but what it exactly does there is still not clear. Recent studies suggest that nurim contains a conserved tripartite consensus sequence also present in the enzyme family of isoprenylcysteine carboxymethyltransferases (ICMTs). ICMTs are involved in processing of proteins containing a CaaX motif. Therefore, an enzymatic function for nurim as a nuclear ICMT has been proposed (Hofemeister and O'Hare, 2005).

1.2.3.7 Otefin

Otefin is a 45 kD protein identified in *Drosophila* with no apparent homology to other known proteins (Padan *et al.*, 1990). It contains one transmembrane domain and a

large hydrophilic domain rich is serines and threonines. It is localised in the INM where it was shown to interact with the *Drosophila* lamins Dm_1, Dm_2 and Dm_{mit} (Goldberg *et al.*, 1998). It is proposed that otefin plays an essential role in nuclear envelope assembly in *Drosophila* by facilitating the attachment of membrane vesicles to chromatin (Ashery-Padan *et al.*, 1997).

1.2.3.8 Bocksbeutel

In an attempt to find LEM domain containing proteins in *Drosophila* the CG9424 or Bocksbeutel gene was identified, which encodes two isoforms, Bocksbeutel α and β. The α isoform contains one transmembrane domain close to the C-terminus and was shown to be localised to the INM (Wagner *et al.*, 2004).

1.2.3.9 LUMA

LUMA is a 45 kD protein with no sequence similarity to any other known protein identified by subcellular proteomics (Dreger *et al.*, 2001). It has three to four putative transmembrane domains and its NE localisation was shown by immunofluorescence studies.

1.3 The Nuclear Pore Complex (NPC)

In eukaryotic cells the NE by enclosing and protecting the genome forms a barrier to the nucleo-cytoplasmic trafficking of molecules. To overcome this barrier cells possess elaborate structures, of about 125 MDa in size, called nuclear pore complexes

(NPCs), which perforate the NE at regular intervals allowing transport of molecules across the membrane. NPCs consist of multiple copies of proteins, rich in phenylalanine-glycine (FG) repeats, called nucleoporins. Proteomic investigations reveal about 30 proteins as NPC components (Cronshaw *et al.*, 2002), although the whole structure including associated proteins is composed of probably more than 50 proteins (Fontoura *et al.*, 1999).

Although the overall structure of NPCs was known for some time advances in microscopy techniques allowed a better insight in the structure of NPCs and the distribution of its components (Krull *et al.*, 2004). NPCs display an eightfold rotational symmetry and consist of a central spoke ring complex at the level of the NE pore membrane, and filaments that extend from the rings towards the cytoplasm and the nucleoplasm. The central spoke ring extends into the NE lumen and contains a channel of about 40 nm through which molecules are transported across the membrane. The complex includes several other rings like the star and the thin ring on the cytoplasmic side and the nucleoplasmic ring on the nucleoplasmic side. From each ring eight filaments protrude towards the cytoplasm and the nucleoplasm. Nucleoplasmic filaments form branches at their ends, which are woven together to form a basket-like structure (Goldberg and Allen, 1996; Goldberg *et al.*, 1997).

Although transport of small molecules of up to 9 nm or less than 60 kD is allowed by passive diffusion, bigger molecules need to be transported by distinct steps that involve interactions with other proteins (Goldberg, 2004). Molecules are transported across the membrane by recognition of certain sequences, the Nuclear Localisation Signal (NLS) for import and the Nuclear Export Signal (NES) for export, by specific

receptors. The directionality of the transport is determined by a small GTPase called Ran, which forms a gradient with its GDP form abundant in the cytoplasm and its GTP form in the nucleus (Gorlich *et al.*, 1996).

In general, import involves the association of the NLS with importin α, which serves as an adaptor for importin β, which in turn docks the complex on the NPC (Adam *et al.*, 1989) by interacting specifically with FG repeat nucleoporins (Rexach and Blobel, 1995), Nup358 being probably one of them (Wu *et al.*, 1995). The next step involves the translocation of the molecule through the central spoke ring via the transporter. Although the existence of this structure is still controversial (Stoffler *et al.*, 2003), it has been described as a structure that is localised in the central channel and can adopt an 'open' or 'close' conformation (Akey, 1990). As the importin-cargo complex finally enters the nucleoplasmic side it is retained in the basket via an interaction with Nup153 and Tpr (Shah *et al.*, 1998) allowing RanGTP to bind importin β and release it from the cargo. In a reverse process, export of RNAs, RNPs and proteins from the nucleus involves formation of a complex with an export receptor called exportin and movement through the nucleoplasmic basket, the transporter and the cytoplasmic filaments towards the cytoplasm (Dahlberg and Lund, 1998).

1.4 The Nuclear Lamina

The lamina is a meshwork of proteins called lamins that underline the nucleoplasmic side of the INM in a discontinuous manner (Paddy *et al.*, 1990). Although their main reported distribution is perinuclear the presence of lamins in the nuclear interior has

also been reported. Localisation of lamins in intranuclear foci could correspond to intermediate assembly stages of lamins before their incorporation into the peripheral lamina (Bridger *et al.*, 1993; Goldman *et al.*, 1992; Sasseville and Raymond, 1995) or to lamins as stable components of the nuclear matrix (Hozak *et al.*, 1995; Muralikrishna *et al.*, 2004; Neri *et al.*, 1999).

Lamins are type V intermediate filaments (IFs) (Aebi *et al.*, 1986) that display the characteristic tripartite molecular organisation of all IFs with a central α-helical rod domain flanked by a globular, non-helical N-terminal 'head' and C-terminal 'tail' domain (Herrmann and Aebi, 2004). Unlike cytoplasmic IFs however, lamins possess six heptad repeats and two phosphorylation sites on their rod domain (Ottaviano and Gerace, 1985) and a CaaX motif in their tail domain that allows farnesylation and carboxymethylation of the C-terminal cysteine residue (Kitten and Nigg, 1991; Vorburger *et al.*, 1989).

Based on their sequence, expression pattern and biochemical properties they are divided in two major classes: A- and B- type lamins. In mammals, B-type lamins comprise lamins B_1, B_2 and B_3, which are encoded by two genes, LMNB1 for B_1 and LMNB2 for B_2 and B_3, and are expressed in embryonic and differentiated cells. A-type lamins consist of lamins A, C, AΔ10 and C_2, which are alternative spliced products of the same gene, LMNA, and are expressed in differentiated cells only (Stuurman *et al.*, 1998).

Although still not completely understood, a number of functions have been assigned to the lamina. The organisation of lamin filaments underneath the nuclear envelope

allows the lamins to act as a load-bearing complex providing structural support to the nucleus and controlling nuclear size and shape. At the same time lamins are part of complexes that include other INM proteins like LAPs, LBR and emerin, NPC components (Smythe *et al.*, 2000), DNA (Luderus *et al.*, 1994; Stierle *et al.*, 2003), chromatin (Glass *et al.*, 1993) and transcription factors like Rb (Ozaki *et al.*, 1994), SREBPs (Lloyd *et al.*, 2002), GCL (Nili *et al.*, 2001) and MOK2 (Dreuillet *et al.*, 2002). Due to these interactions, apart from their structural role, lamins are implicated in other cellular functions like anchoring of INM proteins and NPCs at the nuclear envelope, DNA replication and RNA transcription (Hutchison, 2002).

1.5 Nuclear Envelope dynamics during the cell cycle

With the exception of some unicellular eukaryotes, most higher eukaryotic cells undergo an 'open' mitosis disassembling their NE at the onset of cell division. This disassembly is needed so that the mitotic spindle, which is localised in the cytoplasm, can gain access and attach to chromosomes facilitating their correct segregation. This is a highly complicated process that requires the disassembly of all nuclear components, like the NPCs, the lamina and the nuclear membranes with their proteins. In a reverse process at the end of mitosis the NE reforms, enclosing the chromatin.

The exact mechanisms underlying these processes are still under debate. The older and more traditional view is that upon mitosis the NE breaks down into vesicles, which are targeted back to chromatin at the end of mitosis and fuse to reform the NE (Wiese and Wilson, 1993), while a more recent model suggests that the NE does not

vesiculate but becomes indistinguishable from the ER by diffusion of its proteins throughout an intact ER network (Ellenberg, 2002).

Evidence for a vesiculation of the NE comes mainly from studies using cell-free extracts prepared from amphibian *Rana pipiens* (Lohka and Masui, 1983) or *Xenopus laevis* (Lohka and Maller, 1985; Newport and Spann, 1987) oocytes or from Chinese Hamster Ovary (CHO) cells (Burke and Gerace, 1986). Fractionation of such cell-free systems further revealed that the NE disassembles into two types of vesicles: one set of small vesicles that has the ability to bind chromatin in an ATP-independent process and a second set that has the ability to fuse to chromatin-bound vesicles in a process that requires ATP and GTP (Newport and Dunphy, 1992; Vigers and Lohka, 1991). The different vesicle populations were found to be enriched in NE proteins leading to the conclusion that they are nuclear-specific and distinct from the bulk of the ER (Drummond *et al.*, 1999; Lourim and Krohne, 1993). The NE vesiculation could be 'domain specific' with vesicles originating and containing proteins from either the inner, outer or pore membrane only (Buendia and Courvalin, 1997; Chaudhary and Courvalin, 1993) or 'mixed' with vesicles carrying proteins from more than one NE domain (Wiese *et al.*, 1997). In both cases reassembly of the NE at the end of mitosis would require the targeting and binding of nuclear vesicles to chromatin. This interaction is thought to be mediated by an integral membrane protein since treatment of vesicles with trypsin abolishes their ability to bind chromatin (Wilson and Newport, 1988), and possible candidates include lamins, LBR and otefin. Following binding, vesicles fuse enclosing chromatin with a double-membrane NE and mature NPCs form allowing protein import, which leads to lamina formation and nuclear growth (Gant and Wilson, 1997).

In the second model, INM proteins are retained at the NE during interphase by interacting with other nuclear components like chromatin or the lamina. At the beginning of mitosis phosphorylation abolishes these interactions allowing INM proteins to diffuse freely in the ER resulting in an equilibrated distribution throughout an intact and functionally continuous mitotic ER. In a reverse process dephosphorylation at the end of mitosis allows INM proteins to establish again the interactions with chromatin that will immobilise them, wrapping progressively chromatin and reforming the NE (Ellenberg, 2002). In favour of this model come studies on the fate of INM proteins during mitosis in mammalian cells, where a dispersal of proteins within a continuous ER/NE membrane network is observed (Ellenberg *et al.*, 1997; Yang *et al.*, 1997). Dispersal of INM proteins in the ER could happen according to a 'random diffusion model', where proteins would diffuse throughout the ER or according to a 'domain model', where proteins would diffuse in the intact ER but gather in specific locations establishing microdomains enriched in nuclear proteins (Collas and Courvalin, 2000).

Supporting the second model come also studies in which the Nuclear Envelope Breakdown (NEBD) is attributed to a progressive disassembly of the NPCs or to a microtubule-induced tearing of the lamina. Based on the entry kinetics of dextrans in the nucleus of maturing starfish oocytes a progressive disassembly of NPCs was shown to lead to an increased permeability of the NE as a first step followed by expanding fenestrations leading to complete permeabilisation (Lenart *et al.*, 2003; Terasaki *et al.*, 2001). Alternatively, NEBD is caused by spindle microtubules (MTs), which attach to the NE by dynein pulling it towards the centrosomes. Pulling forces then cause indentations near the centrosomes and tension on the opposite side, which

are responsible for tearing the lamina and pulling away the NE from the chromosomes (Beaudouin *et al.*, 2002; Salina *et al.*, 2002). The argument of the latter model against vesiculation lies on the fact that vesiculation is preceded by lamina phosphorylation, which destabilises the NE leading to permeabilisation, but in this study lamin B1 was found to be dispersed only after the NE breaks down, implying that phosphorylation is not the mechanism for NEBD (Beaudouin *et al.*, 2002). However, a recent study showed that the lamin B1 network can sustain much greater deformations than the ones the spindle MTs can cause on NE. It seems, thus, that the lamin network needs to be weakened first by a biochemical modification like phosphorylation and this would allow MTs to tear the lamina and cause NEBD (Panorchan *et al.*, 2004).

Although the two models of 'vesiculation' and 'ER dispersal' are very dissimilar they are not mutually exclusive. Since the data obtained supporting the first or the second model originate from cell-free extracts and mitotic cells, respectively, their differences could be attributed to the different nature of these two systems. While, on one hand, the observed vesicles could simply be the result of cell homogenisation during extract preparation, on the other hand, oocytes contain stockpiles of materials required for several and rapid cell divisions and could therefore contain nuclear envelope precursor vesicles which are absent from somatic cells. Furthermore, the substrate for NE assembly in egg extracts is sperm chromatin, which is highly condensed, and when decondensed, gives rise to pronuclear NE which are quite different from somatic nuclei (Collas and Courvalin, 2000).

1.6 The INM protein Emerin

Emerin is encoded by the STA gene, which was identified in 1994 by positional candidate cloning on chromosome Xq28, as the gene responsible for the X-linked form of Emery Dreifuss Muscular Dystrophy (EDMD) (Bione *et al.*, 1994). Sequencing of the gene revealed that it is 2.1 kb long, has six exons and contains an open reading frame of 762 nucleotides that encodes emerin (Bione *et al.*, 1995). Subsequent production of emerin specific antibodies revealed a localisation for emerin at the INM of normal tissues and its absence from nuclei of EDMD patients (Manilal *et al.*, 1996; Nagano *et al.*, 1996; Yorifuji *et al.*, 1997). Emerin is ubiquitously expressed in most tissues showing a higher expression in skeletal muscle and heart.

Although mainly localised in the INM, localisation of emerin in other cellular compartments has also been reported. In COS-7 cells emerin was localised in intranuclear spots and fibres that could, however, correspond to NE invaginations (Fairley *et al.*, 1999; Manilal *et al.*, 1998) while a cytoplasmic localisation at the intercalated discs in heart and cultured cardiomyocytes has also been reported (Cartegni *et al.*, 1997). Emerin was also detected in the plasmalemma and cytoplasm of platelets, blood cells that lack nuclei and arise from the cytoplasmic fragmentation of megakaryocytes (Squarzoni *et al.*, 2000). However, both of these studies used polyclonal antibodies, and it has been shown that after affinity purification of a polyclonal antibody against emerin, localisation at the intercalated discs was no longer detectable (Manilal *et al.*, 1999). Also although no plasma membrane association of emerin was found in COS-7 and C2C12 cells, a staining in the ER in

close proximity to the NE was observed (Fairley *et al.*, 1999) leaving the issue of the cytoplasmic localisation of emerin under debate.

1.6.1 Structure

Emerin is a type II integral INM protein of 254 amino acids (aa). It consists of a large hydrophilic N-terminal domain in the nucleoplasm, a single transmembrane (TM) domain (aa 223-243) and a small C-terminal domain in the lumenal space. It is a serine-rich protein with more than 15% of its amino acids being serines mainly clustered in a region between residues 170-200, and it contains 22 possible phosphorylation sites and a bipartite NLS between amino acids 35-46 (Tews, 1999).

Its main characteristic feature is the LEM domain (residues 1-45). Originally it was identified as a domain common in LAP2, Emerin and MAN1 but it is also present in two *C. elegans* proteins (M01D7.6 and W01G7.5) and in the *D. melanogaster* protein otefin. The three-dimensional solution structure of the LEM domain as revealed by Nuclear Magnetic Resonance (NMR) spectroscopy comprises a three-residue N-terminal α helix and two large parallel α helices separated by a loop of conserved hydrophobic residues. LEM domains are connected to a highly divergent LEM-like domain, which shares only 18% identity with the LEM domain but displays a very similar three-dimensional structure, and they are both thought to be protein-protein interaction domains (Laguri *et al.*, 2001; Wolff *et al.*, 2001).

1.6.2 Emerin dynamics during the cell cycle

Emerin is localised at the NE during interphase. Although it contains a bipartite NLS at its N-terminal domain, its proper INM localisation is not mediated by it. Unlike soluble proteins, which are targeted to the nucleus by a NLS through NPCs, the mechanism for nuclear targeting of integral membrane proteins differs and does not involve NLSs (Soulham and Worman, 1995). Instead INM proteins reach the NE by an ER diffusion/retention model. Newly synthesised emerin enters the ER membrane anchored by its TM domain and diffuses laterally till it reaches the INM through the pore membrane. At the INM, emerin gets immobilised by interacting with other NE components, like lamins, using its nucleoplasmic domain. The regions of emerin responsible for its proper localisation have been specified by monitoring the localisation of c-myc or GFP-emerin deletion mutants. While an emerin construct consisting of the entire nucleoplasmic domain and lacking the TM domain (aa 3-228) was localised in the nucleus diffusely rather than concentrated at the periphery, another construct consisting of the TM domain only (aa 197-254) was localised in the ER membranes and not in the nucleus, showing that the TM domain is necessary but not sufficient for a proper INM localisation. Although emerin is anchored at the NE by its TM, a sequence in the nucleoplasmic domain, narrowed down to residues 117-170, was shown to be necessary to retain emerin in the INM (Ostlund *et al.*, 1999; Tsuchiya *et al.*, 1999).

At the onset of mitosis when the NE disassembles the interactions that retain INM proteins at the NE are abolished and this process is regulated by phosphorylation. Emerin contains several phosphorylation sites and was shown to undergo a cell-cycle

dependent phosphorylation appearing hyperphosphorylated in four different forms in metaphase and early S-phase cells (Ellis *et al.*, 1998). The fate of emerin during mitosis has been monitored in human HEp2 (Dabauvalle *et al.*, 1999) and HeLa cells (Haraguchi *et al.*, 2000; Haraguchi *et al.*, 2001). In prophase when chromatin starts to condense emerin is still localised at the NE while in metaphase when the nuclear membranes disassemble emerin is localised throughout the cytoplasm. In both cell types emerin was found to be recruited early in the nuclear assembly process, five minutes after the metaphase to anaphase transition, in early telophase, and was focally concentrated in the 'core' region of chromosomes near the spindle poles. The 'core' localisation was maintained for further three to four minutes after which emerin was uniformly distributed around chromosomes in late telophase. The 'core' localisation of emerin was shown to depend on its interaction with chromatin protein BAF since when emerin LEM domain mutants that do not bind BAF and when BAF mutants that do not bind emerin were used, emerin failed to localise in the 'core' region. Further analysis of HeLa cells by live cell imaging revealed that emerin co-exists in the inner and outer 'core' region of anaphase chromatin, adjacent to the midspindle and spindle poles respectively, with LAP2α, LAP2β and lamin C, in contrast to lamin B and LBR which first assembled to more peripheral regions (Dechat *et al.*, 2004).

1.6.3 Emerin interacting proteins

The identification of emerin as the first INM protein involved in a muscular dystrophy, in 1994, drew intense attention in identifying its interacting proteins with the ultimate goal of understanding its function. Emerin has been shown so far to

interact with several structural and gene regulatory proteins. Its best characterised binding partners so far though include lamins and BAF.

1.6.3.1 Lamins

There are several reports that support an interaction between emerin and lamins. A first indication arose from an immunofluorescence study on Green Monkey Kidney cells (COS-7) with emerin and lamin specific antibodies that showed a co-localisation of emerin with lamins A/C, B1 and B2 in interphase and a partial co-localisation during mitosis (Manilal *et al.*, 1998). Further support for this interaction came from co-immunoprecipitation experiments. An antibody raised against emerin aa 114-183 co-precipitated lamins B and A/C from C2C12 myoblast and rat hepatocyte nuclear extracts (Fairley *et al.*, 1999). A later study confirmed the co-immunoprecipitation of lamins A, C and B1 with emerin in rabbit reticulocyte lysates and showed by competition experiments that although emerin can interact *in vitro* with all lamins its preferred interaction is with lamin C (Vaughan *et al.*, 2001). The same study further showed that in cell lines where lamin A is absent, lamin C is mislocalised in the nucleolus and lamins B1 and B2 are normal, emerin is mislocalised in the ER forming aggregates. When lamin A is transfected back to these cells emerin relocalises correctly to the NE while transfection of lamin B1 is not able to rescue emerin localisation. Thus, although emerin is able to interact with lamin B *in vitro* their interaction *in vivo* is rather doubtful.

A direct interaction between emerin and lamin A was demonstrated by Biomolecular Interaction Analysis (BIA). Application of full-length emerin on lamin A immobilised

on a BIAcore biosensor chip, which measures changes in surface plasmon resonance angle produced by changes in total mass at the surface of the chip, confirmed the interaction of the two proteins (Clements *et al.*, 2000).

The emerin-lamin A interaction was shown to require aa 70-178 of emerin and aa 384-566 of lamin A. The residues of emerin responsible for binding lamin A were mapped by blot overlay assays. Bacteria lysates containing full-length and mutant emerin forms were resolved on gels, transferred to nitrocellulose and incubated with ^{35}S-labelled lamin A. The assay showed that lamin A was able to interact with full-length emerin but not with emerin containing mutations in the central region of the protein between aa 70-178. All other mutants including LEM-domain mutations were able to bind lamin A (Lee *et al.*, 2001). The region of lamin A responsible for binding emerin was investigated by a yeast-two-hybrid system. Full-length emerin was cloned into a vector containing the GAL4 binding domain and different lamin A truncated genes were cloned in vectors containing the GAL4 activating domain. Examination of all combinations revealed that the first half of the lamin A tail domain, between aa 384-566, was responsible for binding emerin (Sakaki *et al.*, 2001).

1.6.3.2 BAF and MAN1

Barrier-to-autointegration factor (BAF) is a DNA-bridging protein that can interact simultaneously with DNA and the LEM domain of LAP2, attaching chromatin to the INM (Shumaker *et al.*, 2001). The ability of BAF to interact with the LEM domain of emerin was investigated by blot overlay experiments in which emerin mutants were immobilised on blots and incubated with ^{35}S-BAF. As for LAP2, BAF was shown to

interact with emerin aa 1-43, which comprise the LEM domain (Lee *et al.*, 2001). A direct interaction of BAF with emerin in living cells has also been demonstrated by Fluorescence Resonance Energy Transfer (FRET) analysis in which repeated photobleaching of YFP-emerin resulted in increase in the fluorescence of CFP-BAF confirming their direct association (Shimi *et al.*, 2004). In the same study Fluorescence Recovery After Photobleaching (FRAP) and Fluorescence Loss In Photobleaching (FLIP) analysis of BAF and its binding partners showed that BAF exists in two separate pools in the cell, a nuclear and a cytoplasmic, that do not mix with each other, and that BAF diffuses rapidly as opposed to emerin and LAP2, which are immobile at the NE. Thus, a 'touch and go' model is proposed according to which BAF interacts frequently but transiently with emerin in interphase.

BAF has the ability to bind MAN1, another INM protein containing a LEM domain. Unexpectedly, affinity chromatography, microtiter and blot overlay assays showed that the N-terminal domain of MAN1 can bind, except BAF, emerin and lamins A and B1 as well, while the C-terminal region of MAN1 can interact with other known emerin binding partners including GCL and Btf. The proposed MAN1 binding region of emerin was shown to include the nucleoplasmic domain of emerin without the LEM domain (Mansharamani and Wilson, 2005). These findings suggest that emerin and MAN1 associate *in vivo*, overlapping functionally, and comes in agreement with RNAi experiments in *C. elegans* embryos where knock-down of MAN1 alone caused a 15% embryonic lethality only while knock-down of emerin and MAN1 together caused a 100% embryonic lethality (Liu *et al.*, 2003).

1.6.3.3 Gene regulatory binding partners

Supporting a role for emerin in affecting gene expression, several gene regulatory proteins have been reported to interact with emerin. Protein Germ Cell Less (GCL) was shown to co-immunoprecipitate with emerin in nuclear extracts prepared from HeLa cells. A microtiter well binding assay with full-length and mutant emerin fragments immobilised on wells and incubated with ^{35}S-GCL showed that GCL binds to emerin residues 34-83, 175-196 and 207-217. Although GCL did not bind the LEM domain like BAF, in competition experiments GCL and BAF did compete for emerin binding (Holaska *et al.*, 2003).

Adding to the list of gene regulatory binding partners a yeast-two-hybrid screen of a human heart cDNA library with full-length emerin as bait identified, apart from lamin A, a nuclear splicing associated factor called YT521-B. The interaction was confirmed by co-immunoprecipitation and BIAcore analysis while a microtiter well binding assay with emerin mutants showed that, like GCL, YT521-B bound the two emerin regions flanking the lamin A binding domain partially overlapping the BAF and lamin-A binding regions (Wilkinson *et al.*, 2003).

In a similar yeast-two-hybrid assay, with full-length emerin used to screen a HeLa cDNA library, a transcriptional repressor called Btf was identified as an emerin interacting protein. The interaction was confirmed with a blot overlay and microtiter well binding assay and was shown to require emerin residues 45-83 and 175-217. The same yeast-two-hybrid screen that identified Btf, however, failed to identify other

known emerin binding partners like lamin A and BAF, while co-immunoprecipitation of emerin and Btf from HeLa lysates also failed (Haraguchi *et al.*, 2004).

The latest indication of emerin involvement in gene regulation involves β-catenin, a down-stream effector of the canonical wnt-signalling pathway. Observations on X-EDMD fibroblasts indicate that absence of emerin leads to unusual growth characteristics with cells failing to enter quiescence upon serum withdrawal. This auto-stimulatory growth results from activation of the canonical wnt pathway since X-EDMD cells in low serum display an accumulation of de-phosphorylated β-catenin, which cannot be degraded, in the nucleus. It is, thus, proposed that emerin binds β-catenin at the NE helping to target nuclear β-catenin for destruction (Markiewicz, personal communication).

1.6.3.4 Structural binding partners

In addition to lamins, emerin has been shown to interact with other proteins that provide structural support to the nucleus. Nesprins are proteins that are rich in spectrin repeats and comprise several isoforms, which connect the cytoskeleton with the nucleoskeleton. An interaction between emerin and nesprin 1α isoform was shown by a blot overlay and microtiter well binding assay using the entire nucleoplasmic domain of emerin (Mislow *et al.*, 2002). In the same study nesprin 1α was shown to interact with lamin A also, implying that it is able to crosslink emerin and lamin A at the NE. More recently, a second isoform of nesprins, nesprin 2, was also shown to interact with emerin by co-immunoprecipitation experiments in vascular smooth muscle cell lysates (Zhang *et al.*, 2005).

Although the presence of actin in the nucleus is still under debate there are several reports about an association of emerin with nuclear actin. Actin was first shown to co-immunoprecipitate with emerin in C2C12 myoblast extracts (Fairley *et al.*, 1999). Actin also co-immunoprecipitated with emerin and lamin A/C in late stages of differentiation of C2C12 myotubes and in mature muscle fibres, and this interaction seemed to be regulated by protein phosphorylation (Lattanzi *et al.*, 2003). In another investigation on emerin binding partners in HeLa nuclear extracts, by affinity chromatography, β-actin was pulled-down. The interaction was further confirmed by co-sedimentation, co-immunoprecipitation and blot overlay assays and was shown to require the entire nucleoplasmic domain of emerin (Holaska *et al.*, 2004). In the same investigation aII spectrin and myosin I were also identified as potential emerin interacting proteins (Bengtsson and Wilson, 2004). These interactions place emerin as part of a nuclear actin cortical network where emerin stabilises and promotes formation of actin filaments by binding to the minus end of F-actin. Short actin filaments are in turn cross-linked to aII spectrin by protein 4.1 and the whole network is thought to provide structural support to the nucleus (Holaska *et al.*, 2004).

1.7 The nuclear envelope and disease

Several human diseases have been associated with defects in genes encoding NE proteins. A large proportion of them are associated with mutations in lamins A/C and emerin and are also known as laminopathies or envelopathies. The best characterised laminopathy so far is Emery-Dreifuss muscular dystrophy, which was the first muscular dystrophy discovered to be caused by a defect in a nuclear envelope protein.

1.7.1 Emery-Dreifuss Muscular Dystrophy (EDMD)

EDMD is a rare form of muscular dystrophy. It was first described in 1966 by Emery and Dreifuss who examined a large Virginian family affected with an X-linked muscular dystrophy (Emery and Dreifuss, 1966). The term 'Emery-Dreifuss muscular dystrophy' was not adopted, however, till 1979 when suggested by Rowland *et al.* who described families with similar symptoms (Rowland *et al.*, 1979). EDMD is caused by mutations in either of two genes, the *STA* gene that encodes emerin and the *LMNA* gene that encodes lamin A/C. Mutations in the *STA* gene give rise to the X-linked recessive form of EDMD while mutation in the *LMNA* gene result an Autosomal-Dominant (AD) form.

Typical EDMD can be defined by a triad of clinical features: early contractures of the Achilles tendons, elbows and post-cervical muscles, muscle wasting and weakness proximal in the upper arms and distal in the lower legs and cardiac conduction defects, which slowly progress towards complete heart block. Smooth muscle function is not affected and mental retardation is not a feature of the disorder (Emery, 2000).

1.7.1.1 X-linked EDMD

X-EDMD has an early onset at the age of 3-5 years with the first symptoms being unstable gait, repeated falls and toe walking because of contractures in the Achilles tendons. Limited flexion of the elbows and neck is also observed, which later progresses to the whole spine overlapping clinically with the rigid spine syndrome

(Kubo *et al.*, 1998). Cardiac defects appear usually in the second decade of life and become worse with age. A study on 18 EDMD patients for a period of 1 to 30 years identified a broad spectrum of cardiac abnormalities. Arrythmias developed in all patients as bradyarrythmias and tachyarrythmias including atrial fibrillation/flutter, which led to atrial standstill and embolic stroke (Boriani *et al.*, 2003). Autopsy on two affected males and one carrier showed that the most significant abnormalities were in the atria with a marked loss of the myocardium and its replacement by fibrous and adipose tissue (Fishbein *et al.*, 1993). Cardiac defects account for the most common cause of death in EDMD patients, which is sudden death, making insertion of a pacemaker life-saving. Since cardiac abnormalities do not correlate with muscle disability it has been proposed that unrecognisable cases could contribute to the sudden unaccountable deaths in healthy young adults (Emery, 2000). However, a screen of more than 3000 individuals with heart conduction system disease and inserted pacemaker identified only one with an emerin mutation showing that the clinical relevance of X-EDMD in heart conduction disease is very low (Vytopil *et al.*, 2004).

Mutations in the *STA* gene occur throughout the gene with no particular 'hot spots'. The majority of mutation are nonsense, frameshift or splice site mutations resulting from base substitutions, small deletions and insertions (Yates and Wehnert, 1999). Although truncated emerin molecules could be produced in these cases a complete emerin absence is observed. This could be either due to mRNA instability or due to protein instability because it cannot fold properly or it cannot integrate into the membrane properly. It is proposed that the last option is the most probable cause of emerin absence since a mutation in the TM domain of emerin was shown to result in a

complete absence of the protein but normal mRNA levels were detected (Manilal *et al.*, 1998).

Although the majority of mutations are null resulting in complete loss of emerin, a few mutations have been identified that lead to reduced levels of expression. These include two in-frame deletions that result removal of amino acids 95-99 (Δ95-99) and 236-241 (Δ236-241) and four missense mutations, which are single substitutions (S54F, Q133H, P183H and P183T). These mutations produce modified forms of emerin. P183T mutation has been shown to cause a milder phenotype in affected individuals with a later age of onset of the first symptoms (Yates *et al.*, 1999). At the same position a proline substitution for a histidine has also been reported. In both cases (P183T/H) emerin is expressed in normal amounts and size but it is displays an altered subcellular distribution and solubilisation properties. Unlike wild-type emerin, mutant emerin in no longer confined to the nuclear fraction and it can be extracted with 1% Triton in the absence of salt indicating that its interactions with the nuclear lamina are weakened (Ellis *et al.*, 1999).

Families with the two in-frame deletions Δ95-99 and Δ236-241 express reduced amounts of emerin but display clinical features identical with patients that carry null mutations lacking emerin completely (Manilal *et al.*, 1998; Yates *et al.*, 1999). The behaviour of emerin mutants Δ95-99, Δ236-241, S54F, P183H and P183T was further studied by transfection of GFP-mutants in C2C12 myoblasts. All mutants displayed reduced targeting and retention at the nuclear envelope in comparison to wild-type emerin and the targeting of the deletion mutations was more severely affected than the two missense mutants. Mutant Δ236-241 was the most severely

mislocalised one since absence of the transmembrane domain did not allow its membrane integration (Fairley *et al.*, 1999).

The final known missense mutation to date is a g to t substitution at nucleotide 993. The mutation is responsible for a Q to H substitution of amino acid 133 and it can also give rise to a number of alternatively spliced mRNAs. The mutation was shown to cause reduced levels of emerin compared to controls (Mora *et al.*, 1997). However, transfection of COS-7 cells with the GFP-mutant did not show an altered localisation relative to wild-type emerin and BIAcore analysis showed that the mutant retained the ability to interact with lamin A. It is, thus, likely that this mutation causes pathogenesis either by reducing emerin levels due to altered mRNA splicing or by disturbing the interaction with another, yet unidentified, partner (Holt *et al.*, 2001).

Since the majority of mutations are null leading to complete absence of emerin, X-EDMD can in most cases be diagnosed at the protein level by immunoblotting and immunofluorescence on skin fibroblasts and leukocytes (Manilal *et al.*, 1997) or by an even less invasive method of cell scraping from the oral mucosa of the cheek (Sabatelli *et al.*, 1998). Unlike X-EDMD mutations, AD-EDMD cannot be detected at the protein level by immunohistochemistry. Instead diagnosis depends on mutation analysis.

X-EDMD displays a high degree of heterogeneity, both inter- and intrafamilial. The same emerin mutation was shown to cause different phenotypes in two German families and also different clinical features in two brothers of the same family (Hoeltzenbein *et al.*, 1999). Furthermore, although cardiac problems appear in the

second decade, one case of a very early onset has been reported in two brothers at the age of six and nine (Talkop *et al.*, 2002). Contributing to the disease variability is the fact that cardiac involvement does not correlate with the degree of muscle involvement. Severe heart failure has been observed in patients with very mild muscular disability (Boriani *et al.*, 2003; Vohanka *et al.*, 2001) and a sudden death of a female carrier has also been reported (Fishbein *et al.*, 1993).

Management of the disease involves limitation of deformities through exercise and physiotherapy while corrective surgery for lengthening of Achilles tendon or elbow flexion can relieve the effects of the contractures. Since sudden death by heart failure is the most common cause of death and it can even affect female carriers, the early diagnosis and monitoring of patients is very important. In most cases insertion of a pacemaker can be life-saving and heart transplantations have also been reported in several patients (Kichuk Chrisant *et al.*, 2004; Merchut *et al.*, 1990). The small size of the coding region of the *STA* gene makes it also a good candidate for gene therapy. Using this approach, a direct delivery of the gene to the conducting system of the heart could have an important clinical effect (Emery, 2000).

1.7.1.2 Autosomal EDMD

Although most cases of EDMD are X-linked a more rare autosomal dominant (AD-EDMD) form also exists. A study on a French family identified the responsible gene on chromosome 1q21. The gene, which is called *LMNA*, encodes lamins A and C by alternative splicing (Bonne *et al.*, 1999). Three cases of an autosomal recessive inherited form (AR-EDMD) have also been reported. A patient was identified

homozygous for a H222Y mutation while his parents, which were first cousins, were heterozygous for the mutation and not affected by the disease (Raffaele Di Barletta *et al.*, 2000). The cases of a woman, also born from consanguineous parents, and of five children affected by EDMD with an autosomal recessive inheritance have also been described (Takamoto *et al.*, 1984; Taylor *et al.*, 1998).

AD-EDMD displays clinical features very similar to those of X-EDMD with early onset of contractures, muscle wasting and weakness but cardiomyopathy is more prevalent than in the X-linked form. Also, unlike X-EDMD, the majority of mutations in AD-EDMD are missense mutations leading to the production of an equimolar mixture of normal and mutated lamins while emerin levels are normal (Morris, 2001). A domain specific phenotype has been proposed according to which mutations in different domain of lamins A/C cause different phenotypes. A study on the mutations and phenotype of 11 families led to the hypothesis that rod domain mutations are responsible for cardiac defects while mutations in the tail domain cause skeletal myopathy (Fatkin *et al.*, 1999). However, several reports contradict this hypothesis. Two families with missense mutations in the central rod domain of the lamin A/C gene displayed the full clinical spectrum of EDMD including humeropelvic weakness and contractures, cardiomyopathy with conduction system disease and sudden death (Felice *et al.*, 2000). Another study on ten patients bearing mutations in the rod and tail domain showed a coexistence of EDMD and cardiac disease in the rod domain mutations while the severity of cardiac defects was not related to the domain of the mutations (Sanna *et al.*, 2003).

1.7.2 Other laminopathies

In the past years mutations in the LMNA gene have been shown to cause a wide spectrum of phenotypes and the term laminopathies has been adopted to collectively describe them. Laminopathies include the following disorders: Limb-girdle muscular dystrophy 1B (LGMD-1B), Dilated cardiomyopathy with conduction system disease (DCM-CD), Dunnigan-type familial partial lipodystrophy (FPLD), Autosomal Recessive Charcot-Marie-Tooth type 2 (AR-CMT2), Mandibuloacral Dysplasia (MAD), Werner syndrome (WS) and Hutchinson-Gilford progeria syndrome (HGPS).

1.7.2.1 Limb girdle muscular dystrophy-1B

LGMD-1B affects mainly the proximal limb-girdle musculature and comprises 15 different types inherited as both autosomal dominant and recessive forms. The LGMD-1B type is characterised by slowly progressive pelvic girdle weakness with late involvement of humeral muscles. Unlike EDMD lower legs are not affected. Contractures of elbows and the Achilles tendons are not observed but cardiological abnormalities are (Van der Kooi *et al.*, 1996). Screening of 79 patients from three families diagnosed with LGMD-1B identified LMNA mutations in all three families demonstrating that LGMD-1B and AD-EDMD are allelic disorders. The three mutations were an in-frame deletion in exon 3 (ΔK208), a missense mutation in exon 6 (R377H) and a splice donor site of intron 9 creating a truncated protein of 571 amino acids (Muchir *et al.*, 2000).

1.7.2.2 Dilated cardiomyopathy with conduction system disease

DCM-CD is a myocardial disorder characterised by a four-chamber dilation of the heart and impaired systolic function leading to congestive heart failure and sudden death. It is a highly heterogenous disorder mostly with an autosomal dominant inheritance. The first indication of an LMNA involvement was in 1999 when Fatkin *et al.* identified five LMNA missense mutations in patients with DMC-CD. Each mutation caused cardiac defects with no contractures or skeletal myopathy (Fatkin *et al.*, 1999). The number of LMNA mutations causing DCM-CD, however, has risen and at least eight mutations are known so far (Morris, 2001).

1.7.2.3 Dunnigan-type Familial Partial Lipodystrophy

Dunnigan-type FPLD is a rare autosomal dominant disease characterised by marked loss of subcutaneous adipose tissue from the extremities and trunk after the onset of puberty and accumulation of excess fat in the head and neck areas. A study on five Canadian kindreds with FPLD identified a missense mutation in LMNA gene (R482Q) (Cao and Hegele, 2000). Two more studies, one on ten (Shackleton *et al.*, 2000) and another on 15 families (Speckman *et al.*, 2000) with FPLD identified five further mutations. All FPLD causing mutations are clustered in the tail region of lamins between exons 8 and 11.

1.7.2.4 Charcot-Marie-Tooth

Charcot-Marie-Tooth (CMT) disease constitutes a heterogenous group of hereditary motor and sensory neuropathies and are divided into demyelinating or type 1 (CMT1) and axonal or type 2 (CMT2). The first association of the LMNA gene with autosomal recessive axonal CMT2 was reported in three consanguineous Algerian families. The main symptoms of the patients included early onset of muscle weakness and wasting predominantly in the distal lower limbs, foot deformities, walking difficulties associated with reduced or absent tendon reflexes and sensory impairment. Mutation analysis revealed a missense mutation in exon 5 causing an R298C substitution (De Sandre-Giovannoli *et al.*, 2002).

1.7.2.5 Mandibuloacral dysplasia

Mandibuloacral dysplasia (MAD) is a rare autosomal recessive disorder characterised by postnatal growth retardation, mandibular and clavicular hypoplasia, acroosteolysis, delayed closure of the cranial suture, joint contractures and types A and B patterns of lipodystrophy. Analysis of five consanguineous Italian families that included nine affected individuals led to linkage of MAD to chromosome 1q21 by homozygosity mapping. Sequencing of the LMNA gene revealed that all patients had a missense mutation, R527H. Immunofluorescence analysis of skin fibroblasts from patients homozygous for the disease showed nuclear abnormalities that involved nuclear envelope lobulation and a honeycomb labelling for lamin A/C (Novelli *et al.*, 2002).

1.7.2.6 Hutchinson-Gilford progeria

Hutchinson-Gilford progeria (HGP) is a rare autosomal syndrome of accelerated aging with an average age of death at 13.4 years due to coronary artery disease. Clinically it is characterised by postnatal growth retardation, midface hypoplasia, premature atherosclerosis, absence of subcutaneous fat, alopecia and generalised osteodysplasia with osteolysis and pathologic fractures. LMNA analysis of HGP affected children, revealed two patients with a heterozygous C to T transition at nucleotide 1824 in exon 11. The mutation has no effect on the translated amino acid (G608G) but it activates a cryptic splice donor site predicted to remove fifty amino acids from the tail of lamin A leaving lamin C unaffected. Immunofluorescence analysis of lymphocytes from patients showed a major loss of lamin A expression, normal lamin C and a mislocalisation of lamin B1 in the nucleoplasm. Morphologically nuclei exhibited altered size and shape with nuclear envelope interruptions and extrusion of chromatin in the cytoplasm (De Sandre-Giovannoli *et al.*, 2003; Eriksson *et al.*, 2003). The same point mutation leading to nuclear abnormalities in HGP patients was also identified by Eriksson *et al.* while Cao *et al.* reported further mutations R471C, R527C, G608S and c.2036C>T (Cao and Hegele, 2003; Eriksson *et al.*, 2003).

1.7.2.7 Werner syndrome

Werner syndrome (WS) is an autosomal recessive progeroid syndrome characterised by scleroderma-like skin changes, cataract, short stature, greying/thinning of the hair, diabetes mellitus, soft tissue calcification and premature atherosclerosis. It is caused

by mutations in WRN, which belongs to a family of DNA helicases. A study of 129 patients diagnosed with an atypical WS, which did not harbour a mutation at WRN, identified three LMNA missense mutations, R133L, L140R and A57P. The clinical features of the LMNA patients included short stature, grey or sparse hair, diabetes mellitus, cardiovascular defects, osteoporosis, lipodystrophy and muscular atrophy. Immunofluorescence on patients fibroblasts revealed irregularly shaped nuclei with leakage of chromatin in the cytoplasm (Chen *et al.*, 2003). The previously reported mutation, R133L, was also identified by Caux *et al.* in a patient with clinical features overlapping between WS and FPLD. The patient presented generalised lipoatrophy with metabolic alterations like insulin resistance and liver steatosis, distinctive subcutaneous manifestations without fat accumulation in the face, neck or trunk, as in FPLD, and cardiac abnormalities involving both endocardium and myocardium. Typical WS symptoms like cataract, short stature and skeletal abnormalities were absent. Immunofluorescence on skin fibroblasts revealed nuclear deformations by herniations of various sizes and shapes and a disorganisation of A-type lamins with a honeycomb staining pattern (Caux *et al.*, 2003).

In total, 69 mutations of the LMNA gene have been reported so far and they are responsible for a wide spectrum of diseases. Several of these mutations, though, have been reported to cause phenotypes with clinical features overlapping between different disorders. A patient with a S143F point mutation in the rod domain of lamin A has been reported combining early myopathy with progeria. Initially she presented congenital weakness in neck muscles, muscle atrophy and rigidity of the spine with no elbow and Achilles tendons contractures. During subsequent years additional progeroid clinical features developed including growth retardation, sclerodermatous

skin lesions, acroosteolysis, sparse hair and loss of subcutaneous fat (Kirschner *et al.*, 2005). Interestingly, a mutation at the same position leading to a serine substitution by a proline (S143P) is reported in a patient with dilated cardiomyopathy but no involvement of skeletal muscles (Karkkainen *et al.*, 2004). A 15-bp deletion from -3 to +12 including the initiation translation codon resulting in a null mutation was identified in a German family. The affected individuals had a unique phenotype, with clinical features that are shared between EDMD and CMT2, suffering from both, neurogenic and myogenic abnormalities (Walter *et al.*, 2005). Also, two mutations, one in the head domain (R28W) and one in the rod domain (R62G) were identified in two families, which presented a Dunnigan type-FPLD, but unlike other FPLD cases, also suffered from cardiomyopathy including cardiac conduction defects, atrial fibrillation and heart failure due to ventricular dilation (Garg *et al.*, 2002). The identification of overlapping lamin-associated disorders indicates that they might represent a functional continuum of related disorders rather than separate diseases (Bonne and Levy, 2003).

1.7.3 Possible disease mechanisms

So far no human diseases have been associated with B-type lamins indicating that they are essential for life. Indeed, lamin B1 knockout mice die a few minutes after birth and exhibit abnormal lung development, bone ossification, misshapen nuclei, impaired differentiation and premature senescence (Vergnes *et al.*, 2004). In contrast, mutations in A-type lamins and emerin are associated with EDMD while a number of other LMNA mutations are implicated in a wide spectrum of disorders. Although emerin and lamins are ubiquitously expressed, mutations seem to affect cardiac and

skeletal tissues selectively and it is still not clear why that is. Several hypotheses have been formulated, however, to explain this tissue specificity.

The 'structural' hypothesis proposes that lamins contribute to the structural integrity of the nuclear envelope and provide mechanical support to the nucleus. Lamin filaments are thought to act as a tensegrity element for the nucleus forming a load-bearing cage-like structure that underlies the nuclear envelope affecting nuclear shape and helping to resist deformations (Hutchison, 2002). Absence of lamins or emerin in disease would destabilise the lamin association with the NE, and the lamina as a whole would become less effective as a load-bearing structure. This in turn would render the NE vulnerable to damage, especially in contractile tissues like the skeletal and cardiac muscle that are under high mechanical stress, leading to cell death and tissue damage (Hutchison *et al.*, 2001). Cell death due to nuclear fragility would be less deleterious in skeletal muscle fibres, which are a syncitium. In contrast, loss of few key cells in the heart by random cell death could lead to a complete block of the conduction pathway (Morris, 2000).

In support to this model come observations of nuclear defects in cells of X- and AD-EDMD patients. Absence of emerin was shown to cause structural alterations at the nuclear periphery including focal detachment of the peripheral heterochromatin from the NE (Ognibene *et al.*, 1999) and nuclear fragility leading to focal loss of nuclear membrane and chromatin extrusion into the cytoplasm (Fidzianska *et al.*, 1998). Ultrastructural studies of muscle nuclei form AD-EDMD patients showed also aberrant nuclear architecture with focal loss of chromatin and sarcoplasmic invaginations into the nucleoplasm (Fidzianska and Hausmanowa-Petrusewicz,

2003). Similar results were observed in lamin A/C knockout mice with irregularly shaped nuclei and herniations of the NE (Sullivan *et al.*, 1999).

The importance of NE proteins in maintaining nuclear structural integrity has been demonstrated in experiments where lamin A/C deficient mouse fibroblasts have been subjected to mechanical stretching (Lammerding *et al.*, 2004) or compaction forces (Broers *et al.*, 2004). Lmna -/- deficient fibroblasts showed a decreased mechanical stiffness and impaired viability under strain in comparison to control nuclei underlying the importance of the lamina in providing structural support to the nucleus. The contribution of the lamina in strength and flexibility of nuclei during shear and extension has also been shown in *Xenopus* oocytes, where it is proposed that the lamina forms a compressed network of interconnected rods with an elastic extensibility and a limited compressibility acting as a molecular shock absorber (Dahl *et al.*, 2004).

Although the 'structural' hypothesis explains nicely the cardiac and skeletal muscle defects, it is probably not a universal model since it cannot explain other laminopathies like FPLD. It is highly unlikely that adipocyte nuclei would ever be subjected to forces comparable to those that are encountered in muscle. An alternative, 'gene expression' hypothesis has been proposed according to which emerin and lamins are involved in tissue specific gene expression (Cohen *et al.*, 2001). According to this model disease may arise from the downstream effects of mutations on chromatin structure or gene expression that are caused by lamina disorganisation, failure to provide attachment sites for transcriptional regulators or reduced binding affinity for other essential partners (Wilson *et al.*, 2001). Moreover,

since all affected tissues in emerin-lamin diseases (muscle, fat, cartilage, bone and tendons) arise from the same progenitor, mesenchymal stem cells, it is proposed that tissue specificity is because of effects of mutations on this particular cell lineage (Wilson, 2000).

Transcriptionally inactive heterochromatin is known to be localised at the nuclear periphery. Lamins and INM proteins provide attachment sites for chromatin by interacting either with chromatin directly or with chromatin associated proteins like HP1 and BAF, and in lamin A/C null cells detachment of chromatin from the NE is frequently observed. Moreover, a growing number of transcription factors, mainly repressors, are reported to interact with emerin and lamins. The retinoblastoma protein (Rb), which binds transcription factor E2F and represses transcription by recruiting histone deacetylase, was shown to anchor at the nucleus by an interaction with LAP2α-lamin A/C complexes (Markiewicz *et al.*, 2002; Ozaki *et al.*, 1994). Lamin A was also shown to bind the transcription factor domain of sterol response element binding protein (SREBP1). SREBP1 is an adipocyte differentiation factor and reduced binding to lamin A could explain the effect of lamin mutations in adipose tissues in FPLD (Lloyd *et al.*, 2002). Emerin has also been implicated in a number of interactions involving transcription factors like GCL, Btf and YT521-B (Haraguchi *et al.*, 2004; Holaska *et al.*, 2003; Wilkinson *et al.*, 2003).

Although very different the two models of 'mechanical stress' and 'gene expression' are not mutually exclusive and disease mechanisms could be explained by the combination of both.

1.8 The *Xenopus* cell-free system

Cell-free systems are widely used in studies of cellular processes like mitosis or DNA replication or in analysing nuclear structures. Several cell-free systems have been developed over the past years arising from mammalian Chinese Hamster Ovary (CHO) cells (Burke and Gerace, 1986), sea urchin eggs (Cameron and Poccia, 1994) or Drosophila embryos (Berrios and Avilion, 1990). The most widely used system, however, is based on amphibian eggs. The first amphibian cell-free system described derived from *Rana pipiens* eggs (Lohka and Masui, 1983) but the most common source of eggs till now remains *Xenopus laevis* (Lohka and Maller, 1985).

Fully grown *Xenopus* oocytes are physiologically arrested in first meiotic prophase. Upon exposure to progesterone oocytes complete meiotic maturation, undergoing breakdown of the NE, chromosome condensation and spindle formation, and arrest in the second meiotic metaphase. Frogs are then induced by gonadotropin to lay eggs, which under natural conditions are fertilised immediately. Upon fertilisation the NE of the sperm breaks down, chromatin decondenses and a new NE is assembled to form the male pronucleus using precursors stored in the egg cytoplasm. This procedure of pronuclear formation can be mimicked *in vitro* using egg extracts in which egg chromosomes have been removed after centrifugation. Since *Xenopus* oocytes contain stockpiles of nuclear components like histones, nuclear membrane components, nuclear pores and enzymes, derived egg extracts can support many rounds of nuclear assembly around exogenously added protein-free DNA. *Xenopus* and human sperm, and lambda DNA have been successfully used as templates for the assembly of intact nuclei in *Xenopus* egg extracts (Lohka, 1998).

Xenopus cell-free extracts present several advantages over other systems. They are easy to maintain and give rise to many eggs that can support the assembly of many nuclei, around a wide variety of exogenously added DNA. In contrast mammalian cells give rise to relatively little material and do not store large amount of nuclear components so they can support the assembly of very limited amount of nuclei. The main advantage of mammalian extracts is that they are derived from cells whose nuclear proteins are well characterised as opposed to the *Xenopus* system where many proteins are still not identified (Lohka, 1998). Still, the ease by which *Xenopus* extracts can be manipulated, either through fractionation or through depletion of different components, makes them a powerful tool for the study and dissection of complicated cellular processes.

1.9 Aims of this thesis

The great importance of the nucleus as a cellular organelle is clearly unquestionable. The discovery of NE proteins that are involved in tissue-specific muscular dystrophies is a subject under investigation with still no definite answers. With the ultimate goal to contribute to the understanding of the function of emerin, the INM protein involved in the X-linked form of Emery-Dreifuss muscular dystrophy, this work was conducted with the following aims:

- To investigate the role of different domains of emerin in chromatin decondensation and NE assembly in the *Xenopus* cell-free system. This was achieved by the addition of bacterially expressed and purified emerin peptides, at increasing concentrations, in nuclear assembly reactions.

- To investigate the presence of LEM domain containing proteins, including endogenous emerin, in the *Xenopus* egg system. This was important in order to explain the inhibitory effect of the exogenously added emerin LEM domain, on membrane recruitment to chromatin during the NE assembly.

- To identify new binding partners of emerin that could provide an explanation for the inhibitory effect of the emerin LEM domain on chromatin decondensation and NE assembly. This was achieved by co-precipitation experiments using emerin peptides as the bait and the *Xenopus* cytosol as the source of interacting proteins.

- As a result of identifying β-tubulin as an emerin interacting protein, the final aim of this work was to investigate the involvement of emerin in the organisation of the microtubule network. This was achieved by investigating whether the absence of emerin in X-EDMD cells affects cytoskeletal microtubules.

CHAPTER 2

MATERIALS AND METHODS

2.1 Expression, extraction and purification of human emerin constructs

Four DNA constructs encoding human emerin amino acids 1-70, 1-176, 73-180 and 1- 220 were kindly provided by Dr Ryszard Rzepecki. The constructs were provided cloned into vectors pET29b, which add a His-tag to the C-terminus of the expressed proteins, and were used to transform *Escherichia coli* Tuner (DE3) pLysS cells. The bacterially expressed proteins were extracted and purified under both, native and denaturing conditions.

2.1.1 Preparation of competent bacteria and transformation with emerin DNA

Competent Tuner (DE3) pLysS cells were prepared using a rubidium chloride method (Ano and Shoda, 1992). Bacteria were grown overnight in LB-Agar plates (10 gr/lt tryptone, 5 gr/lt yeast extract, 10 gr/lt NaCl, 2% agar) containing 15 μg/ml Kanamycin and 34 μg/ml Chloramphenicol (Sambrook *et al.*, 1989). Next day a single colony was inoculated in 2.5 ml of LB at 37°C, overnight, shaking at 225 rpm. The entire overnight culture was transferred the following day to 250 ml LB containing 20 mM $MgSO_4$ and inoculated till OD_{600} 0.4-0.8. Cells were collected by centrifugation at 4500g for 5 minutes at 4°C and pellets resuspended in 50 ml of buffer TFBI (30 mM NaOAc, 10 mM $CaCl_2$, 50 mM $MnCl_2$, 100 mM RbCl, 15% glycerol, pH 5.8), incubated for 5 minutes at 4°C and collected by centrifugation at 4500g for 5 minutes at 4°C. Pellets were resuspended in 10 ml of buffer TFBII (10 mM MOPS, 75 mM $CaCl_2$, 10 mM RbCl, 15% glycerol, pH 6.5). Cells were incubated on ice for 15-60 minutes, aliquoted into 100 μl, snap frozen in liquid N_2 and stored at -80°C.

Competent *E. coli* cells were transformed with emerin DNA encoding for amino acids 1-70, 1-176, 73-180 and 1-220. For each transformation reaction 100 µl of competent cells were mixed with 1 µl of DNA and incubated on ice for 30 minutes. Bacteria were heat shocked at 42°C for 1 minute and returned to ice, where 400 µl of LB was added. Cells were incubated at 37°C for 1 hour and 100 µl of each reaction mix were plated onto LB-Agar plates containing Kanamycin (15 µg/ml) and Chloramphenicol (34 µg/ml). Plates were incubated overnight at 37°C. A single colony was picked next day and inoculated overnight (at 37°C) into 5 ml LB including the appropriate antibiotics. The overnight culture was divided into 1 ml aliquots, 30% sterile glycerol was added and bacteria were stored at -80°C.

2.1.2 Protein expression

For protein expression a sterile loop was used to pick transformed bacteria from frozen glycerol stocks. Bacteria were inoculated overnight at 37°C in 5 ml LB medium containing 15 µg/ml Kanamycin and 34 µg/ml Chloramphenicol. The 5 ml overnight cultures were transferred next day to 500 ml of LB medium containing Kanamycin and Chloramphenicol at the same concentrations, and grown for about 4 hours up to OD 0.4-0.8. Bacteria were induced with 1 mM isopropyl-β-thiogalactoside (IPTG), grown for another 4 hours and, finally, collected by centrifugation at 5000g for 10 minutes. Pellets were stored overnight at -22 °C.

2.1.3 Protein extraction

For native purification, overnight pellets were suspended in 20 ml of Basic Buffer (100 mM NaH_2PO_4/10 mM Tris pH 7.8) containing 0.1% Tween 20 and 10 mM

Imidazole, and bacteria were sonicated three times for 30 sec, with 1 min intervals, on ice. The lysate was centrifuged at 10,000g for 30 minutes at 4°C, the supernatant (Supernatant 1) was collected and the pellet was extracted with 10 ml of Basic Buffer containing 1% Triton X-100. After a further centrifugation at 12,000g for 10 minutes at 4°C the supernatant (Supernatant 2) was removed and any insoluble material collected as a pellet was solubilised with 10 ml of Basic Buffer containing 8 M Urea (Supernatant 3). Aliquots of all supernatants were collected for SDS-PAGE analysis and the rest was stored at -80°C until use for protein purification.

For purification under denaturing conditions, bacteria pellets were suspended in 15 ml of 1xBasic Buffer/8 M Urea/10 mM Imidazole and incubated for 1 hour at room temperature for the pellet to solubilise completely. All solubilised proteins were collected as the supernatant (Supernatant 4) after a centrifugation at 10,000g for 30 minutes at room temperature and used directly for purification.

2.1.4 Protein purification

Purification of all emerin constructs was performed using the Ni-NTA Superflow of Qiagen (Catalog number 30410). This product consists of nickel-nitrilotriacetic acid (Ni-NTA) coupled to Superflow resin, which is highly cross-linked 6% agarose. The resin is provided as a suspension in 30% ethanol and has a binding capacity of 5-10 mg/ml of any protein tagged with six consecutive histidines.

As starting material for the purification of constructs extracted under native conditions, Supernatants 1 and 2 of the extraction procedure were combined. A 1 ml bead volume, which was pre-washed with an equal volume of Basic Buffer containing 10 mM Imidazole was added to the protein extract. The sample was

incubated for 30 minutes at 4°C on a roller and then poured into an empty PD-10 column. After the beads settled at the bottom of the column and the flowthrough was collected, non-specific binding was removed by washing with 50 ml of Basic Buffer containing 300 mM NaCl and 20 mM Imidazole, pH 8.0. The His-tagged protein constructs were eluted with 6 ml of Basic Buffer containing 300 mM NaCl and 250 mM Imidazole pH 8.0. 1 ml elution fractions were collected. A small aliquot of all steps was removed for SDS-PAGE analysis and for determination of protein concentration by the Bradford microassay procedure. The rest was snap frozen in liquid nitrogen and stored at -80°C. The elution fraction of each construct with the highest protein concentration was later thawed, dialysed against Modified Extraction Buffer (MEB) (25 mM potassium gluconate, 10 mM hemi-magnesium gluconate, 20 mM Hepes pH 7.5, 300 μM PMSF, Protease Inhibitor Cocktail at 1:100 dilution) for 3 hours with 3 buffer changes using the Microdialyser system by Pierce. Dialysed elution fractions were divided into 20 μl, snap frozen in liquid nitrogen and stored at -80°C.

For purification of proteins under denaturing conditions the same procedure was used with the only differences being that all incubations and buffers were at room temperature rather than 4°C and all buffers included 8 M Urea and had no NaCl. After purification denatured peptides were refolded by dialysing against MEB for 3 hours with 3 buffer changes using a Microdialyser (Figure 2.1).

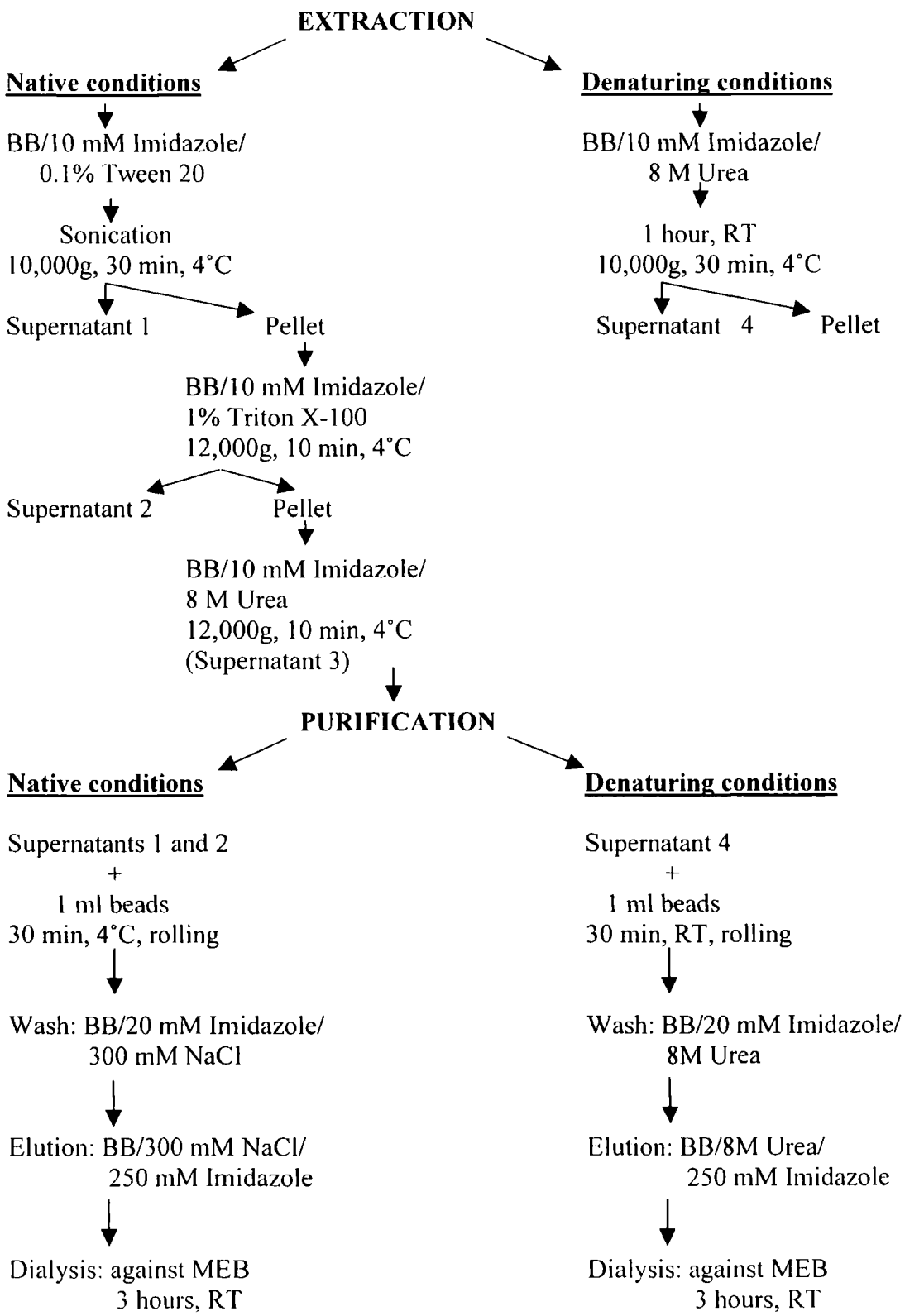

Figure 2.1: A summary of the extraction and purification procedure of emerin peptides 1-70, 1-176, 1-220 and 73-180.

2.1.5 Determination of the molecular weight and molarity of emerin samples

The molecular weight of the emerin peptides was calculated in two ways: one according to their electrophoretic mobility on SDS gels and another according to their amino acid composition.

For the calculation of the apparent molecular weights according to the migration on SDS gels the UVI Band software was used. This software allows selection of specific bands and calculation of their molecular weight in kDaltons provided that a set of markers with known molecular weights is used in parallel.

For the calculation of the molecular weights according to the amino acid composition the ProtParam tool by ExPASy was used, which is found in the following website: http://us.expasy.org/tools/protparam.html. The ProtParam tool allows the computation of various physical and chemical parameters, including the molecular weight, for a sequence entered by the user.

The molarity of all emerin samples was calculated using the following formula:

$$\frac{\text{Concentration in mg/ml}}{\text{Molecular weight in Daltons}}$$

For the molarity calculations, the values used were the concentrations of the dialysed samples (by Bradford) and the molecular weights as calculated with the ProtParam tool.

2.1.6 Determination of protein concentration using the Bradford Microassay.

All protein concentrations were determined using the Bio-Rad Protein Assay, which is based on the differential colour change of the dye Coomassie Brilliant Blue G-250 in response to various protein concentrations. For the Microassay procedure 800 µl of bovine serum albumin (BSA) standards and diluted samples were added to 200 µl of concentrated dye and absorbance was checked at 595 nm. For the standard curve a stock solution of 5 mg/ml of BSA was used to prepare several dilutions ranging from 0 to 50 µg of protein per ml. The BSA standards were prepared as following:

Sample No	**1**	**2**	**3**	**4**	**5**	**6**
BSA (µl)	0	1	2	4	8	10
H_2O (µl)	800	799	798	796	792	790
Dye Concentrated (µl)	200	200	200	200	200	200
Protein (µg)	**0**	**5**	**10**	**20**	**40**	**50**

All OD_{595} readings of the BSA standards were plotted against the amount of protein in µg and a line-of-best-fit with the equivalent equation was applied to the chart. All samples with unknown protein concentrations were prepared by adding 10 µl of each sample to 790 µl of H_2O. 200 µl of concentrated dye was added to the mixture and the OD_{595} was measured. As blank 800 µl of H_2O were used with 200 µl of dye. The amount of µg contained in the 10 µl of each sample was then calculated using the equation displayed on the standard curve ($y = 29.173x$, where x is the OD_{595} and y is the amount of µg in question). To find the concentration of each sample in µg/µl µg values were divided by 10.

2.2 Cell-free *Xenopus* egg extracts

2.2.1 Preparation of unfractionated *Xenopus* egg extract (LSS)

For the preparation of *Xenopus* egg extracts a method described by Hutchison CJ (1993) was used, originally adapted from Lohka M and Maller J (1985). Female frogs were induced to lay eggs by injection of two hormones: Pregnant mares'serum gonadotropin (PMSG, Intervet Ltd) was injected into the dorsal lymph sack, at a concentration of 50 iu/frog, a week before collection of eggs, and Human chorionic gonadotropin (Chorulon, Intervet Ltd), at 500 iu/frog, the day before egg collection.
At the day of preparation, eggs were collected in a 110 mM NaCl solution. Eggs of different frogs were kept in separate beakers in order to avoid contamination of good with bad quality eggs. Bad quality eggs, usually laid in strings and lacking the normal dark-and-white hemisphere appearance, were carefully discarded.

As a first step, the jelly coat of the eggs was removed by replacing the saline tap-water with 500 ml of dejelly solution (110 mM NaCl, 20 mM Tris-HCl pH 8.5, 1 mM DTT). Eggs were left in the dejelly solution, avoiding vigorous mixing, for 5-7 minutes. Eggs were then washed three times in large volumes (2 lt) of saline tap-water followed by three washes in ice-cold Extraction Buffer (EB) (100 mM KCl, 5 mM $MgCl_2$, 20 mM Hepes pH 7.5, 2 mM 2-mercaptoethanol). Necrotic eggs, usually white in appearance, were removed during the washing procedure.

Eggs were subsequently packed in centrifuge tubes in a minimal amount of buffer and centrifuged at 10,000g, for 10 minutes, at 4°C in a swinging-bucket rotor.

Centrifugation resulted in crushing of the eggs and formation of three layers: a yellow lipid cap on top, a middle ooplasmic layer and a grey pellet containing yolk, pigment granules and egg cortices. The middle ooplasmic layer was carefully removed by side puncture with an 18G needle attached to a syringe and transferred to a clean centrifuge tube. The extract was supplemented with Protease Inhibitor Cocktail (Sigma P8340, used at 1:100) containing the following inhibitors: AEBSF 104 mM, Aprotinin 0.08 mM, Leupeptin 2 mM, Bestatin 4 mM, Pepstatin A 1.5 mM and E-64 1.4 mM. Cytochalasin B was also added to a final concentration of 50 μg/ml, and the extract was centrifuged again at 10,000g, for 10 minutes, at 4°C. After the second centrifugation the middle ooplasmic layer was again removed by side puncture. Finally, 5% glycerol was added and the egg extract was snap frozen in liquid nitrogen in 15 μl droplets and stored at -140°C. Since this type of unfractionated extract is prepared by centrifugation at 10,000g, it is also called Low Speed Supernatant (LSS).

2.2.2 Fractionation of LSS into membrane and cytosolic components

Fractionation of LSS into membrane and cytosolic parts was achieved by high-speed ultracentrifugation as described by Lohka MJ (1998). Specifically, LSS was prepared as described above but after the second 10,000g centrifugation, the ooplasmic layer was transferred into 2 ml TLS-55 tubes and centrifuged at 200,000g, for 75 minutes in an Optima TLX table-top ultracentrifuge (Beckman Instruments Inc.). After the centrifugation the extract was fractionated into four main layers: a yellow lipid cap on top followed by a broad layer called S_{200}, a loosely packed layer of membranes called NEP-A and a pellet of yolk, glycogen and pigments. The layer containing the NEP-A membranes was carefully removed by side puncture with an 18G needle and mixed

with an equal volume of Modified Extraction Buffer (MEB) containing 60% sucrose. The NEP-A fraction was then aliquoted into 100 µl, snap frozen in liquid nitrogen and stored at -140°C. The S_{200} was also removed by side puncture and transferred to a new 2 ml TLS-55 tube and centrifuged at 200,000g for 4 hours at 4°C. This centrifugation step resulted in four fractions: a thin lipid cap on top, a clear supernatant which corresponds to the cytosol, a membrane layer called NEP-B and a pellet containing glycogen and ribosomes. The cytosolic and NEP-B layers were removed by side puncture. The cytosol was divided into 100 µl aliquots and snap frozen, whereas the NEP-B was first mixed with an equal volume of Modified Extraction Buffer containing 60% sucrose and then aliquoted in 100 µl. All aliquots were stored at -140°C.

2.2.3 *Xenopus* sperm preparation

Demembranated *Xenopus* sperm heads were used as a template in all nuclear assembly reactions. Sperm preparation was as described in Hutchison CJ (1993). Testes were isolated from male frogs and put on glass petri dish where any fat and connective tissue was carefully removed. Testes were then transferred to another petri dish containing 3 ml of Barth X buffer (88 mM NaCl, 2 mM KCl, 0.33 mM $Ca(NO_3)_2$, 0.41 mM $CaCl_2$ and 0.82 mM $MgSO_4$) and chopped into small pieces with a dissection scissors. All small pieces were finally homogenised gently with a loose-fitting glass pestle. After removal of any particulate material 10% DMSO and newborn calf serum (NCS) were added to the sperm suspension, which was then divided into 0.5 ml aliquots, containing approximately 5 x 10^6 sperms each. Each aliquot was subsequently diluted to 3 ml with SuNaSp buffer (0.25 M sucrose, 75

mM NaCl, 0.5 mM spermidine and 0.5 mM spermine) and the sperm was recovered in a pellet by centrifugation at 3000g for 15 minutes at room temperature. The pellet was then resuspended in 200 µl of SuNaSp and the number of sperms was determined using a haemocytometer. Sperm was stripped of the plasma membrane and nuclear envelope by addition of 40 µl of 1 mg/ml lysolecithin (phosphatidylcholine) and gentle agitation at room temperature for 90 minutes. The reaction was terminated by the addition of 3 ml of ice-cold SuNaSp containing 3 mg/ml BSA, and the sperm was recovered by centrifugation at 3000g for 15 minutes. Finally, the sperm was resuspended in SuNaSp to a final concentration of 5 x 10^4/µl, aliquoted in 5 µl, snap frozen in liquid nitrogen and stored at -140°C.

2.3 Nuclear assembly using the *Xenopus* cell-free system

All nuclear assembly experiments were performed using unfractionated egg extract (LSS) that was rapidly defrosted at room temperature. Typical assembly reactions for immunofluorescence included 25 µl egg extract and demembranated sperm at a final concentration of 10^3/µl. For immunoblotting analysis 100 µl of egg extract and 10^3/µl of *Xenopus* sperm were used. Nuclei were fully assembled after 80 minutes incubation at room temperature (21°C). All reactions were supplemented with an energy generating system that consisted of Adenosine Triphosphate (ATP), Phosphocreatin (PC) and Creatine phosphokinase (CPK). ATP was prepared as a 200 mM solution in 10 mM Hepes (pH 7.2) containing 1 mM DTT, and used at a 1:100 dilution. PC was prepared as a 1 M solution in 10 mM Na phosphate (pH 7.4), and used at a 1: 50 dilution. Finally, 0.5 mg/ml of CPK in 50% Glycerol /10 mM Hepes (pH 7.5) were prepared and used at a 1:100 dilution.

2.3.1 Time-course study of nuclear envelope assembly

The steps of nuclear envelope assembly in *Xenopus* egg extract were studied by a time-course experiment. Specifically, five reactions were set up, as described above, and incubated at room temperature for 0, 10, 20, 40 or 80 minutes. For fixation, 175 µl of EGS (ethylene glycol bis-(succinic acid N-hydroxysuccinimide ester)) were added to each sample, which was then incubated at 37°C for 30 minutes and kept on ice till all reactions had finished. To isolate chromatin, 100 µl of each sample were loaded onto 300 µl SNIB (60 mM KCl, 15 mM Tris pH 7.5, 15 mM NaCl, 1 mM β-mercaptoethanol, 0.15 mM spermine, 0.5 mM spermidine) containing 30% Sucrose and centrifuged at 4000g for 10 minutes. Coverslips were then processed by immunofluorescence using antibodies specific for nucleoporins (antibody 414, 1:100 dilution), for NEP-A vesicles (antibody CEL13A, undiluted), NEP-B vesicles (antibody 4G12, undiluted) or emerin (antibody aE70, undiluted).

2.3.2 Effect of emerin constructs on nuclear envelope assembly

To test the effect of emerin on nuclear envelope assembly, each bacterially expressed construct was added to a typical nuclear assembly reaction at a 0.5 µM, 4 µM or 8 µM concentration. Nuclei were allowed to assemble at room temperature for 80 minutes. 100 µl of each sample were layered over 300 µl of SNIB/30% sucrose in cytology chambers and centrifuged at 4000g for 10 minutes onto coverslips, which were processed by indirect immunofluorescence with antibodies specific for FG-repeat nucleoporins (414), pre-pore nucleoporins (Nup107), NEP-A vesicles (CEL13A) and NEP-B vesicles (4G12). Chromatin was visualised by DAPI mounted in Mowiol.

For immunoblotting analysis, 100 µl of samples were diluted up to 1 ml with ice-cold Extraction Buffer and layered over 500 µl of SNIB/30% Sucrose in eppendorf tubes. Nuclei were pelleted at 4000g for 10 minutes. Pellets were suspended in 10 µl 1x SDS-sample buffer, boiled, analysed by SDS-PAGE and immunoblotted with antibody 414.

2.4 Chromatin binding ability of emerin

To check the chromatin binding ability of emerin by immunofluorescence, the four protein constructs were incubated individually with either condensed or decondensed *Xenopus* sperm chromatin for 15-30 minutes at RT and fixed with 4% formaldehyde at 4 °C for 10 minutes. Samples were loaded onto cushions containing 300 µl SNIB/30% sucrose and centrifuged at 4000g for 10 minutes. Coverslips were removed from the cushions and processed by indirect immunofluorescence. The NCL-Emerin antibody (1:30 diluted in PBS containing 1% NCS) was applied for 1 hour at RT. Coverslips were washed five times in 1x PBS and stained with FITC-Donkey anti- Mouse (1:50 dilution) for 1 hour, at RT. After a final wash in 1x PBS, DNA was stained with DAPI and slides were stored at 4 °C.

2.4.1 Sperm decondensation

When decondensed sperm was used, decondensation was achieved by incubating sperm chromatin with Pfaller buffer (250 mM sucrose, 50 mM KCl, 2.5 mM $MgCl_2$, and 10 mM Hepes/NaOH pH 7.4) containing Poly-Glutamic acid at a concentration of 2 µg/µl, for 30 minutes at RT.

2.5 Cell culture

The following cell lines were used in this work: normal Human Dermal Fibroblasts (HDF), fibroblasts from four patients with X-linked EDMD (X-EDMD 1, 2, 3 and 4 cells), and two cell lines derived from *Xenopus laevis*, XTC and XLK cells, which are *Xenopus* tadpole and *Xenopus* kidney cells, respectively. *Xenopus* cell lines were maintained at room temperature in L-15 medium (Sigma). Human cell lines were grown in Dulbecco's modified Eagle's medium (DMEM) supplemented with 10 units/ml penicillin, 50 µg/ml streptomycin and 10% v/v NCS, and maintained at 37°C in a humidified atmosphere containing 5% CO_2 until 70-80% confluence. Serial passage was performed in the presence of trypsin and 0.5% EDTA.

2.6 Gel electrophoresis and Immunoblotting

2.6.1 1-Dimensional gel electrophoresis

Electrophoretic analysis of proteins was performed under reducing conditions (Laemmli, 1970) using the Protean II minigel system of BioRad. Samples were mixed with an equal volume of 2x SDS-sample buffer (125 mM Tris-HCl, pH 6.8, 2% SDS, 100 mM DTT, 5% Glycerol and 0.2% of Bromophenol blue), heated at 95°C for 3 minutes and resolved on gels at 100 Volts in Tank Buffer (25 mM Tris, 250 mM Glycine and 0.1 % SDS). Depending on the size of the proteins of interest resolving gels of 8% to 15% were used for higher resolution in the upper or lower part of the gel, respectively.

2.6.2 2-Dimensional gel electrophoresis

All protein samples analysed by 2-D gel electrophoresis were precipitated in 5 volumes of ice-cold acetone overnight at -22°C. Proteins were collected by centrifugation at 14,000 rpm for 3 minutes and pellets were suspended in 125 µl of Lysis Buffer (8 M Urea/ 2 M Thiourea/ 4% CHAPS) and incubated for 2 hours at room temperature for the pellet to solubilise completely. Samples were then prepared for electrophoresis in the following sample buffer:

1 µl of Bromophenol blue
2.5 µl of Pharmacyte ampholytes
5 µl of 1M DTT
116.5 µl of protein sample
Total volume: 125 µl

Samples were vortexed, centrifuged for 5 minutes at 13,000 rpm and dispensed into a loading tray. Isoelectric focusing gel strips of pH 4-7 were layered over each sample, carefully to avoid formation of air bubbles, overlaid with paraffin oil and left for 12-24 hours at room temperature to re-hydrate. Next day, the gels were rinsed in ddH_2O, placed on a 2-D electrophoresis apparatus and run in three stages for 6500 Volt hours. After isoelectric focusing the gels were rinsed in ddH_2O and incubated in Equilibration Buffer (6 M Urea/ 30% Glycerol/ 50 mM Tris pH 8.8/ 10% SDS/0.01% Bromophenol blue) containing 64 mM DTT for 15 minutes. Gels were then incubated in Equilibration Buffer containing 262 mM Iodoacetamide for further 15 minutes with constant agitation, rinsed in 1x Tank Buffer and loaded on top of 12%

acrylamide gels (without the stacking gel). SDS markers absorbed on small Whatman papers were placed on the left side of each gel, which was then immersed with 0.5% agarose and run at 100 Volts.

2.6.3 Coomassie staining

After electrophoresis, gels were either stained with normal Coomassie Brilliant Blue or Colloidal Coomassie. For the simple Coomassie staining, gels were placed directly in the dye consisting of 40% methanol, 10% acetic acid, 0.1% Coomassie Blue G-250 and stained at room temperature overnight with constant agitation. Gels were destained with 40% methanol, 10% acetic acid for up to 4 hours with several changes of the solution.

For the Colloidal Coomassie staining, gels were first fixed in a solution consisting of 40% methanol and 10% acetic acid for 1 hour, washed twice in ddH_2O and incubated with the dye overnight with constant agitation. For each gel the dye was prepared by mixing 40 ml of Colloidal Coomassie blue stain (0.1% Coomassie blue G-250, 10% w/v ammonium sulphate, 2% v/v orthophosphoric acid) with 10 ml of methanol. Destaining of the gels required washes with ddH_2O up to 4 hours with several changes.

2.6.4 Silver staining

For silver staining of gels, a method compatible with mass spectroscopy was employed. Gels were fixed after electrophoresis in 40% ethanol/10% acetic acid twice for 15 minutes and sensitised with 0.2% Na thiosulphate/6.8% Na acetate/30% ethanol for 30 minutes with constant agitation. Gels were washed 3 times, for 5 minutes each, with ddH_2O and incubated with 0.25% silver nitrate for 20 minutes. After a brief rinse with ddH_2O proteins were visualised with 2.5% Na carbonate/ 0.04% formaldehyde for 2-5 minutes and development was stopped with 1.46% EDTA for 10 minutes. Gels were finally washed 3 times, for 5 minutes each, with ddH_2O.

2.6.5 Immunoblotting

For immunoblotting analysis after electrophoresis, polypeptides were transferred to nitrocellulose membrane (Protran by Schleicher & Schuell Bioscience) for 1 hour at room temperature or overnight at 4°C in Transfer Buffer (25 mM Tris, 200 mM Glycine, pH 9.2 plus 20% Methanol) at 250 mA. Nitrocellulose membranes were rinsed briefly with Blot Rinse Buffer (BRB) (10 mM Tris, pH 7.4, 150 mM NaCl and 1 mM EDTA) and incubated in BLOTTO (4% milk powder (w/v) in BRB containing 0.1% Tween-20) for 16 hour at 4°C or for 1 hour at room temperature with constant shaking. Membranes were washed three times in BRB/0.1% Tween 20, for 10 minutes each wash and incubated with primary antibodies appropriately diluted in BRB/0.1% Tween 20/1% NCS for 1 hour at room temperature with constant agitation. Membranes were washed again three times for 10 minutes each with

BRB/0.1% Tween 20 and then incubated with the appropriate HRP-conjugated secondary antibody for 1 hour at room temperature. After a final wash of the membranes in BRB/0.1% Tween 20, bands were visualised by enhanced chemiluminescence using ECL reagents (Amersham Life Science) mixed at a ratio of 1:1 v/v.

To perform immunoblotting experiments on normal HDF, X-EDMD fibroblasts, XTC and XLK cell lines, cells were collected at passage 7 in 2 ml ice-cold PBS and centrifuged at 4000 rpm in a bench top centrifuge for 3 minutes at 4°C. Cell pellets were resuspended in 200 µl of CSK buffer (10 mM Pipes-KOH, pH 6.8, 10 mM KCl, 300 mM sucrose, 3 mM $MgCl_2$, 1 mM EGTA, 1.2 mM PMSF) containing 0.5% Triton X-100 and 10 units/ml DNase I and incubated on ice for 7 minutes. Subsequently, 200 µl of 2xSDS sample buffer was added and samples were boiled, resolved by 1-dimensional gel electrophoresis and immunoblotted as described above. For immunoblotting analysis of nuclei assembled in *Xenopus* egg extracts, 100 µl of egg extract was used with 10^3/µl sperm and incubated for 80 minutes at room temperature. Samples were then diluted up to 1 ml with ice-cold Extraction Buffer, layered over 500 µl of SNIB/30% Sucrose and centrifuged at 4000g for 10 minutes. The nuclei containing pellets were suspended in 10 µl 1x SDS-sample buffer, boiled, analysed by 1-D SDS-PAGE and immunoblotted. When fractionated *Xenopus* egg extracts were used, NEP-A, NEP-B and cytosolic samples were mixed with an equal volume of 2x SDS sample buffer and used for 1-D gel electrophoresis and Western blotting.

2.7 Indirect Immunofluorescence

For immunofluorescence analysis of cells, normal HDF, *Xenopus* XTC and XLK cells were grown on 13 mm glass coverslips until 70 –80% confluence, fixed in 3.5% Para-formaldehyde in 1xPBS for 10 minutes, permeabilised by incubation in PBS containing 0.5% Triton X-100 for 5 minutes at 4°C and washed twice in 1x PBS for five minutes at room temperature. For two antibodies only, the β-tubulin and pericentrin antibody, normal and X-EDMD HDF were fixed with ice-cold methanol:acetone (1:1) for 5 minutes at 4°C, washed with 1x PBS and then incubated with the primary antibodies.

For immunofluorescence analysis of nuclei assembled in *Xenopus* egg extracts, after assembly, nuclei were fixed with the cross linking agent ethylene glycol bis-(succinic acid N-hydroxysuccinimide ester) or EGS (50 µl EGS diluted in 5 ml of 1/3 strength of Extraction Buffer) for 30 minutes at 37°C. 100 µl of each sample were then layered over 300 µl of SNIB containing 30% Sucrose in a cytology chamber at the bottom of which a coverslip was attached using wax. Nuclei were centrifuged onto the coverslips at 4000g for 10 minutes. Coverslips were removed by melting the wax on a hotplate, air-dried for 5 minutes and incubated with the primary antibody.

Primary antibodies were applied for 1 hour at room temperature in a humidified chamber, and coverslips were washed 5 times in 1x PBS. Secondary FITC- or TRITC-conjugated antibodies were applied 1 hour at room temperature in the dark and coverslips were washed five times in 1x PBS. Chromatin was visualised with

DAPI mounted in Mowiol (12% Mowiol, Calbiochem, 30% glycerol, 120 mM Tris-HCl, pH 8.5, 2.5% DABCO, 1 μg/ml DAPI).

2.8 Antibodies

A list of all antibodies used in this work is shown in Table 2.1.

2.9 Microscopy

Slides were viewed using a Zeiss Axioplan fluorescence microscope fitted with a 40X and a 100X/1.30 oil immersion Plan-NEOFLUAR lens. Images were collected using a 12 bit CCD camera using the IPLAB Spectrum software.

For imaging of Microtubules in cells confocal laser scanning microscopy was employed. A LMS 510 META (Zeiss) microscope equipped with 40X and 63X/1.10 lens was used. Z-series were collected in Multi-track Mode averaging the background 4 times at a scan speed of 500 lines per minute and a resolution of 1024 x 1024.

All montages were assembled in Adobe Photoshop 6.0.

Antibody	Antigen	Host	IF dilution	IB dilution	Source/Reference
NCL-Emerin	Emerin aa 1-222	Mouse	1:30	1:250	Novocastra Ltd
aE70	Emerin aa 1-70	Rabbit	undiluted	1:250	Dr. Rzepecki R
414	FG-repeat nucleoporins	Mouse	1:100	1:2000	Babco
Nup107	Nup107	Rabbit	1:50	—	Dr. Mattaj I
4G12	p78 on NEP-B	Mouse	—	undiluted	Drummond S *et al.*, 1999
CEL13A	p45 on NEP-A	Mouse	—	undiluted	Lyon C, 1995
LAP12	LAP2β	Mouse	—	1:100	Prof. Foisner R.
Anti-tubulin	β-tubulin	Mouse	1:100	—	Sigma
Pericentrin	pericentrin	Rabbit	1:500	—	Abcam
JOL2	Lamin A/C	Mouse	1:30	—	Dyer *et al.*, 1997
HRP-anti-M/R			—	1:2000	Jackson Immunoresearch Inc.
FITC-anti-M/R			1:50	—	Stratech

Table 2.1: A list of all primary and secondary antibodies used in this work. IF: Immunofluorescence, IB: Immunoblotting.

2.10 Identification of *Xenopus* emerin

2.10.1 Purification of the LAP12 antigen

The antigen recognised by antibody LAP12 on the NEP-A vesicle population was attempted to be identified by affinity chromatography purification by two main approaches, one based on protein G beads and another one based on anti-mouse IgG beads.

For the protein G beads purification a Sepharose 4B Fast Flow (Sigma, Catalog number P3296) column was used prepared with recombinant streptococcal protein G expressed in *E. coli* from which the albumin-binding region has been genetically altered. The beads, which were provided as a suspension in 20% ethanol, were cyanogen bromide activated with a 1 atom spacer arm and a binding capacity of >20 mg human IgG per ml.

The anti-mouse IgG beads were obtained from Calbiochem (Catalog number 121937, 2 ml). This column consisted of beaded agarose matrix, which had 1-2 mg of affinity purified anti-mouse IgG/ml immobilised and was provided as a suspension in PBS containing 0.02% NaN_3.

All purifications were performed in eppendorf tubes where different buffers were added and mixed with the beads by pippeting up and down gently. After each step beads were collected by a slow centrifugation at 500 rpm for 5 minutes at 4°C. The purification involved the following steps:

i. LAP12 binding to the beads: For the purification, 150 µl of beads were transferred in an eppendorf tube and washed four times with 500 µl of 100 mM Na_2HPO_4, pH 6.8 to remove the ethanol. After the final wash 150 µl of the LAP12 antibody were mixed with 150 µl of 100 mM Na_2HPO_4, pH 6.8, added to the beads and incubated for 2 hours at room temperature on a roller. Non-specifically bound antibodies were washed off with 500 µl of 100 mM Na_2HPO_4, pH 6.8 containing 140 mM NaCl. This step was repeated four times.

ii. Incubation with NEP-A extract: 100 µl of NEP-A vesicles where thawed and diluted 1:10 with 1x PBS, pH 7.5 containing 1% Triton X-100 detergent to solubilise membrane bound proteins. In order to investigate the optimum conditions for the antigen-antibody interaction to take place, membranes were also extracted under varying pH conditions and also in presence of detergents other than Triton-X 100. Specifically, NEP-A membranes were extracted with 1x PBS pH 7.5 containing 0.1% SDS or 0.5% Tween 20, and with 1x PBS containing 1% Triton-X 100 at pH 6.5, 7.5 or 8.5. The NEP-A extract was then added to the beads together with Protease Inhibitor Cocktail (1:100) and incubated overnight at 4°C or for two hours at room temperature on a roller. To remove any non-specifically bound material beads were washed three times with 500 µl of 1x PBS/0.1% Triton X-100, two times with 1x PBS/0.1% Triton X-100/0.02% SDS and one time with 1x PBS/0.1% Triton X-100/1 M NaCl.

iii. Elution of antigen-antibody complexes: Antigens that were specifically bound to the antibody were eluted with 250 µl of 50 mM Glycine pH 2.3. This step was repeated four times. 1 ml elution fractions were collected. A small aliquot of each fraction was removed for SDS-PAGE analysis and the rest was snap frozen in liquid

nitrogen and stored at -80°C. Alternatively, elution was attempted with 6 M Urea, with 100 mM Orthophosphoric acid pH 12.5 and with 1.5 M KSCN.

In order to investigate the optimal conditions for the LAP12 antigen purification protein G beads were also used in conjunction with the cross-linking reagent glutaraldehyde. For the IgG beads the cross-linking step with glutaraldehyde was always necessary. In these occasions, after the LAP12 binding step, the beads were incubated with an equal volume of 100 mM Na_2HPO_4 pH 6.8/140 mM NaCl/0.02% glutaraldehyde for two hours at room temperature on a roller. Subsequently, an equal to the beads volume of 1x PBS containing 200 mM ethanolamine, pH 7.5 was added. Beads were incubated with ethanolamine for one hour at room temperature and washed two times with three column volumes of 1x PBS. The rest of the procedure involving addition of NEP-A, washing of non-specific binding and elution, was as described above.

2.10.2 Production and affinity purification of antibody aE70

An antibody against the first seventy amino acids of human emerin was raised in rabbit and kindly provided by Dr Rzepecki. The polyclonal serum was used for further purification of the antibody by affinity chromatography using a HiTrap NHS-activated HP, 1 ml column (Amersham Biosciences). The column consists of highly cross-linked agarose beads with six atoms spacer arms attached to the matrix by epichlorohydrine and activated by N-hydroxysuccinimide (NHS). It is designed for the covalent coupling of ligands containing primary amino groups and it is provided

in 100% isopropanol to prevent deactivation of the NHS groups. The purification of the aE70 antibody involved the following steps:

i. Setting up the column: Just before use the top-cap of the column was removed and a drop of ice-cold 1 mM HCl was applied to avoid air bubbles. The HiTrap luer adaptor was connected to the top of the column and the twist-off end was removed. Isopropanol was washed out by applying 6 ml of ice-cold 1 mM HCl to the column. All buffers were applied using a 10 ml syringe connected to the luer adaptor at the top of the column and at a flow rate of ½ drop/second.

ii. Binding of the antigen to the column: Human emerin peptide 1-70, purified previously on a Ni^{+2}-bead column, was defrosted and dialysed against 2 lt of Standard Coupling Buffer (0.2 M $NaHCO_3$, pH 8.3). Dialysis was performed at room temperature for three hours with three buffer changes, one every hour. The antigen was used at a concentration of 5 mg/ml in a final volume of 1 ml and was injected in the column immediately after the isopropanol was washed out. The column was then sealed and incubated for 30 minutes at +25°C.

iii. Washing and deactivation: A series of washes with Buffer A (0.5 M ethanolamine, 0.5 M NaCl, pH 8.3) and Buffer B (0.1 M acetate, 0.5 M NaCl, pH 4) was used in order to deactivate any excess NHS groups that had not coupled to the antigen and to wash out the non-specifically bound antigens. The buffers were injected in the column in the following order: 6 ml Buffer A, 6 ml Buffer B and 6 ml Buffer A. The column was left for 30 min at room temperature at this stage and the washes continued with the injection of 6 ml Buffer B, 6 ml Buffer A and 6 ml Buffer B. The pH of the column was then neutralised by washing with 10 ml of 10 mM Tris, pH 7.5.

iv. Binding of aE70 antibody to the column: 1.5 ml of the rabbit polyclonal serum was diluted 1:10 in 10 mM Tris, pH 7.5 and applied to the column. The antibody was passed through the column three times at a very slow flow rate to ensure maximum binding.

v. Washing: Non-specifically bound antibody molecules were washed out with 20 ml of 10 mM Tris, pH 7.5 followed by 20 ml of 10 mM Tris, pH 7.5 containing 500 mM NaCl.

vi. Elution: Antibody elution was performed under low and high pH conditions (Harlow and Lane, 1988). Antibodies bound by acid sensitive interactions were eluted with 10 ml of 100 mM Glycine pH 2.5. 1 ml fractions were collected in eppendorf tubes containing 100 µl of 1 M Tris pH 8.0 in order to neutralise the pH of the elution fractions. The column was then washed with 10 ml of 10 mM Tris pH 8.8. Antibodies bound by base sensitive interactions were eluted with 10 ml of 100 mM Triethylamine pH 11.5. Again 1 ml fractions were collected in tubes containing 100 µl of 1 M Tris pH 8.0.

The absorbance of all elution fractions at 280 nm was measured using a spectrophotometer. All elution fractions were dialysed separately against 1x PBS/0.02% NaN_3 overnight at 4°C. Next day elution fractions were further dialysed for 4 hours with two buffer changes and stored separately at 4°C.

2.10.3 Sequence similarity between human and *Xenopus* emerin amino acids 1-70

A nucleotide sequence corresponding to *Xenopus* emerin can be accessed from the National Centre for Biotechnology Information (NCBI at www.ncbi.nlm.nih.gov)

database (Accession Number BG407317). The sequence, which corresponds only to the first 507 nucleotides of emerin, was imported into BioEdit Sequence Alignment Editor, version 5.0.9 and translated. The first 70 amino acids of *Xenopus* emerin were subsequently inserted into BioEdit together with the first 70 amino acids of human emerin and a consensus sequence was created displaying the amino acids that are identical between the two sequences and their position.

2.11 Identification of new binding partners of emerin

2.11.1 Investigation of emerin binding partners in *Xenopus* egg cytosol by co-precipitation experiments.

In order to identify new potential binding partners for emerin the four protein constructs consisting of amino acids 1-70, 1-176, 1-220 and 73-180 were freshly expressed, extracted and purified, as described in section 1, and immediately incubated with cytosol derived from fractionated *Xenopus* egg extract in an Immunoprecipitation procedure. For this experiment, both, emerin peptides purified in their native form and peptides refolded after purification in Urea, were used.

Specifically, for each emerin peptide, immediately after its purification, the protein concentration of each elution fraction was determined using the Bradford microassay procedure, and a volume corresponding to 250 μg was dialysed against MEB for 3 hours at room temperature using the Microdialyser.

Each emerin construct (250 µg protein/50 µl beads) was then allowed to re-bind to Ni^{+2}- beads for 15 minutes at room temperature. The Ni^{+2}- beads prior to emerin binding were washed four times with 200 µl of MEB and incubated with 200 µl of MEB containing 20 mM Imidazole and 1 mg/ml BSA for 15 minutes on a roller in order to reduce any non-specific binding. All co-precipitation steps were performed in eppendorf tubes in a batch method.

Once emerin was bound to the beads 100 µl of *Xenopus* cytosol diluted 1:4 in MEB containing 10 mM Imidazole was added and incubated with the beads for four hours at 4°C on a roller. Beads were subsequently collected and washed two times with 500 µl of MEB containing 100 mM NaCl and 20 mM Imidazole for 15 minutes at 4°C on a roller and one time with 500 µl of MEB containing 250 mM NaCl and 20 mM Imidazole for 15 minutes at 4°C on a roller. Emerin constructs together with any bound cytosolic components were eluted with 100 µl of MEB containing 250 mM NaCl and 250 mM Imidazole. Four elution fractions were collected, pooled together and precipitated by the addition of 1.5 ml of ice-cold acetone for one hour on ice. Samples were centrifuged at 14,000g for 10 minutes, pellets were re-suspended in 40 µl of 1x SDS sample buffer, boiled and analysed by one dimensional SDS-PAGE electrophoresis on 12% and 15% gels. Alternatively, after acetone precipitation samples were centrifuged at 14000g for 10 minutes and pellets were resuspended in 125 µl Lysis Buffer (3 M Urea/2 M Thiourea/4% CHAPS). Samples were incubated with the Lysis Buffer for 2 hours at room temperature till pellets were completely solubilised and processed by 2-D gel electrophoresis. Gels were stained by Colloidal Coomassie overnight or Silver stained.

As a control, Ni^{+2}- beads were incubated with cytosol alone diluted 1:4, in the absence of any emerin construct. Washing, elution and precipitation of elution fractions was performed exactly as described above.

2.11.2 Identification of emerin binding partners by MALDI-TOF Mass Spectrometry

Matrix-assisted laser desorption/ionisation time-of-flight (MALDI-TOF) Mass spectrometry was employed for the identification of emerin binding proteins via peptide mass fingerprinting.

Specifically, 1-D and 2-D gels were carefully examined and any bands or spots that could correspond to emerin interacting proteins were picked from the gel and subjected to trypsin digestion. The trypsin digestion, mass spectrometry and database search for the identification of emerin binding proteins were performed by the staff of the Proteomics facility at the University of Durham.

Tryptic digestion was performed on a ProGest Workstation from Genomic solutions using the standard ProGest long trypsin protocol. Briefly, gel spots were washed in 25 mM bicarbonate buffer and destained and desiccated in concentrated acetonitrile. The gel pieces were rehydrated in 50 mM bicarbonate buffer and the protein spot was reductively alkylated with DTT and iodoacetamide. After several washes in bicarbonate buffer, 200 ng/sample of buffered modified trypsin was added and digestion performed for 8 hours at 37°C. Following digestion the peptide extracts were lyophilised in a vacuum concentrator, resuspended in 10 ml 0.1% formic acid

and introduced into a Voyager DE-STR (Applied Biosystems) mass spectrometer. All MALDI spectra acquired were internally calibrated using the trypsin autolysis peaks 842.5 and 2211.11 m/z present in the spectra. The generated peptide masses for each sample (fingerprints) were then matched to theoretical tryptic digests of proteins from a complete non-redundant human NCBInr database. The database search was performed using the MASCOT (www.matrixscience.com) software at a mass accuracy of 50 parts per million (ppm). During the search oxidised methionines and carbarmidomethyl cysteines were allowed as potential amino acid modifications. All results obtained from a MASCOT search have a MOWSE score assigned to them. The MOWSE score is a molecular weight search algorithm which takes into account the number of peptides that match, the number of fragment ions that match, the accuracy at which they match, and a weighing for large peptide matches (Pappin *et al.*, 1993). For each sample checked the protein with the highest MOWSE score is reported as a positive result.

2.11.3 Investigation of the emerin-profilin interaction by the yeast two-hybrid system

The interaction between emerin and profilin was investigated by the yeast two-hybrid system (Fields and Song, 1989) using full-length human emerin cloned in plasmid pAs2 (prepared by Dr. Alvarez-Reyes M), which contains the Binding domain of GAL4, and plant profilin 2 cloned in plasmid pAct2, which contains the GAL4 Activating domain (kindly provided by Prof. P. Hussey). Yeast strains AH109 and Y187 were used as the recipients for plasmids pAs2 and pAct2, respectively.

2.11.3.1 Yeast transformation

Yeast cells AH109 and Y187 were grown on YPDA-Agar plates (20 g/L Tryptone, 10 g/lt Yeast Extract, 20 g/lt Glucose, 1% Agar, pH 5.8, 0.003% Adenine Hemisulphate) at 30°C for 3 days. One to two large colonies from each plate were inoculated in 10 ml of YPD medium (no agar), in 250 ml sterile flasks, overnight at 30°C with constant agitation at 200 rpm. Next day yeast cells were harvested in a sterile 50 ml Universal tube by centrifugation at 1000g for 3 min, the supernatant was removed, and cells were washed in 50 ml of sterile ddH_20. Cells were then collected by centrifugation and the pellet was resuspended in 1.5 ml of 1x LiTE buffer consisting of 0.4 M Lithium Acetate in TE buffer (10 mM Tris, pH 7.5/1 mM EDTA). Cells were again collected and resuspended in 0.5 ml of 1x LiTE.

Transformation reactions were set up consisting of the following:

100 µl of the LiAc yeast cell suspension
1 µg of plasmid DNA
160 µg of single-stranded salmon sperm
10 µg DMSO
600 µl of 1x PEG/LiTE (as 1x LiTE but using 50% PEG 4000 as the solvent)

The transformation mixture was incubated for 30 minutes at 30°C in a waterbath and cells were heat shocked by transferring them at 42°C in a water bath and incubating them for 30 minutes. Yeasts were collected by centrifugation and the cell pellet was washed with 1 ml of sterile ddH_20. 100 µl of the transformed yeast sample was plated onto the appropriate SD-dropout medium (6.7 g/lt Yeast Nitrogen Base, 20 g/lt glucose, 1% Agar). Transformed AH109 cells were spread onto SD plates

supplemented with 0.74 g/lt –Trp and Y187 cells onto SD plates supplemented with 0.69 g/lt –Leu. Plates were incubated at 30°C for 2–4 days until colonies appeared.

2.11.3.2 Yeast mating and diploid selection

For the mating of transformed AH109 and Y187 cells, 3 colonies from each plate were picked with a sterile tip and suspended separately in 30 µl of sterile ddH_2O (samples E1, E2 and E3 for emerin, and P1, P2 and P3 for profilin). 3 µl of each emerin sample were spotted on a YPDA-A plate and left to dry for a few minutes. 3 µl of each profilin sample was then spotted on top of an emerin sample in the following combinations:

E1 - P1	E2 – P1	E3 – P1
E1 – P2	E2 - P2	E3 – P2
E1 – P3	E2 – P3	E3 - P3

Cells were left to mate for two days at 20°C. To select for the diploids, cells from each combination were picked with a loop and spread separately on SD plates supplemented with –Leu/Trp dropout at 0.64 g/lt. Plates were incubated for 2 days at 30°C.

2.11.3.3 Assessment of emerin-profilin interaction

From each SD –Leu/Trp plate, carrying yeast combinations E1-P1 to E3-P3, a large colony was picked with a sterile tip and suspended in 30 µl of sterile ddH_2O. 3 µl of each combination was then spotted on 2 SD –Leu/Trp, 1 SD –Leu/Trp/His, 1 SD –Leu/Trp/Ade and 1 SD –Leu/Trp/His/Ade plates in the following pattern:

E1 - P1	E2 – P1	E3 – P1
E1 – P2	E2 - P2	E3 – P2
E1 – P3	E2 – P3	E3 - P3

The above combination of plates was necessary in order to investigate the emerin-profilin interaction under both, medium (SD –Leu/Trp/His) and high stringency (SD – Leu/Trp/Ade) conditions, and in order to perform a β-galactosidase assay (SD – Leu/Trp). All plates were left at 30°C for 3 days for the yeast to grow.

2.11.3.4 β-galactosidase assay

To further investigate whether emerin and profilin interact yeast diploids that grew on a SD –Leu/Trp plate were used for a β-galactosidase assay. Plasmid pAs2, containing the DNA-binding domain of GAL4 and emerin, had previously been tested and found negative for auto-activating expression of the reporter gene (Alvarez-Reyes, 2004). For the β-galactosidase assay a sterile Whatman filter was placed on the surface of the plate and left overnight for the yeast to adhere to the filter. Next day the filter was removed, submerged in liquid N_2 for 5 seconds and placed on an empty plate with the yeast colonies facing up. Another filter, pre-soaked in 2 ml of Z-buffer (11.1 g/lt $Na_2HPO_4 \cdot 2H_2O$, 5.5 g/lt $NaH_2PO_4 \cdot H_2O$, 0.75 g/lt KCl and 0.25 g/lt $MgSO_4 \cdot 7H_2O$, pH 7.0, containing 39 mM β-mercaptoethanol and 0.33 mg/ml X-gal) was then placed on top. The filters were covered and kept at room temperature for the development of blue colour in case of an interaction between the proteins.

2.11.4 Position of Microtubule Organising Centre (MTOC) in normal and X-EDMD cells

The position of the MTOC relative to the nucleus was observed in two normal and four X-EDMD fibroblast cell lines with two antibodies, one against β-tubulin and one against the centrosomal protein pericentrin. Cells were grown till 80% confluence, fixed in ice-cold methanol:acetone (1:1) for 5 minutes at 4°C, washed in 1x PBS and processed by immunofluorescence as described in section 2.7. Cells were observed with a Carl Zeiss live-cell imaging fluorescence microscope.

In the β-tubulin stained cells the position of the MTOC was visible as the brightest stained area from which MTs seemed to emanate towards the cell periphery. For each cell line, 200 cells were observed for the position of the MTOC and scored as 'near' when the MTOC was attached or right next to the nucleus or as 'distant' when the MTOC was positioned far away from the nucleus.

In the pericentrin stained cells centrosomes were clearly visible as circular areas in the cytoplasm. Parallel staining with a lamin A/C antibody (JOL2) allowed the measurement of the exact distance of the MTOC from the nuclear envelopes. For each cell line 200 cells were photographed in total and the closest possible distance from the centre of each centrosome to the nuclear envelope was measured and displayed in μm. The 200 measurements from each cell line were used to calculate the average distance of the MTOC from the nucleus. In order to compare control and X-EDMD cells average distances were displayed in a graph and a paired t-test assuming unequal variances was performed using the excel software. Also, for each

cell line frequency histograms were created to show the distribution of the data. In this case distances were divided in four groups: 0, 0.1-1, 1.1-3.5 and 3.5 and above μm. For each cell line the number of cells featuring MTOCs in the above categories was calculated and displayed on a graph.

CHAPTER 3

INVESTIGATION OF EMERIN FUNCTION USING THE *XENOPUS* CELL-FREE SYSTEM

3.1 INTRODUCTION

Emerin is an inner nuclear membrane protein, which when mutated gives rise to the X-linked form of Emery-Dreifuss muscular dystrophy (X-EDMD). Muscular dystrophies are a large and heterogenous group of disorders characterised by progressive loss of muscle strength and integrity. The majority of them are caused either by mitochondrial defects altering the cell energy generation or by defects in the dystroglycan or sarcoglycan complexes leading to loss of integrity of the muscle membrane (Toniolo and Minetti, 1999).

Emerin was the first nuclear protein that was discovered to be the cause of a muscular dystrophy, X-EDMD (Bione *et al.*, 1994). Surprisingly, although expressed in most human tissues, absence of emerin in EDMD patients selectively affects skeletal and cardiac muscle. Why a defect in a nuclear envelope protein causes muscular dystrophy and why the effect is seen on particular tissues only are questions with still no definite answers.

The majority of X-EDMD cases are caused by mutations which lead to a complete loss of emerin. It seems, thus, that understanding the function of emerin and its interactions under normal conditions is an important step in elucidating the disease mechanism. Recent work has identified several binding partners for emerin. The best characterised interactions so far include lamins A/C (Clements *et al.*, 2000; Vaughan *et al.*, 2001) and a chromatin associated protein called Barrier-to-autointegration factor (Lee *et al.*, 2001; Shimi *et al.*, 2004). Other proposed binding partners include transcription factors GCL (Holaska *et al.*, 2003), Btf (Haraguchi *et al.*, 2004) and

YT521-B (Wilkinson *et al.*, 2003) and structural proteins like nesprins (Mislow *et al.*, 2002; Zhang *et al.*, 2005) and actin (Holaska *et al.*, 2004; Lattanzi *et al.*, 2003).

Based on these interactions, two major hypotheses have been formulated for the function of emerin. One hypothesis suggests that emerin is part of a structural network that connects the nucleoplasm with the cytoplasm and provides structural support to the nucleus. Absence of emerin could lead to the destabilisation or weakening of this complex affecting the mechanical stability of the nuclear membrane. This could have devastating effects on tissues that are under rigorous movements and mechanical stress like skeletal and cardiac muscles. Interactions of emerin with lamins, which form a load-bearing complex in the inner side of the nuclear envelope, and with nesprins, which are large proteins spanning the nuclear envelope and connecting emerin with the cytoskeleton are in support to this model. On the other hand, emerin is proposed to anchor chromatin at the nuclear periphery via its interaction with chromatin protein BAF and detachment of chromatin in X-EDMD cells has been observed (Fidzianska *et al.*, 1998). This, combined with reported interactions with transcription factors like GCL, Btf and YT521-B led to a second hypothesis of emerin as a regulator of gene expression and chromosome organisation.

In the present study, the *Xenopus* cell-free system was employed to investigate the function of emerin. Cell-free extracts derived form *Xenopus laevis* eggs (Lohka and Masui, 1983) faithfully reproduce nuclear assembly *in vitro*. Addition of sperm chromatin in interphase extracts leads to sperm decondensation and formation of nuclei that are indistinguishable from nuclei formed *in vivo*. In general, the process

involves the recruitment and binding of nuclear envelope precursor vesicles to chromatin and vesicle fusion to form a double-layered nuclear envelope followed by NPC and lamina formation.

Fractionation of extracts by centrifugation at 150,000g, for 2 hours results separation of soluble from membrane material and complete nuclear assembly was shown to require both, the cytosolic and membrane components (Lohka and Masui, 1984). Further fractionation including two centrifugation steps at 200,000g, one for 75 minutes and another for 4 hours, revealed that the membrane components consist of two vesicle populations. The two vesicle populations are called NEP-A and NEP-B for Nuclear Envelope Precursor fractions A and B, and have distinct roles in nuclear envelope assembly (Vigers and Lohka, 1991). NEP-B vesicles have the ability to bind chromatin and are involved in the initial targeting of membranes to chromatin. Also the density of NPCs in nuclear envelopes is dependent on the abundance of NEP-B showing a role for them in the assembly of NPCs. Supporting that, an enrichment of some nucleoporins in the NEP-B fraction has been shown. In contrast, NEP-A vesicles do not have the ability to bind chromatin but they can fuse to pre-bound vesicles and are necessary, together with NEP-B and the cytosol, to form a complete nuclear envelope (Vigers and Lohka, 1991; Vigers and Lohka, 1992).

The biochemically and functionally distinct nature of NEP-A and NEP-B vesicles was further analysed by the production of an antibody against NEP-B fraction and by an antibody against LBR (Drummond *et al.*, 1999). While the LBR antibody reacted with a protein contained in NEP-A vesicles only, called LBRx, the NEP-B antibody reacted with a 78 kD protein contained in the NEP-B fraction, which was named

NEP-B78. Nuclear assembly was shown to require both vesicle populations with NEP-B vesicles containing the chromatin binding ability and NEP-A vesicles the fusogenic ability. The vesicle-specific antibodies were also used in nuclear assembly reactions in *Xenopus* egg extracts and in kidney cells (XLK-2). In both cases they showed an ordered recruitment of vesicles around chromatin with NEP-B vesicles appearing earlier than NEP-A vesicles, further confirming the distinct nature of the two populations.

The *Xenopus* cell-free system was considered as an appropriate tool to investigate the function of emerin because it mediates nuclear assembly by distinct steps that have already been characterised (Drummond *et al.*, 1999) and it has been used successfully in the past to study the function of other INM proteins (Gant *et al.*, 1999). In the present study the ordered recruitment around chromatin and distinct nature of nuclear envelope precursor vesicles described by Drummond *et al.*, was confirmed by the use of different antibodies. To investigate the role of different emerin domains in this process, four human emerin peptides consisting of amino acids 1-70, 1-176, 1-220 and 73-180 were expressed in bacteria and purified. Each peptide was added to *Xenopus* nuclear assembly reactions at different concentrations and the effect on nuclear vesicle recruitment and NPC formation was monitored. Finally, the chromatin binding ability of each peptide was tested using condensed *Xenopus* sperm and artificially decondensed *Xenopus* sperm by poly-glutamic acid.

3.2 RESULTS

3.2.1 Time-course study of nuclear envelope assembly in *Xenopus*

Pronuclei formation in *Xenopus* egg extracts was monitored in a time-course manner by immunofluorescence with antibodies that recognise nuclear envelope precursor vesicles and nucleoporins. Nuclei were allowed to assemble for 0, 10, 20, 40 and 80 minutes at room temperature, fixed with EGS for 30 minutes at 37°C, layered over SNIB/30% Sucrose and centrifuged at 4000g for 10 minutes onto coverslips. During nuclear formation, chromatin decondensation was visualised by DAPI and recruitment of FG-nucleoporins by antibody 414 (Figure 3.1). Binding of NEP-B and NEP-A vesicles to chromatin was monitored by antibodies 4G12 and CEL13A, respectively (Figures 3.2 and 3.3).

As shown by the DAPI staining (Figures 3.1, 3.2 and 3.3), in all three cases pronuclear formation proceeded normally, with chromatin undergoing progressive decondensation with time. At 0 minutes *Xenopus* sperm chromatin was found in its characteristic thin and elongated form (panels a), which progressively decondensed (10 and 20 minutes, panels b and c) till it acquired a round shape at 40 minutes (panels d). Longer incubation caused enlargement of the nuclei (80 minutes, panels e).

FG-nucleoporins, as detected by antibody 414, were recruited around chromatin at an early stage of the NE assembly process, at 10 minutes (Figure 3.1 b). The first vesicles that appeared around chromatin belonged to the NEP-B population. Like FG-

nucleoporins, NEP-B vesicles also bound to chromatin, at 10 minutes (Figure 3.2 b), whereas NEP-A vesicles appeared later, at 20 minutes (Figure 3.3 c). At 40 and 80 minutes complete nuclear envelopes could be observed (Figures 3.1, 3.2, 3.3, d and e). The above results confirm, by the use of a different set of antibodies, the sequence reported by Drummond *et al.* according to which NEP-B vesicles appear early around chromatin and are followed by NEP-A vesicles.

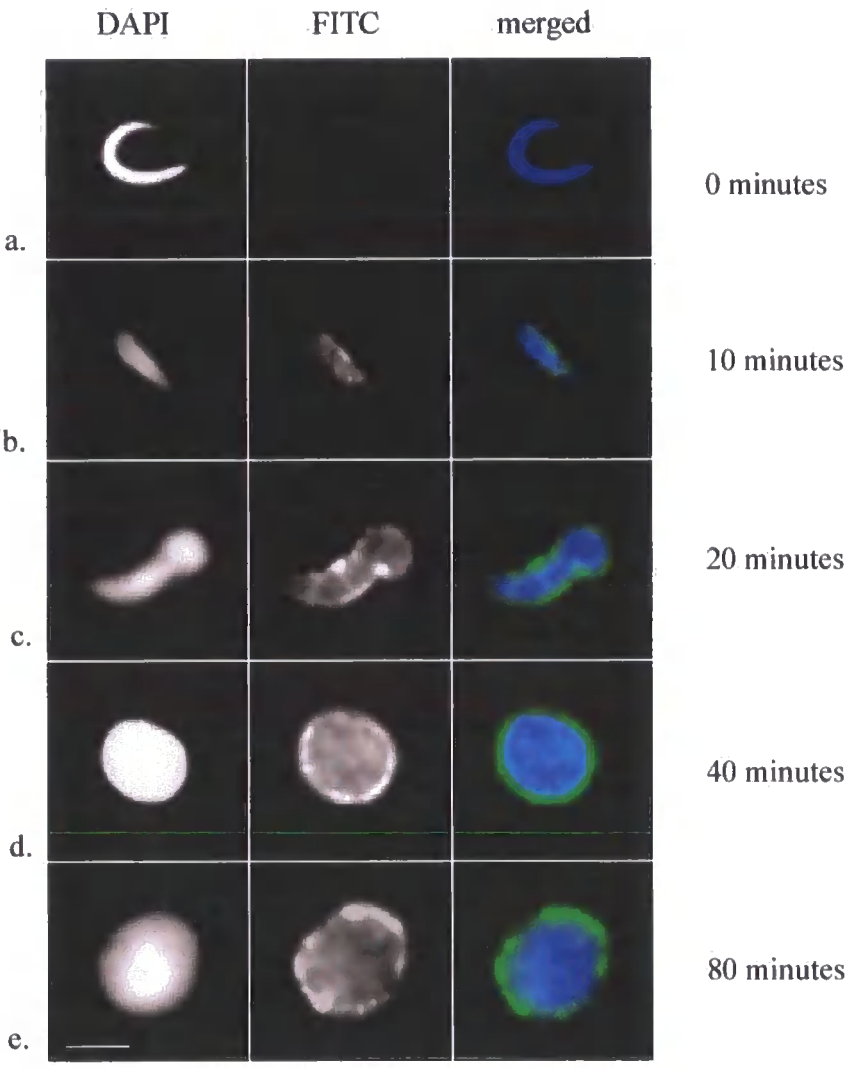

Figure 3.1: NPC formation during nuclear assembly in *Xenopus* egg extracts.

Nuclei were assembled at room temperature and stained at several time points, ranging from 0 to 80 minutes, with antibody 414 (FITC). The first nucleoporins around chromatin were observed at 10 minutes (b). At 20 minutes (c) recruitment of nucleoporins had increased and at 40 and 80 minutes (d and e) a rim staining was observed. Chromatin decondensation was visualised by DAPI. Bar is 10 μm.

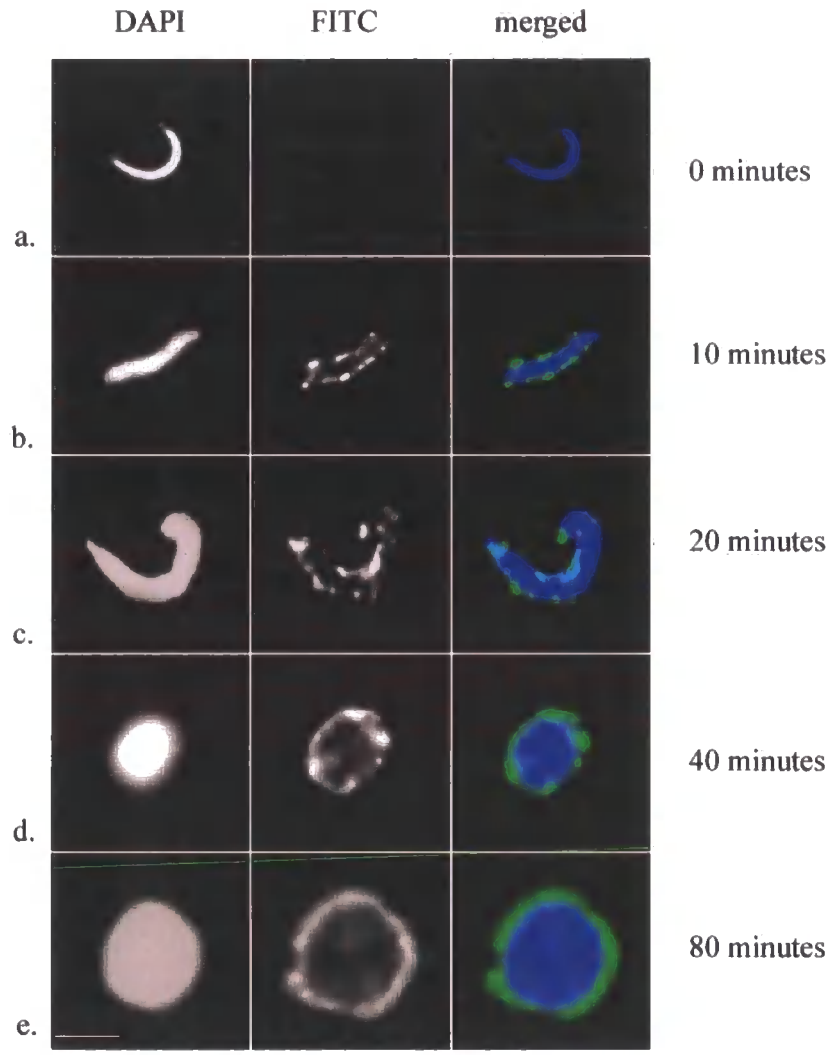

Figure 3.2: Recruitment of NEP-B vesicles to chromatin during nuclear assembly in *Xenopus* egg extracts.

Nuclei were allowed to assemble for 0, 10, 20, 40 and 80 minutes and stained with antibody 4G12 (FITC), which recognises protein NEP-B78. The NEP-B population showed a recruitment pattern similar to that of nucleoporins. The first vesicles appeared around chromatin at 10 minutes (b), an increased staining was observed at 20 and 40 minutes (c and d) and a complete rim staining at 80 minutes (e). Chromatin was visualised by DAPI. Bar is 10 μm.

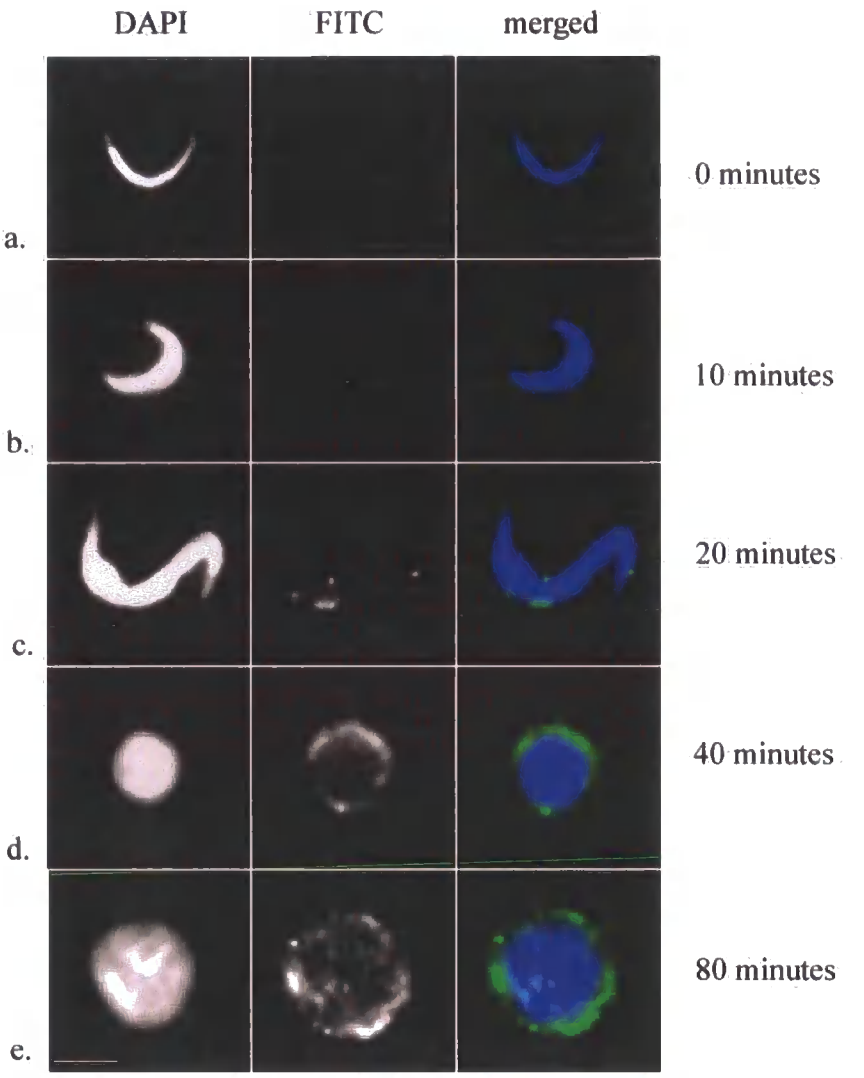

Figure 3.3: Recruitment of NEP-A vesicles to chromatin during nuclear assembly in *Xenopus* egg extracts.

Nuclei were allowed to assemble for 0, 10, 20, 40 and 80 minutes and stained with antibody CEL13A (FITC). As for NPCs and NEP-B vesicles an increased staining with time was observed. However, the first NEP-A vesicles appeared around chromatin at a later stage, after 20 minutes of initiation of nuclear assembly (b). At 40 and 80 minutes a rim staining was observed (d and e). Chromatin was visualised by DAPI. Bar is 10 μm.

3.2.2 Purification of emerin deletion mutants

3.2.2.1 Expression

Human emerin constructs consisting of amino acids 1-70, 1-176, 1-220 and 73-180 contained in pET29b vectors were expressed in bacteria cells for 4 hours after induction with 1 mM IPTG and collected by centrifugation. Bacteria pellets were snap frozen in liquid N_2 and stored at -80°C. A schematic representation of the four peptides is shown in Figure 3.4.

3.2.2.2 Extraction

Bacteria pellets were suspended in Basic Buffer containing 0.1% Tween 20, sonicated and collected again by centrifugation. Pellets were subjected to sequential extractions with Basic Buffer containing 1% Triton X-100 and Basic Buffer containing 8 M Urea. Aliquots of the supernatants after sonication and supernatants after Triton and Urea extractions were analysed by SDS-PAGE (Figure 3.5).

As the figure shows the majority of peptide 1-70 was released in the Sonicate (Figure 3.5 a, lanes 2 and 5) and only a small fraction was released after the Triton and the Urea extraction (Figure 3.5 a, lanes 3-4 and 6-7). For the rest of the peptides, although a considerable amount was released in the Sonicate and the Triton supernatant, the majority was solubilised with Urea (Figure 3.5 b, c and d, lanes 4 and 7).

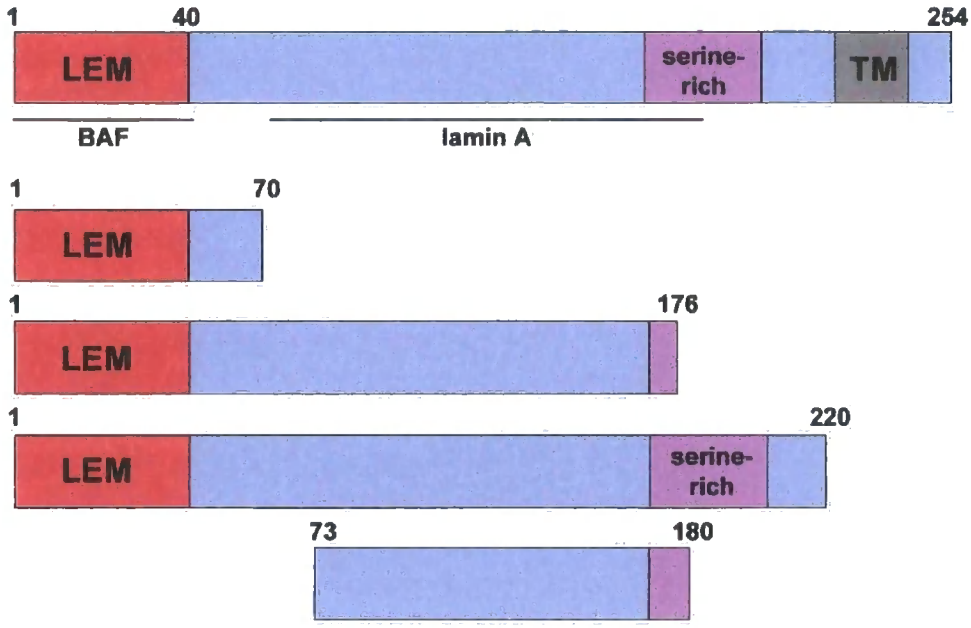

Figure 3.4: A schematic presentation of the four emerin deletion mutants used in this study.

The four emerin peptides consisting of amino acids 1-70, 1-176, 1-220 and 73-180 are shown compared to full-length emerin which is shown at the top. Regions corresponding to the BAF and lamin A binding domains are indicated with bars. Important domains like the LEM domain (aa 1-40), the serine-rich region (aa 170-200) and the transmembrane domain (TM) (aa 223-243) of emerin are also shown.

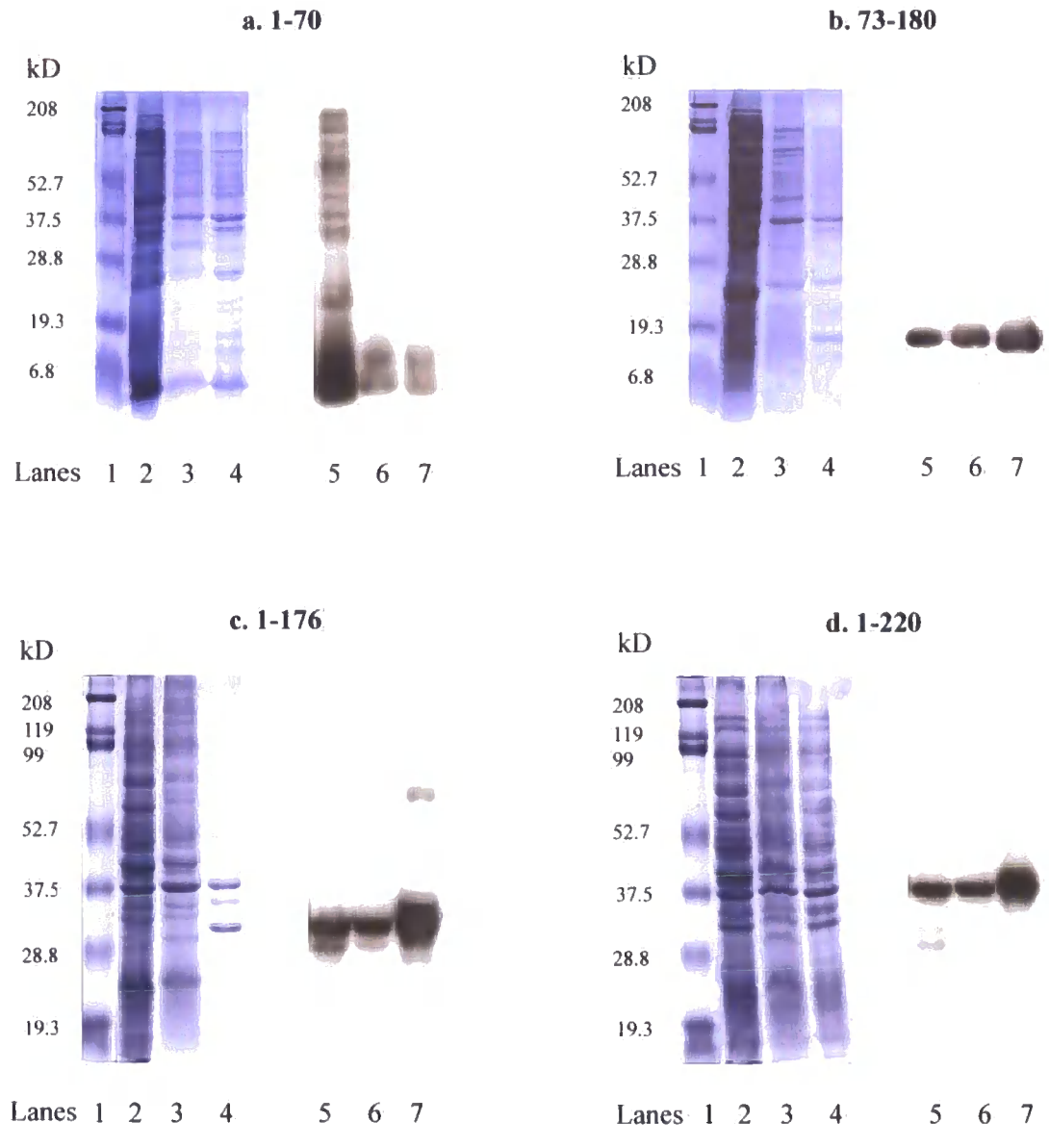

Figure 3.5: Extraction of human emerin peptides 1-70, 73-180, 1-176 and 1-220.

Bacterially expressed emerin peptides were extracted in sequential steps with Basic Buffer in presence of 0.1% Tween 20 (lanes 2 and 5), 1% Triton X-100 (lanes 3 and 6) and 8 M Urea (lanes 4 and 7). Aliquots were analysed by SDS-PAGE and gels were stained with Coomassie (lanes 1-4) or transferred to nitrocellulose and analysed by Immunoblotting with NCL-Emerin antibody (lanes 5-6). Pre-stained markers and their corresponding molecular weights in kD are shown in lanes 1.

3.2.2.3 Purification

Purification of the peptides was performed under native conditions by Immobilised Metal Affinity Chromatography (IMAC), using Ni^{+2}-beads that specifically recognise the histidine-tag. For each peptide supernatants after sonication and Triton extraction were pooled together and incubated with the beads. The flowthrough was collected in order to check whether sufficient binding of all peptides to the column had occurred. Beads were then washed to remove any unbound and non-specifically bound material and peptides were eluted with 6 ml elution buffer. 1 ml elution fractions were collected. Two aliquots of each elution fraction were removed: one for SDS-PAGE analysis and one for determination of protein concentration by the Bradford Microassay procedure.

SDS-PAGE analysis of the elution fractions showed that all peptides were successfully eluted at their expected molecular weight (Figure 3.6) and were mainly concentrated in elution fractions 2 and 3 (lanes 11 and 12). A doublet of proteins of about 70 kD co-purified with all emerin peptides. Mass spectrometric analysis (as described in Chapter 5) identified one as a member of the *E. coli* Heat Shock Protein family (HSP70) (Figure 3.6, lanes 3-8).

For each protein construct the elution fraction with the highest protein concentration was dialysed against Pfaller buffer using the microdialyser system, aliquoted in 20 µl, snap frozen in liquid nitrogen and stored at -80°C till further use.

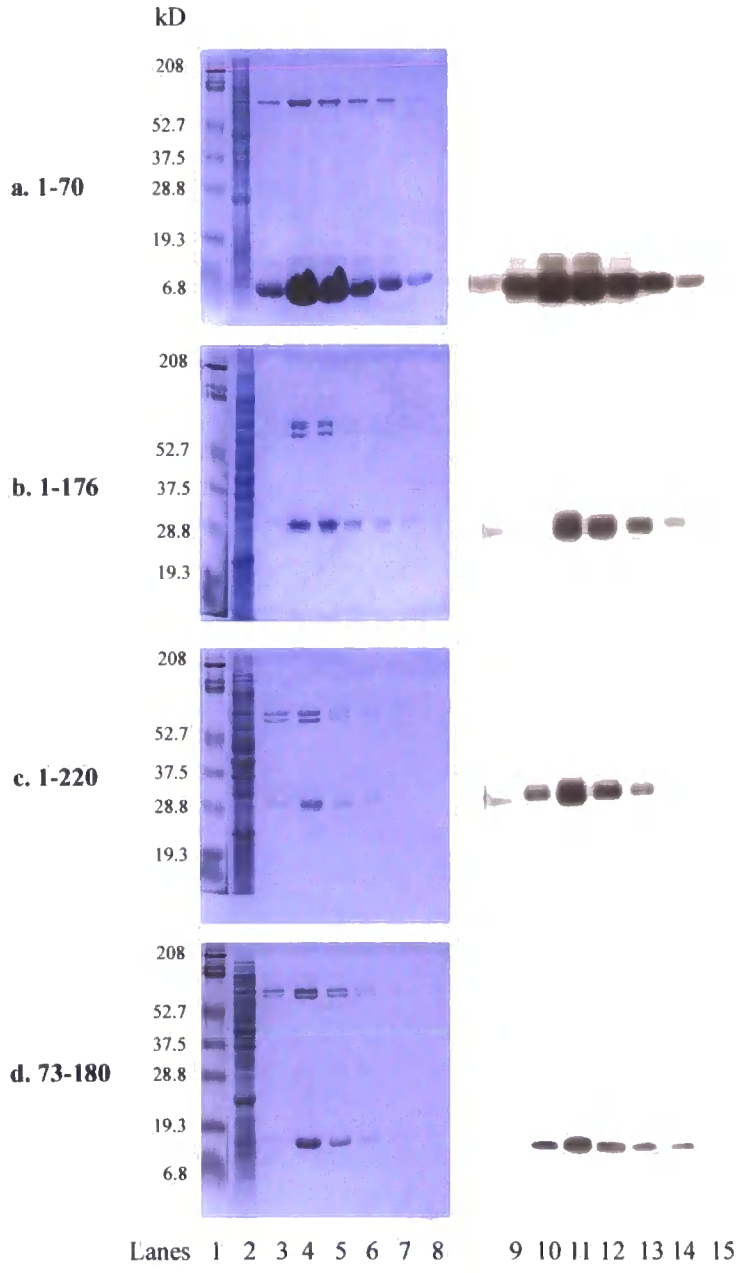

Figure 3.6: Purification of emerin peptides 1-70, 1-176, 1-220 and 73-180.

All emerin peptides were purified in their native conformation by affinity chromatography. 6 elution fractions were collected and aliquots analysed by SDS-PAGE. Gels were stained with Coomassie (lanes 1-8) or Immunoblotted with antibody NCL-Emerin (lanes 9-15). Lanes 3-8 and 10-15 correspond to elution fractions 1-6. The collected flowthrough for each peptide is shown in lanes 2and 9. Markers and the molecular weights corresponding to them are shown in lanes 1.

3.2.2.4 Determination of the molecular weight of the emerin peptides

To calculate the molecular weight of the emerin peptides according to their electrophoretic mobility, all peptides were resolved on a 15% SDS gel and detected by Immunoblotting with an emerin specific antibody (NCL-Emerin by Novocastra). The UVI band software was then used to divide the blot in five lanes: Lane 1 for the markers and lanes 2, 3, 4 and 5 for emerin 1-70, 73-180, 1-176 and 1-220, respectively (Figure 3.7). The bands corresponding to the markers and emerin peptides were selected. After a molecular weight value in kD was assigned to each marker band, the software calculated and displayed a value for each emerin peptide (in kD). The relative molecular weights (Mr), as calculated by the software, for emerin 1-70, 73-180, 1-176 and 1-220 were 8.773 kD, 13.090 kD, 29.478 kD and 30.104 kD, respectively.

The molecular weights of the emerin peptides were also calculated based on their amino acid composition. The four sequences were entered in the ProtParam website of ExPASy (http://us.expasy.org/tools/protparam.html) which returned the following values for the peptides:

Emerin 1-70: 8018.8 Daltons

Emerin 73-180: 12446.3 Daltons

Emerin 1-176: 20204.8 Daltons

Emerin 1-220: 24898.9 Daltons

The above results are in agreement with full-length emerin whose Mr (34 kD) is always higher than the predicted one from its amino acid composition (29kD).

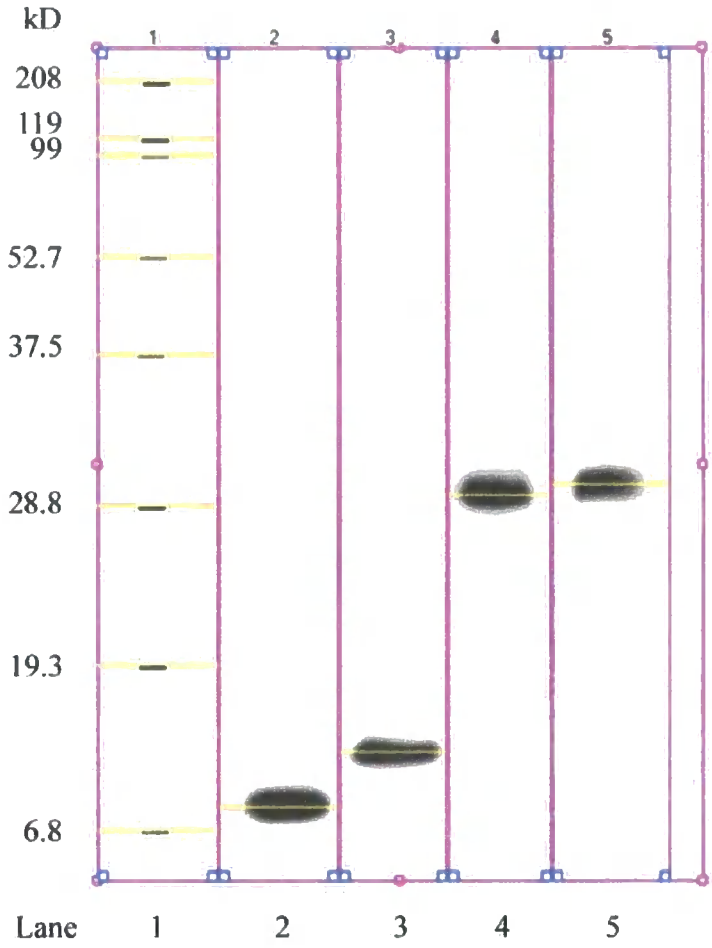

Figure 3.7: Calculation of the apparent molecular weights of emerin peptides using the UVI band software.

Aliquots of all emerin peptides were immunoblotted with NCL-Emerin antibody and the blot was used with the UVI band software, which assigned a molecular weight to each peptide relatively to markers with known molecular weights (lane 1). Lanes 2, 3, 4 and 5 correspond to emerin peptides 1-70, 73-180, 1-176 and 1-220, respectively.

3.2.2.5 Bradford Microassay on emerin elution fractions

The concentration of all elution fractions was determined by the Bradford Microassay procedure. A standard curve was firstly prepared with dilutions of BSA ranging from 0 to 50 μg. The absorbance at 595 nm was plotted against the μg of the samples and a line-of-best-fit with the equivalent equation was applied (Figure 3.8).

10 μl of each elution fraction were appropriately diluted (in 790 μl of H_2O and 200 μl of concentrated dye) and the absorbance at 595 nm was measured. The amount in μg contained in the 10 μl of each sample was calculated using the equation displayed on the standard curve. The concentration of each sample was found by multiplying the μg values by 10.

The protein concentration was then used to calculate the molarity of each elution fraction by dividing the mg/ml value by the molecular weight of each construct. The results of the Bradford Microassay procedure for each elution fraction and the molarity values are shown in Table 3.1.

a.

BSA (µg)	OD_{595} (nm)
0	0
5	0.307
10	0.524
20	0.964
40	1.341
50	1.465

b.

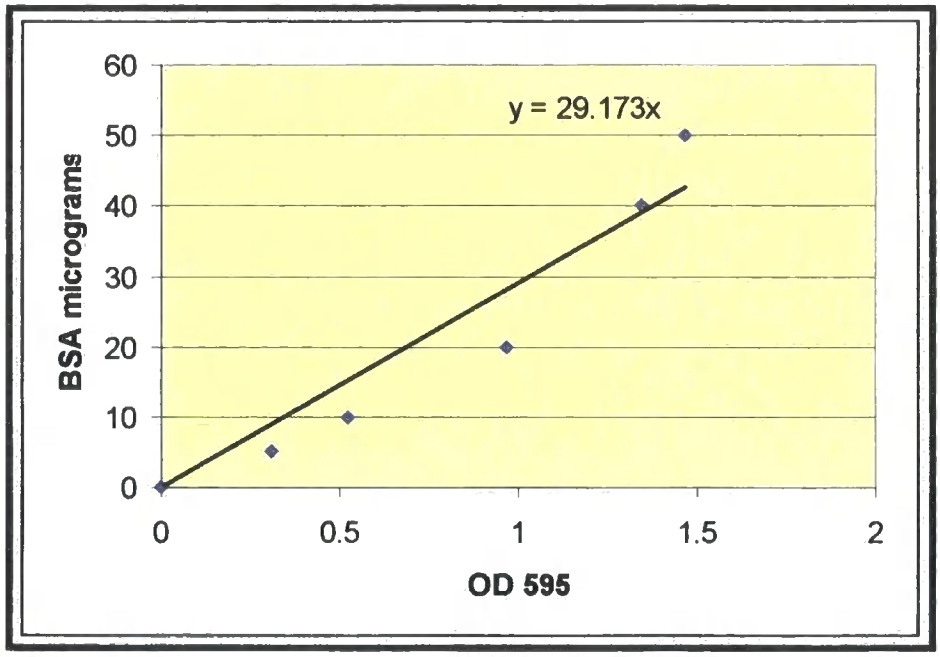

Figure 3.8: Bradford standard curve used for calculation of protein concentrations.

a: for the standard curve 5 dilutions of BSA were prepared and the absorbance of each at 595 nm was calculated using a spectrophotometer.

b: the standard curve was produced by plotting the amount of BSA (µg) against the OD_{595}.

	Emerin 1-70			Emerin 1-176			Emerin 1-220			Emerin 73-180		
	OD_{595} (nm)	Concentr. (mg/ml)	Molarity (µM)	OD_{595} (nm)	Concentr. (mg/ml)	Molarity (µM)	OD_{595} (nm)	Concentr. (mg/ml)	Molarity (µM)	OD_{595} (nm)	Concentr. (mg/ml)	Molarity (µM)
EF1	0.785	2.29	285.5	0.069	0.20	9.89	0.089	0.25	10	0.090	0.26	20.9
EF2	1.240	3.61	450.2	0.946	2.75	136.1	0.538	1.57	63	0.845	2.46	197.7
EF3	1.158	3.37	420.3	0.641	1.86	92.1	0.172	0.50	20	0.325	0.94	75.5
EF4	0.992	2.89	360.4	0.210	0.61	30.1	0.094	0.27	10.8	0.112	0.32	25.7
EF5	0.664	1.93	240.7	0.103	0.30	14.8	0.058	0.16	6.4	0.046	0.13	10.4
EF6	0.211	0.61	76.07	0.052	0.15	2.6	0.0	0	0	0.020	0.05	4

Table 3.1: Determination of protein concentration of elution fractions by the Bradford Microassay method.

The absorbance at 595 nm of each elution fraction (EF) of each peptide are displayed together with the calculated concentration and Molarity of each sample.

3.2.3 Effect of emerin mutants on nuclear envelope assembly

The effect of each emerin deletion mutant on nuclear envelope assembly was investigated in typical nuclear assembly reactions consisting of unfractionated *Xenopus* egg extract (LSS), *Xenopus* sperm and energy. The emerin mutants were included in the reactions at three different concentrations: a low concentration of 0.5 μM, an intermediate concentration of 4 μM and a high concentration of 8 μM. This way, competition experiments were established in which the exogenously added emerin would compete with the endogenous emerin for binding partners during the nuclear assembly process.

Pronuclei were allowed to assemble for 80 minutes at 21°C, fixed with EGS for 30 minutes at 37°C, layered over SNIB/30% Sucrose and centrifuged at 4,000g for 10 minutes onto coverslips. As a control assembly reactions consisting of LSS, sperm and energy, in absence of any emerin mutant, were used.

The assembly of the nuclear envelope was investigated with two antibodies that specifically recognise proteins contained in nuclear envelope precursor vesicles A and B (NEP-A and NEP-B). The effect of emerin constructs consisting of amino acids 1-70, 1-176, 1-220 and 73-170 are shown in Figures 3.9, 3.10, 3.11 and 3.12, respectively.

As shown in the figures, when emerin peptides were added at a concentration of 0.5 μM chromatin decondensation occurred normally (compare Figures 3.9 – 3.12, a and

b versus control). Similarly, there was no effect on vesicle binding to chromatin as shown by antibodies 4G12 and CEL13A (Figures 3.9 - 3.12, a and b).

However, at higher concentrations (4 μM and 8 μM) mutants 1-70 and 1-176 showed a strong inhibitory effect on nuclear envelope precursor vesicle recruitment to chromatin and chromatin decondensation. Both mutants preferentially inhibited NEP-A binding, since at 4 μM NEP-A was almost absent from the surface of chromatin, whereas NEP-B was largely unaffected (Figures 3.9 and 3.10, c and d). At 8 μM NEP-B was depleted from the surface of chromatin but still to a lesser extend than NEP-A (Figures 3.9 and 3.10, e and f).

In contrast, emerin mutants 1-220 and 73-180 had little or no effect on nuclear assembly (Figures 3.11 and 3.12, c and d).

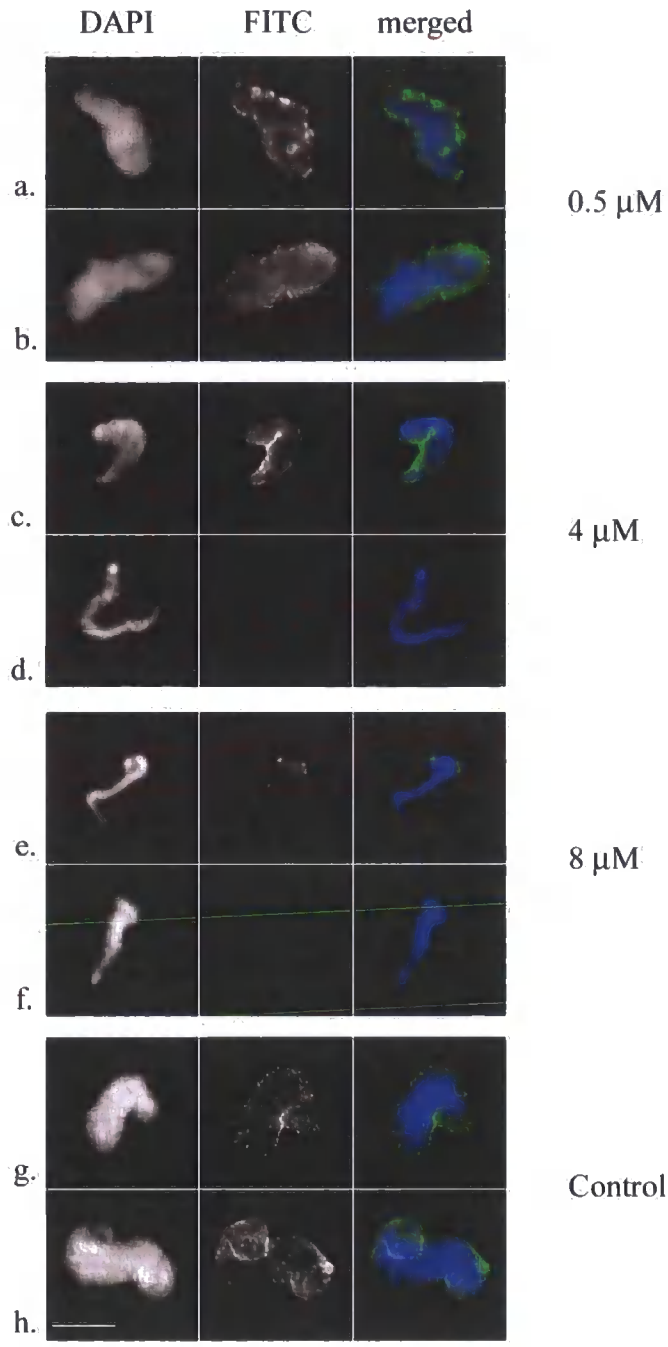

Figure 3.9: Effect of emerin 1-70 on nuclear assembly in *Xenopus* egg extracts.

Human emerin 1-70 was added to assembling nuclei at three concentrations: 0.5 µM (a and b), at 4 µM (c and d) and at 8 µM (e and f). Monitoring of NE vesicle recruitment to chromatin was achieved with two antibodies: 4G12 for NEP-B vesicles (a, c, e and g) and CEL13A for NEP-A vesicles (b, d, f and h). Chromatin was stained with DAPI. Bar is 10 µm.

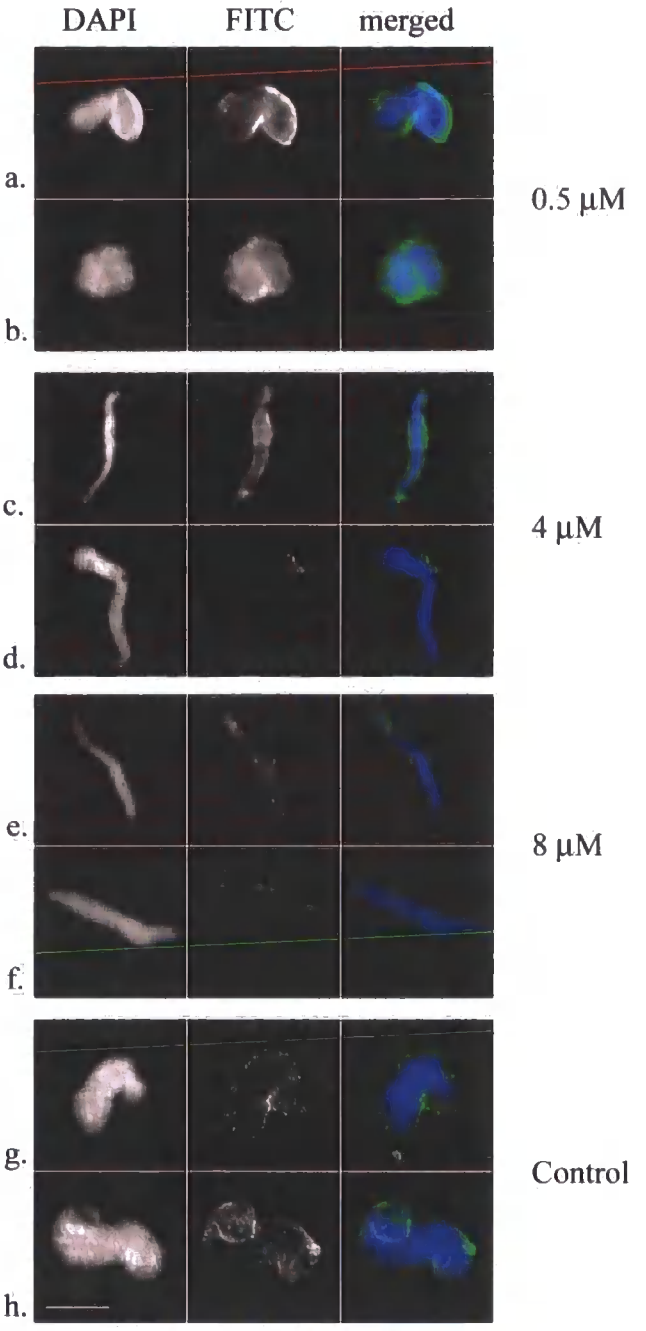

Figure 3.10: Effect of emerin 1-176 on nuclear assembly in *Xenopus* egg extracts.

Human emerin 1-176 was added to assembling nuclei at three concentrations: 0.5 µM (a and b), at 4 µM (c and d) and at 8 µM (e and f). Monitoring of NE vesicle recruitment to chromatin was achieved with two antibodies: 4G12 for NEP-B vesicles (a, c, e and g) and CEL13A for NEP-A vesicles (b, d, f and h). Chromatin was stained with DAPI. Bar is 10 µm.

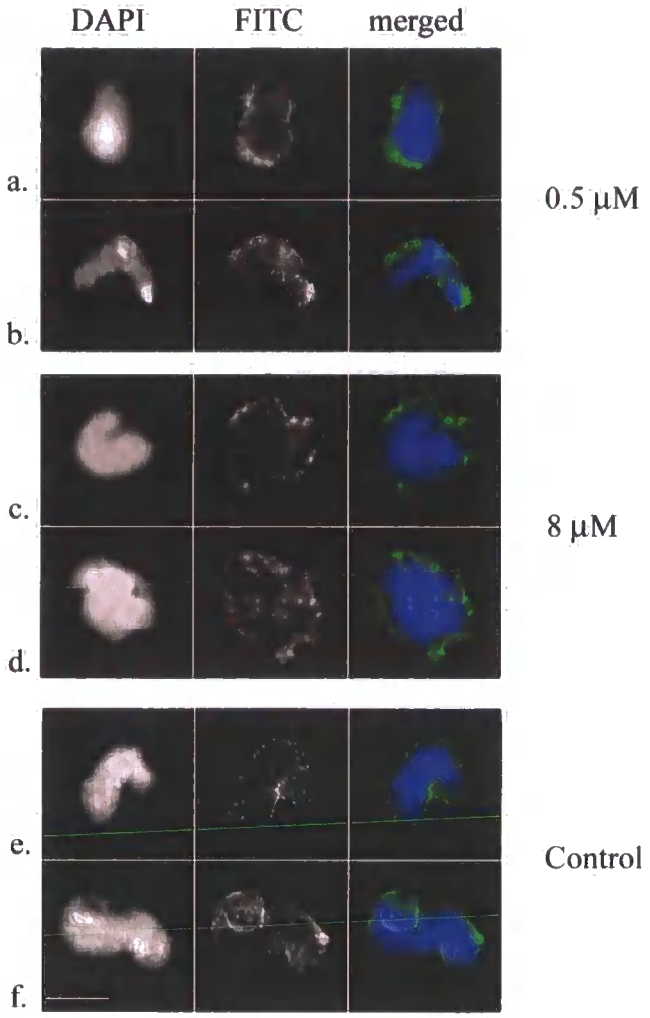

Figure 3.11: Effect of emerin 1-220 on nuclear assembly in *Xenopus* egg extracts.

Human emerin 1-220 was added to assembling nuclei at two concentrations: 0.5 μM (a and b) and 8 μM (c and d). Monitoring of NE vesicle recruitment to chromatin was achieved with two antibodies: 4G12 for NEP-B vesicles (a, c, and e) and CEL13A for NEP-A vesicles (b, d and f). Chromatin was stained with DAPI. Bar is 10 μm.

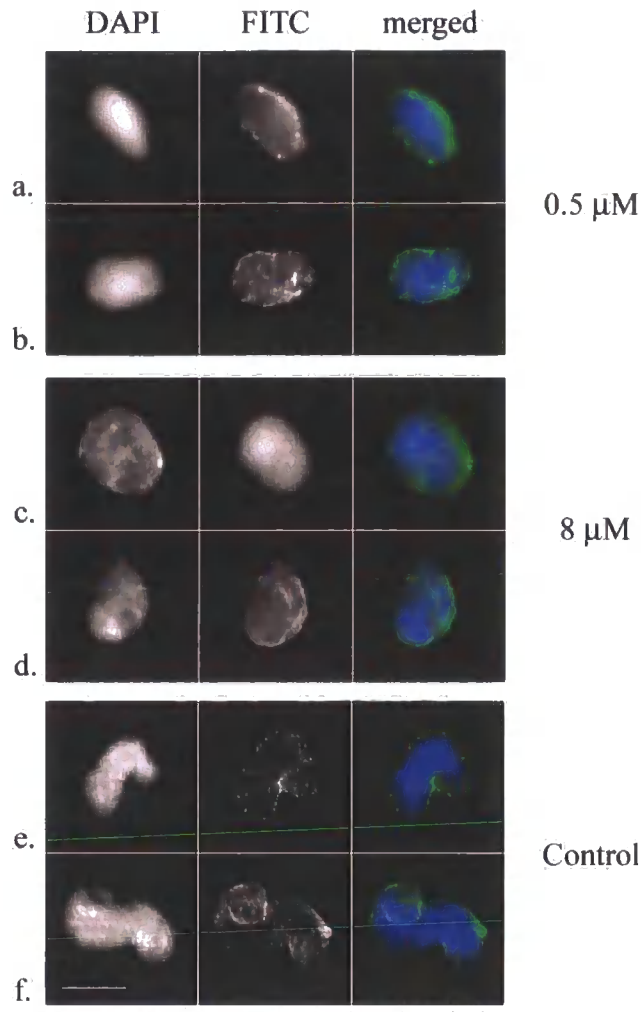

Figure 3.12: Effect of emerin 73-180 on nuclear assembly in *Xenopus* egg extracts.

Human emerin 73-180 was added to assembling nuclei at two concentrations: 0.5 µM (a and b) and 8 µM (c and d). Monitoring of NE vesicle recruitment to chromatin was achieved with two antibodies: 4G12 for NEP-B vesicles (a, c, and e) and CEL13A for NEP-A vesicles (b, d and f). Chromatin was stained with DAPI. Bar is 10 µm.

3.2.4 Effect of emerin mutants on Nuclear Pore Complex assembly.

The effect of the four emerin mutants on nucleoporins recruitment to chromatin was assessed using two antibodies: 414, which recognises four FG-repeat nucleoporins (p62, Nup153, Nup214 and Nup358), and Nup107, which recognises nucleoporins present in the very early stages of NPC assembly.

As for NEP-vesicle recruitment, nuclei were allowed to assemble for 80 minutes at 21°C, in the presence of 0.5 μM, 4 μM and 8 μM of emerin mutant peptides, fixed with EGS, layered over SNIB/30% Sucrose and centrifuged at 4000g for 10 minutes onto coverslips.

Staining with antibody 414 revealed that in control nuclei FG-nucleoporins displayed a nuclear rim staining (Figure 3.13, k). At 0.5 μM none of the emerin mutants inhibited the accumulation of FG-nucleoporins at the NE (Figure 3.13 a, d, g and i). Chromatin decondensation was inhibited with higher concentrations of mutants 1-70 and 1-176. However, 414 staining was only reduced at the highest concentration of 8 μM (Figure 3.13, c and f). Thus, the effects of 1-70 and 1-176 on NPC assembly (as detected by antibody 414) were very similar to the effects on NEP-B vesicles. In contrast to peptides 1-70 and 1-176, peptides 1-220 and 73-180 did not inhibit chromatin decondensation or NPC formation even when added at 8 μM (Figure 3.13 h and j).

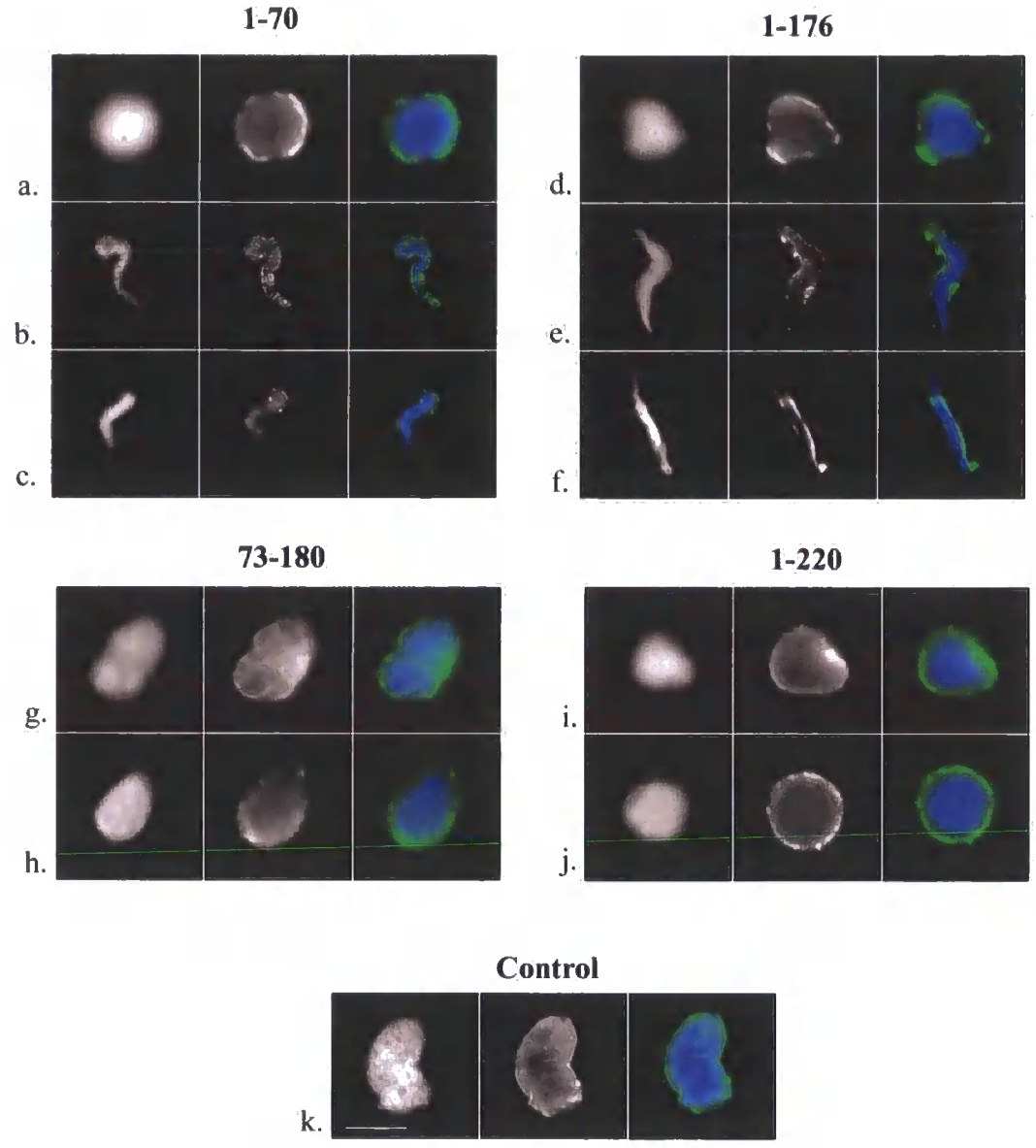

Figure 3.13: Effect of emerin peptides 1-70, 1-176, 73-180 and 1-220 on NPC assembly in *Xenopus* egg extracts.

Emerin peptides 1-70 (a-c), 1-176 (d-f), 73-180 (g-h) and 1-220 (i-j) were added to assembling nuclei at 0.5 μM (a, d, g and i), at 4 μM (b and e) and at 8 μM (c, f, h and j). To monitor recruitment of nucleoporins around chromatin all nuclei were stained with antibody 414 (FITC). Control reactions contained nuclei assembled in absence of any exogenous emerin (k). Chromatin was visualised with DAPI. Bar is 10 μm.

Nuclei with the condensed chromatin phenotype were further characterised for the specific type of nucleoporins that were recruited to them (Figure 3.14 a). Nuclei were allowed to assemble for 80 minutes at room temperature in presence of 8 μM of emerin 1-70 and 1-176 (Figure 3.14 a, lanes 3 and 4, respectively), centrifuged through SNIB/30% Sucrose and the pelleted nuclei were analysed by immunoblotting with antibody 414 which recognises four nucleoporins: Nup358, Nup214, Nup153 and p62.

Two control reactions were run in parallel. In lane 1, chromatin was incubated in *Xenopus* egg extract in absence of any emerin peptide. In lane 2, egg extract was analysed in absence of emerin and sperm to see whether any nucleoporins could pellet without being associated with chromatin.

As the figure shows at 8 μM the main inhibitory action of the emerin mutants was, firstly, on Nup153 and, secondary, on p62. Nucleoporins 214 and 358 were not affected. Densitometric analysis of the bands was performed for the quantification of the above results. UVI band software was used to calculate the intensity of all bands. The software assigned to each band a volume number, which corresponds to the sum of intensities of the pixels of the band. The intensities of the control bands (Figure 3.14 a, lane 1) were then set as the maximum (100%) intensities. The intensity of the bands in presence of 8 μM emerin 1-70 and 1-176 was calculated as a percentage relatively to the control intensities. Quantification shows that more than 95% of nucleoporins 358 and 214 were detected around chromatin in inhibited nuclei compared to the controls. Nup153 was the most severely affected since only 18-

23.7% of the protein was recruited in inhibited nuclei. p62 was also significantly affected since the amount detected in inhibited nuclei was only 55.6-61.4% of the normal levels in the control reaction (Figure 3.14 a).

To test whether early stages of NPC assembly were affected in inhibited nuclei, immunofluorescence analysis using the Nup107 antibody was performed on nuclei assembled in presence of 8 μM of emerin 1-70 and 1-176 (Figure 3.14 b). In both cases although chromatin had a condensed phenotype as expected, recruitment of the Nup107 complex nucleoporins was not inhibited.

Figure 3.14: Analysis of NPC assembly on emerin inhibited nuclei.

Nuclei assembled in presence of 8 μM of emerin 1-70 and 1-176 were analysed by Immunoblotting with antibody 414 (a) and by Immunofluorescence with antibody Nup107 (b).

***(a):** Immunoblotting analysis with antibody 414 showed reduced amounts of Nup153 and p62 in presence of emerin 1-70 and 1-176 (a, lanes 3 and 4, respectively). No effect was observed on Nup358 and Nup214 compared to controls (a, lanes 1 and 2). Densitometric analysis of the bands is shown in the table underneath the blot. Volume numbers correspond to the sum of the intensities of the pixels of each band as given by the UVI band software. The intensities of the control bands (lane 1) are set as 100%. The intensities of the bands in the inhibited nuclei are calculated as a percentage relatively to the control bands. For p62 final intensity volumes were calculated by subtracting the intensity of the band in the negative control (lane 2) from the bands in lanes 1, 3 and 4. The extremely reduced levels of Nup153 and p62 compared to control reactions are highlighted in bold. L1, L2, L3 and L4 correspond to Lane 1, Lane 2, Lane 3 and Lane 4, respectively.*

***(b):** Recruitment of pre-pore nucleoporins was not inhibited as shown by Immunofluorescence with Nup107 antibody (FITC). Chromatin was stained with DAPI. Bar is 10 μm.*

a.

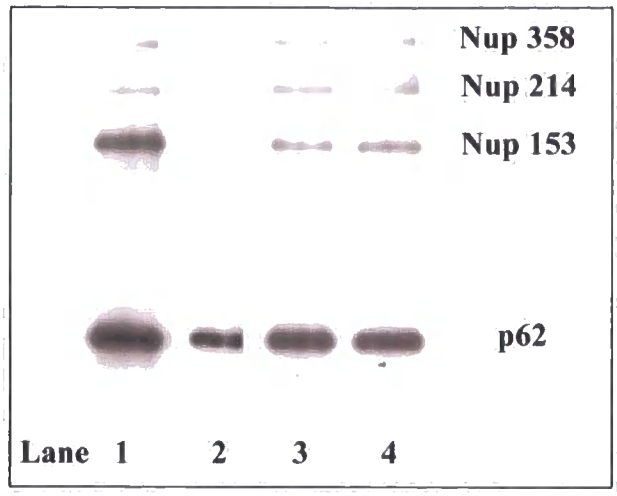

	Control (L1)		1-70, 8μM (L3)		1-176, 8 μM (L4)	
	volume	%	volume	%	volume	%
Nup358	8355	100	7976	95.5	8231	98.5
Nup214	20044	100	19563	97.6	19924	99.4
Nup153	152698	100	27478	**18**	36120	**23.7**
p62	250273 (L1) - 107433 (L2) 142840	100	153643 (L3) - 107433 (L2) 46210	**32.4**	139118 (L4) - 107433 (L2) 31685	**22.2**

b.

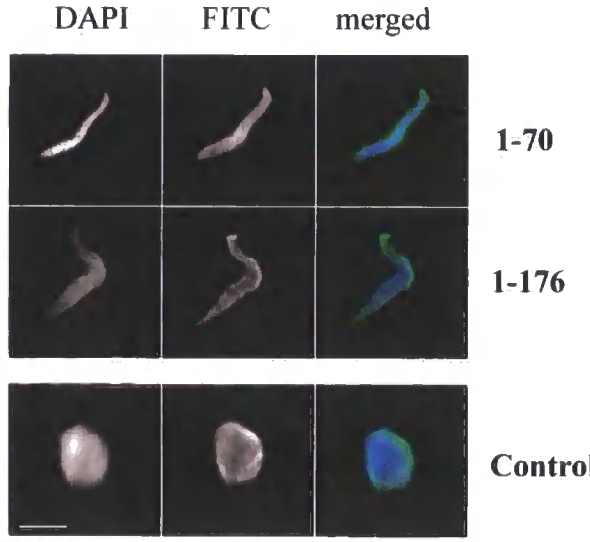

Figure 3.14: Analysis of NPC assembly on emerin inhibited nuclei.

3.2.5 Investigation on the chromatin binding ability of emerin

In order to test the ability of emerin to interact with chromatin each emerin peptide was incubated with condensed, and poly-glutamic acid induced decondensed *Xenopus* sperm chromatin for 15-30 minutes at room temperature. Samples were then fixed with 4% formaldehyde and centrifuged through SNIB/30% Sucrose onto coverslips. The presence of emerin on the chromatin was checked by immunofluorescence with NCL-Emerin antibody, which is specific for human emerin while sperm chromatin was visualised with DAPI (Figure 3.15).

As shown by the DAPI staining treatment of sperm with poly-glutamic acid caused extensive decondensation of the chromatin (Figure 3.15 b, d, f and h) compared to untreated sperms which have a condensed morphology (Figure 3.15 a, c, e and g).

When decondensed chromatin was incubated with emerin peptides all of them were able to bind to decondensed chromatin (Figure 3.15 b, d, f and h). When condensed chromatin was used instead, peptides 1-70, 1-176 and 73-180 were not able to bind to chromatin (Figure 3.15 a, c and e). Peptide 1-220, however, showed a unique characteristic of being able to bind to condensed chromatin as well (Figure 3.15 g).

A summary of the results obtained for each emerin peptide is shown in Table 3.2.

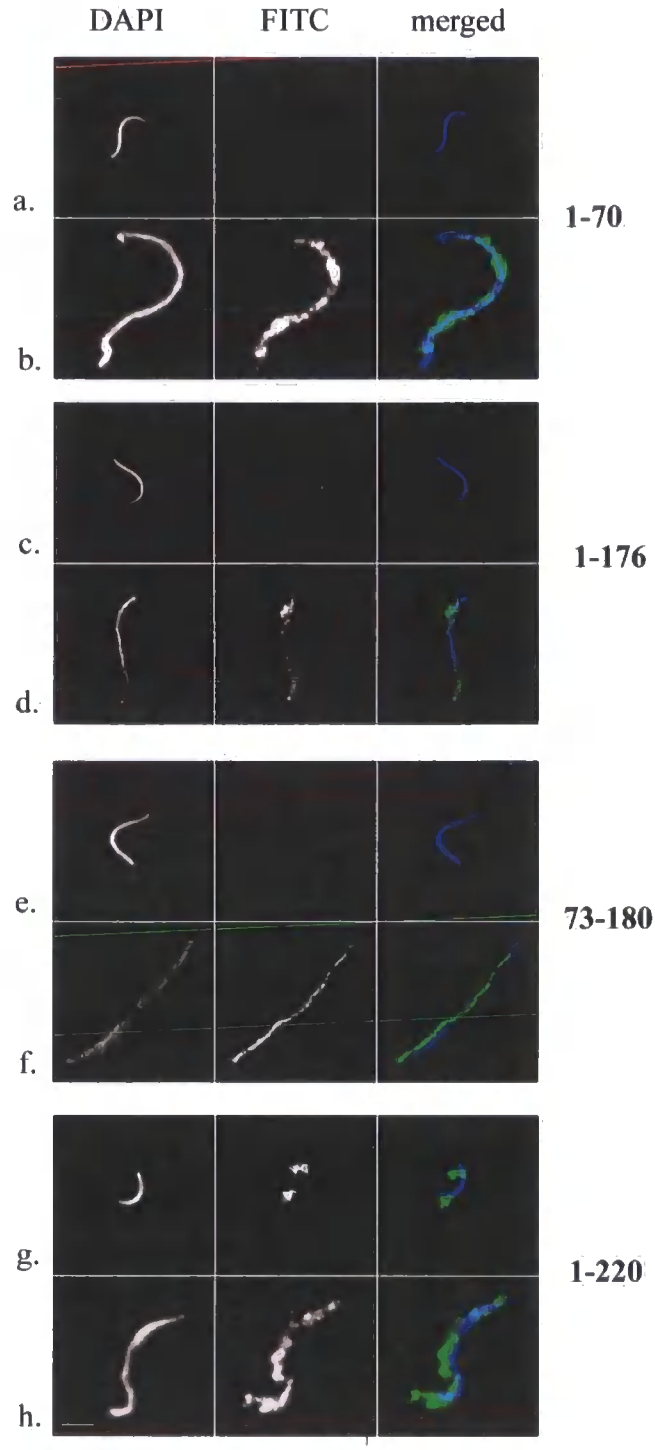

Figure 3.15: Investigation of chromatin binding ability of emerin.

Emerin peptides 1-70, 1-176, 1-220 and 73-180 were incubated with condensed (a, c, e and g) and decondensed (b, d, f and h) Xenopus sperm chromatin, and their ability to interact with chromatin was investigated by immunofluorescence with NCL-Emerin antibody (FITC). Chromatin was visualised with DAPI (blue). Bar is 10 μm.

Emerin	Added concentration	NEP-B binding	NEP-A binding	Chromatin decondensation	NPC assembly	Chromatin binding ability
1-70	0.5 µM	+ + +	+ + +	+ + +	+ + +	Condensed : no Decondensed : yes
	4 µM	+ +	+	—	+ +	
	8 µM	+	—	—	—	
1-176	0.5 µM	+ + +	+ + +	+ + +	+ + +	Condensed : no Decondensed : yes
	4 µM	+ +	+	—	+ +	
	8 µM	+	—	—	—	
1-220	0.5 µM	+ + +	+ + +	+ + +	+ + +	Condensed : yes Decondensed : yes
	8 µM	+ + +	+ + +	+ + +	+ + +	
73-180	0.5 µM	+ + +	+ + +	+ + +	+ + +	Condensed : no Decondensed : yes
	8 µM	+ + +	+ + +	+ + +	+ + +	

Table 3.2: A summary of the effect of emerin peptides on NEP-A and NEP-B binding to chromatin, Chromatin decondensation and NPC assembly on nuclei assembled in Xenopus egg extracts.

The ability of each peptide to bind to condensed and decondensed chromatin is also shown. Symbols correspond to: + + + : normal, + + : slightly inhibited, + : considerably inhibited, — : completely inhibited in comparison to results from control reactions where nuclei were assembled in the absence of any emerin peptide.

3.3 DISCUSSION

In this chapter the function of emerin was investigated using the *Xenopus* cell-free system. As a first step, the order and dynamics of nuclear assembly in *Xenopus* egg extracts was investigated. Previous work has shown that nuclear assembly requires two vesicle populations, NEP-B and NEP-A. The first population displays chromatin binding properties and the latter fusogenic properties (Vigers and Lohka, 1991). Immunofluorescence studies using a NEP-B-specific antibody and an antibody against human LBR showed an ordered recruitment of vesicles around chromatin with NEP-B appearing first and followed by NEP-A (Drummond *et al.*, 1999).

In this chapter the ordered process of nuclear envelope assembly around chromatin and the existence of two distinct vesicles populations shown by Drummond *et al.* was reconfirmed by a set of experiments that included antibodies not used before. Nuclear envelope assembly around demembranated sperm chromatin was monitored in a time-course manner over a period of 80 minutes. Antibodies 4G12 and CEL13A were used to detect nuclear membranes and antibody 414 to detect FG-nucleoporins. 4G12 antibody was used as a marker for NEP-B vesicles. The antibody was produced by Drummond S. by immunising mice with the NEP-B fraction of *Xenopus* egg extracts (Drummond *et al.*, 1999). The antibody was shown to recognise a 78 kD protein present in the MP2 (or NEP-B) membrane fraction. The second antibody, CEL13A, was produced by Lyon C. using isolated pronuclei formed in unfractionated *Xenopus* egg extracts to immunise BALB/c mice (Lyon, 1995). The antibody was shown to recognise an integral membrane protein of 40 kD present in the whole membrane fraction. Whether the antibody was contained in a particular membrane fraction,

NEP-A or NEP-B, was not tested in that study. Functional characterisation of the antigen showed that it is probably involved in maintaining chromatin structure since depletion of extracts from the CEL13A antigen resulted nuclei with decondensed but unstructured and stringy-looking chromatin, which were not enclosed by a nuclear envelope (Lyon, 1995). The use of these antibodies reconfirmed the existence of two distinct vesicle populations. NEP-B vesicles, as detected by antibody 4G12, were involved in the earliest stages of nuclear assembly appearing around chromatin at 10 minutes after initiation of assembly. In contrast, CEL13A antibody showed a different staining pattern with the first signal around chromatin appearing at 20 minutes. CEL13A is a membrane-specific antibody that does not recognise any soluble proteins present in the cytosol of *Xenopus* egg extracts (Lyon, 1995). The timing of recruitment of the CEL13A-detected vesicles is comparable with the LBR containing vesicles described in Drummond *et al.*, which appeared around chromatin at 15-30 minutes after nuclear assembly initiation.

The formation of NPCs on pronuclei assembled in this system was monitored by antibody 414, which recognises four FG-nucleoporins: p62, nup358, nup214 and nup153. 414 antibody displayed a similar staining pattern with the NEP-B specific antibody 4G12, detecting the first nucleoporins around chromatin at 10 minutes. A correlation between NEP-B vesicles and NPCs has already been reported by Vigers and Lohka. NEP-B vesicles seem to be able to recruit nucleoporins since the number of NPCs formed in nascent nuclear envelopes depends on the availability of NEP-B vesicles (Vigers and Lohka, 1991). The NEP-B fraction was also shown to be enriched in some nucleoporins including p62, which is one of the nucleoporins recognised by antibody 414 (Vigers and Lohka, 1992). The formation of some NPCs

at an early stage of nuclear assembly in *Xenopus* egg extracts has also been described before in FEISEM studies, in which mature NPCs were observed on patches of flattened membranes at 8-10 minutes after initiation of assembly (Wiese *et al.*, 1997).

To investigate the role of emerin in this highly coordinated process of nuclear envelope assembly, four human emerin constructs were provided by Dr Rzepecki. The constructs encode for emerin amino acids (aa) 1-70, 1-176, 1-220 and 73-180 and were chosen because they represent regions of emerin known to interact with other proteins or regions of unknown so far function. All peptides except 73-180 contain the LEM domain (aa 1-45), which mediates binding to chromatin protein BAF. Peptides 1-176, 1-220 and 73-180 contain the lamin A binding domain (aa 70-178). Peptide 1-220 contains, except the BAF and lamin A binding domains, a third serine-rich region consisting of aa 180-220 of unknown function.

The provided emerin constructs were expressed in bacteria cells and subjected to sequential extractions under native and denaturing conditions. The behaviour of each peptide was examined by SDS-PAGE on Coomassie stained gels and by Immunoblotting with an emerin-specific antibody. Although a considerable amount of all peptides was extracted under native conditions, maximum extraction of peptides 1-176 and 1-220 was achieved under denaturing conditions in presence of urea. Formation of inclusion bodies that consist of insoluble protein aggregates and require denaturing reagents to be solubilised are often observed when overexpressing foreign proteins in *E. coli*. This could be due to differences in size with small peptides easier obtained in their soluble form and bigger peptides forming inclusion bodies. Inclusion bodies could arise by the inappropriate aggregation of partially folded or malfolded

peptides, and bigger peptides could be at higher risk of inappropriate folding than smaller ones. Since retention of the biological activity was important for subsequent experiments only fractions obtained by native extraction were used for purification. Peptides were tagged with six consecutive histidines allowing purification by Immobilised Affinity Chromatography (IMAC). IMAC employs the ability of polyhistidine tracts to bind tightly to metal ions like Ni^{2+}, Zn^{2+} or Cu^{2+}, immobilised on a resin. Elution of the protein is achieved by a competing chelator like imidazole. Although the level of contaminants when using this method is relatively low, a couple of contaminant proteins were observed copurifying with all emerin peptides. The contaminants were seen as a doublet of bands at about 70 kD one of which was later (Chapter 5) identified as chaperone HSP70. Chaperones are proteins whose main role is the binding of unfolded or partially folded forms of other proteins (Hendrick and Hartl, 1995) and are commonly observed bound to purified peptides.

The molecular weight of each peptide was calculated according to their electrophoretic mobility on SDS-gels. Peptides 1-70, 1-176, 1-220 and 73-180 migrated as proteins of 8.8, 29.5, 30.1 and 13.1 kD, respectively. The observed molecular weights were higher than the molecular weights calculated according to their amino acid composition. This a general property of emerin. Full-length emerin migrates on SDS-PAGE slower, as a 34 kD protein, compared to its predicted size of 29 kD probably due to post-translational modifications (Manilal *et al.*, 1996).

After purification each emerin peptide was added to nuclear assembly reactions at various concentrations ranging from a very low one of 0.5 μM to a high one of 8 μM. The effect on recruitment of vesicles and nucleoporins was observed with antibodies

4G12, CEL13A and 414. The peptides fell into two categories: one, including peptides 1-220 and 73-180, did not have an effect on nuclear assembly compared to control reactions at any concentration added while in the other category peptides 1-70 and 1-176 showed a strong inhibitory effect on nuclear assembly when added at a high concentration. The inhibitory effect was dose-dependent. The higher the amount of the peptide added the stronger the inhibitory effect. In any case inhibition of NEP-A vesicles was always stronger than NEP-B vesicles and nucleoporins. This was more obvious when a middle concentration of peptides was used (4 μM) at which NEP-A vesicles were selectively inhibited over NEP-B. Inhibited nuclei were small-sized with condensed chromatin showing an impairment in chromatin decondensation.

The fact that emerin peptides 1-70 and 1-176 inhibited nuclear assembly, whereas peptide 73-180, which lacks the LEM domain was unable to cause the same effect, indicates that the LEM domain is responsible for the inhibition. A similar role for the LEM domain of another INM protein, LAP2, has also been shown (Shumaker *et al.*, 2001). When the N-terminal region of LAP2, which contains the LEM domain, was added to *Xenopus* nuclear assembly reactions at 10 μM, an arrest in nuclear envelope assembly and condensed chromatin were observed. Addition of LAP2 peptides with mutations in the LEM domain failed to cause the same inhibition.

The inhibitory effect of emerin peptides 1-70 and 1-176 at 8 μM could be explained by their ability to out compete endogenous emerin (or endogenous LEM domain proteins in total) for binding partners, due to their higher concentration. The preferential inhibition of NEP-A vesicles suggests that exogenous emerin competes

with components residing in NEP-A vesicles. One possible explanation for the inhibitory effect is that exogenously added emerin occupies sites on chromatin not allowing nuclear precursor vesicles to attach to chromatin and form a complete nuclear envelope. This could be mediated by an interaction with BAF, a chromatin protein that is known to interact with LEM domain proteins. A function for BAF in binding LEM domain proteins during nuclear assembly and mediating thereby attachment of chromatin to the inner nuclear membrane has already been reported. When BAF mutants that cannot bind emerin were included in *Xenopus* nuclear assembly reactions at high concentrations, they produced nuclei with condensed chromatin devoid of nuclear membranes (Segura-Totten *et al.*, 2002). Thus, DNA-bound BAF must interact with LEM domain proteins to recruit membranes and promote chromatin decondensation and nuclear growth.

The effect of emerin peptides on NPC formation was investigated by immunofluorescence and immunoblotting with the 414 antibody. Again, only peptides 1-70 and 1-176 had an inhibitory effect on recruitment of nucleoporins to chromatin. This effect was much milder though compared to the inhibition of NEP vesicles. The main inhibitory effect as revealed by immunoblotting was on Nup153 and p62. Nup358 and 214 were not affected. Densitometric analysis showed that Nup153 was most severely affected. Only 1/5 (~ 20%) of the nucleoporin was recruited around chromatin in inhibited nuclei compared to control reactions. Immunofluorescence analysis of mitotic NRK cells has shown before an early recruitment of Nup153 to chromatin during NE reassembly, which could be independent of membrane recruitment to chromatin (Bodoor *et al.*, 1999). In *Xenopus*, however, time-course studies using egg extracts revealed a late recruitment

of Nup153 that requires the prior formation of the lamina (Smythe *et al.*, 2000). The results presented in this chapter support a recruitment of Nup153 that is dependent on nuclear membrane recruitment to chromatin since inhibition of NE formation in presence of exogenous emerin greatly reduced the amount of Nup153 around chromatin.

p62 levels around chromatin were also reduced in presence of exogenous emerin but to a lesser extent than Nup153. Approximately 55% of the protein was detected in inhibited nuclei compared to controls by densitometry. In the *Xenopus* system, p62 is recruited to chromatin earlier than Nup153, at 20 minutes after initiation of nuclear assembly (Smythe *et al.*, 2000). This timing is consistent with the early recruitment of NEP-B vesicles around chromatin presented by Drummond *et al.* (1999) and in the present study. Thus, the milder inhibition of p62 by exogenous emerin could be due to the milder inhibition of the emerin peptides on NEP-B vesicles. A previously reported co-fractionation of p62 with NEP-B vesicles (Vigers and Lohka, 1992) further supports the above explanation.

In contrast to Nup153 and p62, nucleoporins 358 and 214 were not affected by the presence of exogenous emerin since nearly equal amounts were detected in control and inhibited by emerin nuclei. Nups 358 and 214 are localised in the cytoplasmic side of the NPC unlike Nup153, which is positioned in the nucleoplasmic side and p62, which is symmetrically located on the NPC. The fact that cytoplasmic components of the NPC were not affected by exogenous emerin could be explained by the milder inhibition of NEP-B vesicles. NEP-B vesicles are enriched in ER/ONM proteins (Drummond *et al.*, 1999), which could interact or recruit the cytoplasmic

facing nucleoporins 214 and 358 to chromatin. Although no direct proof exists, an association of ER/ONM components of NEP-B with Nups 214 and 358 provides a possible explanation for the selective inhibition of nucleoplasmic nucleoporins.

One of the earliest stages of NPC formation involves the binding of nucleoporins of the Nup107 complex to chromatin. The complex consists of Nup107, Nup133, Nup96, Nup160 and Sec13 and is thought to form pre-pores, which serve as attachment sites for subsequent recruitment of other nucleoporins (Belgareh *et al.*, 2001). Pre-pores were first observed by Sheehan et al. (1988) as short-lived transient structures at very early time points during assembly, which mediate formation of mature NPCs. Depletion of Nup107 by RNAi in HeLa cells was shown to cause the co-depletion of several other nucleoporins among which were the 414 antigens Nup214, Nup358, Nup153 and p62 (Boehmer *et al.*, 2003; Walther *et al.*, 2003). Depletion of Nup107 from *Xenopus* egg extracts also led to absence of staining with antibody 414 as observed by immunofluorescence on assembled nuclei (Walther *et al.*, 2003). In the same study, however, 414 nucleoporins associated only weakly with chromatin in the absence of membranes even when the Nup107 complex was present. Thus, in *Xenopus* the stable binding of 414 nucleoporins to chromatin requires the presence of both, the Nup107 complex and nuclear membranes. Nuclei assembled in presence of high concentrations of emerin peptides 1-70 and 1-176 although had a reduced staining for 414 nucleoporins were not inhibited regarding binding of Nup107 to chromatin. Thus, the reduced staining observed for antibody 414 was probably a result of the impaired vesicle recruitment on chromatin caused by the emerin mutants.

A rather surprising result was observed for peptide 1-220, which failed to inhibit nuclear assembly although it contains the LEM domain. There are two possible explanations for this. One explanation is that the region specific to this peptide, between residues 176 and 220, mediates an interaction with a yet unidentified partner This interaction could confer a unique ability to this peptide, compared to the others, to promote chromatin decondensation. Alternatively, the inability of this peptide to inhibit assembly could be due to the simple fact that it is inactive. Indeed, during the purification of all peptides, 1-220 was the most difficult one to obtain in a soluble form and to keep it soluble over long periods. This peptide was always more sensitive in freezing/thawing cycles and had a tendency to precipitate much easier than any other peptide probably due to its bigger size. Thus, although the non-inhibitory effect of 1-220 could be functionally significant concerns should be noted about its correct folding and functionality during the assay.

To test whether peptide 1-220 has the unique ability to promote chromatin decondensation due to an interaction with a chromatin protein, the chromatin binding ability of all peptides was investigated. Condensed and decondensed *Xenopus* sperm chromatin was used for this purpose. All of the peptides had the ability to interact with decondensed chromatin. When condensed chromatin was used no signal was detected for peptides 1-70, 1-176 and 73-180. This is can be easily explained considering the extremely compact nature of condensed chromatin, which would make any emerin binding sites inaccessible. Remodelling chromatin artificially, by poly-glutamic acid, would expose binding sites allowing peptides to attach to decondensed chromatin. In contrast to the other peptides, emerin 1-220, was observed attached to condensed chromatin as well. The ability of peptide 1-220 to interact with

condensed chromatin, probably via a chromatin-associated protein, would suggest a role in chromatin remodelling. However, the possibility that what is observed on condensed chromatin is aggregates of the peptide, rather than a real interaction, cannot be ruled out. The unstable nature of the peptide does not allow a clear interpretation of the above result.

CHAPTER 4

INVESTIGATION OF NOVEL LEM-LIKE DOMAIN PROTEINS IN THE *XENOPUS* SYSTEM

4.1 INTRODUCTION

In the previous chapter, the inhibitory effects on NE assembly of peptides including the LEM domain of emerin were investigated using the *Xenopus* cell-free system. LEM domain containing human emerin peptides were shown to inhibit certain aspects of nuclear assembly highlighting a potentially important role of either emerin or other LEM domain proteins in nuclear assembly. The inhibitory effect was thought to be mediated by the competition of exogenously added peptides with endogenous proteins for binding partners. Therefore, as a next step it was important to investigate the presence of endogenous emerin in the experimental system used.

Emerin is a conserved protein during evolution. It has been detected by immunoblotting in various vertebrate cell lines that include human, rat, mouse, marsupial, hamster and *Xenopus* cells (Dabauvalle *et al.*, 1999). Human emerin consists of 254 amino acids, has a predicted molecular weight (Mr) of 29 kD but runs on SDS-PAGE gels as a 34 kD protein. In rat, emerin was identified as a 260 residue protein that exhibits 74% identity to human emerin. It has a Mr of 29,675 but runs on SDS-PAGE gels as two bands of 36 and 38 kD (Ellis *et al.*, 1998). In mouse, cloning of the emerin gene revealed a cDNA that encodes a 259 residue protein which is 73% identical and 79% similar to human emerin and 93% identical and 95% similar to rat emerin. The mouse emerin has a predicted molecular weight of 29.4 kD (Small *et al.*, 1997). Emerin has also been detected by immunoblotting as a 34 kD protein in rabbit cells (Manilal *et al.*, 1996).

The emerin sequence of several species including human, mouse, rat, chimpanzee, dog, *C.elegans* and *Xenopus*, has been published and is available online. The size and accession numbers of the available emerin sequences so far are presented below.

Species	Amino acids	NCBI Accession number
Homo sapiens	254	S50834
Mus musculus	259	NP031953
Rattus norvegicus	260	NP037080
Pan troglodytes	247	XP521335
Canis familiaris	170	XP549369
Caenorhabtitis elegans	166	NP490907
Xenopus laevis	180	AAR37361 (Xemerin1) AAX09328 (Xemerin2)

At the time of this study, the complete amino acid sequence of *Xenopus* emerin was not available online. Recently, two emerin isoforms have been described in *Xenopus*. Both consist of 180 amino acids and differ by 24 amino acids scattered throughout the sequence (Gareiss *et al.*, 2005).

In the present chapter, two antibodies were used in order to attempt to identify LEM domain proteins, including emerin, in *Xenopus*: an antibody against the LEM domain of LAP2 (LAP12 antibody) and an antibody against the LEM domain of human emerin (aE70 antibody). Characterisation of the LAP12 antigen was unsuccessful. Therefore, only antibody aE70 was used in subsequent experiments. The specificity of the antibody for human emerin was initially confirmed using normal HDF and HDF from patients with X-EDMD, which lack emerin. Attempts to identify *Xenopus*

emerin using the aE70 antibody were based on the high similarity of the sequence the antibody was raised against (human emerin amino acids 1-70) with the *Xenopus* emerin amino acids 1-70 (49% identical, 66% similar). Immunoblotting and immunofluorescence experiments were performed on *Xenopus* somatic cells and fractionated egg extracts. The timing of incorporation of the aE70 antigen into reforming nuclear envelopes was also investigated using unfractionated egg extracts.

4.2 RESULTS

4.2.1 Attempted purification of the LAP12 antigen

Western Blotting analysis of fractionated *Xenopus* egg extracts with the LAP12 antibody, which recognises the LEM domain of human LAP2β, revealed a major 36 kD band recognised by the antibody, localised in the NEP-A fraction (Figure 4.1). In order to identify this protein by mass spectroscopy pull-down experiments of the antigen were attempted. The antibody was immobilised either on protein G beads or anti-mouse IgG beads and incubated with solubilised fractions of NEP-A.

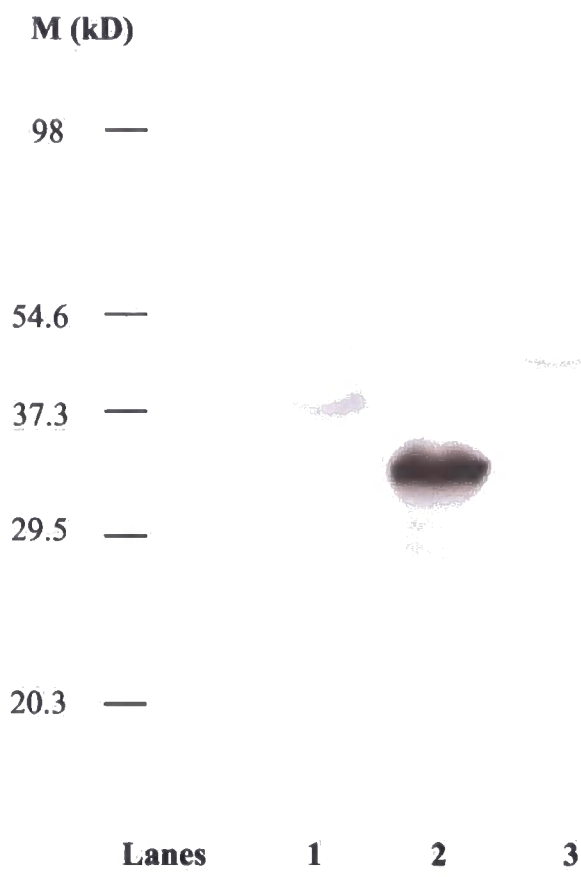

Figure 4.1: Immunoblotting analysis of NEP-A, NEP-B and cytosolic fractions of *Xenopus* egg extracts with the LAP12 antibody.

Aliquots of Xenopus cytosol (lane 1), NEP-A (lane 2) and NEP-B (lane 3) fractions were resolved on a 12% gel and immunoblotted with antibody LAP12 (1:100). As shown the main protein recognised by the antibody resides in the NEP-A fraction and has a molecular weight of about 36 kD. The markers (in kD) are shown on the left.

4.2.1.1 Protein G beads

LAP12 antibody was immobilised on protein G beads and incubated with NEP-A membranes extracted with 1x PBS, pH 7.5 containing 1% Triton X-100. After removal of non-specifically bound material, antibody-antigen complexes were eluted with 50 mM Glycine pH 2.3. Samples of all fractions were analysed by Western Blotting with the LAP12 antibody (Figure 4.2 a). The Western blot revealed that none of the elution fractions contained the 36 kD band. Instead the antigen was contained in the flowthrough fraction (Figure 4.2 a, lane 2) indicating either that the antigen was not able to bind to the antibody or that the antigen was not eluted under these conditions.

To distinguish between these two possibilities the experiment was repeated in the same way with the difference that before elution the beads were divided into three equal volumes, which were eluted under different conditions. Specifically, the first bead sample was subjected to elution with 1.5 M KSCN (Figure 4.2 b, lanes 9-12), the second with 100 mM Orthophosphoric acid pH 12.5 (Figure 4.2 b, lanes 13-16) and the third with 6 M Urea (Figure 4.2 b, lanes 17-20). Aliquots of the remaining beads after elution were also analysed (Figure 4.2 b, lanes 21-23). Western blot analysis showed that none of the elution fractions contained the antigen, which again was exclusively contained in the flowthrough fraction (Figure 4.2 b, lane 2). Also the antigen did not remain on the beads after elution. When aliquots of the beads were analysed only the light and heavy IgG chain of the antibody were detected and none of the antigen (lanes 21-23).

Figure 4.2: Immunoprecipitation experiment of the LAP12 antigen using protein G beads.

Xenopus NEP-A fractions were extracted with PBS containing 1% Triton X-100, pH 7.5 (starting material) and incubated with LAP12 antibody immobilised on protein G beads. The flowthrough was collected and beads washed and eluted under different conditions. Aliquots of all samples were analysed by SDS-PAGE and immunoblotted with antibody LAP12. Asterisks indicate the position of the LAP12 antigen

a: *Lane 1: starting material, Lane 2: flowthrough, Lanes 3-5: washes with PBS/0.1% Triton X-100, Lanes 6-7: washes with PBS/0.1% Triton X-100/0.02% SDS, Lane 8: wash with PBS/0.1% Triton X-100/1M NaCl, Lanes 9-12: elution with 50 mM Glycine pH 2.3.*

b: *Lane 1: starting material, Lane 2: flowthrough, Lanes 3-5: washes with PBS/0.1% Triton X-100, Lanes 6-7: washes with PBS/0.1% Triton X-100/0.02% SDS, Lane 8: wash with PBS/0.1% Triton X-100/1M NaCl, Lanes 9-12: elution with 1.5 M KSCN, Lanes 13-16: elution with 100 mM Orthophosphoric acid pH 12.5, Lanes 17-20: elution with 6 M Urea, Lanes 21-23: beads after elution with KSCN, Orthophosphoric acid and Urea, respectively.*

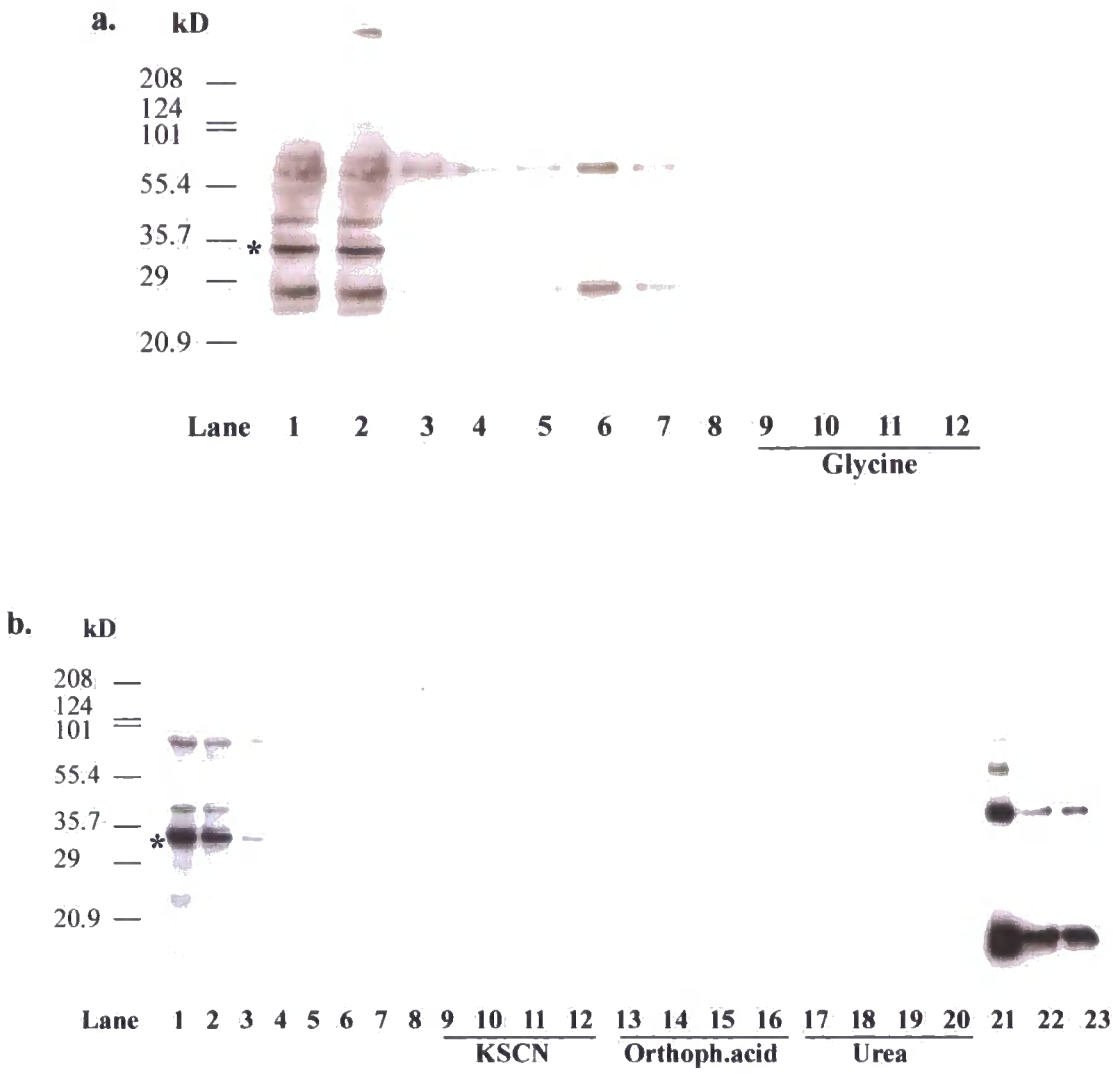

Figure 4.2: Immunoprecipitation experiment of the LAP12 antigen using protein G beads.

4.2.1.2 anti-mouse IgG beads

Since no antibody-antigen interaction was detected using the protein G beads a different approach was used, which involved immobilising the antibody on anti-mouse IgG beads. An extra step of cross-linking the antibody to the beads with 0.02% glutaraldehyde was required in this case. The Immunoprecipitation experiment was repeated as described above. A NEP-A aliquot was extracted with PBS/1% Triton X-100, pH 7.5 and incubated with the antibody. The beads were then washed, eluted with 50 mM Glycine pH 2.3 and samples of all fractions were analysed by Western blotting (Figure 4.3 a). As the figure shows again no antigen was detected in the elution fractions. Instead all the protein was contained in the flowthrough (Figure 4.3 a, lane 2).

The significance of different detergents and pH values in the antibody-antigen binding step was also assessed. Different NEP-A samples were extracted in the presence of a strong denaturing detergent like 0.1% SDS (Figure 4.3 b) or a mild detergent like 0.5% Tween 20 (Figure 4.3 c), and in presence of 1% Triton-X 100 at pH 6.5 (Figure 4.3 d) and pH 8.5 (Figure 4.3 e). NEP-A extracts were incubated with the beads, which were subsequently washed, suspended in SDS sample buffer and analysed by Western blotting. As the figure shows none of these conditions proved sufficient for an antigen-antibody interaction to take place. Furthermore, when Tween 20 was used (Figure 4.3 c) the protein was not extracted from the membrane at all.

Figure 4.3: Immunoprecipitation experiment of the LAP12 antigen using IgG beads.

Xenopus NEP-A fractions were incubated with LAP12 antibody immobilised on IgG beads. To investigate optimum binding conditions aliquots were extracted with PBS/ 1% Triton X-100, pH 7.5 (a), with PBS/0.1% SDS (b), with PBS/0.5% Tween 20 (c), with PBS/1% Triton X-100 pH 6.5 (d) and with PBS/1% Triton X-100 pH 8.5 (e).

The position of the LAP12 antigen is shown by asterisks.

***a:** Lane 1: starting material, Lane 2: flowthrough, Lanes 3-5: washes with PBS/0.1% Triton X-100, Lanes 6-7: washes with PBS/0.1% Triton X-100/0.02% SDS, Lane 8: wash with PBS/0.1% Triton X-100/1M NaCl, Lanes 9-12: elution with 50 mM Glycine pH 2.3.*

***b - e:** Lane 1: starting material, Lane 2: flowthrough, Lanes 3-5: washes with PBS, Lane 6: beads after washes.*

In all cases the extracted protein was contained in the flowthrough fraction (lanes 2) except in case (c) where the protein was not extracted with Tween 20. A small amount of protein detected on the beads in (e), lane 6 was not reproducible.

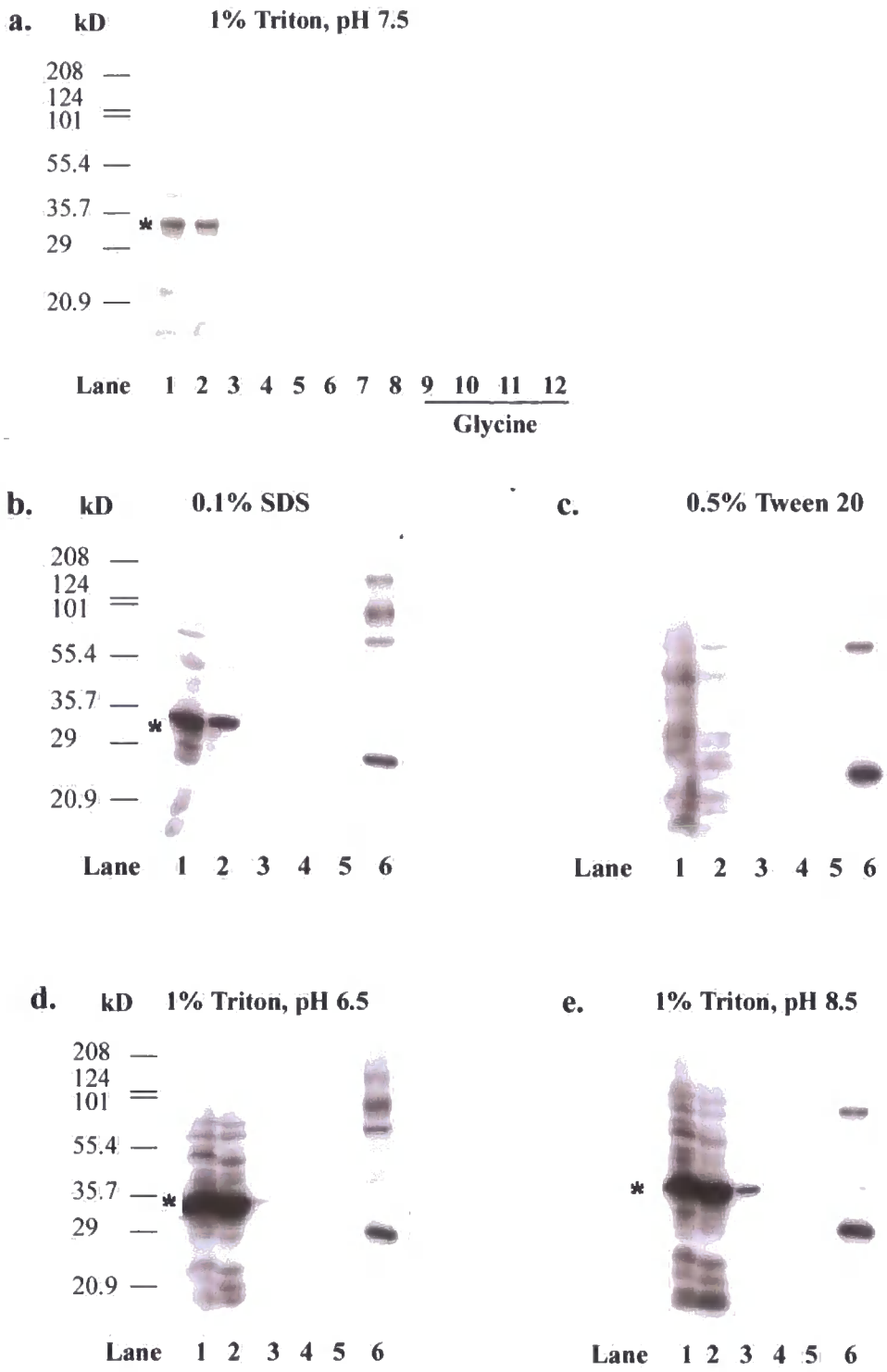

Figure 4.3: Immunoprecipitation experiment of the LAP12 antigen using IgG beads.

To ensure that the antibody binding site on the antigen was not masked by an interaction with any other protein of the membrane, NEP-A fractions were stripped of peripheral and lumenal proteins by washes with MEB containing 500 mM NaCl and 100 mM Na_2CO_3, respectively. The remaining integral membrane proteins were extracted with 1% Triton-X 100, pH 7.5. Extracts were incubated with LAP12-beads, which were washed and eluted with 50 mM Glycine, pH 2.3. Analysis of the samples showed that all of the antigen was again contained in the flowthrough fraction (Figure 4.4).

Figure 4.4: Immunoprecipitation of the LAP12 antigen after clean up of NEP-A membranes from non-integral proteins.

NEP-A membranes were incubated with 500 mM NaCl and 100 mM Na_2CO_3 for removal of peripheral and lumenal proteins, respectively, extracted with PBS/1% Triton X-100 (lane 1) and incubated with LAP12 antibody on protein G beads. After collection of the flowthrough (lane 2) beads were washed with PBS (lanes 3-5) and eluted with 50 mM Glycine pH 2.3 (lanes 6-9). Beads after elution are shown in lane 10. The majority of the protein was contained in the flowthrough.

4.2.2 Purification of antibody aE70

As an alternative approach, an antibody against amino acids 1-70 of human emerin, raised in rabbit, was kindly provided by Dr. R. Rzepecki. The polyclonal serum was then used to further purify the antibody by affinity chromatography on an antigen column. The purification procedure included binding of the antigen (bacterially expressed and purified human emerin peptide consisting of amino acids 1-70) on NHS-activated agarose beads, incubation with the rabbit polyclonal serum diluted 1:10, removing of non-specific binding and antibody elution.

To elute antibodies that are bound by acid- and base-sensitive interactions to the column, elution was performed under conditions of low and high pH, respectively. Thus, 10 ml of 100 mM Glycine pH 2.5 were used to collect ten 1 ml elution fractions and 10 ml of 100 mM Triethylamine pH 11.5 were used to collect another set of ten 1 ml elution fractions. The pH of all elution fractions was neutralised with 1 M Tris pH 8.0. Since it was important to obtain the antibody as concentrated as possible all elution fractions were kept separately and their absorbance at 280 nm was measured in order to find which fraction contained the majority of the antibody. Subsequently, all elution fractions were separately dialysed against PBS/0.02% NaN_3, aliquoted and stored at -20°C.

Measurement of the absorbance at 280 nm (Table 4.1) showed that the majority of the antibody eluted in fraction 2, under both low and high pH conditions.

Elution Fractions-low pH	OD_{280}	Elution Fractions-high pH	OD_{280}
1	-.022	1	-.023
2	**0.140**	**2**	**0.170**
3	-.013	3	-.038
4	0.005	4	-.046
5	0.016	5	0.001
6	-.035	6	-.003
7	0.017	7	-.050
8	0.023	8	-.035
9	0.017	9	-.050
10	0.011	10	0.003

Table 4.1: Measurement of absorbance at 280 nm of elution fractions of purified antibody aE70.

Antibody aE70 was eluted with 100 mM Glycine pH 2.5 (low pH) and 100 mM Triethylamine pH 11.5 (high pH) and the OD_{280} was measured for all elution fractions. The antibody eluted almost exclusively in one fraction (fraction 2) and it eluted almost equally in low and high pH conditions.

4.2.3 Characterisation of the aE70 antigen in human cells

To confirm the successful purification of the antibody, aliquots of elution fractions 2, from both low and high pH elution, were used to detect the antigen in Western blotting experiments. Thus, human emerin peptide 1-70 was resolved on a 15% gel and blotted with elution fractions 2, diluted 1:1000 in BRB/Tween 20/1% NCS (Figure 4.5 a, lanes 1 and 2). In both cases the antigen was correctly recognised as a band of ~ 8 kD.

To further confirm that the protein recognised by the antibody is emerin, normal Human Dermal Fibroblasts (HDF) and fibroblasts from a patient with X-EDMD were analysed by immunoblotting with aE70. In the case of normal HDF the antibody recognised a band of 34 kD (Figure 4.5 a, lane 3), corresponding to human emerin. The band was absent from cells from the X-EDMD patient, which lack emerin (Figure 4.5 a, lane 4). Normal HDF were also grown on coverslips till 80% confluence, fixed with methanol: acetone 1:1 and analysed by immunofluorescence with aE70 (Figure 4.5 b). The antibody gave a rim staining as expected for emerin, an INM protein. Taken together these data show that the antibody is specific for human emerin.

Figure 4.5: Characterisation of the aE70 antigen by immunoblotting and immunofluorescence.

Polyclonal serum of antibody aE70, raised in rabbit against human emerin aa 1-70, was purified on an antigen column. The antibody was eluted with 100 mM Glycine pH 2.5 and 100 mM Triethylamine pH 11.5 and was mainly contained in one elution fraction. Aliquots of each elution fraction, after low and high pH elution, were analysed by Immunoblotting (a, lanes 1 and 2, respectively). In both cases the antigen, emerin peptide 1-70, was recognised confirming the successful purification of the antibody.

Normal HDF (a, lane 3) and X-EDMD fibroblasts (a, lane 4) were also analysed by Immunoblotting with purified aE70. In normal HDF the antibody recognised a protein of 34 kD, which corresponds to emerin. The identity of this protein as emerin is further reconfirmed by the absence of the band in X-EDMD fibroblasts.

Normal HDF were also analysed by immunofluorescence with aE70 (FITC), which gave a rim staining as expected for an INM antibody (b). Chromatin was stained with DAPI. Scale bar is 10 μm.

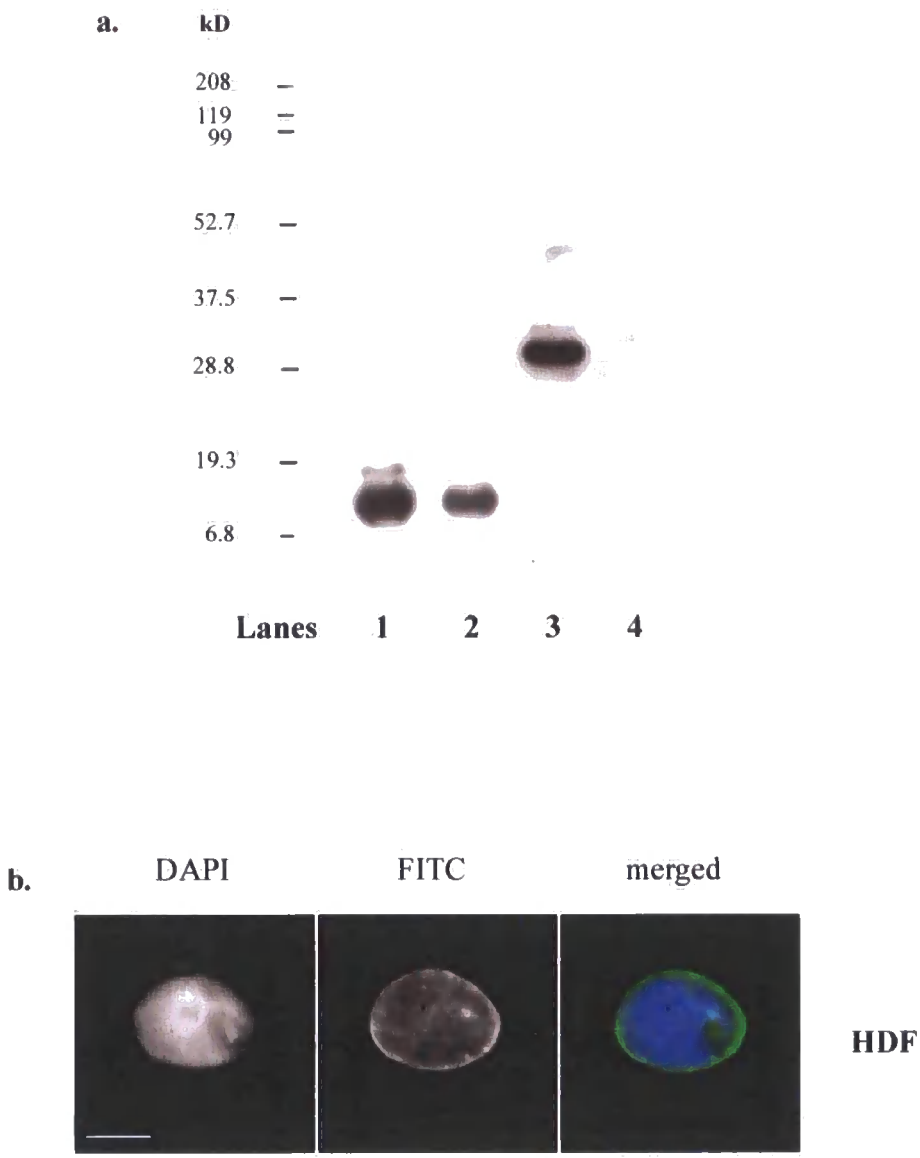

Figure 4.5: Characterisation of the aE70 antigen by immunoblotting and immunofluorescence.

4.2.4 Characterisation of the aE70 antigen in *Xenopus*.

4.2.4.1 Sequence similarity between human and *Xenopus* emerin amino acids 1-70.

Since the aE70 antibody was raised against the first 70 amino acids of human emerin, before attempting to identify an emerin homologue in *Xenopus*, the sequence similarity of human and *Xenopus* emerin was compared. The complete sequence of *Xenopus* emerin was not available at the time of this study. Instead, a nucleotide sequence consisting of 507 bp that corresponds to *Xenopus* emerin could be freely accessed via the NCBI webpage (NCBI at www.ncbi.nlm.nih.gov, Accession number BG407317). The nucleotide sequence, starting from the first ATG, was imported into the BioEdit Sequence Alignment Editor and translated to obtain the corresponding amino acid sequence (Figure 4.6).

```
1     ATG GAA AAT TAT AAA CAC ATG ACT GAC GAT GAA CTT ATT GAA ACC   45
1      M   E   N   Y   K   H   M   T   D   D   E   L   I   E   T   15

46    CTG CAG AAA TGC AAC ATC ACA CAT GGT CCT ATT GTC GGT ACT ACT   90
16     L   Q   K   C   N   I   T   H   G   P   I   V   G   T   T   30

91    CGG ACT TTA TAT GAG AAG AAA CTT TAT GAA TAT GAA CGC AGC AAG   135
31     R   T   L   Y   E   K   K   L   Y   E   Y   E   R   S   K   45

136   ACT AGG AAT CCG TAT CCT CTA GGT TCC TAC GAG AGC AAA ACA CAC   180
46     T   R   N   P   Y   P   L   G   S   Y   E   S   K   T   H   60

181   TAC AGA AAC AGA GCG AAT GAA GAG GAC TTG GCG GAT GAG AAT TAT   225
61     Y   R   N   R   A   N   E   E   D   L   A   D   E   N   Y   75

226   TAC GAA GAG AAA ACA GTT ACC AGA ACC TAC CAG TAT CCC CAA GCA   270
76     Y   E   E   K   T   V   T   R   T   Y   Q   Y   P   Q   A   90

271   CGA CCA CGA ACC ACC TTT GAT CGG CTT GAA CGA GAA CCA CTC TAT   315
91     R   P   R   T   T   F   D   R   L   E   R   E   P   L   Y   105

316   AAA GAA AAC ACG TAC CAG CCC ATA TCC CAG ATG CGC CAT CTG GGG   360
106    K   E   N   T   Y   Q   P   I   S   Q   M   R   H   L   G   120

361   GCA ACA CAG AGG GTA GAG CCT CGC AGG CCA ATC CGT GTG AAG CAA   405
121    A   T   Q   R   V   E   P   R   R   P   I   R   V   K   Q   135

406   AAT GAA GAG AAA CCC TGT AAG   426   nucleotides
136    N   E   E   K   P   C   K   142   amino acids
```

Figure 4.6: Translation of *Xenopus* nucleotide sequence using the BioEdit Sequence Alignment Editor.

A Xenopus emerin sequence consisting of 142 amino acids was obtained by translating the corresponding nucleotide sequence (NCBI, Accession number BG407317) using the BioEdit software.

The first 70 amino acids of *Xenopus* emerin were then compared with the first 70 amino acids of human emerin (Figure 4.7 a). As the figure shows, the sequences share 28 identical amino acids, which are highlighted in red and 11 conservative substitutions. Conserved hydrophobic residues (L, M, V, I, L) are shown in grey, conserved acidic residues (D, E) in yellow, conserved basic residues (R, K) in green, and conserved uncharged polar residues (S, T, Q, Y, N) in blue.

The percentage of identity and similarity between human and *Xenopus* emerin was calculated by performing a BLAST search using the *Xenopus* sequence as a query (Figure 4.7 b). The search displayed human emerin as the result with the highest matching score confirming that this sequence is a *Xenopus* homologue of human emerin and revealed a 49% sequence identity (matching of identical residues) and a 66% sequence similarity (matching of identical and conserved residues or positives). Noticeably, out of the 28 identical amino acids between the two sequences, 24 are contained within the LEM domain (57% identity, 78% similarity), which consists of amino acids 1-45. Therefore, it is probable that apart from emerin, aE70 antibody will recognise and react with other *Xenopus* proteins containing the LEM domain as well.

a.

b.

>gi|30583641|gb|AAP36065.1| emerin (Emery-Dreifuss muscular dystrophy) [Homo sapiens]

Score = 60.8 bits (146), Expect = 9e-09
Identities = 28/57 (49%), Positives = 38/57 (66%)

```
Query:1 MENYKHMTDDELIETLQKCNITHGPIVGTTRTLYEKKLYEYERSKTRNPYPLGSYES 57
        M+NY  ++D EL   L++ NI HGP+VG+TR LYEKK++EYE  + R   P  S  S
Sbjct:1 MDNYADLSDTELTTLLRRYNIPHGPVVGSTRRLYEKKIFEYETQRRRLSPPSSSAAS 57
```

Figure 4.7: Comparison of sequence similarity between *Xenopus* and human emerin amino acids 1-70.

a: *The sequences starting from the first methionine were aligned and compared for identical and conserved amino acids. The comparison revealed that the two sequences have 28 identical amino acids (red), one conserved acidic substitution (yellow), two conserved basic substitutions (green), three conserved hydrophobic substitutions (grey) and five conserved polar uncharged substitutions (blue).*

b: *A BLAST search was performed using the Xenopus amino acids 1-70. The search showed a 49% sequence identity and a 66% similarity (positives) with human emerin. In the result a consensus sequence with all the identical amino acids between Xenopus (query) and human emerin (sbjct) is also displayed. Conserved residues are designated with the + symbol.*

4.2.4.2 Identification of the aE70 antigen in XTC, XLK cells and fractionated *Xenopus* egg extract.

In order to identify proteins recognised by aE70 antibody in *Xenopus*, XTC and XLK cells were analysed by immunofluorescence (Figure 4.8 a) and immunoblotting (Figure 4.8 b, lanes 4 and 5). Immunofluorescence experiments showed that the antibody stained the rim of the nuclei recognising, thus, a protein localised in the NE (Figure 4.8 a, FITC). Immunoblotting analysis showed that in both cell types the antibody recognises mainly a protein of 85 kD, which could correspond to another *Xenopus* LEM domain protein like MAN1 (See also discussion) (Figure 4.8 b, lanes 4 and 5).

To further characterise the aE70 antigen in fractionated egg extracts aliquots of NEP-A and NEP-B vesicles and the cytosol were analysed by immunoblotting. NEP-A and –B membranes were extracted with EB containing 1% Triton X-100, mixed with an equal volume of SDS-sample buffer and immunoblotted with aE70. A cytosolic aliquot was also mixed with SDS-sample buffer and analysed by western blotting. (Figure 4.8 b, lanes 1, 2 and 3). Between the two vesicle populations the main protein recognised by the antibody resided in NEP-A vesicles and had a Mr of 30 kD (Figure 4.8 b, lane 1). The size of this protein and the high degree of similarity between the human and *Xenopus* LEM domain could suggest that the 30 kD protein corresponds to *Xenopus* emerin. However, no direct proof for that is provided. The antibody also reacted with a soluble cytosolic protein of 37.5 kD (Figure 4.8, lane 3).

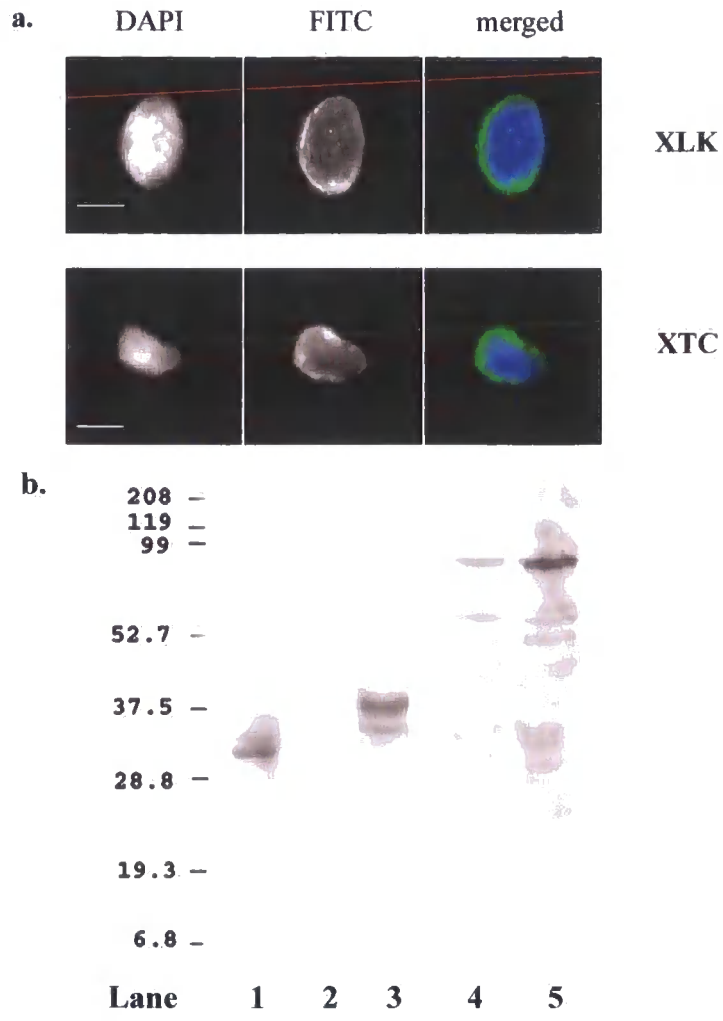

Figure 4.8: Characterisation of the aE70 antigen in *Xenopus*.

Xenopus XLK and XTC cells were grown till 80% confluence, fixed with methanol:acetone and processed by immunofluorescence (a) or immunoblotting (b, lanes 4 and 5) with purified antibody aE70. Aliquots of NEP-A and –B vesicles and the cytosol were also analysed by immunoblotting (b, lanes 1, 2 and 3, respectively). Immunofluorescence experiments in both cell types revealed a clear rim staining, which is characteristic for NE proteins (a, FITC). DAPI was used to stain chromatin. When the antibody was used in immunoblotting experiments on XTC (b, lane 4) and XLK (b, lane 5) it recognised a band of about 85 kD. The antibody also reacted with a protein of about 30 kD on NEP-A vesicles (lane 1), no protein on NEP-B vesicles (lane 2) and a protein of about 37 kD in the cytosol (lane 3). Scale bars are 10 µm.

4.2.5 Time-course study of the aE70 antigen assembly into the nuclear envelope

Since the aE70 antigen was found to be contained within the NEP-A vesicles, a time-course experiment was set up to investigate its incorporation into the reforming nuclear envelope in *Xenopus* egg extracts. Nuclei were assembled at room temperature for 0, 10, 20, 40 and 80 minutes, fixed with EGS, centrifuged onto coverslips and processed by immunofluorescence with aE70 (Figure 4.9).

The first signal appeared around chromatin at 20 minutes after initiation of nuclear assembly and gradually increased (40 minutes) till a uniform staining around the nuclei was observed at 80 minutes. This staining pattern is in agreement with the staining of NEP-A vesicles with antibody CEL13A (compare Figure 4.9 with Figure 3.3) where the first signal was also observed at 20 minutes, in contrast to NEP-B vesicles which appeared around chromatin at 10 minutes (Figure 3.2).

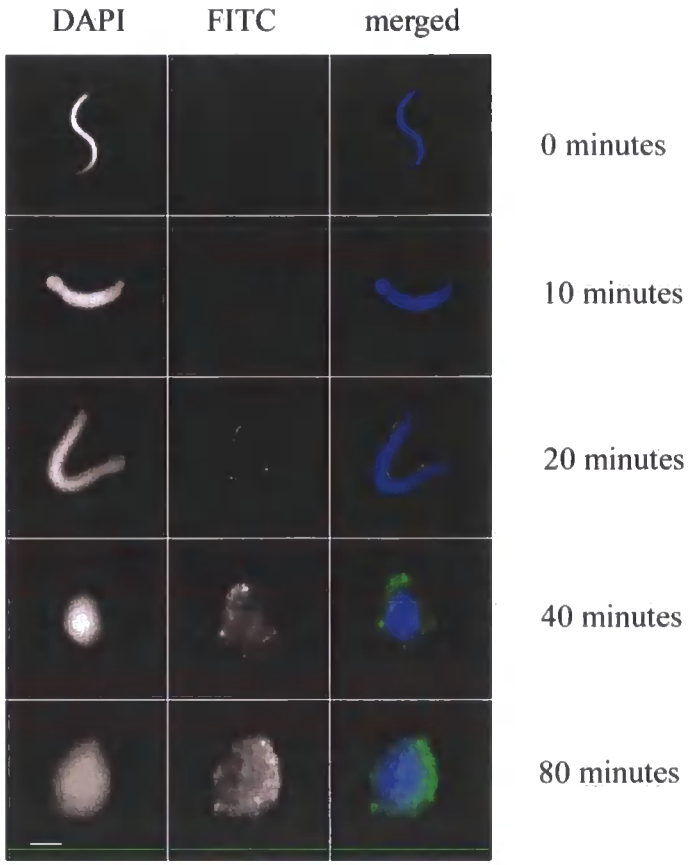

Figure 4.9: Incorporation of the aE70 antigen into the NE during nuclear assembly in *Xenopus* egg extracts.

Nuclei were assembled in Xenopus egg extracts for 0, 10, 20, 40 and 80 minutes and analysed by immunofluorescence with antibody aE70 (FITC). Chromatin decondensation was observed with DAPI. As shown the first appearance of the antigen around chromatin occurred at 20 minutes, which coincides with the appearance of NEP-A vesicles around chromatin. More protein was observed around chromatin at 40 minutes, and at 80 minutes a rim staining was observed. Bar is 10 μm.

4.3 DISCUSSION

Xenopus cell-free extracts are widely used as an experimental system for the functional analysis of nuclear envelope proteins. However, so far little is known about the presence and distribution of several known INM proteins in fractionated egg extracts. Two different antibodies were used in this study to identify emerin in *Xenopus*: a mouse monoclonal antibody called LAP12, and a polyclonal antibody purified on an antigen column called aE70.

LAP12 is a mouse monoclonal antibody that recognises the LEM domain of human LAP2β. The use of this antibody to detect *Xenopus* emerin was justified by the fact that the LEM domain is shared between LAP2 and emerin and it displays a high degree of similarity between the proteins and the species it is found in. Immunoblotting analysis on fractionated egg extract revealed a major band of ~ 34 kD contained in the NEP-A fraction. The LAP12 antigen had the correct size of 34 kD for it to be emerin. Also its identity as any other known LEM domain protein was excluded since the *Xenopus* LAP2 protein (XLAP2) was shown to be absent from egg extracts and oocytes (Lang *et al.*, 1999) and *Xenopus* MAN1 (XMAN1) has a much bigger size with a Mr of 88.5 kD (Osada *et al.*, 2003).

Unfortunately, attempts to obtain the antigen by immunoprecipitation and subsequently identify it were unsuccessful. Although the antigen was recognised on a western blot, no antigen-antibody interaction could take place when the antibody was immobilised on a column. Different approaches were used by immobilising the antibody on protein G or IgG beads with no success in both cases. Also extraction,

binding and elution conditions were varied. Extraction of NEP-A fractions with three detergents ranging from very mild to strong was performed: Tween 20, a very mild detergent that keeps proteins in their native form; Triton X-100, a stronger, non-ionic, weakly denaturing detergent, and Sodium dodecyl sulphate (SDS), an anionic, excellent solubilising but highly denaturing agent were used. pH conditions ranging form 6.5 to 8.5 were also varied to see whether they affect the binding of the antigen to the antibody. Also different elution methods were used. Elution was attempted under both, low and high pH conditions (glycine, pH 2.3 and orthophosphoric acid, pH 12.5, respectively). Harsher elution methods with a dissociating agent like urea and chaotropic ions like SCN^- ions were also employed. None of the above conditions proved efficient for obtaining the LAP12 antigen. Finally, the possibility that the epitope recognised by the antibody is masked by an interaction with another membrane protein was also investigated. NEP-A fractions were treated prior to incubation with the antibody, with a high ionic strength solution (0.5 M NaCl), which results in solubilisation of peripheral membrane proteins, and with Na_2CO_3, which results in removal of lumenal proteins. Again no antigen-antibody interaction was detected. It is not clear why the antigen was recognised by the antibody only in its denatured form on a western blot and not on a column. As investigating the right conditions and possible reasons proved to be very time consuming an alternative approach using a different antibody was employed.

Antibody aE70 was raised against the first 70 amino acids of human emerin and was used in immunoblotting and immunofluorescence experiments in *Xenopus* adult cells and egg extracts. The rabbit polyclonal antibody was first purified on an antigen column to improve its quality. The successful purification of the antibody was

confirmed by immunoblotting experiments in which the antibody was able to recognise its antigen, emerin peptide 1-70. Its specificity for human emerin was confirmed in western blots of normal Human Dermal Fibroblasts (HDF) in which a 34 kD band corresponding to emerin was recognised. The major recognised band was absent from blots of emerin-null X-EDMD fibroblasts further confirming the identity of the protein as emerin. In immunofluorescence microscopy of normal HDF purified aE70 reacted with the nuclear periphery and displayed a rim staining characteristic of INM proteins.

After the specificity of aE70 for human emerin was confirmed the antibody was used in *Xenopus* adult cells and egg extracts. While the present investigation was in progress the full-length sequence of *Xenopus* emerin was not known. However, a partial sequence that included the LEM domain was available online, and this sequence was used to compare the *Xenopus* LEM domain with the human. The comparison revealed that the two sequences share a significant degree of identity (57%) and similarity (78%). Based on this, aE70 was used in an attempt to identify *Xenopus* emerin.

Only very recently, after the completion of the present investigation, the complete sequence of *Xenopus* emerin has been published (Gareiss *et al.*, 2005). According to Gareiss *et al.* there are two emerin homologues in *Xenopus*, Xemerin1 and Xemerin2. Both are 24 kD in size and differ by 24 amino acids scattered throughout the sequence, which implies that they are products of separate genes. When the expression pattern of emerin during embryogenesis was investigated emerin was not

detected in oocytes and eggs. Instead emerin expression was shown to start from stage 43 onwards.

Immunofluorescence microscopy with the aE70 antibody on somatic XLK and XTC cells and in nuclei assembled in unfractionated egg extracts revealed a rim staining indicating the recognition of NE proteins. In immunoblotting experiments of adult XTC and XLK cells the antibody recognised a protein of ~ 85 kD. The size of this protein is too high for it to be emerin, which is 24 kD. Although no protein of that size was detected in somatic cells it is rather unlikely that emerin is not present in adult cells. The inability to detect a protein that could correspond to emerin could be due to the low levels of emerin relative to the 85 kD protein or due to the antibody used. Also tadpoles correspond to stage 40 embryos and emerin was shown to be expressed from stage 43 onwards (Gareiss *et al.*, 2005). Although the identity of the 85 kD protein is not known it could correspond to another *Xenopus* LEM domain protein considering that it is a highly conserved domain. In addition to emerin, two other LEM domain proteins are known in *Xenopus*, XLAP2 and XMAN1.

Studies on *Xenopus* LAP2 revealed that out of the three mammalian LAP2 isoforms (LAP2α, β and γ) only LAP2β is represented in *Xenopus* and its expression is regulated during development. The *Xenopus* homologue of LAP2β, XLAP2, which has a size of 68 kD, is present only in somatic and adult cells and is absent from oocytes and unfertilised eggs. In these early stages of development a second LAP2 related polypeptide with an Mr of 84 kD was detected while another protein of 35 kD, probably unrelated to LAP2, was also detected. Although the expression of the 84 kD protein did decrease during development and was no longer detectable in swimming

tadpoles the possibility that the 84 kD protein is expressed in the adult organism was not ruled out (Lang *et al.*, 1999). In this study a protein of very similar Mr was detected in adult cells. The other known LEM domain protein in *Xenopus*, XMAN1, has an Mr of 88.5 kD and is expressed throughout development with levels that are constant during embryogenesis (Osada *et al.*, 2003). It is not clear whether the 84 kD protein recognised by aE70 corresponds to the *Xenopus* LAP2 or MAN1 protein since the two proteins are 41% identical and 71% similar to each other.

In fractionated *Xenopus* egg extracts, aE70 antibody recognised a protein of ~ 30 kD contained exclusively in NEP-A membranes as revealed by immunoblotting experiments. The size of this protein suggests that it could correspond to *Xenopus* emerin, however, no definite evidence for that is provided. To further characterise the aE70 antigen nuclei were allowed to assemble in unfractionated egg extracts for times ranging from 0 to 80 minutes and processed by immunofluorescence. The aE70 antigen appeared around chromatin at a late stage of nuclear formation displaying a chromatin association pattern similar to that of NEP-A vesicles rather than NEP-B, as described in Chapter 3. This is in agreement with the exclusive localisation of the aE70 antigen in NEP-A membranes as shown by immunoblotting. Even though the exact identity of the aE70 antigen cannot be concluded form the above results, the antibody was shown to recognise in egg extracts a LEM domain protein of ~ 30 kD present in NEP-A membranes and with a similar chromatin association pattern to NEP-A during nuclear assembly.

In addition to aE70, LAP12 antibody raised against the LEM domain of human LAP2β, recognised a protein of 36 kD also localised in the NEP-A membrane

fraction. Thus, in total, two antibodies (aE70 and LAP12) raised against LEM domains recognise two different proteins (30 and 36 kD, respectively), both residing in NEP-A membranes. This provides an explanation for the preferential inhibition of NEP-A recruitment to chromatin by exogenously added LEM domain containing human emerin peptides as described in Chapter 3.

CHAPTER 5

INVESTIGATION OF EMERIN BINDING PARTNERS IN THE *XENOPUS* CYTOSOL

5.1 INTRODUCTION

The importance of emerin at the nuclear envelope and the implications of its absence in disease led to an intense interest in its function. One approach to elucidate the function of a protein is to identify the proteins interacting with it. So far well characterised emerin binding proteins include lamin A, the chromatin protein BAF and transcription factor GCL (Clements *et al.*, 2000; Holaska *et al.*, 2003).

Evidence supporting the above interactions derives mainly from immunofluorescence and immunoprecipitation experiments in mammalian cells. Emerin antibodies were shown to immunoprecipitate lamins A/C and B from C2C12 myoblast and rat hepatocyte nuclear extracts (Fairley *et al.*, 1999) or from rabbit reticulocyte lysates (Vaughan *et al.*, 2001). A direct interaction between emerin and lamin A has been shown using the BIAcore assay (Clements *et al.*, 2000). Blot overlay and microtiter well binding assays were also employed in confirming emerin interactions. In these experiments recombinant emerin was immobilised on nitrocellulose or on microtiter wells, respectively, and incubated with ^{35}S-labelled proteins. Binding of emerin to lamin A (Lee *et al.*, 2001), BAF (Lee *et al.*, 2001; Segura-Totten *et al.*, 2002), GCL (Holaska *et al.*, 2003) and actin (Holaska *et al.*, 2004) was reported this way. Additional attempts to identify emerin binding partners included yeast-two-hybrid screens of a human heart cDNA library and of a HeLa cell cDNA library leading to the identification of YT-521B and Btf, respectively (Haraguchi *et al.*, 2004; Wilkinson *et al.*, 2003).

In this study the four emerin peptides consisting of residues 1-70, 1-176, 1-220 and 73-180 were immobilised via their His-tag on Ni-beads and used to fish for emerin interacting proteins from the cytosolic fraction of *Xenopus* egg extracts. Following washing, emerin peptides and interacting proteins were eluted from the beads and analysed by 1-D and 2-D gel electrophoresis. Two similar experiments in which emerin affinity columns were created and used to identify interacting proteins have been performed in the past. These experiments, however, used nuclear extracts from rat skeletal muscle and liver (Sakaki *et al.*, 2001) and HeLa nuclear extracts (Bengtsson and Wilson, 2004; Holaska *et al.*, 2004). In the present study the *Xenopus* egg cytosol was used for the first time as a source to identify emerin interacting proteins.

For the identification of the emerin interacting candidates Matrix-assisted laser desorption and ionisation time-of-flight mass spectrometry (MALDI-TOF) and peptide mass fingerprinting (PMF) were employed. Two different sets of experiments identified β-tubulin as an emerin interacting protein. Subsequent immunofluorescence analysis of X-EDMD cells, which lack emerin, with a β-tubulin antibody revealed no alterations in the organisation of the MT network. The most prominent phenotype was a mis-localisation of the Microtubule Organising Centre (MTOC) far from the nucleus in cells which lack emerin. This observation was also confirmed with a centrosome-specific antibody.

5.2 RESULTS

5.2.1 Investigation of emerin binding partners in *Xenopus* cytosol by affinity chromatography

In an attempt to identify new binding partners for emerin, peptides consisting of amino acids 1-70, 1-176, 1-220 and 73-180 were used to co-precipitate interacting proteins from *Xenopus* cytosol. The constructs were expressed in bacteria and purified under both, native and denaturing conditions, immobilised on Ni^{+2}-beads and incubated with the cytosol (diluted 1:4) for 4 hours at 4°C. Non-specifically bound proteins were removed with washes in 250 mM NaCl and elution was achieved with high urea concentration (250 mM). Elution fractions were precipitated with ice-cold acetone and analysed by 1-D or 2-D gel electrophoresis. Potential targets were subsequently cut form the gels and identified by mass spectroscopy.

5.2.1.1 1-D gel analysis and mass spectroscopic identification of targets

As a first step, all emerin peptides were purified in their native conformation and incubated with the cytosol. Eluates were resolved on 12% and 15% 1-D gels. Purification of the emerin peptides rarely resulted in 100% pure samples. To avoid picking as positive results proteins that were already present in the emerin samples, as contaminants, during their purification in bacteria, aliquots of the emerin peptides only (not incubated with *Xenopus* cytosol) were resolved on the gels in parallel. As a second control *Xenopus* cytosol was incubated with Ni^{+2}-beads in absence of any

emerin peptide to ensure that none of the positive results with emerin were non specific.

After electrophoresis gels were stained with Coomassie and examined carefully for potential emerin interacting proteins. 12% gels of all samples are shown in Figure 5.1 and 15% gels are shown in Figure 5.2. In both cases, bands that were unique in the emerin-cytosol lanes (Figures 5.1 and 5.2, lanes 4, 6, 8 and 10) were identified as potential targets. Bands that were common between the emerin-cytosol (lanes 4, 6, 8 and 10) and the emerin alone (lanes 3, 5, 7 and 9) and cytosol alone (lanes 2) samples were ignored. Several of the selected targets did not co-precipitate preferentially with one emerin peptide only but with all of them. In that case the band cut out of the gel was randomly selected from lanes 4, 6, 8 or 10.

In total 13 bands were picked from the gels, which are marked with red arrowheads in Figures 5.1 and 5.2. The bands were digested with trypsin and identified by peptide mass fingerprinting. The results of the mass spectroscopy are shown in Table 5.1. For each sample the peptide that was used as bait and the protein with the highest matching score are displayed. All scores were statistically significant except the ones marked with an asterisk. Information on the species and the mass of the identified proteins is also provided.

As the table shows, although care was taken to avoid false positives by using two types of control (emerin only and cytosol only), four of the targets (samples 1, 4, 9 and 12) were identified as *E. coli* proteins. This clearly shows that the resolution of 1-D gels is not sufficient to eliminate false positive results. Although two of the *E. coli* proteins (samples 4 and 9) did not appear as statistically significant results, one

protein, sample 1, was identified as DNAK with a very high score. The presence of DNAK, which is the bacterial homologue of HSP70, was probably required during the purification of the emerin peptides for correct folding. The second *E. coli* protein, sample 12, is a common contaminant when Ni^{+2}–beads are being used.

Furthermore, incubation of the beads with BSA prior to addition of the cytosol in an attempt to reduce non specific binding of proteins to the beads, ironically resulted in albumin as one of the identified targets (sample 6). Also, samples 7 and 11 were identified as human emerin and could correspond to degradation products of the purified peptides and samples 5 and 13 could not be identified. Sample 8 was identified as a *Xenopus* protein MGC83078. A BLAST search using the corresponding amino acid sequence was performed and the protein with the highest matching score proved to be the *E. coli* protein peroxiredoxin. Considering that peroxiredoxin is one of the ten most abundant proteins in *E. coli* it is rather unlikely that this is a functionally significant result (Wood *et al.*, 2003).

Thus, out of the 13 samples, only 3 *Xenopus* proteins were considered as potentially significant, samples 2, 3 and 10, which correspond to calcineurin or protein phosphatase 2B, tubulin β2 and profilin 1. As a first step, the interaction of one of them, profilin, with emerin was further investigated.

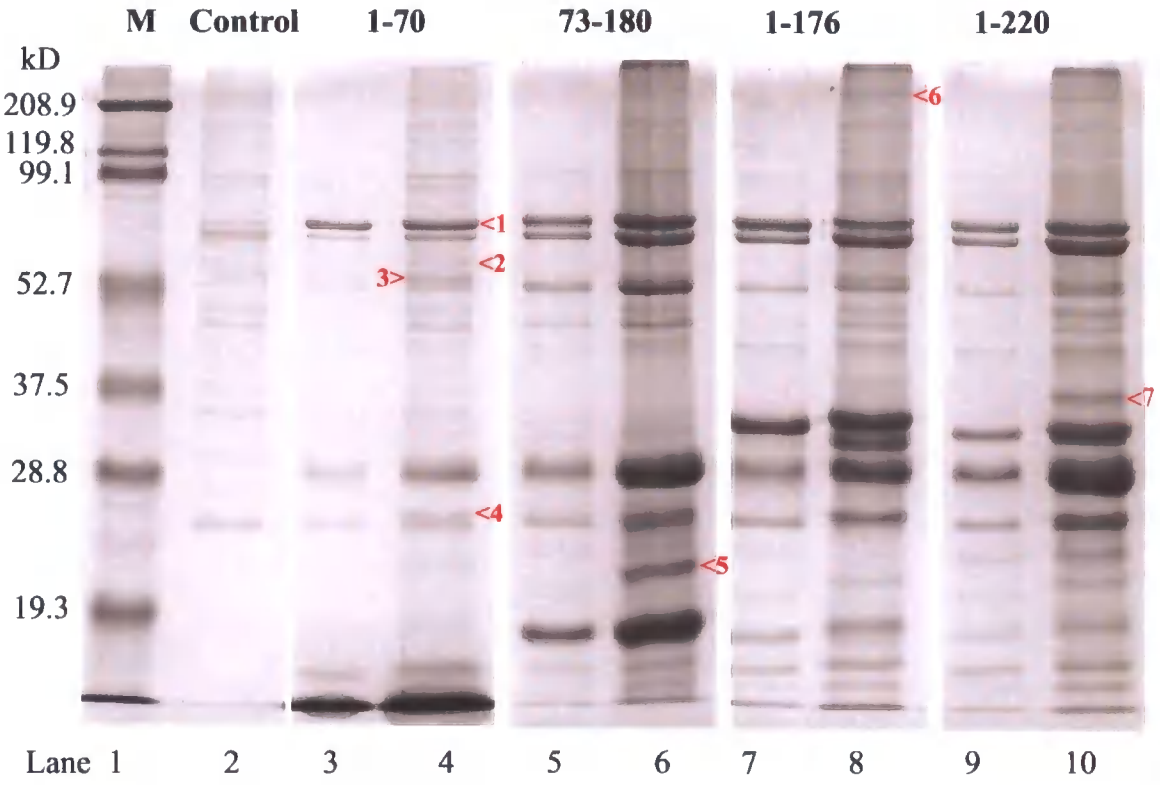

Figure 5.1: Co-precipitation of emerin interacting proteins from *Xenopus* cytosol and analysis by 1-D SDS-PAGE on a 12% gel.

Emerin peptides 1-70, 73-180, 1-176 and 1-220 were incubated with Xenopus cytosol in order to identify new binding partners and resolved on a 12% gel. The gel was loaded as following: Lane 1: Markers (kD), Lane 2: Control (Beads + Xenopus cytosol only), Lane 3: 1-70 only, Lane 4: 1-70 + Cytosol, Lane 5: 73-180 only, Lane 6: 73-180 + Cytosol, Lane 7: 1-176 only, Lane 8: 1-176 + Cytosol, Lane 9: 1-220 only, Lane 10: 1-220 + Cytosol.

Seven bands that were unique to the emerin-cytosol lanes, marked with red arrowheads, were cut from the gel and sent for mass spectroscopic analysis.

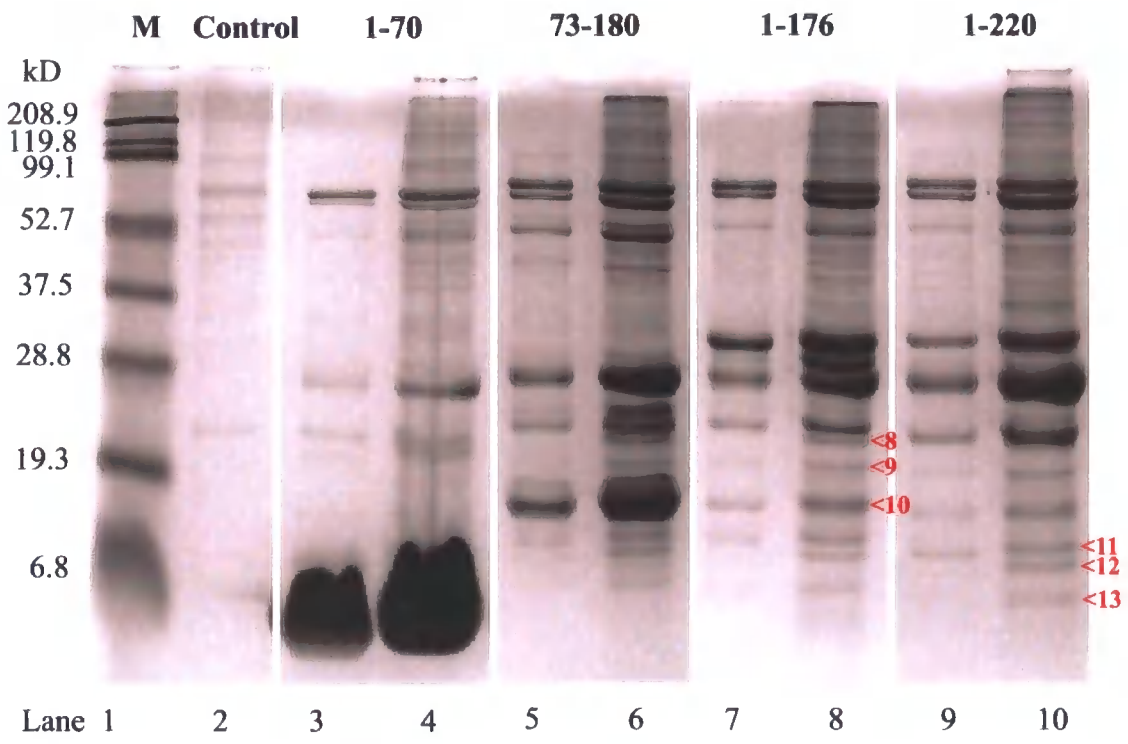

Figure 5.2: Co-precipitation of emerin interacting proteins from *Xenopus* cytosol and analysis by 1-D SDS-PAGE on a 15% gel.

Emerin peptides 1-70, 73-180, 1-176 and 1-220 that were incubated with Xenopus cytosol were also resolved on a 15% gel. The gel was loaded as following: Lane 1: Markers (kD), Lane 2: Control (Beads + Xenopus cytosol only), Lane 3: 1-70 only, Lane 4: 1-70 + Cytosol, Lane 5: 73-180 only, Lane 6: 73-180 + Cytosol, Lane 7: 1-176 only, Lane 8: 1-176 + Cytosol, Lane 9: 1-220 only, Lane 10: 1-220 + Cytosol. Six bands (No 8-13), marked with red arrowheads, were cut from the gel and sent for mass spectroscopic analysis.

Sample	Bait	Highest match	Species	Mass	Score
1	1-70	DNAK	*E. coli*	69.165	234
2	1-70	Calcineurin catalytic subunit	*X. laevis*	58.059	56
3	1-70	Tubulin β2	*X. laevis*	50.072	76
4	1-70	Cap-Dna recognition	*E. coli*	23.683	56 *
5	73-180	No hit	—	—	—
6	1-176	Albumin	*B. taurus*	71.244	56
7	1-220	Emerin	*H. sapiens*	29.033	76
8	1-176	MGC83078	*X. laevis*	22.653	71
9	1-176	Ecs1486	*E. coli*	21.441	73 *
10	1-176	Profilin 1	*X. laevis*	16.925	90
11	1-220	Emerin	*H. sapiens*	29.056	212
12	1-220	Ni^{+2}-responsive regulatory protein	*E. coli*	15.199	79
13	1-220	No hit	—	—	—

Table 5.1: Mass spectroscopic identification of proteins co-precipitating with emerin as shown on 1-D gels.

Bands 1-13 that were selected from 12% and 15% gels (shown in Figures 5.1 and 5.2) were identified by peptide mass fingerprinting. The table summarises the results showing for each sample which emerin peptide was used as the bait, the highest corresponding match, the species it belongs to, its molecular weight (in kD) and its score. Scores marked with an asterisk, although the highest for the corresponding samples, were statistically insignificant. All other scores were statistically significant.

5.2.1.2 Investigation of the emerin-profilin interaction by the yeast-two-hybrid assay

To examine whether profilin is able to interact with emerin, the yeast-two-hybrid system was employed. Emerin, cloned in a vector that contains the Binding domain of GAL4, and profilin, cloned in a vector that contains the Activating domain, were transformed into yeast, which were then mated and selected for diploids. The occurrence of an interaction was assessed by plating the diploids on plates with four media combinations: SD –Leu/Trp, SD –Leu/Trp/His, SD –Leu/Trp/Ade and SD –Leu/Trp/His/Ade. After a 3-day incubation at 30°C yeast growth was observed only in medium stringency conditions, namely in the SD –Leu/Trp and SD –Leu/Trp/His plates (Figure 5.3). No growth developed in the SD –Leu/Trp/Ade and SD –Leu/Trp/His/Ade plates.

Diploids grown on a SD –Leu/Trp plates were also used for the β-galactosidase assay. After addition of the substrate of the enzyme (X-gal) and incubation at room temperature no development of blue colour was observed. Since diploid growth was observed only in medium stringency conditions and the β-galactosidase assay was negative it can be concluded that an emerin–profilin interaction did not occur in this assay.

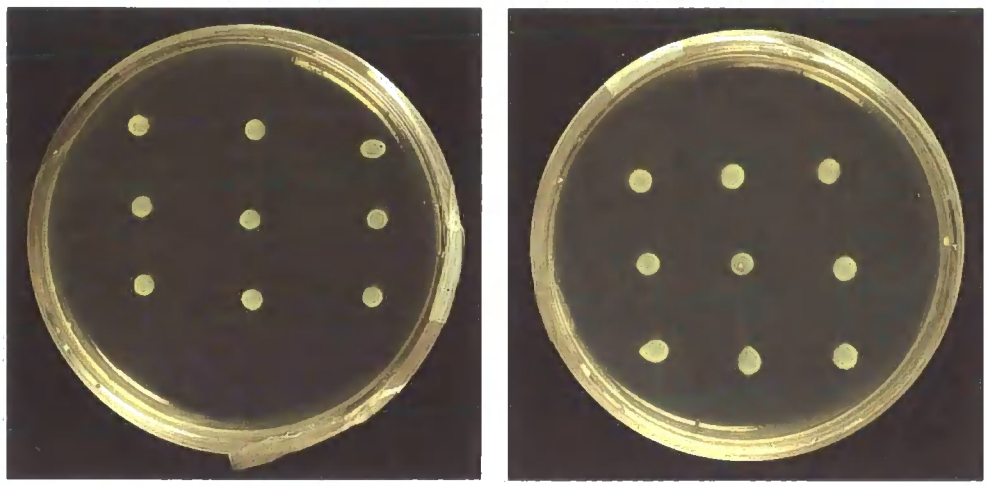

SD -Trp/Leu **SD -Trp/Leu/His**

Figure 5.3: Investigation of the emerin-profilin interaction using the yeast-two-hybrid system.

The picture shows the growth of yeast cells transformed with emerin and profilin on plates containing SD –Leu/Trp, SD –Leu/Trp/His.

5.2.1.3 2-D gel analysis and mass spectroscopic identification of targets

The resolution provided by 1-D gel electrophoresis did not prove to be sufficient to eliminate false positive results in the emerin co-precipitation experiments since many of the selected targets turned out to be *E. coli* proteins (Table 5.1).

Thus, the analysis of the samples by 2-D gel electrophoresis was considered to be more appropriate. Pull-down experiments were performed exactly as described earlier (Section 5.2.1) and precipitated elution fractions were loaded on pH 4-7 gel strips for the first dimension, and on 12% SDS gels for the second dimension. As a control, both emerin peptides alone and *Xenopus* cytosol incubated with beads in absence of emerin, were used in parallel.

Also one target protein identified by 1-D gel electrophoresis was the *E. coli* HSP70 probably bound to human emerin peptides during their purification (Young *et al.*, 2004). HSP70 being a chaperone would have the ability to bind other proteins of the *Xenopus* cytosol during the co-precipitation procedure. So even if proteins were selected that are unique in the emerin-cytosol samples and absent from both control types there is still a possibility that they are bound to HSP70 rather than emerin. Indeed, for all of the already identified proteins like calcineurin and tubulin, several reports exist about their ability to interact with HSP70 (Marchesi and Ngo, 1993; Sanchez *et al.*, 1994; Someren *et al.*, 1999).

For this reason emerin peptides were purified in presence of urea in an attempt to destroy the emerin-HSP70 interaction removing this way the chaperone as a

contaminant. After purification, peptides were refolded by dialysing for 3 hours at room temperature against MEB and subsequently used for the co-precipitation experiments. Only emerin peptides 1-70 and 73-180 were analysed this way since their small size allowed successful refolding. For comparison peptides purified in their native form were also analysed by 2-D gel electrophoresis.

Results for peptide 1-70, used after purifying it in its native conformation, are shown in Figure 5.4. Careful examination of the gels revealed three proteins that specifically co-precipitated with emerin, shown with a red, green and blue arrowhead in Figure 5.4 b. A fourth spot marked with a black arrowhead was chosen to confirm its identity as HSP70. The four protein spots were cut out of the gel and sent for mass spectroscopic analysis. The proteins were identified as HSP70 (black) and tubulin-β2 (red). Proteins marked with a green and blue arrowhead could not be identified.

To ensure that the presence of tubulin is because of an interaction with emerin and not HSP70 the same experiment was performed but this time using emerin purified in urea and refolded. The results are shown in Figure 5.5. Although examination of the gels revealed as before very few protein spots unique in the emerin-cytosol gel (gel b) in comparison to controls, the spot corresponding to tubulin was still present (gel b, red arrowhead). Furthermore, purification of emerin in presence of urea successfully removed HSP70 as a contaminant showing that co-precipitation of tubulin is due to an interaction with emerin. The absence of HSP70 is shown with the black arrowhead in gel b (compare black arrowhead in Figure 5.5 b with black arrowhead in Figure 5.4 b).

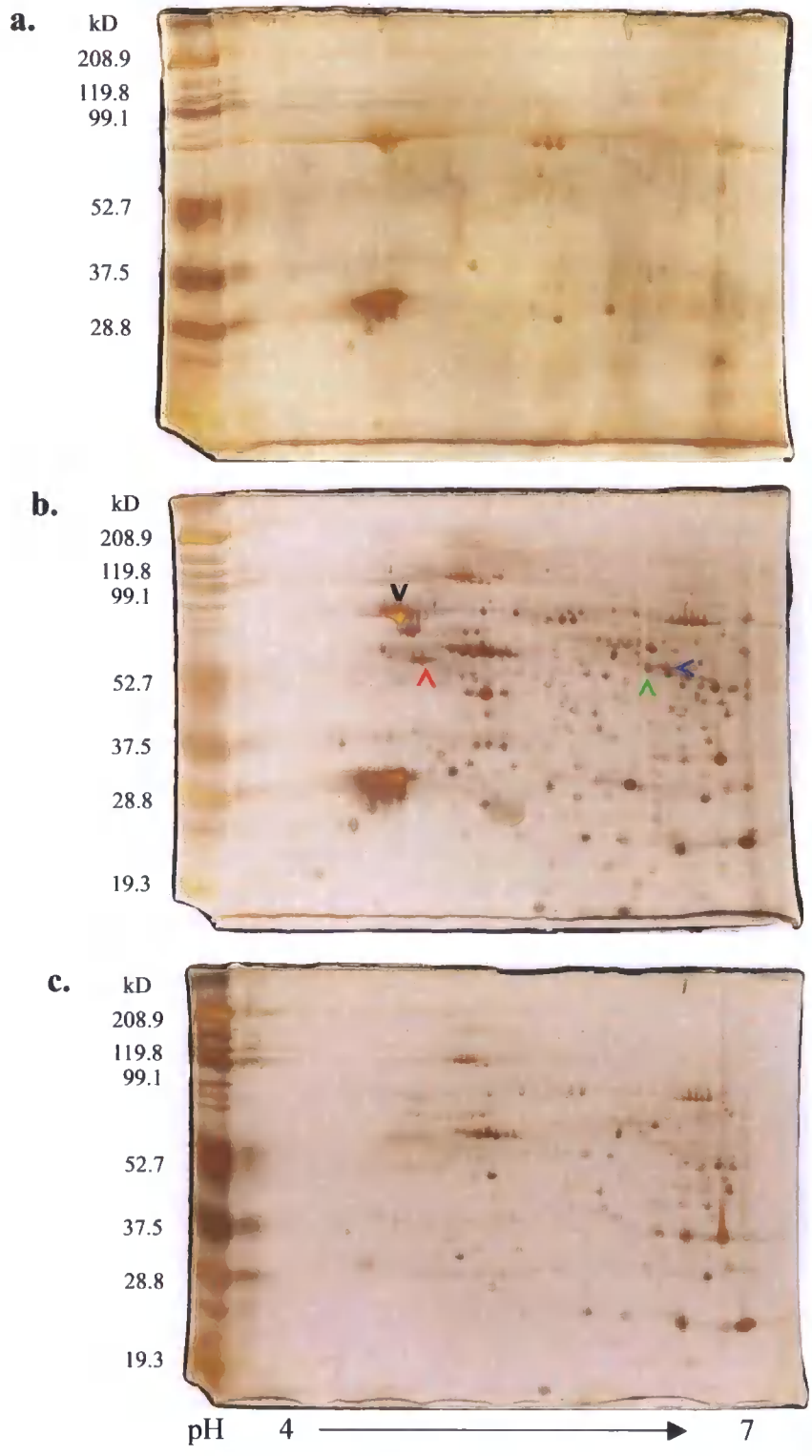

Figure 5.4: Co-precipitation of *Xenopus* cytosolic proteins with emerin peptide 1-70 purified under native conditions.

a: *emerin 1-70 only,* ***b:*** *emerin 1-70 – Xenopus cytosol,* ***c:*** *Xenopus cytosol only*

Coloured arrowheads indicate spots that were sent for mass spectroscopic analysis.

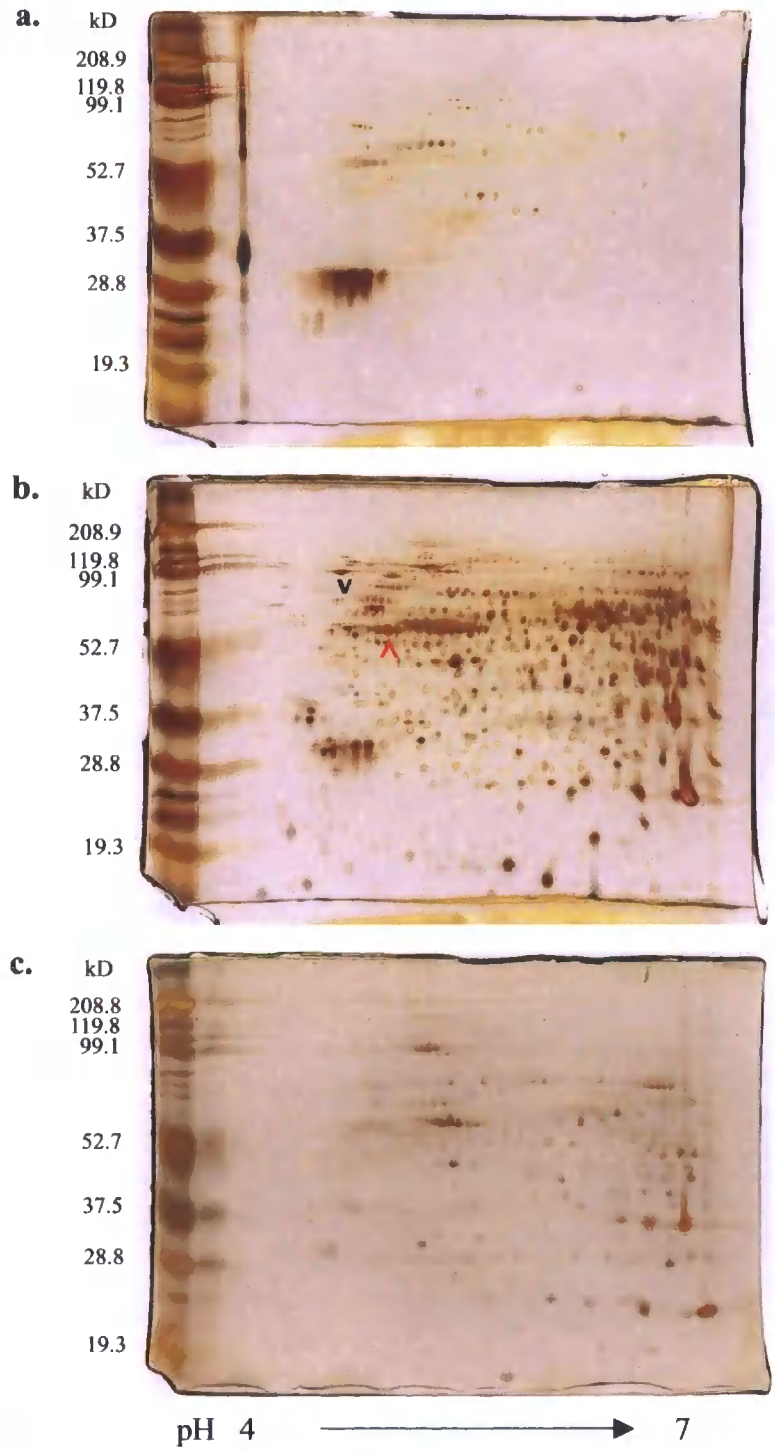

Figure 5.5: Co-precipitation of *Xenopus* cytosolic proteins with emerin peptide 1-70 purified under denaturing conditions.

a: *emerin 1-70 only,* ***b:*** *emerin 1-70 – Xenopus cytosol,* ***c:*** *Xenopus cytosol only*

The red arrowhead indicates a protein spot that was sent for mass spectroscopic analysis. The absence of HSP70 is shown by the black arrowhead.

In a similar way emerin 73-180 was used to co-precipitate *Xenopus* cytosolic proteins. The results are shown in Figures 5.6 and 5.7. When emerin was purified in its native conformation except from HSP70 (Figure 5.6 b, black arrowhead), tubulin-β2 was also detected (Figure 5.6 b, red arrowhead). As for emerin 1-70, the interaction with tubulin (Figure 5.7 b, red arrowhead) was still present in the absence of HSP70 (Figure 5.7 b, black arrowhead). The identity of two more protein spots (Figure 5.7 b, grey and turquoise arrowheads) could not be found.

A summary of all mass spectrometric data obtained from 2-D gels (Figures 5.4-5.7) is presented in Table 5.2. Although four of the selected targets could not be identified (samples 1-4) tubulin-β2 was identified as an interacting protein with emerin amino acids 1-70 and 73-180. The interaction seemed to be emerin specific since it occurred even in the absence of HSP70, when urea purified and refolded emerin peptides were used. The acquired MS spectrum of the peptide identified as β-tubulin is shown in Figure 5.8.

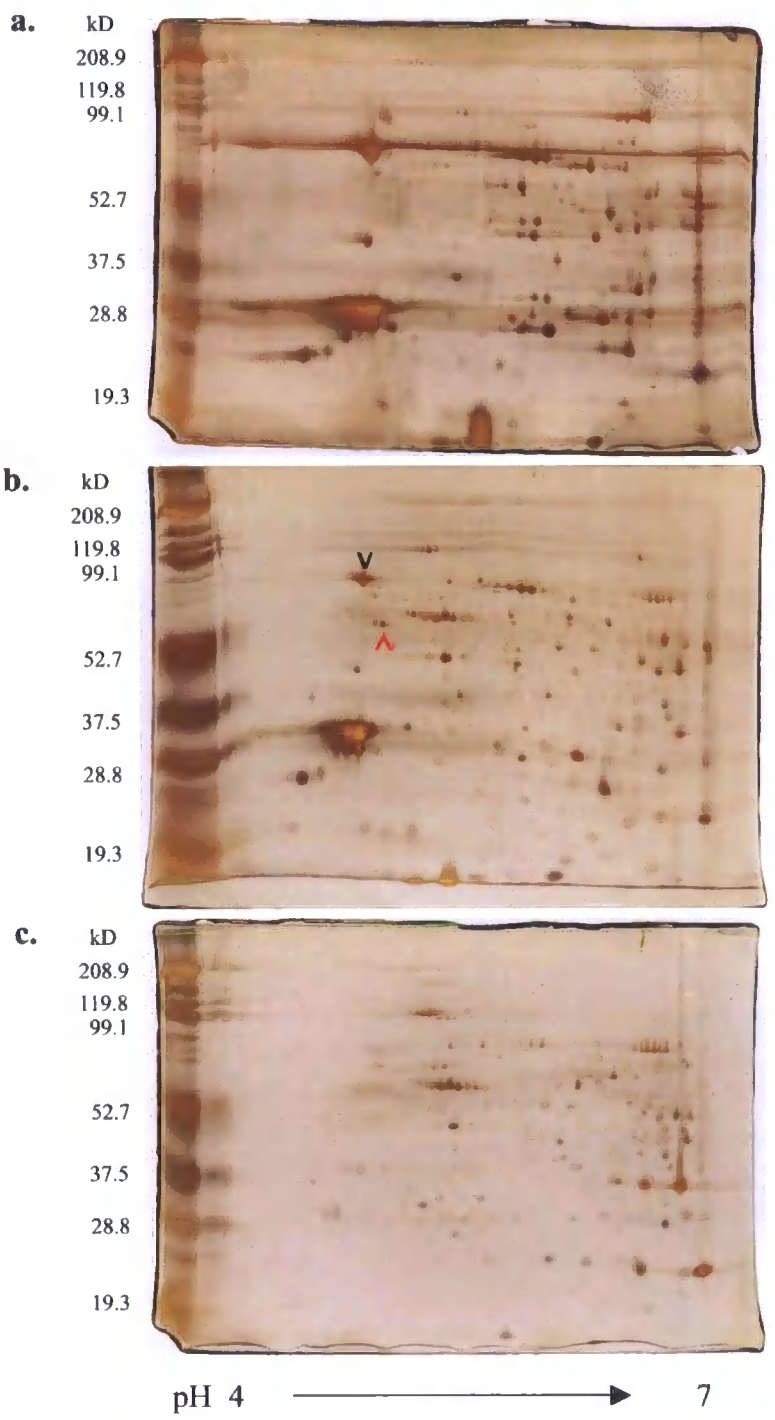

Figure 5.6: Co-precipitation of *Xenopus* cytosolic proteins with emerin peptide 73-180 purified under native conditions.

a: *emerin 73-180 only,* ***b:*** *emerin 73-180 – Xenopus cytosol,* ***c:*** *Xenopus cytosol only*

Black and red arrowheads indicate protein spots that were sent for mass spectroscopic analysis.

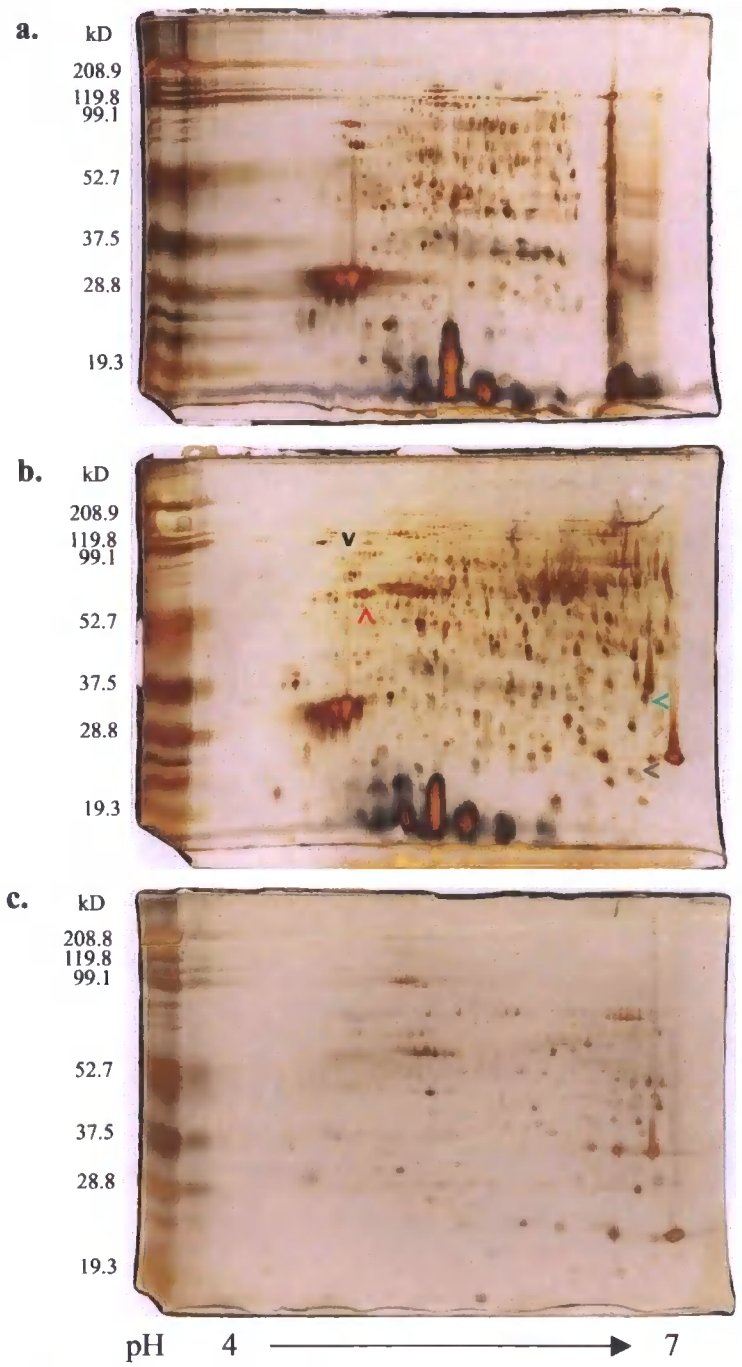

Figure 5.7: Co-precipitation of Xenopus cytosolic proteins with emerin peptide 73-180 purified under denaturing conditions.

a: *emerin 73-180 only,* ***b:*** *emerin 73-180 – Xenopus cytosol,* ***c:*** *Xenopus cytosol only*

Grey and turquoise arrowheads indicate protein spots that were sent for mass spectroscopic analysis. The absence of HSP70 is shown by the black arrowhead.

Sample	Bait	Highest match	Species	Mass	Score
> 1	1-70	No hit	—	—	—
> 2	1-70	No hit	—	—	—
> 3	73-180	No hit	—	—	—
> 4	73-180	No hit	—	—	—
> 5	1-70 & 73-180	Tubulin-β2	*X. laevis*	50.233	166
> 6	1-70 & 73-180	HSP70	*E. coli*	69.130	305

Table 5.2: Mass spectroscopic identification of proteins co-precipitating with emerin as shown on 2-D gels.

Samples 1-6, as shown in Figures 5.4 – 5.7 with coloured arrowheads, were digested with trypsin and identified by peptide mass fingerprinting. Tubulin- β2 was identified as a protein interacting with emerin 1-70 and 73-180. The masses of the identified proteins (in kD) and their matching scores are also shown.

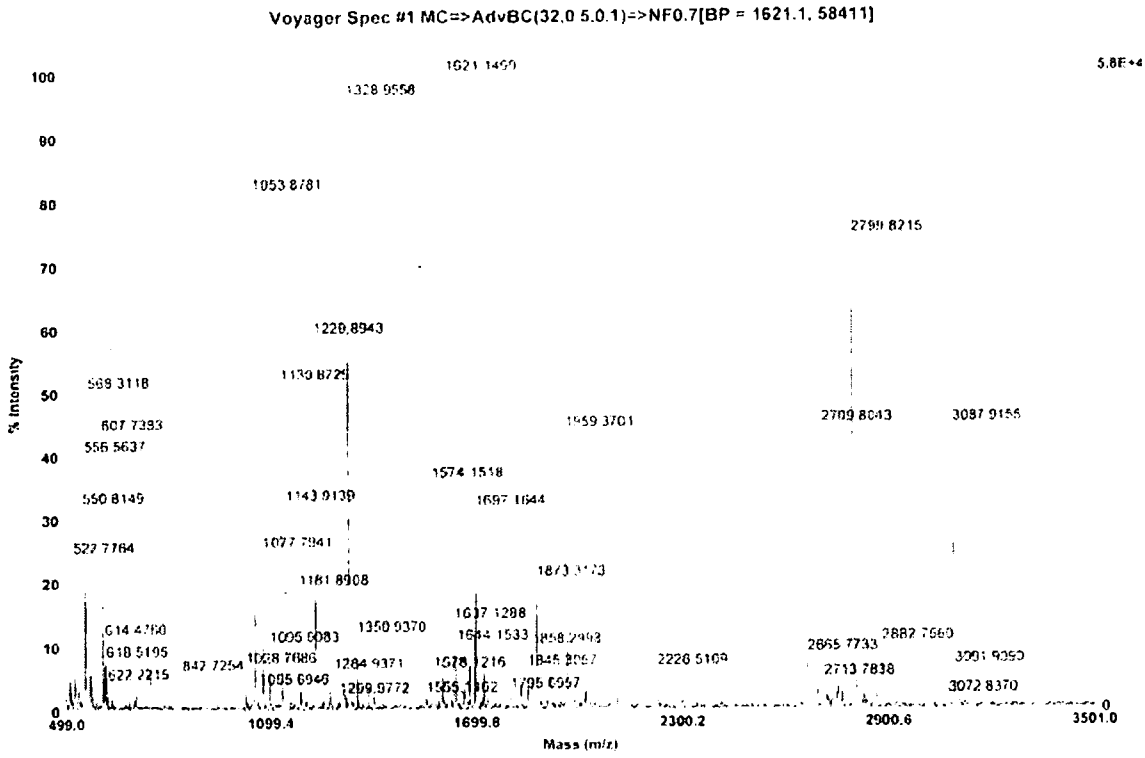

Figure 5.8: β-tubulin MS spectrum.

The acquired MS spectrum for the peptide identified as tubulin by peptide mass fingerprinting is shown. The number of peptides generated after trypsin digestion and their corresponding mass/charge ratio as identified by the mass spectrometer can be seen. Tubulin was identified with a statistically significant score of 166.

5.2.2 Immunostaining of normal HDF and X-EDMD fibroblasts with a β-tubulin antibody

In order to investigate the functional significance of the emerin-tubulin interaction the organisation of the microtubule network in normal and X-EDMD fibroblasts, which lack emerin, was studied. Four different X-EDMD cell lines derived from male patients were used. To keep the anonymity of the donors the cell lines are called X-EDMD 1, 2, 3 and 4. As a control, two normal HDF cell lines were used.

Initially, the level of emerin expression in all cells was checked by immunoblotting with an emerin-specific antibody. Equal loading was standardised according to actin expression. As expected emerin expression was observed in the normal HDF. Three X-EDMD cell lines (2, 3 and 4) were found null for emerin expression. One band of 34 kD corresponding to emerin was detected in X-EDMD cell line 1 (Figure 5.9).

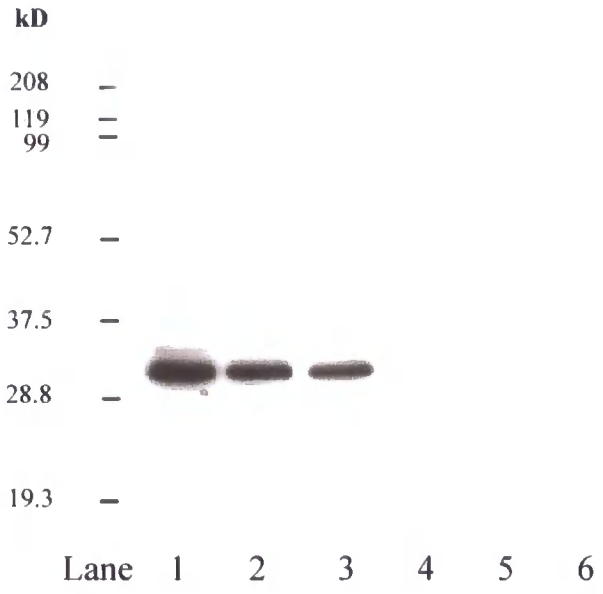

Figure 5.9: Emerin expression in cell lines used in this study.

Four HDF cell lines derived from X-EDMD male patients and two HDF cell lines derived from healthy individuals were used in this study. All cell lines were checked for emerin expression by immunoblotting. Lanes 1 and 2 correspond to HDF obtained from healthy individuals. Lanes 3, 4, 5 and 6 correspond to X-EDMD cell lines 1, 2, 3 and 4, respectively. As expected emerin was detected as a 34 kD band in normal HDF. X-EDMD cell lines 2, 3 and 4 had no detectable emerin. Surprisingly emerin expression was observed in X-EDMD cell line 1.

All cell lines were subsequently grown till 80% confluence, fixed with ice-cold methanol:acetone (1:1) and processed by immunofluorescence with an antibody against β-tubulin. Cells were observed by confocal microscopy.

When normal HDF were stained with anti- β-tubulin (Figures 5.10 and 5.11), the characteristic appearance of microtubules (MTs) starting from the Microtubule Organising Centre (MTOC) and orientated towards the cell periphery was observed. The MTOC was clearly visible as the area with the higher intensity labelling. In most cells the MTOC was positioned in the cell centre, as expected for interphase cells, next to the nuclear envelope.

When X-EDMD cells were examined, as shown in Figures 5.12-5.15, MTs seemed to radiate out of the MTOC into the cell periphery like in control cells. Also, no alterations in the organisation of the MT network were observed between all X-EDMD cell lines and control cells in which MTs were seen as fine lacelike threads. The depicted 'fragmented' and more punctuate staining of MTs in X-EDMD cell lines 1 (Figure 5.12) and 3 (Figure 5.14) does not represent a general feature of these cell lines as it was not a repeatable result.

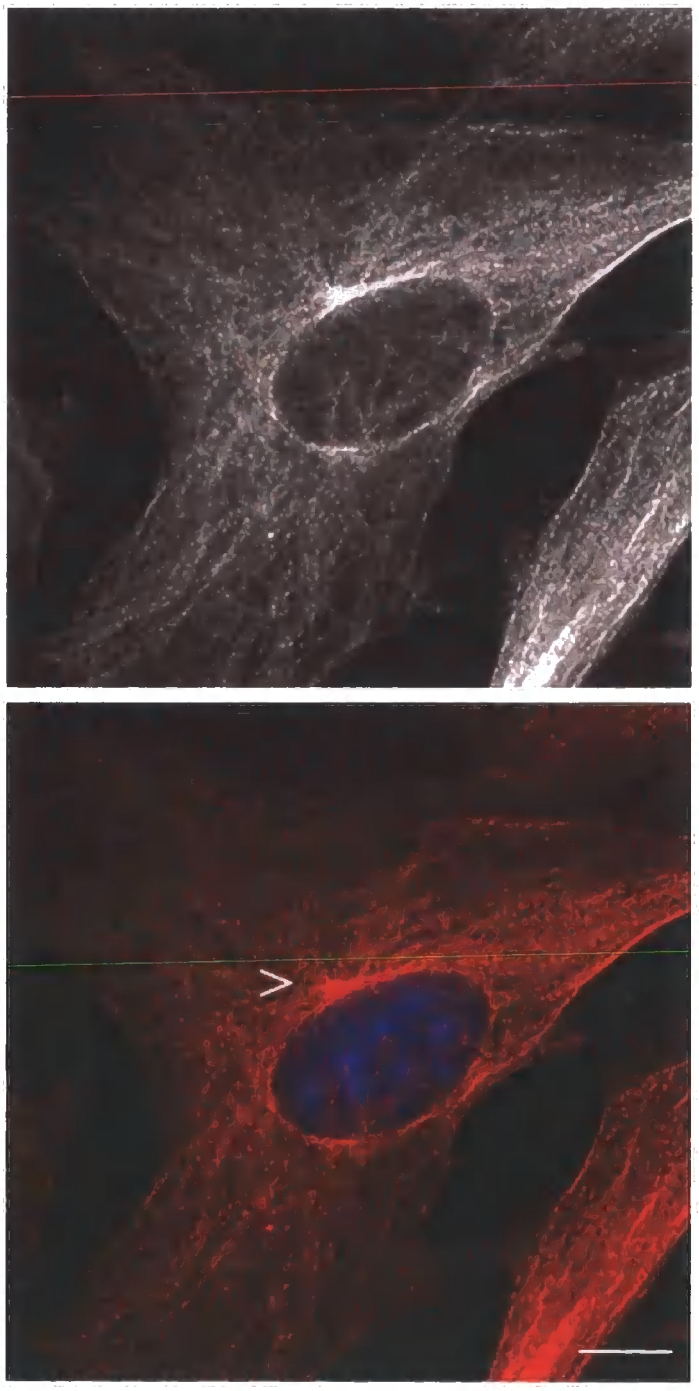

Figure 5.10: Organisation of microtubules in Normal 1 cell line.

Normal fibroblasts were stained with a Cy3 conjugated antibody against β-tubulin and observed by confocal microscopy. The upper panel shows the MTs stained by Cy3 and the lower panel shows the merged image in which chromatin is shown in blue (DAPI) and tubulin in red. The white arrowhead indicates the position of the MTOC in close association with the nucleus. Scale bar is 10 μm.

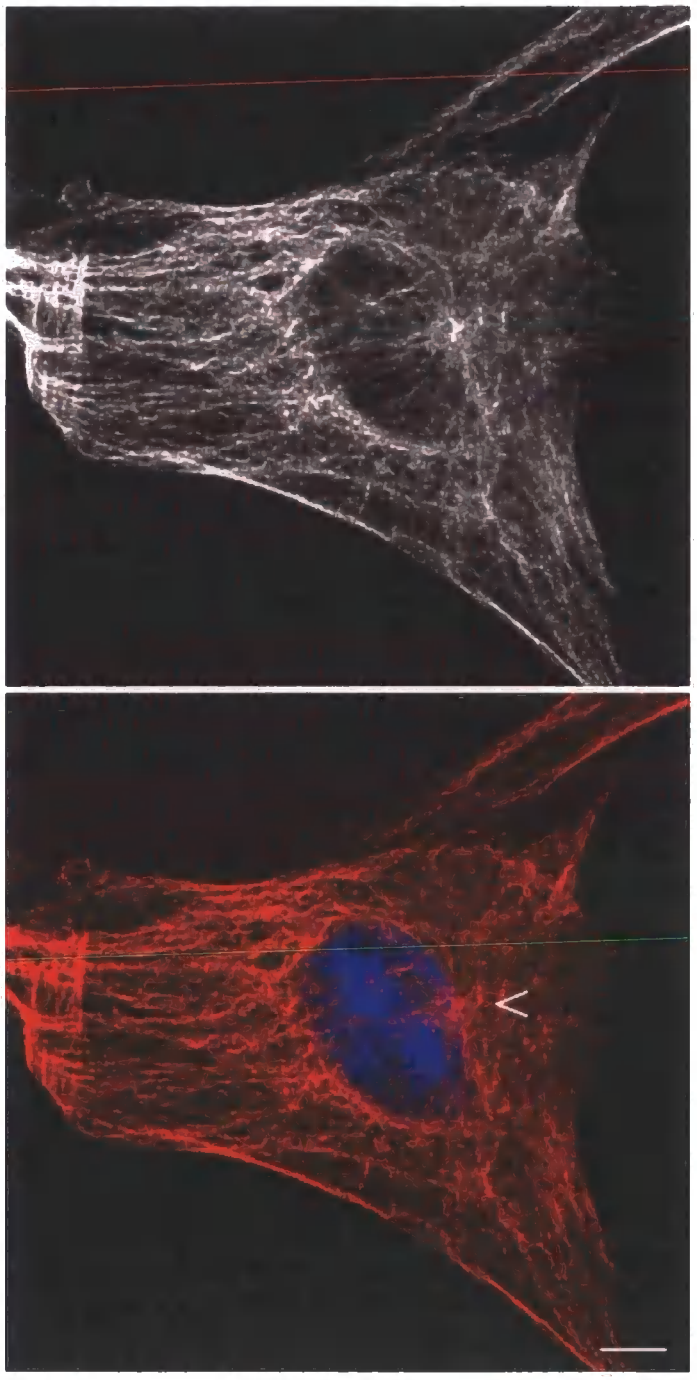

Figure 5.11: Organisation of microtubules in Normal 2 cell line

Normal fibroblasts were stained with a Cy3 conjugated antibody against β-tubulin and observed by confocal microscopy. The upper panel shows the MTs stained by Cy3 and the lower panel shows the merged image in which chromatin is shown in blue (DAPI) and tubulin in red. The white arrowhead indicates the position of the MTOC in close association with the nucleus. Scale bar is 10 μm.

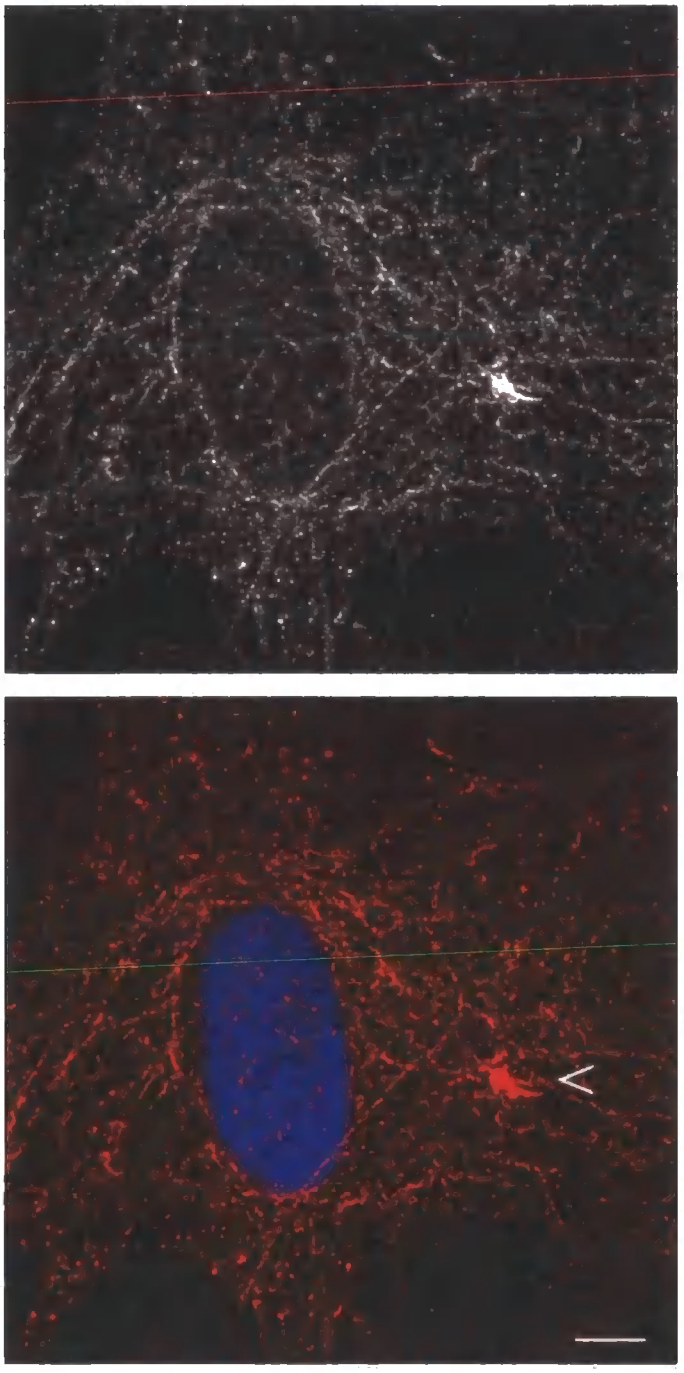

Figure 5.12: Organisation of microtubules in X-EDMD 1 cell line

EDMD fibroblasts were stained with a Cy3 conjugated antibody against β-tubulin and observed by confocal microscopy. The upper panel shows the MTs stained by Cy3 and the lower panel shows the merged image in which chromatin is shown in blue (DAPI) and tubulin in red. The white arrowhead indicates the position of the MTOC positioned in the cell periphery and not associated with the nucleus. Scale bar is 10 μm.

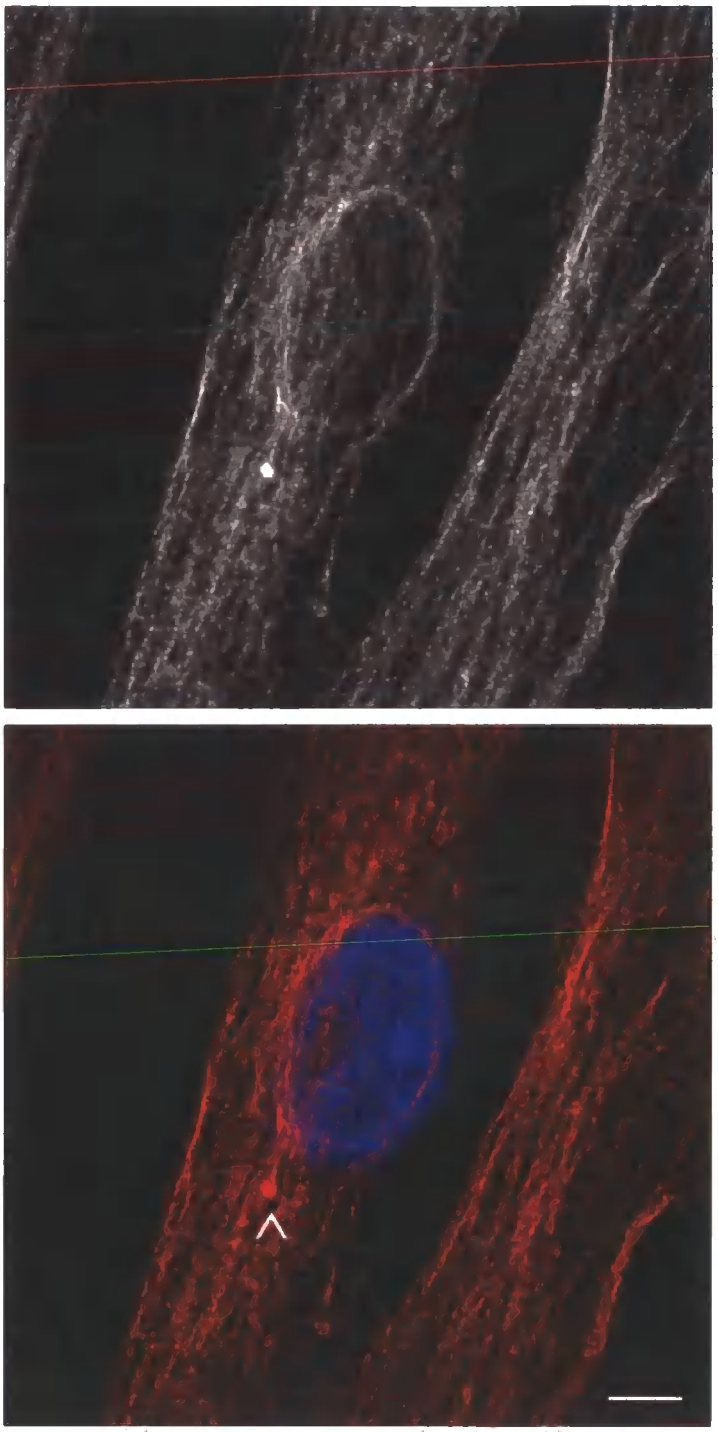

Figure 5.13: Organisation of microtubules in X-EDMD 2 cell line

EDMD fibroblasts were stained with a Cy3 conjugated antibody against β-tubulin and observed by confocal microscopy. The upper panel shows the MTs stained by Cy3 and the lower panel shows the merged image in which chromatin is shown in blue (DAPI) and tubulin in red. The white arrowhead indicates the position of the MTOC positioned in the cell periphery and not associated with the nucleus. Scale bar is 10 μm.

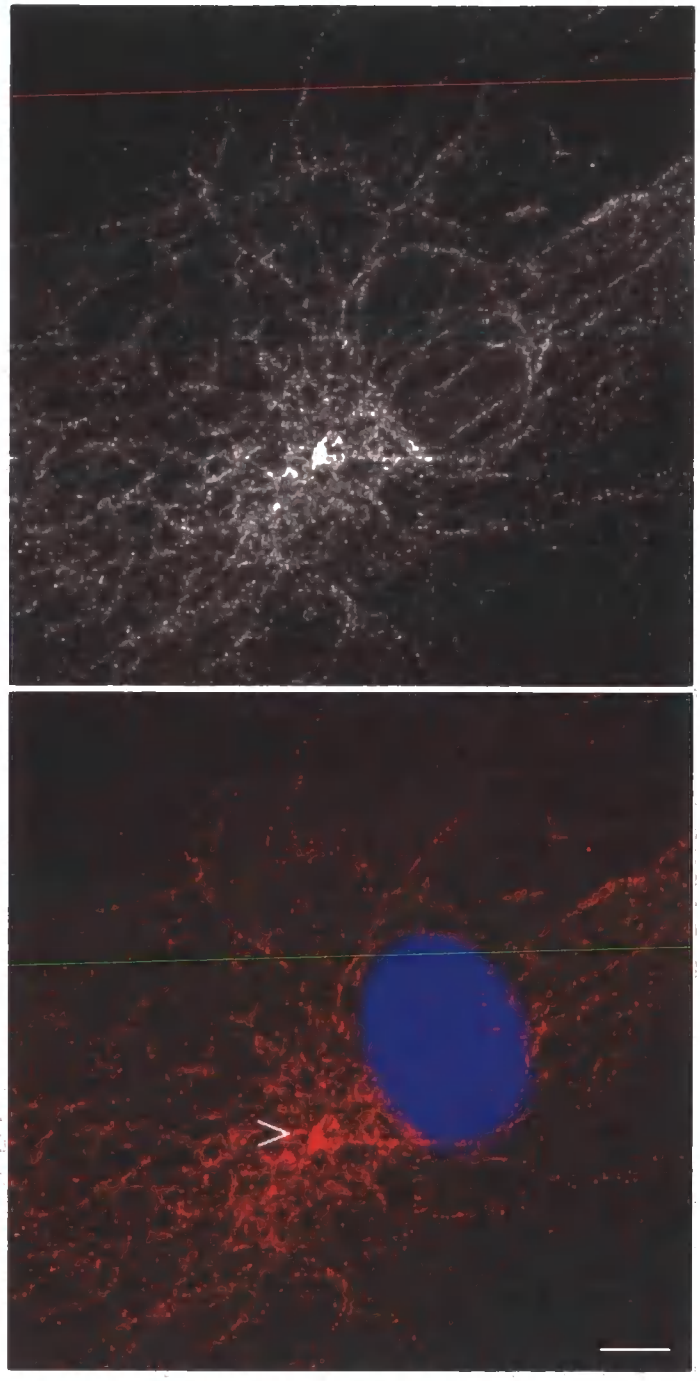

Figure 5.14: Organisation of microtubules in X-EDMD 3 cell line

EDMD fibroblasts were stained with a Cy3 conjugated antibody against β-tubulin and observed by confocal microscopy. The upper panel shows the MTs stained by Cy3 and the lower panel shows the merged image in which chromatin is shown in blue (DAPI) and tubulin in red. The white arrowhead indicates the position of the MTOC positioned in the cell periphery and not associated with the nucleus. Scale bar is 10 μm.

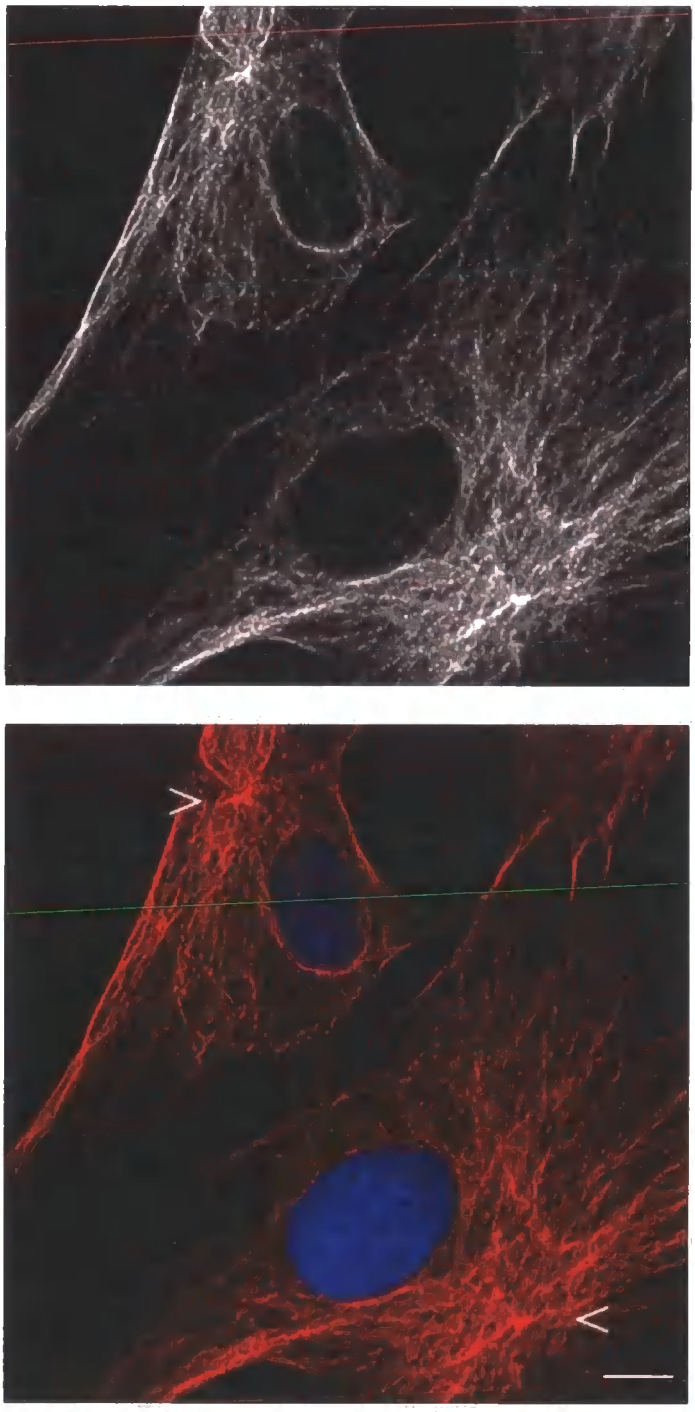

Figure 5.15: Organisation of microtubules in X-EDMD 4 cell line

EDMD fibroblasts were stained with a Cy3 conjugated antibody against β-tubulin and observed by confocal microscopy. The upper panel shows the MTs stained by Cy3 and the lower panel shows the merged image in which chromatin is shown in blue (DAPI) and tubulin in red. The white arrowhead indicates the position of the MTOC positioned in the cell periphery and not associated with the nucleus. Scale bar is 10 μm.

The most prominent difference observed between normal and X-EDMD cells was related to the position of the MTOC relative to the nuclei. In X-EDMD cells a significant proportion of the cells exhibited a mis-localisation of the MTOC towards the cell periphery and not in contact with the nucleus. To ensure that there was a significant difference, 200 cells of each cell line were observed for the MTOC position (Figure 5.16). MTOCs were scored as 'near' or 'distant' depending on whether they were attached or detached from the nuclei, respectively. As the figure shows in the two normal cell lines the majority of the cells (86.5% and 81.6%) had a MTOC closely associated with the nucleus, while only 13.5-18.4% had a MTOC positioned at the cell periphery and not associated with the nucleus. The picture was completely different in X-EDMD cells, where a large percentage of cells (between 30.9 and 40%) displayed an abnormally localised MTOC distant from the nucleus (Figure 5.16 a). The percentage of normal and X-EDMD cells scored with an MTOC positioned near or distant from the nucleus is shown in a chart in Figure 5.16 b, in which MTOCs near the nucleus are shown in blue and MTOCs distant the nucleus are shown in red.

Figure 5.16: Position of the MTOC in normal and X-EDMD fibroblasts as seen with the β-tubulin antibody

Normal HDF and HDF derived from patients with X-EDMD were stained with an anti-β-tubulin antibody and observed under a confocal microscope. The position of the MTOC relatively to the nucleus was counted in 200 cells and was also calculated as a percentage.

a: *In the two control HDF cell lines tested, 86.5% and 81.5% of MTOC were found associated with the nuclei and only 13.5% and 18.4% were localised distant to the nucleus. In contrast in X-EDMD fibroblasts derived from four different patients (X-EDMD 1-4) 60-69.1% of cells displayed a normal MTOC position and 30.9-40% of cells had the MTOC abnormally localised far away from the nucleus.*

b: *Plots showing the percentage of cells displaying a normal (near) and abnormal (distant) position of the MTOC in the two normal and four X-EDMD HDF tested.*

a.

HDF	MTOC near the NE		MTOC distant from the NE	
	number of cells	%	number of cells	%
Normal-1	173	86.5	27	13.5
Normal-2	164	81.6	37	18.4
X-EDMD-1	137	67.5	66	32.5
X-EDMD-2	141	69.1	63	30.9
X-EDMD-3	136	66.3	69	33.7
X-EDMD-4	120	60	94	40
Total	~ 200		~ 200	

b.

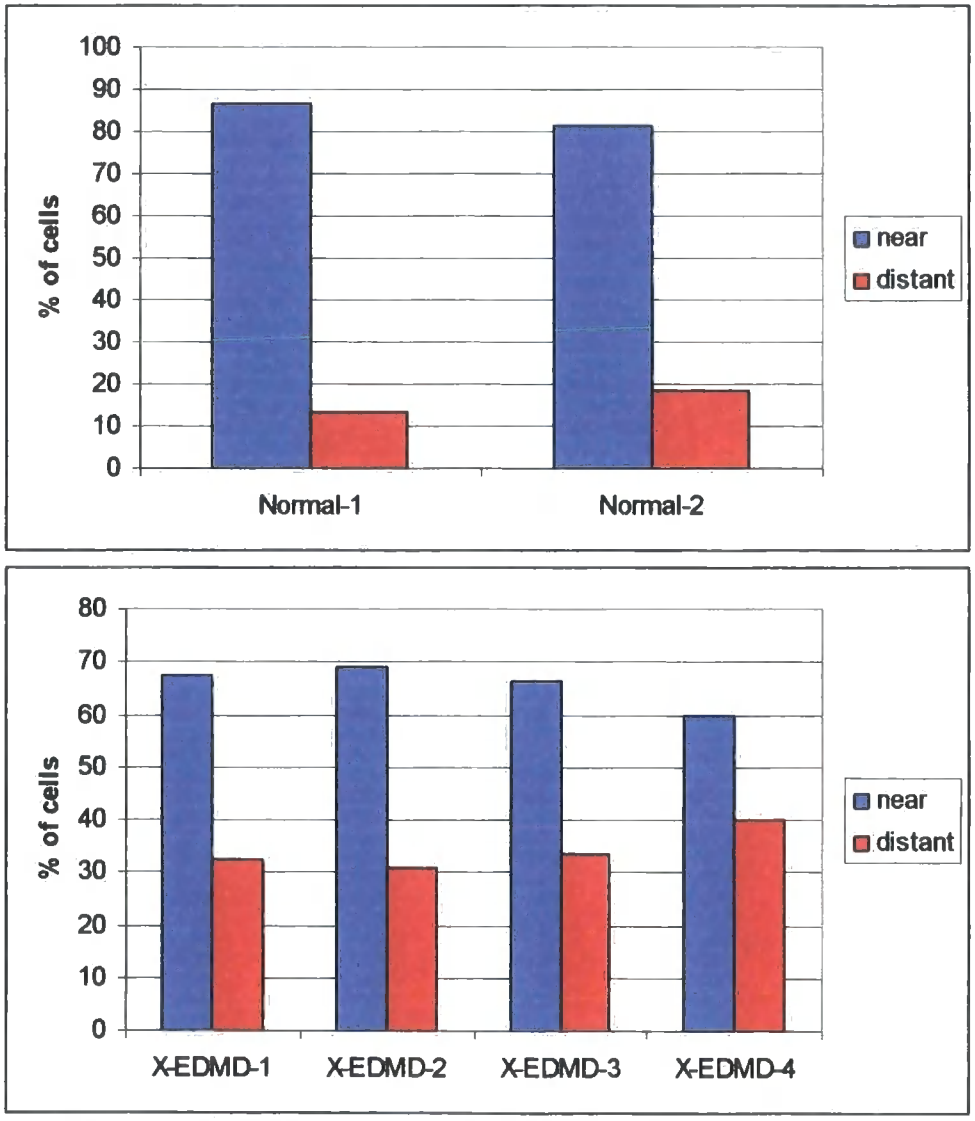

Figure 5.16: Position of MTOC in normal and X-EDMD fibroblasts as seen with the β-tubulin antibody.

5.2.3 Immunostaining of normal and X-EDMD fibroblasts with a centrosome-specific antibody

To confirm the observed detachment of the MTOC from the NE described above normal and X-EDMD fibroblasts were double-stained with a centrosome-specific antibody that recognises the protein pericentrin and with a NE-antibody that recognises lamin A/C. The same two normal and four EDMD cell lines were used as in the β-tubulin staining and cells were observed with a Carl Zeiss live-cell imaging microscope.

In all cell types the lamin A/C antibody gave a rim staining as expected. The pericentrin antibody stained very brightly the centrosomes as circular structures in the cytoplasm while some punctuate staining around the centrosomes was also observed in most cells (Figure 5.17).

Figure 5.17: Centrosome staining in normal and X-EDMD cells.

Two normal and four X-EDMD cell lines were double-stained with antibody JOL2, which recognises lamin A/C (FITC) and with the pericentrin antibody, which stains centrosomes (TRITC). Chromatin was stained with DAPI (blue). ***a and b****: normal HDF.* ***c, d, e and f****: X-EDMD cell lines 1, 2, 3 and 4, respectively.*

All cells are positive for lamin A/C expression (green). Centrosomes are clearly visible as circular structures in the cytoplasm (red) and are marked with white arrowheads. Noticeably, in control cells (a and b) centrosomes are closely associated with the NEs while in X-EDMD cells (c, d, e and f) centrosomes are frequently positioned away from the NE.

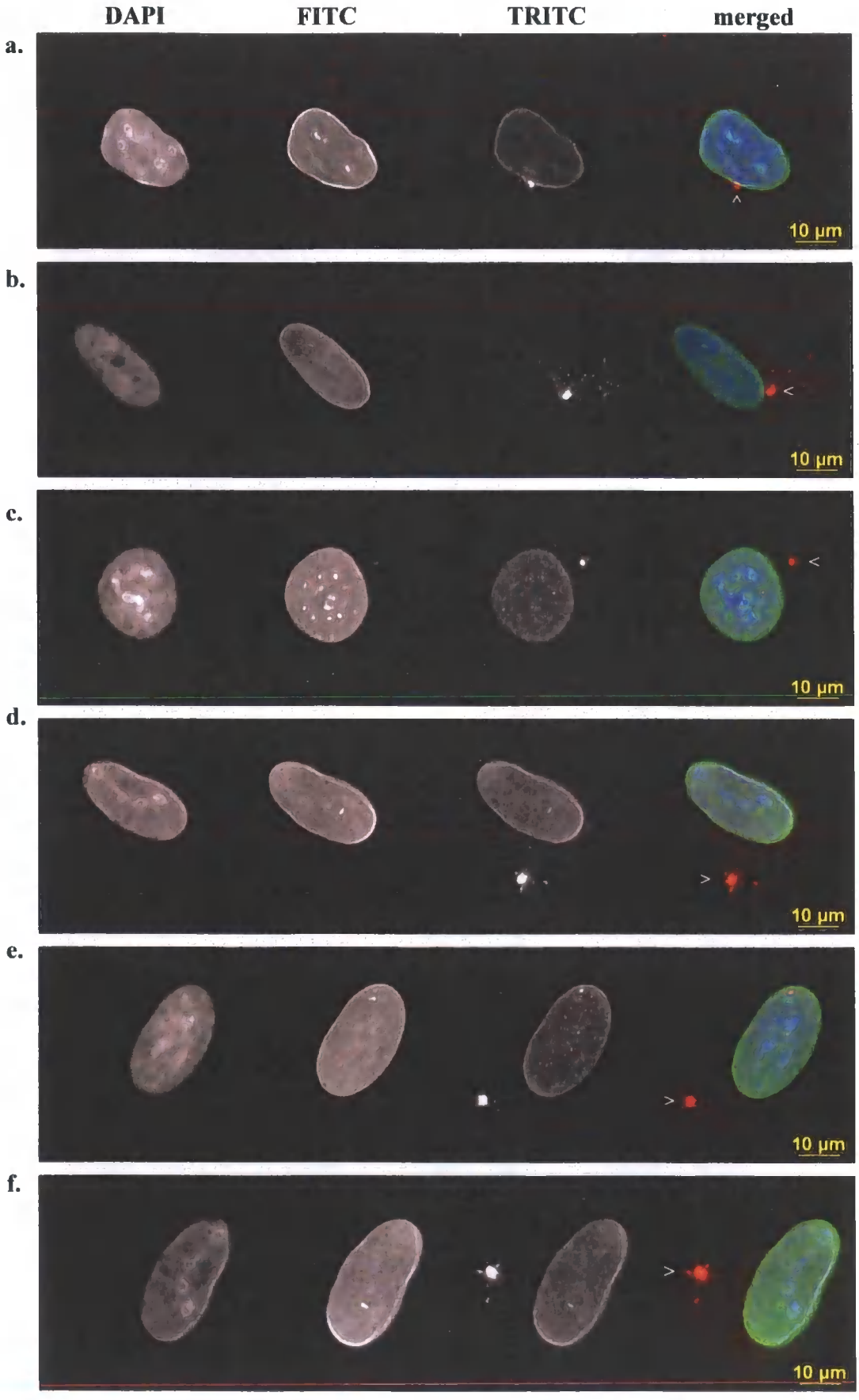

Figure 5.17: Centrosome staining in normal and X-EDMD cells.

Since the pericentrin antibody does not stain MTs, the position of the centrosome in each cell was much more clearly visible than as seen with the β-tubulin antibody. This allowed the measurement of the exact distance of the MTOC from the NE. For each cell line approximately 200 cells were randomly chosen and photographed. The distance from the centre of each centrosome to the NE was then measured and displayed in μm. Examples of images from each cell line with the calculated distances of the centrosomes from the nuclei are shown in Figure 5.18.

The 200 measurements were then used to calculate the average distance of the centrosome from the nucleus in each cell line. In control cells, the average distance was calculated as 1.535 μm (± 0.109) and 1.557 μm (± 0.109) in cell lines Normal 1 and 2, respectively. A twofold increase was observed in X-EDMD cells with distance values of 2.949 μm (± 0.209), 3.623 μm (± 0.257), 3.503 μm (± 0.248) and 3.775 μm (± 0.266) in X-EDMD cell lines 1, 2, 3 and 4, respectively (Figure 5.19 a). A graphical representation of the above results featuring the error bars clearly shows that there is a statistically significant difference in the distance of the centrosome from the nucleus between normal and X-EDMD cells (Figure 5.19 b). Also measurements from X-EDMD and normal cells were compared by performing two-tailed Student's t-tests assuming unequal variances. The obtained t-values between samples Normal 1 and X-EDMD 1, 2, 3 and 4 were 3.65, 5.58, 5.59 and 6.82, respectively. Similarly, t-values for samples Normal 2 and X-EDMD 1, 2, 3 and 4 were 3.79, 5.83, 5.89 and 7.29, respectively. For degrees of freedom ∞, the critical value for P=0.001 is 3.29. Since all t values are larger than 3.29 it can be concluded that there is a statistically significant difference between normal and all X-EDMD cell lines at 0.1% level of significance.

Figure 5.18: Measurements of the distance of the centrosomes from the nuclei in control and X-EDMD cell lines.

For each cell line used images of approximately 200 cells were taken and the distance of the centre of each centrosome from the NE was measured and is displayed in μm. NEs were visualised with the JOL2 antibody, which recognises lamin A/C and are shown in green. Centrosomes were visualised with the pericentrin antibody (red) and chromatin was stained with DAPI (blue). Examples of images featuring the calculated distances are shown. ***a****: normal cell line 1,* ***b****: normal cell line 2,* ***c****: X-EDMD cell line 1,* ***d****: X-EDMD cell line 2,* ***e****: X-EDMD cell line 3 and* ***f****: X-EDMD cell line 4. Note the bigger distances of centrosomes from nuclei in EDMD cell lines compared to control cells.*

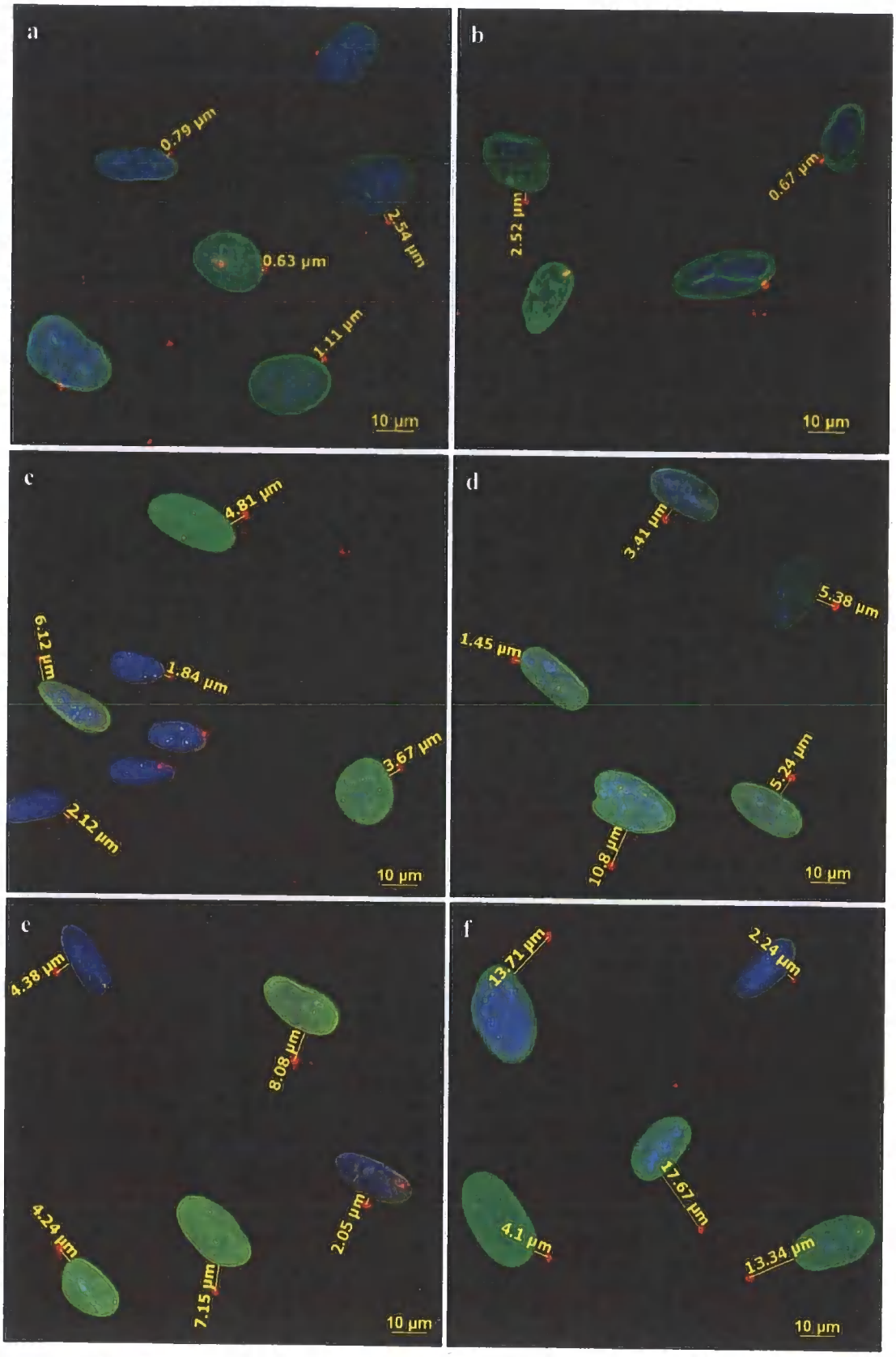

Figure 5.18: Measurements of the distance of the centrosomes from the nuclei in control and X-EDMD cell lines.

a.

Cell line	Mean distance (µm)	Total number of cells	STDV	SEM
Normal 1	1.535	198	2.78	± 0.197
Normal 2	1.557	201	2.19	± 0.154
X-EDMD 1	2.949	199	4.75	± 0.336
X-EDMD 2	3.623	198	4.50	± 0.320
X-EDMD 3	3.503	199	3.63	± 0.257
X-EDMD 4	3.775	201	3.76	± 0.265

b.

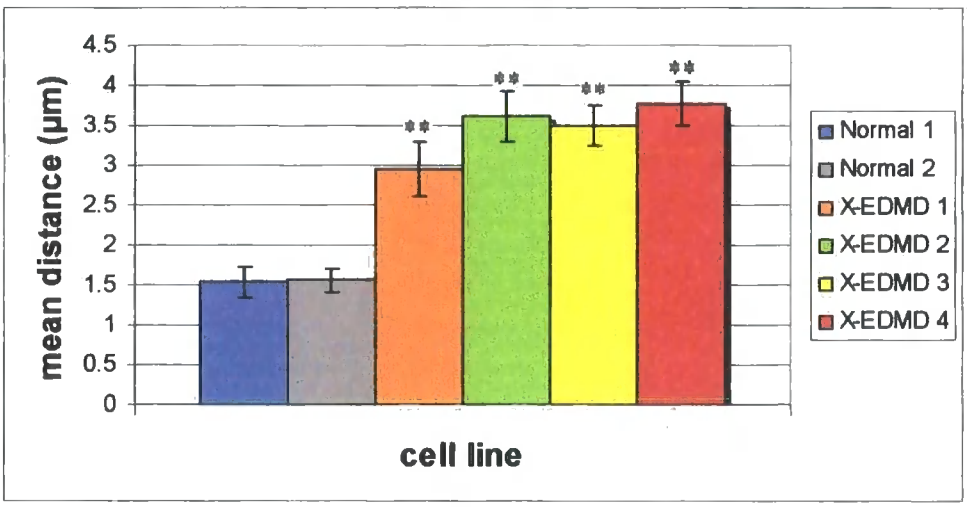

Figure 5-19: Mean distance of centrosomes from nuclei in normal and X-EDMD cell lines.

The distance of the centrosome from the nucleus was measured in approximately 200 cells, in two normal and four X-EDMD cell lines. ***a:*** *the measurements were used to calculate the average distance for each cell line, the standard deviation (STDV) and the Standard Error of the Mean (SEM)* ***b:*** *a graphical representation of the average centrosome distance from the nucleus in all six cell lines used. A statistically significant twofold increase in the centrosome distance in X-EDMD cells compared to normal cells is clearly shown. Asterisks indicate that the means of normal and X-EDMD cells are different at a 0.01% level of significance (d.f. ∞).*

Noticeably, when standard deviations were calculated the nearly 200 measurements were found to deviate much more from the average in X-EDMD cells than in control cells. Thus, for a more complete comparison of normal and X-EDMD cell lines it was considered necessary to include the distribution of the data. For this purpose nuclei were grouped in four categories: nuclei in which the centrosomes co-localised with the NEs (0 μm), nuclei in which the centrosomes were attached to the NEs (0.1–1 μm), nuclei in which the centrosomes were detached and at small distance from the NEs (1.1–3.5 μm), and nuclei in which the centrosomes were detached from the NEs and separated by distances greater than 3.5 μm. For each cell line the number of cells falling in each category was calculated and frequency histograms were created (Figure 5.20). Remarkably, more than half of the control cells had their centrosomes either co-localising with (0μm) or directly attached (0.1–1 μm) to the NEs. In contrast, X-EDMD cells were only poorly represented in these two categories. The picture seemed to reverse when moving away from the nucleus. Approximately one fourth of normal cells had centrosomes localised at distances between 0.1 and 1 μm while X-EDMD were better represented with more than one third of cells scoring in this category. The difference between normal and X-EDMD cells was even bigger at distances greater than 3.5 μm. While the minority of normal cells was observed in this category more than one fourth of X-EDMD cells displayed centrosomes abnormally localised at such a big distance from the nucleus. It should be noted that X-EDMD cell line 1, with its cells almost equally distributed between the four categories, displayed a distribution pattern in-between the normal and the other X-EDMD cell lines.

Figure 5.20: Frequency histograms of the distances of centrosomes from nuclei in normal and EDMD cell lines.

Photographs of nearly 200 cells from two normal and four X-EDMD cell lines stained with the pericentrin antibody were obtained. Cells were divided into four categories regarding the distance of their centrosome from the NE: 0 μm, 0.1-1 μm, 1.1-3.5 μm and > 3.5 μm. The number of cells falling in each category was then calculated and frequency histograms were created. The different cell lines are represented with different colours: blue for Normal 1, grey for Normal 2, orange for X-EDMD 1, green for X-EDMD 2, yellow for X-EDMD 3 and red for X-EDMD 4. The total number of cells scored was: 198 for Normal 1, 201 for Normal 2, 199 for X-EDMD 1, 198 for X-EDMD 2, 199 for X-EDMD 3 and 201 for X-EDMD 4. Numbers inside the bars of the histograms correspond to the number of cells that fell into each category. Immunofluorescence images of representative nuclei for each category are shown in the right side of the histograms.

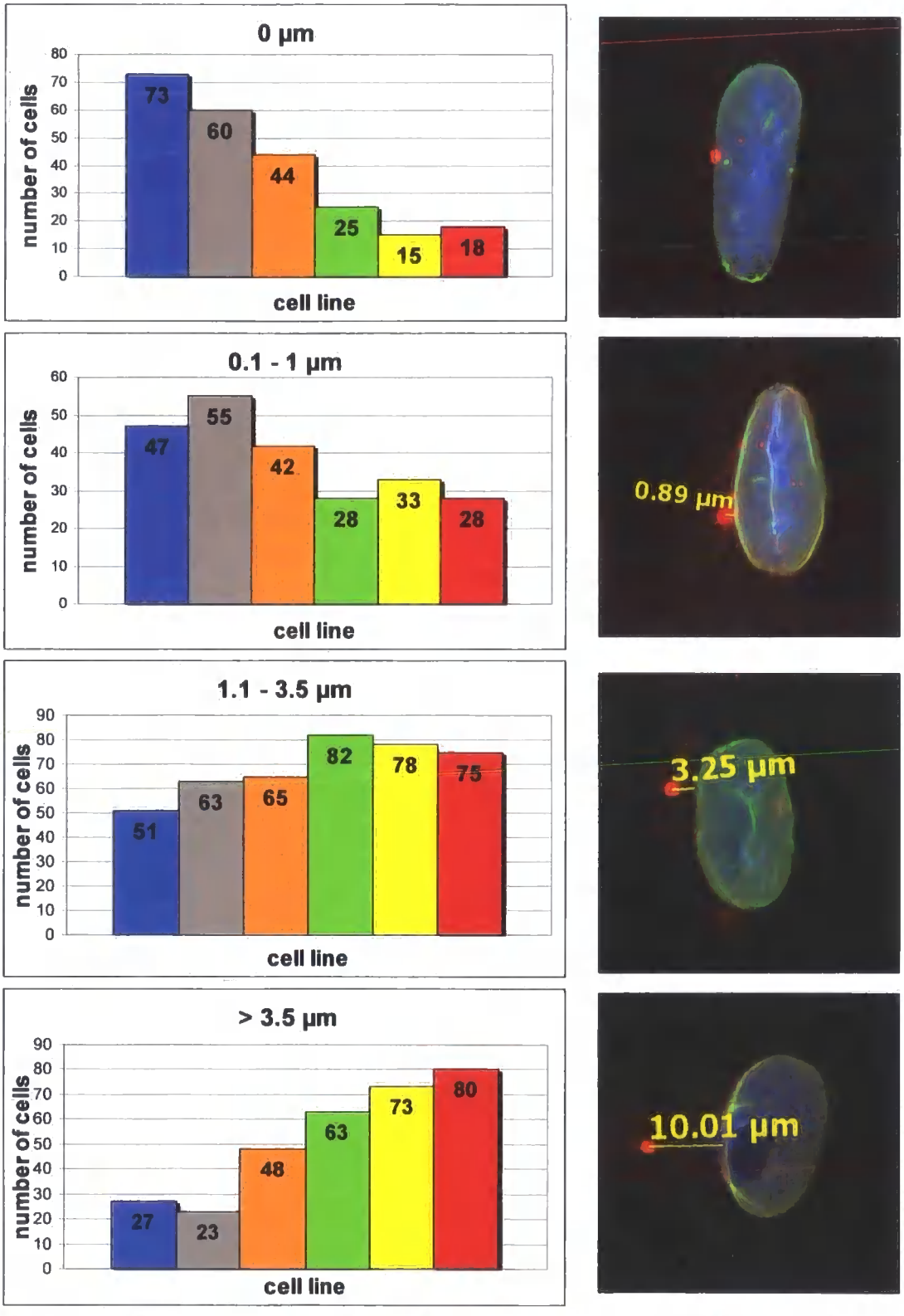

Figure 5.20: Frequency histograms of the distances of centrosomes from nuclei in normal and X-EDMD cell lines.

5.3 DISCUSSION

So far, functional differences of emerin peptides with and without the LEM domain and a LEM domain mediated inhibition of nuclear assembly in *Xenopus* have been demonstrated (Chapter 3). These differences have been attributed to the ability of the LEM domain to compete with endogenous *Xenopus* LEM domain proteins residing in the NEP-A membrane fraction, for chromatin binding (Chapter 4). In the present chapter the possibility that the different behaviour of emerin peptides in nuclear assembly correlated with differences in binding partners was explored. Emerin peptides were immobilised on beads and incubated with *Xenopus* cytosol. Interacting proteins were identified by a combination of gel electrophoresis, mass spectrometry and peptide mass fingerprinting.

Initially samples were analysed by 1-D gel electrophoresis. To avoid false positive results two controls were used: aliquots of purified emerin peptides alone and aliquots of *Xenopus* cytosol incubated with beads in the absence of emerin. Thirteen bands that were uniquely present in the emerin-cytosol lanes were selected and analysed by mass spectrometry (Table 5.1). Unfortunately, most of the bands were identified as contaminating proteins while two could not be identified (possible reasons for that will be discussed later). Among the contaminating bands, four corresponded to *E. coli* proteins DNAK, Ni^{+2}-responsive regulatory protein, Cap-Dna recognition and Ecs1486, the latter two with a statistically insignificant matching score.

DNAK is the bacterial homologue of the mammalian chaperone HSP70. HSP70s are a family of constitutively expressed proteins of about 70 kD found in almost all

organisms that participate in a diverse array of functions. The presence of DNAK in the samples of the purified emerin peptides can be explained by considering their role in protein folding. Chaperones bind to nascent polypeptides on ribosomes or proteins in transit across intracellular membranes and prevent premature misfolding of the peptides. In bacteria this process includes the progressive binding of polypeptides to different chaperones like DNAJ, DNAK and GrpE (Hendrick and Hartl, 1995). Alternatively, it has been shown using a predicting algorithm for DNAK binding motifs within protein sequences, that linker peptide regions (or spacers) that connect proteins to short sequence tags can bind DNAK. A comparison of several pET and pGEX vectors revealed that the connector peptide region of pET29 displays a very high affinity DNAK binding site (Rial and Ceccarelli, 2002). In contrast to DNAK, the presence of the other *E. coli* contaminant, the Ni^{+2}-responsive regulatory protein most probably resulted from a direct interaction of the protein with the Ni^{+2} –beads. Several histidine-rich *E. coli* proteins that are able to bind tightly to Ni^{+2} have been reported as contaminants in purifications of His-tagged proteins (ftp://ftp.ncifcrf.gov/pub/methods/TIBS/jul95.txt).

Two more of the identified proteins from the 1-D gels can be characterised as contaminating: albumin, which was introduced in the experiment when incubating the beads with BSA, and protein MGC83078, which is the *Xenopus* homologue of the *E. coli* protein peroxiredoxin, one of the 10 most abundant proteins in *E. coli*. The two proteins that were identified as human emerin probably correspond to degradation products or modified forms of the purified peptides. Thus, at the level of 1-D gel electrophoresis, out of the thirteen selected bands only three can be considered as

possible emerin interacting partners: calcineurin, a Ca^{2+}/calmodulin dependent Ser/Thr phosphatase, and the two cytoskeletal proteins β-tubulin and profilin.

Since, as described above, most of the obtained results were identified as contaminating proteins despite the use of two types of control, a method with increased resolution power was considered more appropriate for the analysis of the results. 1-D gel electrophoresis although is simple to perform and reproducible it separates proteins on the basis of their molecular masses only and has a limited resolving power. For this reason 2-D gel electrophoresis was employed. 2-D electrophoresis resolves proteins according to their net charge in the first dimension and according to their molecular mass in the second dimension. It is capable of resolving thousands of proteins and peptides from a single complex mixture in a single experiment and produces a resolution far exceeding that obtained in 1-D gels (Fey and Larsen, 2001).

Furthermore, as several connections exist between one of the contaminants, DNAK, and other obtained results like tubulin and calcineurin, caution was taken to remove DNAK from the pull-down experiments. Substrate binding and release from DNAK are coupled to its ATPase activity: in the ATP-bound state DNAK shows a low affinity and fast exchange rate for substrates, whereas in the ADP-bound state it has a high affinity and slow exchange rates for substrates (Palleros *et al.*, 1993a). Therefore, preincubation of protein solutions with Mg-ATP prior to purification has been suggested as a way to dissociate protein-DNAK complexes. It is thought that Mg-ATP results in exchange of ADP with ATP, which then causes a conformational change that triggers substrate release from the complex (Palleros *et al.*, 1993b).

However, in more recent reports addition of ATP to complex mixtures like bacterial lysates does not reduce DNAK contamination but usually increases it. This is probably because the ATP treatment releases DNAK that is bound to unfolded bacterial proteins allowing binding to other proteins including the recombinant protein to be purified. Indeed when the Mg-ATP method was used in this study not only it did not remove DNAK but it resulted in extensive fragmentation of the emerin peptides as detected by western blotting (data not shown). This is consistent with other reports of Mg-ATP making nascent polypeptides more sensitive to proteases (Eggers *et al.*, 1997). As an alternative approach to remove DNAK contamination denatured *E. coli* proteins, which serve as substrates for DNAK, were included to a Mg-ATP buffer before eluting the recombinant protein (Rial and Ceccarelli, 2002).

In the present work extraction and purification of the peptides under denaturing conditions (8M Urea), in absence of Mg-ATP, proved sufficient to remove DNAK. To ensure successful refolding, only the smallest emerin peptides (1-70 and 73-180) were used. Samples were analysed by 2-D gel electrophoresis. For comparison peptides purified under native conditions were also analysed by 2-D electrophoresis. As in 1-D SDS PAGE, 2-D gels were compared to identify spots that were unique in the emerin-cytosol sample and absent from the two controls. Careful examination revealed only few protein spots, which were then cut out of the gels and analysed by mass spectroscopy (Table 5.2). Consistent with the results from 1-D gels, β-tubulin was identified as a protein co-precipitating with emerin. The majority of the analysed protein spots, however, could not be identified. There are several reasons that could explain why some selected targets could not be identified by mass spectrometry.

Also, known emerin binding partners like lamins and BAF were not detected in these pull-down experiments. Possible reasons are discussed below.

MALDI-TOF in combination with 2-D gel electrophoresis and the fast growth of protein databases is a powerful tool that allows rapid protein identification. However, this approach suffers from several methodological limitations. 2-D gel electrophoresis although is the highest resolution protein separation method available is still limited by the number and type of proteins that can be resolved. Very large proteins of more than 100 kD may not enter the gel in the first dimension and very acidic or basic proteins, with a pI below 3 or above 10, are usually not well represented. Also when highly concentrated samples are used the most abundant proteins can dominate the gel making detection of low-copy proteins difficult. This problem cannot be overcome by loading more protein on the gel since the resolution decreases as the amount of the applied protein increases (Fey and Larsen, 2001). The *Xenopus* cytosol used in these pull-down experiments is a highly concentrated fraction (~ 50 mg protein/ml) and had to be diluted 1:4 in order not to overload the beads and to obtain samples that can be resolved on a gel. This could make the detection of proteins that are not abundant difficult. Out the two best characterised emerin binding partners, lamin A and BAF, lamin A is not represented in *Xenopus* egg extracts and hence could not be detected. BAF on the other hand, is represented in the *Xenopus* cytosol and at 25 µM it is an abundant protein (Segura-Totten *et al.*, 2002). In this case it is worth considering that the only reported emerin-BAF interaction by co-immunoprecipitation employed ^{35}S-labelled emerin and BAF that were produced in rabbit reticulocytes (Lee *et al.*, 2001). Unlike eukaryotic systems, however, modifications like phosphorylation, acetylation, glycosylation or disulfide formation

do not occur in prokaryotes. So when searching for binding partners of emerin expressed in *E. coli* interactions that require such modifications will not be detected.

Peptide mass fingerprinting (PMF) has also its limitations. Its ability to identify a protein depends on the presence of the protein in a database. PMF is a very effective method in the analysis of proteins from organisms whose genome is small, completely sequenced and well annotated. The fact that the *Xenopus* sequence is not complete yet could explain why some of the selected targets could not be identified. A study on the origins of uninterpretable masses in PMF revealed a number of other reasons that lead to the non identification of a protein (Karty *et al.*, 2002). Among these are errors in the published genome like incorrectly assigned protein start codons and protein modifications like deamidation and guanidination that give rise to masses that cannot be correctly matched.

Based on the evidence provided so far, β-tubulin was identified as an emerin interacting protein in two different sets of experiments analysed by both 1-D and 2-D gel electrophoresis. Calcineurin and profilin were identified as emerin interacting proteins based on their co-precipitation with emerin 1-70 and 1-176, respectively. The band corresponding to profilin, however, did also co-precipitate with emerin 1-220 and 73-180 but not with 1-70. Unfortunately both, calcineurin and profilin, were not detected in subsequent experiments in which samples were analysed by 2-D SDS-PAGE. Also investigation of the emerin-profilin interaction by the yeast-two-hybrid system did not yield a positive result leaving β-tubulin as the most convincing result based on the assays used in this work.

To investigate the functional significance of an emerin-tubulin interaction fibroblasts derived from four different X-EDMD patients were stained with a β-tubulin antibody. As a control, two HDF cell lines obtained from two unaffected individuals were used. Careful examination of normal and X-EDMD cells under a confocal microscope revealed no major differences regarding MT organisation in the cytoplasm. In both cases MTs seemed to radiate out from the MTOC towards the cell periphery.

The most striking difference between normal and X-EDMD cells was the position of the MTOC relative to the nucleus. While in normal cells the MTOC was observed on one side of the nucleus in X-EDMD cells the MTOC was frequently found located far away from the nucleus. This observation was confirmed in four different X-EDMD cell lines and with two different antibodies, one against β-tubulin and one against the centrosomal protein pericentrin. In both cases, nearly 40% of cells had the MTOC detached from the nucleus while the equivalent in normal cells was on average less than 15%. Possible explanations and implications of the above result will be discussed in the General Discussion (Chapter 6).

CHAPTER 6

GENERAL DISCUSSION

6.1 Overview

The *Xenopus* cell-free system has been extensively used in the past to study the process of nuclear envelope formation and the function of nuclear proteins. In this study, it was used to investigate the function and binding partners of the INM protein emerin. The results presented in this work lead to the following main conclusions:

(a) In *Xenopus*, nuclear envelope assembly proceeds by the ordered recruitment of distinct vesicle populations to chromatin and requires the interaction of LEM domain containing, membrane associated proteins with chromatin.

(b) Emerin is able to interact, either directly or indirectly, with the cytoskeletal protein β-tubulin and is involved in maintaining the correct position of the Microtubule Organising Centre (MTOC) near the NE.

6.2 Nuclear envelope assembly in *Xenopus*

To date, the exact mechanism of NEBD and reassembly after mitosis is still under debate. One of the existing models includes NE vesiculation and reassembly from discrete vesicles (Wiese and Wilson, 1993). This involves the initial binding of nuclear envelope precursor (NEP) vesicles to chromatin, fusion of vesicles into an ER-like network, enclosure of the chromatin, and NE expansion (Mattaj, 2004). Alternatively, dispersal of proteins into the ER upon NEBD, and retention at chromatin during reassembly has been suggested. This is thought to occur by modified binding

characteristics of INM proteins to chromatin, which is regulated by phosphorylation/dephosphorylation cycles (Ellenberg, 2002).

The present study has provided clear evidence to support the existence of distinct membrane populations in *Xenopus* (NEP-A and –B) that are recruited to chromatin in an ordered manner during NE assembly. Successful nuclear assembly was shown to require both membrane populations, and the interaction of membrane components with chromatin. Consistent with the evidence provided in this study, four more integral membrane proteins, contained either in the NEP-A or NEP-B fraction, have been shown to differ in their timing of incorporation into *in vitro* assembled pronuclei. Furthermore, the growth of oocyte germinal vesicles as an *in vivo* model for NE assembly provided additional evidence for the existence of distinct NEP populations. FESEM and thin section TEM of whole isolated *Xenopus* oocyte germinal vesicle NEs during growth phases identified large, ribosome studded vesicles, fused to the ONM, and smaller, smooth vesicles that were close to, docked with or fused to the ONM. In view of the above results it can be hypothesised that nuclear assembly in *Xenopus* egg extracts proceeds by the binding of NE-specific NEP-B vesicles to chromatin at approximately the same time as binding of pre-pore complexes. Binding of NEP-B vesicles promotes chromatin decondensation and further recruitment of FG-repeat nucleoporins, and is followed by the binding and fusion of ER-like NEP-A membranes. This streaming and fusion leads to enclosure of the chromatin and formation of mature NPCs (Salpingidou *et al.*, 2005; submitted for publication).

The existence of distinct NE vesicle populations presented here reflects the fundamental difference between somatic and embryonic systems. In contrast to somatic

cells, egg systems contain stockpiles of materials to support the generation of many cells, and in any one cell division only a fraction of this material is used. Therefore, storing of proteins separately from each other might function in order to limit the formation of inappropriate structures, and could explain the observed segregation of different NE proteins into discrete NEP populations in eggs.

The role of the LEM domain in nuclear assembly was highlighted in this study by the fact that emerin peptides containing the LEM domain were able to inhibit nuclear decondensation, binding of NEP vesicles to chromatin and correct NPC assembly. The ability of the emerin LEM domain to interfere with nuclear assembly, as opposed to emerin peptides lacking the LEM domain, raised important questions on the functional differences between the emerin domains. To address this question affinity chromatography was employed to investigate the binding partners of emerin in the *Xenopus* system.

6.3 Emerin interacting proteins

In this study an emerin affinity column was created to screen the *Xenopus* cytosol for interacting proteins. Mass spectrometric analysis identified three potential emerin binding proteins: calcineurin, profilin and β-tubulin. Since β-tubulin was the only repeatable result in this work emphasis was given in investigating the emerin-tubulin relationship. However, the significance of the other two identified proteins should not be dismissed and, therefore, a brief description of them will be given below. Further work in the future involving other protein-protein interaction methods could clarify whether an interaction of calcineurin or profilin with emerin occurs.

6.3.1 Calcineurin

Calcineurin is a Ca^{2+}/Calmodulin dependent Ser/Thr phosphatase widely distributed throughout eukaryotic cells. It consists of a catalytic subunit, which binds calmodulin and a regulatory subunit, which binds Ca^{2+} (Ito *et al.*, 1989). Although it is generally believed that 50% of calcineurin is cytosolic and 50% is bound to the plasma membrane (Yakel, 1997) several reports of calcineurin in the nucleus exist (Momayezi *et al.*, 2000; Nakazawa *et al.*, 2001; Usuda *et al.*, 1996).

Calcineurin is a critical transducer of calcium signals that influence development, adaptation and disease of cardiac and skeletal muscle. Involvement of a calcineurin-dependent pathway in cardiac hypertrophy has already been shown. Transgenic mice that express an activated form of calcineurin in the heart develop dramatic cardiac enlargement that progresses to dilated cardiomyopathy, heart failure and sudden death (Molkentin *et al.*, 1998). In skeletal muscle, calcineurin is involved in the signalling of muscle-fibre type conversion. Activated calcineurin is able to transform myofibres into slow oxidative muscle fibres, resulting in muscle responding and adapting to environmental needs (Olson and Williams, 2000). Calcineurin is also implicated in skeletal muscle differentiation by activating MEF2 and MyoD transcription factors (Friday *et al.*, 2003), and in muscle regeneration via NFATc1 and GATA2 dependent pathways (Sakuma *et al.*, 2003). In further support of an involvement of calcineurin in muscle regeneration is the fact that cyclosporine A, an inhibitor of calcineurin, prevents muscle regeneration in response to damage (Abbott *et al.*, 1998). This could also explain why patients treated with cyclosporine A show severe skeletal muscle weakness (Goy *et al.*, 1989). Considering that absence of emerin leads to defects in cardiac and

skeletal muscle, an interaction between emerin and calcineurin could explain at least partly the tissue specificity of X-EDMD. Interestingly, an association between muscle A-kinase anchoring protein (mAKAP) and nesprin-1α has been reported recently. mAKAP is part of a signalling complex that is involved in transducing cAMP and Ca^{+2} at the NE of heart muscle cells. This signalling complex is involved in the selective activation of NFATc transcription factor by the β-adrenergic receptor and the calcium-dependent phosphatase calcineurin (Pare *et al.*, 2005). Apart from mAKAP, nesprin-1α is also known to interact with emerin. Further work that could provide more solid evidence on the emerin-calcineurin interaction would be of great importance. It would implicate emerin and calcium ion signalling in the development of muscular dystrophy and cardiomyopathy in X-EDMD.

6.3.2 Profilin

Profilin is part of the large number of the actin binding proteins. By interacting with the barbed ends of actin filaments, profilin is one of the major components that control actin polymerisation. A nuclear localisation for profilin has also been reported and based on its co-localisation with speckles and Cajal bodies a role for nuclear profilin:actin complexes in pre-mRNA splicing has also been proposed (Skare *et al.*, 2003). Although the existence of nuclear actin is still controversial, interactions between emerin and actin in the nucleus have already been reported (Fairley *et al.*, 1999; Holaska *et al.*, 2004; Lattanzi *et al.*, 2003). It is proposed that emerin binds the pointed end of F-actin and stimulates actin polymerisation by stabilising the actin filaments. In this way, emerin is part of a nuclear actin cortical network that provides structural support to the nucleus (Holaska *et al.*, 2004).

6.3.3 β-tubulin

Clearly, the most convincing result as an emerin interacting protein from the experiments presented in this work is β-tubulin, as it was repeatable in different sets of experiments, analysed by both, 1-D and 2-D gel electrophoresis. However, tubulin is the major constituent protein of cytoplasmic microtubules (MTs) while emerin is an INM protein, separated from the cytoplasm by the ONM and NE lumen. Hence, the important question arises as how these two proteins could interact.

One possible way that emerin could interact with tubulin is if the latter would be localised in the nucleus. Although tubulin has generally been thought as a protein exclusively localised in the cytoplasm several reports exist about a nuclear localisation of tubulin. Early studies on tissue culture cells report on tubulin distributed throughout the nucleus and in association with chromatin (Menko and Tan, 1980). A more recent study identified the β_{II} isotype of tubulin in the nuclei of cultured rat kidney mesangial cells (Walss *et al.*, 1999). However, unlike most other normal cell lines mesangial cells have the ability to proliferate rapidly in culture by self-producing growth factors and undergoing autocrine-mediated proliferation. Further studies on several cancer cell lines confirmed a nuclear localisation for β_{II}-tubulin and proposed a function in accelerating DNA and RNA synthesis (Walss-Bass *et al.*, 2002). As, however, localisation of β-tubulin in the nucleus is restricted to cells that are characterised by rapid proliferation it seems unlikely that an interaction of emerin with tubulin in the nucleus could be a general phenomenon in normal cells.

A more plausible scenario would be if emerin and tubulin interact during mitosis when the boundary that separates them in interphase, the nuclear envelope, no longer exists. Several aspects of mitosis, including NEBD and assembly of emerin into the reforming NE at the end of mitosis, seem connected with MTs.

MTs have been implicated in the process of NEBD. In prophase, the NE has been shown to form two indentations at antidiametrical sites of the nucleus, which contain the centrosomes that will later form the spindle pole, and MTs. Also, using a marker for the plus-ends of MTs it has been shown that in late prophase, when the NE breaks down, MTs grow towards the nucleus and plus-ends concentrate near the nucleus in a ring of ~ 2-3 μm in width (Piehl and Cassimeris, 2003). Initially, it was suggested that the MTs that are contained in the NE indentations, elongate as mitosis progresses pushing and eventually penetrating the nucleus leading to NEBD (Georgatos *et al.*, 1997). Subsequent studies, however, found no evidence of MTs piercing the nuclear membranes. Instead it is proposed that dynein, a MT minus-end-directed motor protein, associates with the NE before NEBD, stabilising MTs and favouring their growth in close association with the NE. It then pulls NE components towards the centrosomes leading to the formation of the observed NE invaginations. The tension created distal from the centrosomes, leads to detachment of nuclear membranes from chromatin (Beaudouin *et al.*, 2002; Piehl and Cassimeris, 2003; Salina *et al.*, 2002). Once the NE is broken, tubulin can gain access to NE proteins. A role for tubulin in binding NE components at this stage of the cell cycle has already been reported. Binding of M31, the mouse homologue of human HP1 protein, to NEs was shown to be inhibited by a cytosolic factor, which was identified as β2- α2/6-tubulin. Experiments showed that the inhibitory effect was mediated by tubulin blocking the M31-binding sites at the NE.

Non-polymeric tubulin was shown to interact with intact NEs with a high affinity. M31 is known to mediate the recruitment of NE precursors to chromatin during NE reassembly at the end of mitosis. It was, therefore, hypothesised that during NEBD soluble tubulin binds to NE membranes preventing premature interactions between fragments of the NE and M31. In a reverse process, dissociation of tubulin from NE-derived membranes could occur at subsequent stages of mitosis, when the spindle fully develops, and the concentration of soluble tubulin drops (Kourmouli *et al.*, 2001). In a similar scenario it could be hypothesised that when the NE breaks down, tubulin binds to emerin thereby preventing its premature association with its chromatin associated partner BAF.

At this point, it is also worth considering that interactions between NE fragments and other elements of the cytoskeleton have been reported suggesting a role for the cytoskeleton in membrane partitioning during cell division. In prometaphase-arrested cells, vimentin filaments were observed extending towards the cell periphery closely associated with vesicles ranging in diameter from 100 to 400 nm. The vesicles were morphologically different from flat membrane cisternae and tubular elements representing the ER and Golgi apparatus. Immunoelectron microscopy revealed that the vimentin associated vesicles carry lamin B and p58 (or LBR) on their surface while they are depleted of ER and Golgi markers. An interaction between vimentin and lamin B was also shown by co-immunoprecipitation. Based on the above, it was proposed that vimentin filaments act as transient docking sites for NE-derived vesicles during mitosis sorting these vesicles away from ER and Golgi membranes. Alternatively, the interaction of NE vesicles with IFs could serve to prevent premature association of the vesicles with the surface of chromosomes (Maison *et al.*, 1995).

Interestingly, several lines of evidence support a close association between emerin and MTs at the end of mitosis when the NE reassembles. Observations on the fate of emerin during mitosis in human Hep2 cells by confocal microscopy have shown some overlapping staining of emerin with β-tubulin at the spindle poles in metaphase indicating that some emerin containing vesicles are associated with the mitotic spindle poles. In anaphase and early telophase, emerin was found on the chromosome surfaces but initially focally concentrated in the areas of the spindle poles (Dabauvalle *et al.*, 1999). Observations of GFP-emerin in living HeLa cells and endogenous emerin by immunofluorescence further confirmed the enrichment of emerin in the central core region of chromosomes behind the spindle pole (Haraguchi *et al.*, 2000). At the core region, emerin was shown to co-exist with A-type lamins and LAP2α while other nuclear membrane proteins like lamin B, LBR and LAP2β were localised in more peripheral chromosome areas (Dechat *et al.*, 2004). Although in close proximity to MTs, the core region localisation of emerin near the spindle poles does not seem to depend on MTs but on BAF since, when MTs were depolymerised, emerin still localised at the core region (Haraguchi *et al.*, 2001). However, this does not rule out the possibility that once near the spindle poles emerin could gain MT binding activity.

Finally, it is also possible that emerin and tubulin do interact in interphase via an indirect mechanism and that other components that mediate the interaction were not detected in the experiments performed. Taking into account the observed detachment of the MTOC from nuclei in X-EDMD cells, which lack emerin, an indirect link between emerin and MTs in interphase seems not improbable. The recently

discovered giant spectrin-repeat containing proteins that localise at the NE and connect the nucleus with the cytoskeleton would be ideal candidates for this scenario.

6.4 Emerin and the Microtubule Organising Centre (MTOC)

With the aim of investigating the functional significance of the emerin-tubulin interaction X-EDMD cell lines, which lack emerin, were stained with a β-tubulin antibody. The most striking abnormality observed in all X-EDMD cell lines, was the detachment of the MTOC from the nucleus, which was localised at distances at least double than in control cells.

In cells, minus-ends of MTs emanate from and are organised by the MTOC, an organelle that is also known as the centrosome in vertebrate cells or the spindle pole body in yeast. Centrosomes play a fundamental role in the organisation of cells. They regulate the number, distribution and dynamics of MTs within the cell and orchestrate the generation and orientation of the bipolar mitotic spindle. Centrosomes are actively maintained at the cell centre by several kinds of forces. In mammalian cells it is thought that the cell centre position is maintained by pulling forces applied to the MTs by dynein at the cell cortex. Pushing forces on the centrosome MTs exerted by the actomyosin complex also contribute to the centrosome positioning (Burakov *et al.*, 2003).

In interphase, centrosomes are associated with the nucleus. In some organisms like *S. cerevisiae* the MTOC, most commonly known as spindle pole body is embedded in the NE. Unlike the spindle pole body, however, the centrosome is not embedded at the NE,

and the link between centrosomes and nuclei has been mysterious (Raff, 1999). MTs and dynein have been implicated in playing an important role in the attachment of the centrosome to the nucleus while recent studies in *C.elegans* and *Drosophila* have identified more proteins involved in this process.

Cytoplasmic dynein is a minus-end-directed microtubule motor that is involved in several cellular processes like centrosome migration, spindle morphogenesis, cytokinesis or acting as a kinetochore motor. In addition to the above, studies in *Drosophila* have revealed a role for dynein in the attachment of centrosomes to nuclei. In dynein mutant embryos a detachment of centrosomes from the NE was observed. The detachment was either permanent or in some cases centrosomes detached briefly and then moved back to the nucleus and reattached. The role of dynein in the nuclear attachment of the centrosome could be explained by a localisation of dynein at the NE where it could act as a minus-end motor to draw in centrosomal MTs. Alternatively, dynein could be localised at the centrosome where it could act to stabilise the attachment of nucleated MTs that are themselves required for nuclear attachment (Robinson *et al.*, 1999).

In *C.elegans*, protein ZYG-12 has been identified as essential for the centrosome-nucleus attachment. The *zyg-12* gene encodes three isoforms, ZYG-12 A, B and C. All isoforms belong to the Hook family of proteins, which are thought to act as linker proteins between membrane compartments and the MT cytoskeleton. Unlike the Drosophila and human Hook proteins, ZYG-12 B and C isoforms encode a transmembrane domain at their C-terminus and show a centrosomal and NE localisation. In *C.elegans zyg-12* mutant embryos, centrosomes fail to associate with

nuclei throughout interphase. This leads to formation of aberrant spindles, chromosome segregation defects and ultimately embryonic lethality. ZYG-12 can interact with components of the dynein complex and its localisation at the NE requires SUN-1, a SUN-domain containing NE protein. Based on this, a two-step model has been proposed for the attachment of centrosomes to nuclei in *C.elegans*. Initially, dynein is recruited to the nucleus via an interaction of ZYG-12 at the NE with the dynein light intermediate chain. Dynein then translocates towards the minus-ends of MTs organised by the centrosome, bringing the centrosome in close proximity to the nucleus. In the second dynein-independent step, ZYG-12, which is localised in the NE in a SUN-1-dependent manner and at the centrosome, mediates a direct attachment of the two organelles by homodimerisation (Malone *et al.*, 2003).

Further studies on nuclear migrations that occur during the embryonic development of *C.elegans*, identified protein UNC-84 as the missing link between the centrosome and the nucleus. UNC-84 comprises two isoforms, A and B, which contain a transmembrane region and are associated with the NE although it is not clear yet whether they are localised at the inner or outer nuclear membrane. Both contain a C-terminal SUN-domain, which is highly similar to the C-terminus of Sad1, a NE protein that is thought to anchor the spindle pole body to the NE. In *unc-84* mutants mispositioned and unanchored nuclei that were able to move around within the cytoplasm were observed. The mutations that affected the function of UNC-84 required for nuclear anchoring were localised in the SUN domain. Since nuclear anchoring in a cell could be achieved by forces transmitted to the nucleus through the centrosome it was initially proposed that UNC-84 could function to couple the nucleus and the centrosome (Malone *et al.*, 1999). Subsequent studies, however, challenged the above

hypothesis. When centrosomes were localised in *C.elegans* unc-84 null cells centrosome localisation was indistinguishable from wild-type embryos suggesting that UNC-84 is not involved in the nuclear anchorage of the centrosome. Instead based on the dependence of its NE localisation on lamin expression, it is proposed that UNC-84 and its partner UNC-83 form a structural bridge that connects the spectrin-repeat containing protein ANC-1, which is localised at the ONM to the lamina in the INM. This connection would then function to transfer forces between the structural elements of the nucleus and molecular motors of the cytoskeleton (Lee *et al.*, 2002).

Studies in *Drosophila* have also shed some more light in the nature of the centrosome-nucleus association. Recently, Klarsicht, a large protein that contains a KASH (Klarsicht, Anc-1, Syne-1 Homology) domain, was shown to localise to the NE where it can interact with lamins. Based on the fact that in Klarsicht and lamin *Drosophila* mutants the MTOC is detached from the nucleus it is hypothesised that these proteins form a bridge that connects the MTOC with the nucleus. In this complex, Klarsicht is localised at the ONM via its KASH domain and is linked by one or more proteins to the lamins in the INM. At the same time the N-terminal portion of Klarsicht is linked to MTs by dynein tethering this way the MTOC to the NE (Patterson *et al.*, 2004).

The implication of the KASH domain containing protein Klarsicht in maintaining the MTOC-nucleus association seems very interesting considering that nesprins 1 and 2 also contain a KASH domain at their C-terminus and are known to interact with lamins and emerin. Although the nesprin ortholog in *Drosophila* is the giant protein MSP300 and Klarsicht shares no other similarity with nesprins than the KASH domain, it is

possible that Klarsicht performs the NE and cytoplasmic functions of nesprins while MSP300 has a more muscle specific role in *Drosophila* (Zhang *et al.*, 2005).

Nesprins 1 and 2, also known as Enaptin and NUANCE are gigantic proteins that belong to the α-actinin family of actin binding proteins. Structurally they comprise three main domains: an N-terminal actin binding domain, a large helical rod domain that contains multiple spectrin-repeats (SRs) and a C-terminal TM domain. At the C-terminus, and including the TM domain, is the KASH domain, a 62 residue region that is shared between the *Drosophila* Klarsicht, Anc-1 and Syne-1 proteins. Except nesprin-1 and -2 giant, the nesprin family comprises many other N-terminally truncated isoforms (Zhang *et al.*, 2001). The different nesprin isoforms are localised at the NE, cytoplasm and nuclear interior while immunoelectron microscopy revealed that even the large isoforms like Nesprin-2 giant/NUANCE are able to localise at both sides of the NE. Interactions between the last SRs at the C-terminal regions of both, nesprin 1α and nesprin 2 with emerin have already been reported (Libotte *et al.*, 2005; Mislow *et al.*, 2002; Zhang *et al.*, 2005).

Considering that nesprins localise at both the inner and outer nuclear membrane, and that they can interact with emerin it is not unlikely that they are part of complex that connects emerin with the MTOC. It has already been suggested for nesprin-2/NUANCE that it could serve as a platform for anchoring the dynein-dynactin complex. Interestingly, when cells were treated with Latrunculin A, a drug that depolymerises actin filaments, nuclei acquired an irregular shape with wrinkled invaginations, in which cytoplasmic nesprin-2/NUANCE and actin aggregates accumulated. These NE invaginations greatly resembled the MT containing finger-like projections observed in

cells just before NEBD. Based on this observation, which implies a link between nesprin-2/NUANCE and the pericentrosomal astral complex, the authors suggested a role for nesprin-2/NUANCE in the spatial organisation of a MT-dependent machinery linking it to the NE (Zhen *et al.*, 2002).

6.5 Emerin in disease

Since the discovery that mutations in the emerin gene cause Emery-Dreifuss muscular dystrophy several hypotheses have been formulated to explain how a NE protein can lead to the disease phenotype. The two most appealing explanations so far include the 'structural' model and the 'gene expression' model, in which mutations lead to an increased nuclear fragility or to gene expression defects, respectively.

There is increasing evidence that strengthens the idea that the nucleus is not an isolated organelle but is linked to cytoskeletal elements. The discovery of nesprins, the giant proteins that localise to both sides of the NE, connecting NE proteins with the cytoskeleton, is one of them. Additionally, lamin mutations cause the autosomal dominant form of EDMD and in lamin null-cells a disorganisation of the actin, tubulin and vimentin cytoskeleton and their detachment from the nucleus has been reported (Broers *et al.*, 2004). The present work provides further evidence for the close association of the nucleus with the cytoskeleton supporting the 'structural' hypothesis model. The direct or indirect association of emerin with tubulin and the disturbed appearance of MTs in X-EDMD cells points to the interdependence of the nucleus and the cytoskeleton. Future work on whether other cytoskeletal elements are disturbed in X-EDMD cells would be interesting.

The observed detachment of the MTOC from the nucleus in X-EDMD cells further supports the relationship of emerin with MTs. The immediate question that arises from this observation, however, is what the detachment of the MTOC means in relation to emerin and X-EDMD. Attachment of the centrosome to the nucleus serves several purposes. It maintains the proximity of the centrosomes to chromosomes at the onset of mitosis. Abnormal centrosome positioning could lead to a failure of astral MTs to capture chromosomes upon NEBD producing defects in chromosome segregation. One of the main clinical features of X-EDMD is muscle waste, which implies defective muscle regeneration. The regeneration process requires that satellite cells, which are in a quiescent state, re-enter the cell cycle, proliferate and differentiate into myofibres. As the centrosome attachment to the nucleus is of great importance for a smooth cell cycle any abnormalities arising from the detachment of the centrosomes from the nuclei could interfere with the regeneration process.

Additionally, centrosome attachment to the nucleus is required for positioning the nucleus at the cell centre and to transmit forces to move nuclei during nuclear migrations. This would imply an involvement of emerin in nuclear migrations. Nuclear migrations play an essential role in various processes like the movement of pronuclei during fertilisation, the separation of daughter nuclei during mitosis and the positioning of nuclei in interphase cells. In muscle, nuclear migrations are an important step during differentiation. Skeletal muscles fibres are syncytial. Each fibre contains several hundred myonuclei. Most nuclei are well separated from each other. In developing myotubes nuclei move at high speeds through the cytoplasm and migrate from the centre to the cell periphery. This repositioning of nuclei from the centre to the periphery defines the myotubes to myofibre transition. Interestingly, mispositioned nuclei that fail

to migrate have been observed in X-EDMD muscle tissues (Toniolo *et al.*, 1999). As, however, this has been observed in muscle tissues of patients with other muscular dystrophies as well, more work is needed to support a correlation of emerin with nuclear migrations defects in muscle.

To date several functions have been attributed to emerin. These include the mechanical stability of the nuclear membrane, the regulation of gene expression, the regeneration of muscle fibres and the regulation of calcium levels at the nuclear envelope and nucleoplasm. The present thesis has provided evidence on the association of emerin with tubulin and the MTOC. Clearly more work is needed as to elucidate the nature of this interaction and its functional significance. Understanding the function of nuclear envelope proteins seems of great importance considering the devastating effects of their absence.

REFERENCES

Abbott K. L., Friday B. B., Thaloor D., Murphy T. J. and Pavlath G. K. (1998) Activation and cellular localization of the cyclosporine A-sensitive transcription factor NF-AT in skeletal muscle cells. *Mol Biol Cell* **9 (10)**: 2905-16.

Adam S. A., Lobl T. J., Mitchell M. A. and Gerace L. (1989) Identification of specific binding proteins for a nuclear location sequence. *Nature* **337 (6204)**: 276-9.

Aebi U., Cohn J., Buhle L. and Gerace L. (1986) The nuclear lamina is a meshwork of intermediate-type filaments. *Nature* **323 (6088)**: 560-4.

Akey C. W. (1990) Visualization of transport-related configurations of the nuclear pore transporter. *Biophys J* **58 (2)**: 341-55.

Alberts B., Bray D., Lewis J., Raff M., Roberts K. and Watson J. D. (1989) *Molecular Biology of the Cell.* Garland Publishing Inc, New York.

Alvarez-Reyes M. (2004) Interactions between nuclear lamins and their binding partners in EDMD fibroblasts. PhD Thesis *University of Durham.*

Ano T. and Shoda M. (1992) Ultra-rapid transformation of Escherichia coli by an alkali cation. *Biosci Biotech and Biochem* **56 (9)**: 1505.

Apel E. D., Lewis R. M., Grady R. M. and Sanes J. R. (2000) Syne-1, a dystrophin- and Klarsicht-related protein associated with synaptic nuclei at the neuromuscular junction. *J Biol Chem* **275 (41)**: 31986-95.

Ashery-Padan R., Ulitzur N., Arbel A., Goldberg M., Weiss A. M., Maus N., Fisher P. A. and Gruenbaum Y. (1997) Localization and posttranslational modifications of otefin, a protein required for vesicle attachment to chromatin, during Drosophila melanogaster development. *Mol Cell Biol* **17 (7)**: 4114-23.

Beaudouin J., Gerlich D., Daigle N., Eils R. and Ellenberg J. (2002) Nuclear envelope breakdown proceeds by microtubule-induced tearing of the lamina. *Cell* **108 (1)**: 83-96.

Belgareh N., Rabut G., Baï S. W., van Overbeek M., Beaudouin J., Daigle N., Zatsepina O. V., Pasteau F., Labas V., Fromont-Racine M., Ellenberg J. and Doye V. (2001) An evolutionarily conserved NPC subcomplex, which redistributes in part to kinetochores in mammalian cells. *J Cell Biol* **154**: 1147-60.

Belmont A. (2003) Dynamics of chromatin, proteins, and bodies within the cell nucleus. *Curr Opin Cell Biol* **15 (3)**: 304-10.

Bengtsson L. and Wilson K. L. (2004) Multiple and surprising new functions for emerin, a nuclear membrane protein. *Curr Opin Cell Biol* **16 (1)**: 73-9.

Berrios M. and Avilion A. A. (1990) Nuclear formation in a *Drosophila* cell-free system. *Exp. Cell Res.* **191**: 64-70.

Bione S., Maestrini E., Rivella S., Mancini M., Regis S., Romeo G. and Toniolo D. (1994) Identification of a novel X-linked gene responsible for Emery-Dreifuss muscular dystrophy. *Nat Genet* **8 (4)**: 323-7.

Bione S., Small K., Aksmanovic V. M., D'Urso M., Ciccodicola A., Merlini L., Morandi L., Kress W., Yates J. R., Warren S. T. and et al. (1995) Identification of new mutations in the Emery-Dreifuss muscular dystrophy gene and evidence for genetic heterogeneity of the disease. *Hum Mol Genet* **4 (10)**: 1859-63.

Bodoor K., Shaikh S., Salina D., Raharjo W. H., Bastos R., Lohka M. and Burke B. (1999) Sequential recruitment of NPC proteins to the nuclear periphery at the end of mitosis. *J Cell Sci* **112**: 2253-64.

Boehmer T., Enninga J., Dales S., Blobel G. and Zhong H. (2003) Depletion of a single nucleoporin, Nup107, prevents the assembly of a subset of nucleoporins into the nuclear pore complex. *Proc Natl Acad Sci U S A* **100**: 981-985.

Bonne G., Di Barletta M. R., Varnous S., Becane H. M., Hammouda E. H., Merlini L., Muntoni F., Greenberg C. R., Gary F., Urtizberea J. A., Duboc D., Fardeau M., Toniolo D. and Schwartz K. (1999) Mutations in the gene encoding lamin A/C cause autosomal dominant Emery-Dreifuss muscular dystrophy. *Nat Genet* **21 (3)**: 285-8.

Bonne G. and Levy N. (2003) LMNA mutations in atypical Werner's syndrome. *Lancet* **362 (9395)**: 1585-6; author reply 1586.

Boriani G., Gallina M., Merlini L., Bonne G., Toniolo D., Amati S., Biffi M., Martignani C., Frabetti L., Bonvicini M., Rapezzi C. and Branzi A. (2003) Clinical relevance of atrial fibrillation/flutter, stroke, pacemaker implant, and heart failure in Emery-Dreifuss muscular dystrophy: a long-term longitudinal study. *Stroke* **34 (4)**: 901-8.

Bridger J. M., Kill I. R., O'Farrell M. and Hutchison C. J. (1993) Internal lamin structures within G1 nuclei of human dermal fibroblasts. *J Cell Sci* **104 (Pt 2)**: 297-306.

Broers J. L., Peeters E. A., Kuijpers H. J., Endert J., Bouten C. V., Oomens C. W., Baaijens F. P. and Ramaekers F. C. (2004) Decreased mechanical stiffness in LMNA-/- cells is caused by defective nucleo-cytoskeletal integrity: implications for the development of laminopathies. *Hum Mol Genet* **13 (21)**: 2567-80.

Buendia B. and Courvalin J. C. (1997) Domain-specific disassembly and reassembly of nuclear membranes during mitosis. *Exp Cell Res* **230 (1)**: 133-44.

Burakov A., Nadezhdina E., Slepchenko B. and Rodionov V. (2003) Centrosome positioning in interphase cells. *J Cell Biol* **162 (6)**: 963-9.

Burke B. and Gerace L. (1986) A cell free system to study reassembly of the nuclear envelope at the end of mitosis. *Cell* **44 (4)**: 639-52.

Cameron L. A. and Poccia D. (1994) *In vitro* development of the sea urchin male pronucleus. *Dev. Biol.* **162**: 568-578.

Cao H. and Hegele R. A. (2000) Nuclear lamin A/C R482Q mutation in canadian kindreds with Dunnigan-type familial partial lipodystrophy. *Hum Mol Genet* **9 (1)**: 109-12.

Cao H. and Hegele R. A. (2003) LMNA is mutated in Hutchinson-Gilford progeria (MIM 176670) but not in Wiedemann-Rautenstrauch progeroid syndrome (MIM 264090). *J Hum Genet* **48 (5)**: 271-4.

Cartegni L., di Barletta M. R., Barresi R., Squarzoni S., Sabatelli P., Maraldi N., Mora M., Di Blasi C., Cornelio F., Merlini L., Villa A., Cobianchi F. and Toniolo D. (1997) Heart-specific localization of emerin: new insights into Emery-Dreifuss muscular dystrophy. *Hum Mol Genet* **6 (13)**: 2257-64.

Caux F., Dubosclard E., Lascols O., Buendia B., Chazouilleres O., Cohen A., Courvalin J. C., Laroche L., Capeau J., Vigouroux C. and Christin-Maitre S. (2003) A new clinical condition linked to a novel mutation in lamins A and C with generalized lipoatrophy, insulin-resistant diabetes, disseminated

leukomelanodermic papules, liver steatosis, and cardiomyopathy. *J Clin Endocrinol Metab* **88 (3)**: 1006-13.

Chaudhary N. and Courvalin J. C. (1993) Stepwise reassembly of the nuclear envelope at the end of mitosis. *J Cell Biol* **122 (2)**: 295-306.

Chen L., Lee L., Kudlow B. A., Dos Santos H. G., Sletvold O., Shafeghati Y., Botha E. G., Garg A., Hanson N. B., Martin G. M., Mian I. S., Kennedy B. K. and Oshima J. (2003) LMNA mutations in atypical Werner's syndrome. *Lancet* **362 (9382)**: 440-5.

Chu A., Rassadi R. and Stochaj U. (1998) Velcro in the nuclear envelope: LBR and LAPs. *FEBS Lett* **441 (2)**: 165-9.

Clements L., Manilal S., Love D. R. and Morris G. E. (2000) Direct interaction between emerin and lamin A. *Biochem Biophys Res Commun* **267 (3)**: 709-14.

Cohen M., Lee K. K., Wilson K. L. and Gruenbaum Y. (2001) Transcriptional repression, apoptosis, human disease and the functional evolution of the nuclear lamina. *Trends Biochem Sci* **26 (1)**: 41-7.

Collas I. and Courvalin J. C. (2000) Sorting nuclear membrane proteins at mitosis. *Trends Cell Biol* **10 (1)**: 5-8.

Comings D. E. (1980) Arrangement of chromatin in the nucleus. *Hum Genet* **53 (2)**: 131-43.

Cronshaw J. M., Krutchinsky A. N., Zhang W., Chait B. T. and Matunis M. J. (2002) Proteomic analysis of the mammalian nuclear pore complex. *J Cell Biol* **158 (5)**: 915-27.

Dabauvalle M. C., Muller E., Ewald A., Kress W., Krohne G. and Muller C. R. (1999) Distribution of emerin during the cell cycle. *Eur J Cell Biol* **78 (10)**: 749-56.

Dahl K. N., Kahn S. M., Wilson K. L. and Discher D. E. (2004) The nuclear envelope lamina network has elasticity and a compressibility limit suggestive of a molecular shock absorber. *J Cell Sci* **117 (Pt 20)**: 4779-86.

Dahlberg J. E. and Lund E. (1998) Functions of the GTPase Ran in RNA export from the nucleus. *Curr Opin Cell Biol* **10 (3)**: 400-8.

De Sandre-Giovannoli A., Bernard R., Cau P., Navarro C., Amiel J., Boccaccio I., Lyonnet S., Stewart C. L., Munnich A., Le Merrer M. and Levy N. (2003) Lamin a truncation in Hutchinson-Gilford progeria. *Science* **300 (5628)**: 2055.

De Sandre-Giovannoli A., Chaouch M., Kozlov S., Vallat J. M., Tazir M., Kassouri N., Szepetowski P., Hammadouche T., Vandenberghe A., Stewart C. L., Grid D. and Levy N. (2002) Homozygous defects in LMNA, encoding lamin A/C nuclear-envelope proteins, cause autosomal recessive axonal neuropathy in human (Charcot-Marie-Tooth disorder type 2) and mouse. *Am J Hum Genet* **70 (3)**: 726-36.

Dechat T., Gajewski A., Korbei B., Gerlich D., Daigle N., Haraguchi T., Furukawa K., Ellenberg J. and Foisner R. (2004) LAP2alpha and BAF transiently localize to telomeres and specific regions on chromatin during nuclear assembly. *J Cell Sci* **117 (Pt 25)**: 6117-28.

Dechat T., Korbei B., Vaughan O. A., Vlcek S., Hutchison C. J. and Foisner R. (2000) Lamina-associated polypeptide 2alpha binds intranuclear A-type lamins. *J Cell Sci* **113 (Pt 19)**: 3473-84.

Dechat T., Vlcek S. and Foisner R. (2000) Review: lamina-associated polypeptide 2 isoforms and related proteins in cell cycle-dependent nuclear structure dynamics. *J Struct Biol* **129 (2-3)**: 335-45.

Dellaire G. and Bazett-Jones D. P. (2004) PML nuclear bodies: dynamic sensors of DNA damage and cellular stress. *Bioessays* **26 (9)**: 963-77.

Dreger M., Bengtsson L., Schoneberg T., Otto H. and Hucho F. (2001) Nuclear envelope proteomics: novel integral membrane proteins of the inner nuclear membrane. *Proc Natl Acad Sci U S A* **98 (21)**: 11943-8.

Dreuillet C., Tillit J., Kress M. and Ernoult-Lange M. (2002) In vivo and in vitro interaction between human transcription factor MOK2 and nuclear lamin A/C. *Nucleic Acids Res* **30 (21)**: 4634-42.

Drummond S., Ferrigno P., Lyon C., Murphy J., Goldberg M., Allen T., Smythe C. and Hutchison C. J. (1999) Temporal differences in the appearance of NEP-B78 and an LBR-like protein during Xenopus nuclear envelope reassembly reflect the ordered recruitment of functionally discrete vesicle types. *J Cell Biol* **144 (2)**: 225-40.

Dyer J A, Kill IR, Pugh G, Quinlan RA, Lane EB and Hutchison CJ (1997) Cell cycle changes in A-type lamin associations detected in human dermal fibroblasts using monoclonal antibodies. *Chromosome Res* **5**: 383-394.

Eggers D. K., Welch W. J. and Hansen W. J. (1997) Complexes between nascent polypeptides and their molecular chaperones in the cytosol of mammalian cells. *Mol Biol Cell* **8 (8)**: 1559-73.

Ellenberg J (2002) Dynamics of the nuclear envelope proteins during the cell cycle in mammalian cells. In: *Nuclear envelope dynamics in embryos and somatic cells* (eds Collas), pp: 15-28, Kluwer Academic/Plenum Publisher.

Ellenberg J., Siggia E. D., Moreira J. E., Smith C. L., Presley J. F., Worman H. J. and Lippincott-Schwartz J. (1997) Nuclear membrane dynamics and reassembly in living cells: targeting of an inner nuclear membrane protein in interphase and mitosis. *J Cell Biol* **138 (6)**: 1193-206.

Ellis J. A., Craxton M., Yates J. R. and Kendrick-Jones J. (1998) Aberrant intracellular targeting and cell cycle-dependent phosphorylation of emerin contribute to the Emery-Dreifuss muscular dystrophy phenotype. *J Cell Sci* **111 (Pt 6)**: 781-92.

Ellis J. A., Yates J. R., Kendrick-Jones J. and Brown C. A. (1999) Changes at P183 of emerin weaken its protein-protein interactions resulting in X-linked Emery-Dreifuss muscular dystrophy. *Hum Genet* **104 (3)**: 262-8.

Emery A. E. (2000) Emery-Dreifuss muscular dystrophy - a 40 year retrospective. *Neuromuscul Disord* **10 (4-5)**: 228-32.

Emery A. E. and Dreifuss F. E. (1966) Unusual type of benign x-linked muscular dystrophy. *J Neurol Neurosurg Psychiatry* **29 (4)**: 338-42.

Eriksson M., Brown W. T., Gordon L. B., Glynn M. W., Singer J., Scott L., Erdos M. R., Robbins C. M., Moses T. Y., Berglund P., Dutra A., Pak E., Durkin S., Csoka A. B., Boehnke M., Glover T. W. and Collins F. S. (2003) Recurrent de novo point mutations in lamin A cause Hutchinson-Gilford progeria syndrome. *Nature* **423 (6937)**: 293-8.

Fairley E. A., Kendrick-Jones J. and Ellis J. A. (1999) The Emery-Dreifuss muscular dystrophy phenotype arises from aberrant targeting and binding of emerin at the inner nuclear membrane. *J Cell Sci* **112 (Pt 15)**: 2571-82.

Fatkin D., MacRae C., Sasaki T., Wolff M. R., Porcu M., Frenneaux M., Atherton J., Vidaillet H. J., Jr., Spudich S., De Girolami U., Seidman J. G., Seidman C., Muntoni F., Muehle G., Johnson W. and McDonough B. (1999) Missense mutations in the rod domain of the lamin A/C gene as causes of dilated

cardiomyopathy and conduction-system disease. *N Engl J Med* **341 (23)**: 1715-24.

Felice K. J., Schwartz R. C., Brown C. A., Leicher C. R. and Grunnet M. L. (2000) Autosomal dominant Emery-Dreifuss dystrophy due to mutations in rod domain of the lamin A/C gene. *Neurology* **55 (2)**: 275-80.

Fey S. J. and Larsen P. M. (2001) 2D or not 2D. Two-dimensional gel electrophoresis. *Curr Opin Chem Biol* **5 (1)**: 26-33.

Fidzianska A. and Hausmanowa-Petrusewicz I. (2003) Architectural abnormalities in muscle nuclei. Ultrastructural differences between X-linked and autosomal dominant forms of EDMD. *J Neurol Sci* **210 (1-2)**: 47-51.

Fidzianska A., Toniolo D. and Hausmanowa-Petrusewicz I. (1998) Ultrastructural abnormality of sarcolemmal nuclei in Emery-Dreifuss muscular dystrophy (EDMD). *J Neurol Sci* **159 (1)**: 88-93.

Fields S. and Song O. (1989) A novel genetic system to detect protein-protein interactions. *Nature* **340**: 245-6.

Fishbein M. C., Siegel R. J., Thompson C. E. and Hopkins L. C. (1993) Sudden death of a carrier of X-linked Emery-Dreifuss muscular dystrophy. *Ann Intern Med* **119 (9)**: 900-5.

Foisner R. (2001) Inner nuclear membrane proteins and the nuclear lamina. *J. Cell Sci.* **114**: 3791-2.

Foisner R. and Gerace L. (1993) Integral membrane proteins of the nuclear envelope interact with lamins and chromosomes, and binding is modulated by mitotic phosphorylation. *Cell* **73 (7)**: 1267-79.

Fontoura B. M., Blobel G. and Matunis M. J. (1999) A conserved biogenesis pathway for nucleoporins: proteolytic processing of a 186-kilodalton precursor generates Nup98 and the novel nucleoporin, Nup96. *J Cell Biol* **144 (6)**: 1097-112.

Forterre P. (1995) Thermoreduction, a hypothesis for the origin of prokaryotes. *C R Acad Sci III* **318 (4)**: 415-22.

Fox A. H., Lam Y. W., Leung A. K., Lyon C. E., Andersen J., Mann M. and Lamond A. I. (2002) Paraspeckles: a novel nuclear domain. *Curr Biol* **12 (1)**: 13-25.

Franke W. W., Scheer U., Krohne G. and Jarasch E. D. (1981) The nuclear envelope and the architecture of the nuclear periphery. *J Cell Biol* **91 (3 Pt 2)**: 39s-50s.

Friday B. B., Mitchell P. O., Kegley K. M. and Pavlath G. K. (2003) Calcineurin initiates skeletal muscle differentiation by activating MEF2 and MyoD. *Differentiation* **71 (3)**: 217-27.

Fridkin A., Mills E., Margalit A., Neufeld E., Lee K. K., Feinstein N., Cohen M., Wilson K. L. and Gruenbaum Y. (2004) Matefin, a Caenorhabditis elegans germ line-specific SUN-domain nuclear membrane protein, is essential for early embryonic and germ cell development. *Proc Natl Acad Sci U S A* **101 (18)**: 6987-92.

Furukawa K. (1999) LAP2 binding protein 1 (L2BP1/BAF) is a candidate mediator of LAP2-chromatin interaction. *J Cell Sci* **112 (Pt 15)**: 2485-92.

Furukawa K., Fritze C. E. and Gerace L. (1998) The major nuclear envelope targeting domain of LAP2 coincides with its lamin binding region but is distinct from its chromatin interaction domain. *J Biol Chem* **273 (7)**: 4213-9.

Gant T. M., Harris C. A. and Wilson K. L. (1999) Roles of LAP2 proteins in nuclear assembly and DNA replication: truncated LAP2beta proteins alter

lamina assembly, envelope formation, nuclear size, and DNA replication efficiency in Xenopus laevis extracts. *J Cell Biol* **144 (6)**: 1083-96.

Gant T. M. and Wilson K. L. (1997) Nuclear assembly. *Annu Rev Cell Dev Biol* **13** 669-95.

Gareiss M., Eberhardt K., Kruger E., Kandert S., Bohm C., Zentgraf H., Muller C. R. and Dabauvalle M. C. (2005) Emerin expression in early development of Xenopus laevis. *Eur J Cell Biol* **84 (2-3)**: 295-309.

Garg A., Speckman R. A. and Bowcock A. M. (2002) Multisystem dystrophy syndrome due to novel missense mutations in the amino-terminal head and alpha-helical rod domains of the lamin A/C gene. *Am J Med* **112 (7)**: 549-55.

Georgatos S. D. (2001) The inner nuclear membrane: simple, or very complex? *Embo J* **20 (12)**: 2989-94.

Georgatos S. D., Pyrpasopoulou A. and Theodoropoulos P. A. (1997) Nuclear envelope breakdown in mammalian cells involves stepwise lamina disassembly and microtubule-drive deformation of the nuclear membrane. *J Cell Sci* **110 (Pt 17)**: 2129-40.

Glass C. A., Glass J. R., Taniura H., Hasel K. W., Blevitt J. M. and Gerace L. (1993) The alpha-helical rod domain of human lamins A and C contains a chromatin binding site. *Embo J* **12 (11)**: 4413-24.

Goldberg M. (2004) Import and export at the nuclear envelope. In: *The Nuclear Envelope* (eds D.E. Evans), pp: 115-134, Garland/Bios Scientific Publishers, Abingdon.

Goldberg M., Lu H., Stuurman N., Ashery-Padan R., Weiss A. M., Yu J., Bhattacharyya D., Fisher P. A., Gruenbaum Y. and Wolfner M. F. (1998) Interactions among Drosophila nuclear envelope proteins lamin, otefin, and YA. *Mol Cell Biol* **18 (7)**: 4315-23.

Goldberg M. W. and Allen T. D. (1996) The nuclear pore complex and lamina: three-dimensional structures and interactions determined by field emission in-lens scanning electron microscopy. *J Mol Biol* **257 (4)**: 848-65.

Goldberg M. W., Wiese C., Allen T. D. and Wilson K. L. (1997) Dimples, pores, star-rings, and thin rings on growing nuclear envelopes: evidence for structural intermediates in nuclear pore complex assembly. *J Cell Sci* **110 (Pt 4)**: 409-20.

Goldman A. E., Moir R. D., Montag-Lowy M., Stewart M. and Goldman R. D. (1992) Pathway of incorporation of microinjected lamin A into the nuclear envelope. *J Cell Biol* **119 (4)**: 725-35.

Gorlich D., Pante N., Kutay U., Aebi U. and Bischoff F. R. (1996) Identification of different roles for RanGDP and RanGTP in nuclear protein import. *Embo J* **15 (20)**: 5584-94.

Goy J. J., Stauffer J. C., Deruaz J. P., Gillard D., Kaufmann U., Kuntzer T. and Kappenberger L. (1989) Myopathy as possible side-effect of cyclosporin. *Lancet* **1 (8652)**: 1446-7.

Greber U. F. and Gerace L. (1995) Depletion of calcium from the lumen of endoplasmic reticulum reversibly inhibits passive diffusion and signal-mediated transport into the nucleus. *J Cell Biol* **128 (1-2)**: 5-14.

Haraguchi T., Holaska J. M., Yamane M., Koujin T., Hashiguchi N., Mori C., Wilson K. L. and Hiraoka Y. (2004) Emerin binding to Btf, a death-promoting transcriptional repressor, is disrupted by a missense mutation that causes Emery-Dreifuss muscular dystrophy. *Eur J Biochem* **271 (5)**: 1035-45.

Haraguchi T., Koujin T., Hayakawa T., Kaneda T., Tsutsumi C., Imamoto N., Akazawa C., Sukegawa J., Yoneda Y. and Hiraoka Y. (2000) Live fluorescence imaging reveals early recruitment of emerin, LBR, RanBP2, and Nup153 to reforming functional nuclear envelopes. *J Cell Sci* **113 (Pt 5)**: 779-94.

Haraguchi T., Koujin T., Segura-Totten M., Lee K. K., Matsuoka Y., Yoneda Y., Wilson K. L. and Hiraoka Y. (2001) BAF is required for emerin assembly into the reforming nuclear envelope. *J Cell Sci* **114 (Pt 24)**: 4575-85.

Harlow L. and Lane D. (1988) *Antibodies. A laboratory manual.* Cold Spring Harbor Laboratory Press, Cold Spring Harbor, New York.

Harris C. A., Andryuk P. J., Cline S., Chan H. K., Natarajan A., Siekierka J. J. and Goldstein G. (1994) Three distinct human thymopoietins are derived from alternatively spliced mRNAs. *Proc Natl Acad Sci U S A* **91 (14)**: 6283-7.

Harris C. A., Andryuk P. J., Cline S. W., Mathew S., Siekierka J. J. and Goldstein G. (1995) Structure and mapping of the human thymopoietin (TMPO) gene and relationship of human TMPO beta to rat lamin-associated polypeptide 2. *Genomics* **28 (2)**: 198-205.

Hartmann E., Rapoport T. A. and Lodish H. F. (1989) Predicting the orientation of eukaryotic membrane-spanning proteins. *Proc Natl Acad Sci U S A* **86 (15)**: 5786-90.

Hedges S. B., Chen H., Kumar S., Wang D. Y., Thompson A. S. and Watanabe H. (2001) A genomic timescale for the origin of eukaryotes. *BMC Evol Biol* **1 (1)**: 4.

Hendrick J. P. and Hartl F. U. (1995) The role of molecular chaperones in protein folding. *Faseb J* **9**: 1559-69.

Herrmann H. and Aebi U. (2004) Intermediate filaments: molecular structure, assembly mechanism, and integration into functionally distinct intracellular Scaffolds. *Annu Rev Biochem* **73**: 749-89.

Hodzic D. M., Yeater D. B., Bengtsson L., Otto H. and Stahl P. D. (2004) Sun2 is a novel mammalian inner nuclear membrane protein. *J Biol Chem* **279 (24)**: 25805-12.

Hoeltzenbein M., Karow T., Zeller J. A., Warzok R., Wulff K., Zschiesche M., Herrmann F. H., Grosse-Heitmeyer W. and Wehnert M. S. (1999) Severe clinical expression in X-linked Emery-Dreifuss muscular dystrophy. *Neuromuscul Disord* **9 (3)**: 166-70.

Hofemeister H. and O'Hare P. (2005) Analysis of the localization and topology of nurim, a polytopic protein tightly associated with the inner nuclear membrane. *J Biol Chem* **280 (4)**: 2512-21.

Holaska J. M., Kowalski A. K. and Wilson K. L. (2004) Emerin caps the pointed end of actin filaments: evidence for an actin cortical network at the nuclear inner membrane. *PLoS Biol* **2 (9)**: E231.

Holaska J. M., Lee K. K., Kowalski A. K. and Wilson K. L. (2003) Transcriptional repressor germ cell-less (GCL) and barrier to autointegration factor (BAF) compete for binding to emerin in vitro. *J Biol Chem* **278 (9)**: 6969-75.

Holt I., Clements L., Manilal S. and Morris G. E. (2001) How does a g993t mutation in the emerin gene cause Emery-Dreifuss muscular dystrophy? *Biochem Biophys Res Commun* **287 (5)**: 1129-33.

Hozak P., Sasseville A. M., Raymond Y. and Cook P. R. (1995) Lamin proteins form an internal nucleoskeleton as well as a peripheral lamina in human cells. *J Cell Sci* **108 (Pt 2)**: 635-44.

Huang S. (2000) Review: perinucleolar structures. *J Struct Biol* **129 (2-3)**: 233-40.
Hutchison C.J. (1993). The use of cell-free extracts of Xenopus eggs for studying DNA replication in vitro. In: *The Cell Cycle – A practical approach.* Oxford University Press.
Hutchison C. J. (2002) Lamins: building blocks or regulators of gene expression? *Nat Rev Mol Cell Biol* **3 (11)**: 848-58.
Hutchison C. J., Alvarez-Reyes M. and Vaughan O. A. (2001) Lamins in disease: why do ubiquitously expressed nuclear envelope proteins give rise to tissue-specific disease phenotypes? *J Cell Sci* **114 (Pt 1)**: 9-19.
Hutchison C.J. (2002) Spectrin-repeat proteins: integrating the nucleoskeleton with the cytoskeleton? *The ELSO Gazette* **11** 1-3.
Ito A., Hashimoto T., Hirai M., Takeda T., Shuntoh H., Kuno T. and Tanaka C. (1989) The complete primary structure of calcineurin A, a calmodulin binding protein homologous with protein phosphatases 1 and 2A. *Biochem Biophys Res Commun* **163 (3)**: 1492-7.
Karkkainen S., Helio T., Miettinen R., Tuomainen P., Peltola P., Rummukainen J., Ylitalo K., Kaartinen M., Kuusisto J., Toivonen L., Nieminen M. S., Laakso M. and Peuhkurinen K. (2004) A novel mutation, Ser143Pro, in the lamin A/C gene is common in finnish patients with familial dilated cardiomyopathy. *Eur Heart J* **25 (10)**: 885-93.
Karty J. A., Ireland M. M., Brun Y. V. and Reilly J. P. (2002) Artifacts and unassigned masses encountered in peptide mass mapping. *J Chromatogr B Analyt Technol Biomed Life Sci* **782 (1-2)**: 363-83.
Kessel R. G., Tung H. N., Beams H. W. and Lin J. J. (1986) Is the nuclear envelope a 'generator' of membrane? Developmental sequences in cytomembrane elaboration. *Cell Tissue Res* **245 (1)**: 61-8.
Kichuk Chrisant M. R., Drummond-Webb J., Hallowell S. and Friedman N. R. (2004) Cardiac transplantation in twins with autosomal dominant Emery-Dreifuss muscular dystrophy. *J Heart Lung Transplant* **23 (4)**: 496-8.
Kirschner J., Brune T., Wehnert M., Denecke J., Wasner C., Feuer A., Marquardt T., Ketelsen U. P., Wieacker P., Bonnemann C. G. and Korinthenberg R. (2005) p.S143F mutation in lamin A/C: a new phenotype combining myopathy and progeria. *Ann Neurol* **57 (1)**: 148-51.
Kitten G. T. and Nigg E. A. (1991) The CaaX motif is required for isoprenylation, carboxyl methylation, and nuclear membrane association of lamin B2. *J Cell Biol* **113 (1)**: 13-23.
Kourmouli N., Dialynas G., Petraki C., Pyrpasopoulou A., Singh P. B., Georgatos S. D. and Theodoropoulos P. A. (2001) Binding of heterochromatin protein 1 to the nuclear envelope is regulated by a soluble form of tubulin. *J Biol Chem* **276 (16)**: 13007-14.
Krull S., Thyberg J., Bjorkroth B., Rackwitz H. R. and Cordes V. C. (2004) Nucleoporins as components of the nuclear pore complex core structure and tpr as the architectural element of the nuclear basket. *Mol Biol Cell* **15 (9)**: 4261-77.
Kubo S., Tsukahara T., Takemitsu M., Yoon K. B., Utsumi H., Nonaka I. and Arahata K. (1998) Presence of emerinopathy in cases of rigid spine syndrome. *Neuromuscul Disord* **8 (7)**: 502-7.
Laemmli U.K. (1970) Cleavage of structural proteins during the assembly of the head of bacteriophage T4. *Nature* **227 (5259)**: 680-5.

Lafarga M., Berciano M. T., Pena E., Mayo I., Castano J. G., Bohmann D., Rodrigues J. P., Tavanez J. P. and Carmo-Fonseca M. (2002) Clastosome: a subtype of nuclear body enriched in 19S and 20S proteasomes, ubiquitin, and protein substrates of proteasome. *Mol Biol Cell* **13 (8)**: 2771-82.

Laguri C., Gilquin B., Wolff N., Romi-Lebrun R., Courchay K., Callebaut I., Worman H. J. and Zinn-Justin S. (2001) Structural characterization of the LEM motif common to three human inner nuclear membrane proteins. *Structure (Camb)* **9 (6)**: 503-11.

Lammerding J., Schulze P. C., Takahashi T., Kozlov S., Sullivan T., Kamm R. D., Stewart C. L. and Lee R. T. (2004) Lamin A/C deficiency causes defective nuclear mechanics and mechanotransduction. *J Clin Invest* **113 (3)**: 370-8.

Lang C., Paulin-Levasseur M., Gajewski A., Alsheimer M., Benavente R. and Krohne G. (1999) Molecular characterization and developmentally regulated expression of Xenopus lamina-associated polypeptide 2 (XLAP2). *J Cell Sci* **112 (Pt 5)**: 749-59.

Lattanzi G., Cenni V., Marmiroli S., Capanni C., Mattioli E., Merlini L., Squarzoni S. and Maraldi N. M. (2003) Association of emerin with nuclear and cytoplasmic actin is regulated in differentiating myoblasts. *Biochem Biophys Res Commun* **303 (3)**: 764-70.

Lee K. K., Haraguchi T., Lee R. S., Koujin T., Hiraoka Y. and Wilson K. L. (2001) Distinct functional domains in emerin bind lamin A and DNA-bridging protein BAF. *J Cell Sci* **114 (Pt 24)**: 4567-73.

Lee K. K., Starr D., Cohen M., Liu J., Han M., Wilson K. L. and Gruenbaum Y. (2002) Lamin-dependent localization of UNC-84, a protein required for nuclear migration in Caenorhabditis elegans. *Mol Biol Cell* **13 (3)**: 892-901.

Lenart P., Rabut G., Daigle N., Hand A. R., Terasaki M. and Ellenberg J. (2003) Nuclear envelope breakdown in starfish oocytes proceeds by partial NPC disassembly followed by a rapidly spreading fenestration of nuclear membranes. *J Cell Biol* **160 (7)**: 1055-68.

Libotte T., Zaim H., Abraham S., Padmakumar V. C., Schneider M., Lu W., Munck M., Hutchison C., Wehnert M., Fahrenkrog B., Sauder U., Aebi U., Noegel A. A. and Karakesisoglou I. (2005) Lamin A/C Dependent Localization of Nesprin-2, a Giant Scaffolder at the Nuclear Envelope. *Mol Biol Cell* **16 (7):** 3411-24.

Lin F., Blake D. L., Callebaut I., Skerjanc I. S., Holmer L., McBurney M. W., Paulin-Levasseur M. and Worman H. J. (2000) MAN1, an inner nuclear membrane protein that shares the LEM domain with lamina-associated polypeptide 2 and emerin. *J Biol Chem* **275 (7)**: 4840-7.

Lin F., Morrison J. M., Wu W. and Worman H. J. (2005) MAN1, an integral protein of the inner nuclear membrane, binds Smad2 and Smad3 and antagonizes transforming growth factor-{beta} signaling. *Hum Mol Genet* **14 (3)**: 437-45.

Liu J., Lee K. K., Segura-Totten M., Neufeld E., Wilson K. L. and Gruenbaum Y. (2003) MAN1 and emerin have overlapping function(s) essential for chromosome segregation and cell division in Caenorhabditis elegans. *Proc Natl Acad Sci U S A* **100 (8)**: 4598-603.

Lloyd D. J., Trembath R. C. and Shackleton S. (2002) A novel interaction between lamin A and SREBP1: implications for partial lipodystrophy and other laminopathies. *Hum Mol Genet* **11 (7)**: 769-77.

Lohka M. J. (1998) Analysis of nuclear envelope assembly using extracts of *Xenopus* eggs. In: *Nuclear Structure and Function* (eds Berrios) *Methods in Cell Biology*, pp: 367-395, Academic Press, San Diego.

Lohka M. J. and Maller J. L. (1985) Induction of nuclear envelope breakdown, chromosome condensation, and spindle formation in cell-free extracts. *J Cell Biol* **101 (2)**: 518-23.

Lohka M. J. and Masui Y. (1983) Formation in vitro of sperm pronuclei and mitotic chromosomes induced by amphibian ooplasmic components. *Science* **220 (4598)**: 719-21.

Lohka M. J. and Masui Y. (1984) Roles of cytosol and cytoplasmic particles in nuclear envelope assembly and sperm pronuclear formation in cell-free preparations from amphibian eggs. *J Cell Biol* **98**: 1222-1230.

Lourim D. and Krohne G. (1993) Membrane-associated lamins in Xenopus egg extracts: identification of two vesicle populations. *J Cell Biol* **123 (3)**: 501-12.

Luderus M. E., den Blaauwen J. L., de Smit O. J., Compton D. A. and van Driel R. (1994) Binding of matrix attachment regions to lamin polymers involves single-stranded regions and the minor groove. *Mol Cell Biol* **14 (9)**: 6297-305.

Lyon C. (1995) Immunological studies of the molecular basis of nuclear envelope structure and formation. PhD Thesis *University of Dundee.*

Maison C., Pyrpasopoulou A. and Georgatos S. D. (1995) Vimentin-associated mitotic vesicles interact with chromosomes in a lamin B- and phosphorylation-dependent manner. *Embo J* **14 (14)**: 3311-24.

Maison C., Pyrpasopoulou A., Theodoropoulos P. A. and Georgatos S. D. (1997) The inner nuclear membrane protein LAP1 forms a native complex with B-type lamins and partitions with spindle-associated mitotic vesicles. *Embo J* **16 (16)**: 4839-50.

Malone C. J., Fixsen W. D., Horvitz H. R. and Han M. (1999) UNC-84 localizes to the nuclear envelope and is required for nuclear migration and anchoring during C. elegans development. *Development* **126 (14)**: 3171-81.

Malone C. J., Misner L., Le Bot N., Tsai M. C., Campbell J. M., Ahringer J. and White J. G. (2003) The C. elegans hook protein, ZYG-12, mediates the essential attachment between the centrosome and nucleus. *Cell* **115 (7)**: 825-36.

Manilal S., Nguyen T. M. and Morris G. E. (1998) Colocalization of emerin and lamins in interphase nuclei and changes during mitosis. *Biochem Biophys Res Commun* **249 (3)**: 643-7.

Manilal S., Nguyen T. M., Sewry C. A. and Morris G. E. (1996) The Emery-Dreifuss muscular dystrophy protein, emerin, is a nuclear membrane protein. *Hum Mol Genet* **5 (6)**: 801-8.

Manilal S., Recan D., Sewry C. A., Hoeltzenbein M., Llense S., Leturcq F., Deburgrave N., Barbot J., Man N., Muntoni F., Wehnert M., Kaplan J. and Morris G. E. (1998) Mutations in Emery-Dreifuss muscular dystrophy and their effects on emerin protein expression. *Hum Mol Genet* **7 (5)**: 855-64.

Manilal S., Sewry C. A., Man N., Muntoni F. and Morris G. E. (1997) Diagnosis of X-linked Emery-Dreifuss muscular dystrophy by protein analysis of leucocytes and skin with monoclonal antibodies. *Neuromuscul Disord* **7 (1)**: 63-6.

Manilal S., Sewry C. A., Pereboev A., Man N., Gobbi P., Hawkes S., Love D. R. and Morris G. E. (1999) Distribution of emerin and lamins in the heart and

implications for Emery-Dreifuss muscular dystrophy. *Hum Mol Genet* **8 (2)**: 353-9.

Mansharamani M. and Wilson K. L. (2005) Nuclear membrane protein MAN1: Direct binding to emerin in vitro and two modes of binding to BAF. *J Biol Chem* **280 (14)**: 13863-70.

Marchesi V. T. and Ngo N. (1993) In vitro assembly of multiprotein complexes containing alpha, beta, and gamma tubulin, heat shock protein HSP70, and elongation factor 1 alpha. *Proc Natl Acad Sci U S A* **90 (7)**: 3028-32.

Margulis L., Dolan M. F. and Guerrero R. (2000) The chimeric eukaryote: origin of the nucleus from the karyomastigont in amitochondriate protists. *Proc Natl Acad Sci U S A* **97 (13)**: 6954-9.

Markiewicz E., Dechat T., Foisner R., Quinlan R. A. and Hutchison C. J. (2002) Lamin A/C binding protein LAP2alpha is required for nuclear anchorage of retinoblastoma protein. *Mol Biol Cell* **13 (12)**: 4401-13.

Martin L., Crimaudo C. and Gerace L. (1995) cDNA cloning and characterization of lamina-associated polypeptide 1C (LAP1C), an integral protein of the inner nuclear membrane. *J Biol Chem* **270 (15)**: 8822-8.

Matera A. G. (1998) Of coiled bodies, gems, and salmon. *J Cell Biochem* **70 (2)**: 181-92.

Matera A. G. (2003) Cajal bodies. *Curr Biol* **13 (13)**: R503.

Mattaj I. W. (2004) Sorting out the nuclear envelope from the endoplasmic reticulum. *Nat Rev Mol Cell Biol* **5 (1)**: 65-9.

Menko A. S. and Tan K. B. (1980) Nuclear tubulin of tissue culture cells. *Biochim Biophys Acta* **629 (2)**: 359-70.

Merchut M. P., Zdonczyk D. and Gujrati M. (1990) Cardiac transplantation in female Emery-Dreifuss muscular dystrophy. *J Neurol* **237 (5)**: 316-9.

Mislow J. M., Holaska J. M., Kim M. S., Lee K. K., Segura-Totten M., Wilson K. L. and McNally E. M. (2002) Nesprin-1alpha self-associates and binds directly to emerin and lamin A in vitro. *FEBS Lett* **525 (1-3)**: 135-40.

Mislow J. M., Kim M. S., Davis D. B. and McNally E. M. (2002) Myne-1, a spectrin repeat transmembrane protein of the myocyte inner nuclear membrane, interacts with lamin A/C. *J Cell Sci* **115 (Pt 1)**: 61-70.

Molkentin J. D., Lu J. R., Antos C. L., Markham B., Richardson J., Robbins J., Grant S. R. and Olson E. N. (1998) A calcineurin-dependent transcriptional pathway for cardiac hypertrophy. *Cell* **93 (2)**: 215-28.

Momayezi M., Kissmehl R. and Plattner H. (2000) Quantitative immunogold localization of protein phosphatase 2B (calcineurin) in Paramecium cells. *J Histochem Cytochem* **48 (9)**: 1269-81.

Mora M., Cartegni L., Di Blasi C., Barresi R., Bione S., Raffaele di Barletta M., Morandi L., Merlini L., Nigro V., Politano L., Donati M. A., Cornelio F., Cobianchi F. and Toniolo D. (1997) X-linked Emery-Dreifuss muscular dystrophy can be diagnosed from skin biopsy or blood sample. *Ann Neurol* **42 (2)**: 249-53.

Moreira D. and Lopez-Garcia P. (1998) Symbiosis between methanogenic archaea and delta-proteobacteria as the origin of eukaryotes: the syntrophic hypothesis. *J Mol Evol* **47 (5)**: 517-30.

Morris G. E. (2000) Nuclear proteins and cell death in inherited neuromuscular disease. *Neuromuscul Disord* **10 (4-5)**: 217-27.

Morris G. E. (2001) The role of the nuclear envelope in Emery-Dreifuss muscular dystrophy. *Trends Mol Med* **7 (12)**: 572-7.

Muchir A., Bonne G., van der Kooi A. J., van Meegen M., Baas F., Bolhuis P. A., de Visser M. and Schwartz K. (2000) Identification of mutations in the gene encoding lamins A/C in autosomal dominant limb girdle muscular dystrophy with atrioventricular conduction disturbances (LGMD1B). *Hum Mol Genet* **9 (9)**: 1453-9.

Muralikrishna B., Thanumalayan S., Jagatheesan G., Rangaraj N., Karande A. A. and Parnaik V. K. (2004) Immunolocalization of detergent-susceptible nucleoplasmic lamin A/C foci by a novel monoclonal antibody. *J Cell Biochem* **91 (4)**: 730-9.

Nagano A., Koga R., Ogawa M., Kurano Y., Kawada J., Okada R., Hayashi Y. K., Tsukahara T. and Arahata K. (1996) Emerin deficiency at the nuclear membrane in patients with Emery-Dreifuss muscular dystrophy. *Nat Genet* **12 (3)**: 254-9.

Nakazawa A., Usuda N., Matsui T., Hanai T., Matsushita S., Arai H., Sasaki H. and Higuchi S. (2001) Localization of calcineurin in the mature and developing retina. *J Histochem Cytochem* **49 (2)**: 187-95.

Neri L. M., Raymond Y., Giordano A., Capitani S. and Martelli A. M. (1999) Lamin A is part of the internal nucleoskeleton of human erythroleukemia cells. *J Cell Physiol* **178 (3)**: 284-95.

Newport J. and Dunphy W. G. (1992) Characterisation of the membrane binding and fusion events during nuclear envelope assembly using purified components. *J Cell Biol* **116 (2)**: 295-306.

Newport J. and Spann T. (1987) Disassembly of the nucleus in mitotic extracts: membrane vesicularization, lamin disassembly, and chromosome condensation are independent processes. *Cell* **48 (2)**: 219-30.

Nili E., Cojocaru G. S., Kalma Y., Ginsberg D., Copeland N. G., Gilbert D. J., Jenkins N. A., Berger R., Shaklai S., Amariglio N., Brok-Simoni F., Simon A. J. and Rechavi G. (2001) Nuclear membrane protein LAP2beta mediates transcriptional repression alone and together with its binding partner GCL (germ-cell-less). *J Cell Sci* **114 (Pt 18)**: 3297-307.

Novelli G., Muchir A., Sangiuolo F., Helbling-Leclerc A., D'Apice M. R., Massart C., Capon F., Sbraccia P., Federici M., Lauro R., Tudisco C., Pallotta R., Scarano G., Dallapiccola B., Merlini L. and Bonne G. (2002) Mandibuloacral dysplasia is caused by a mutation in LMNA-encoding lamin A/C. *Am J Hum Genet* **71 (2)**: 426-31.

Ognibene A., Sabatelli P., Petrini S., Squarzoni S., Riccio M., Santi S., Villanova M., Palmeri S., Merlini L. and Maraldi N. M. (1999) Nuclear changes in a case of X-linked Emery-Dreifuss muscular dystrophy. *Muscle Nerve* **22 (7)**: 864-9.

Olson E. N. and Williams R. S. (2000) Remodeling muscles with calcineurin. *Bioessays* **22 (6)**: 510-9.

Osada S., Ohmori S. Y. and Taira M. (2003) XMAN1, an inner nuclear membrane protein, antagonizes BMP signaling by interacting with Smad1 in Xenopus embryos. *Development* **130 (9)**: 1783-94.

Ostlund C., Ellenberg J., Hallberg E., Lippincott-Schwartz J. and Worman H. J. (1999) Intracellular trafficking of emerin, the Emery-Dreifuss muscular dystrophy protein. *J Cell Sci* **112 (Pt 11)**: 1709-19.

Ottaviano Y. and Gerace L. (1985) Phosphorylation of the nuclear lamins during interphase and mitosis. *J Biol Chem* **260 (1)**: 624-32.

Ozaki T., Saijo M., Murakami K., Enomoto H., Taya Y. and Sakiyama S. (1994) Complex formation between lamin A and the retinoblastoma gene product: identification of the domain on lamin A required for its interaction. *Oncogene* **9 (9)**: 2649-53.

Padan R., Nainudel-Epszteyn S., Goitein R., Fainsod A. and Gruenbaum Y. (1990) Isolation and characterization of the Drosophila nuclear envelope otefin cDNA. *J Biol Chem* **265 (14)**: 7808-13.

Paddy M. R., Belmont A. S., Saumweber H., Agard D. A. and Sedat J. W. (1990) Interphase nuclear envelope lamins form a discontinuous network that interacts with only a fraction of the chromatin in the nuclear periphery. *Cell* **62 (1)**: 89-106.

Padmakumar V. C., Abraham S., Braune S., Noegel A. A., Tunggal B., Karakesisoglou I. and Korenbaum E. (2004) Enaptin, a giant actin-binding protein, is an element of the nuclear membrane and the actin cytoskeleton. *Exp Cell Res* **295 (2)**: 330-9.

Palleros D. R., Reid K. L., Shi L. and Fink A. L. (1993a) DnaK ATPase activity revisited. *FEBS Lett* **336 (1)**: 124-8.

Palleros D. R., Reid K. L., Shi L., Welch W. J. and Fink A. L. (1993b) ATP-induced protein-Hsp70 complex dissociation requires K+ but not ATP hydrolysis. *Nature* **365 (6447)**: 664-6.

Pan D., Estevez-Salmeron L. D., Stroschein S. L., Zhu X., He J., Zhou S. and Luo K. (2005) The integral inner nuclear membrane protein MAN1 physically interacts with the R-Smad proteins to repress signaling by the TGFbeta superfamily of cytokines. *J Biol Chem* **280 (16)**: 15992-6001.

Panorchan P., Schafer B. W., Wirtz D. and Tseng Y. (2004) Nuclear envelope breakdown requires overcoming the mechanical integrity of the nuclear lamina. *J Biol Chem* **279 (42)**: 43462-7.

Pappin D.J., Hojrup P. and Bleasby A. (1993) Rapid identification of proteins by peptide-mass fingerprinting. *Curr Biol* **3 (6)**: 327-32.

Pare G. C., Easlick J. L., Mislow J. M., McNally E. M. and Kapiloff M. S. (2005) Nesprin-1alpha contributes to the targeting of mAKAP to the cardiac myocyte nuclear envelope. *Exp Cell Res* **303 (2)**: 388-99.

Pathak R. K., Luskey K. L. and Anderson R. G. (1986) Biogenesis of the crystalloid endoplasmic reticulum in UT-1 cells: evidence that newly formed endoplasmic reticulum emerges from the nuclear envelope. *J Cell Biol* **102 (6)**: 2158-68.

Patterson K., Molofsky A. B., Robinson C., Acosta S., Cater C. and Fischer J. A. (2004) The functions of Klarsicht and nuclear lamin in developmentally regulated nuclear migrations of photoreceptor cells in the Drosophila eye. *Mol Biol Cell* **15 (2)**: 600-10.

Paulin-Levasseur M., Blake D. L., Julien M. and Rouleau L. (1996) The MAN antigens are non-lamin constituents of the nuclear lamina in vertebrate cells. *Chromosoma* **104 (5)**: 367-79.

Piehl M. and Cassimeris L. (2003) Organization and dynamics of growing microtubule plus ends during early mitosis. *Mol Biol Cell* **14 (3)**: 916-25.

Polioudaki H., Kourmouli N., Drosou V., Bakou A., Theodoropoulos P. A., Singh P. B., Giannakouros T. and Georgatos S. D. (2001) Histones H3/H4 form a tight complex with the inner nuclear membrane protein LBR and heterochromatin protein 1. *EMBO Rep* **2 (10)**: 920-5.

Puddington L., Lively M. O. and Lyles D. S. (1985) Role of the nuclear envelope in synthesis, processing, and transport of membrane glycoproteins. *J Biol Chem* **260 (9)**: 5641-7.

Raff J. W. (1999) The missing (L) UNC? *Curr Biol* **9 (18)**: R708-10.

Raffaele Di Barletta M., Ricci E., Galluzzi G., Tonali P., Mora M., Morandi L., Romorini A., Voit T., Orstavik K. H., Merlini L., Trevisan C., Biancalana V., Housmanowa-Petrusewicz I., Bione S., Ricotti R., Schwartz K., Bonne G. and Toniolo D. (2000) Different mutations in the LMNA gene cause autosomal dominant and autosomal recessive Emery-Dreifuss muscular dystrophy. *Am J Hum Genet* **66 (4)**: 1407-12.

Raju G. P., Dimova N., Klein P. S. and Huang H. C. (2003) SANE, a novel LEM domain protein, regulates bone morphogenetic protein signaling through interaction with Smad1. *J Biol Chem* **278 (1)**: 428-37.

Raska I., Koberna K., Malinsky J., Fidlerova H. and Masata M. (2004) The nucleolus and transcription of ribosomal genes. *Biol Cell* **96 (8)**: 579-94.

Rexach M. and Blobel G. (1995) Protein import into nuclei: association and dissociation reactions involving transport substrate, transport factors, and nucleoporins. *Cell* **83 (5)**: 683-92.

Rial D. V. and Ceccarelli E. A. (2002) Removal of DnaK contamination during fusion protein purifications. *Protein Expr Purif* **25 (3)**: 503-7.

Richardson J. C. and Maddy A. H. (1980) The polypeptides of rat liver nuclear envelope. II. Comparison of rat liver nuclear membrane polypeptides with those of the rough endoplasmic reticulum. *J Cell Sci* **43**: 269-77.

Robinson J. T., Wojcik E. J., Sanders M. A., McGrail M. and Hays T. S. (1999) Cytoplasmic dynein is required for the nuclear attachment and migration of centrosomes during mitosis in Drosophila. *J Cell Biol* **146 (3)**: 597-608.

Rolls M. M., Stein P. A., Taylor S. S., Ha E., McKeon F. and Rapoport T. A. (1999) A visual screen of a GFP-fusion library identifies a new type of nuclear envelope membrane protein. *J Cell Biol* **146 (1)**: 29-44.

Rowland L. P., Fetell M., Olarte M., Hays A., Singh N. and Wanat F. E. (1979) Emery-Dreifuss muscular dystrophy. *Ann Neurol* **5 (2)**: 111-7.

Sabatelli P., Squarzoni S., Petrini S., Capanni C., Ognibene A., Cartegni L., Cobianchi F., Merlini L., Toniolo D. and Maraldi N. M. (1998) Oral exfoliative cytology for the non-invasive diagnosis in X-linked Emery-Dreifuss muscular dystrophy patients and carriers. *Neuromuscul Disord* **8 (2)**: 67-71.

Sakaki M., Koike H., Takahashi N., Sasagawa N., Tomioka S., Arahata K. and Ishiura S. (2001) Interaction between emerin and nuclear lamins. *J Biochem (Tokyo)* **129 (2)**: 321-7.

Sakuma K., Nishikawa J., Nakao R., Watanabe K., Totsuka T., Nakano H., Sano M. and Yasuhara M. (2003) Calcineurin is a potent regulator for skeletal muscle regeneration by association with NFATc1 and GATA-2. *Acta Neuropathol (Berl)* **105 (3)**: 271-80.

Salina D., Bodoor K., Eckley D. M., Schroer T. A., Rattner J. B. and Burke B. (2002) Cytoplasmic dynein as a facilitator of nuclear envelope breakdown. *Cell* **108 (1)**: 97-107.

Salpingidou G., Rzepecki R., Kiseleva E., Lyon C., Lane B., Fusiek K., Golebiewska A., Drummond S., Allen T., Ellis J. A., Smythe C., Goldberg M. and Hutchison C. J. (2005) Nuclear Growth and assembly in *Xenopus* oocytes

and egg extracts is mediated by distinct populations of membranes, *J Cell Biol*, submitted for publication.

Sambrook J., Fritsch E.F. and Maniatis T. (1989) *Molecular cloning: a laboratory manual*. Cold Spring Harbor Laboratory Press, Cold Spring Harbor, New York.

Sanchez C., Padilla R., Paciucci R., Zabala J. C. and Avila J. (1994) Binding of heat-shock protein 70 (hsp70) to tubulin. *Arch Biochem Biophys* **310 (2)**: 428-32.

Sanna T., Dello Russo A., Toniolo D., Vytopil M., Pelargonio G., De Martino G., Ricci E., Silvestri G., Giglio V., Messano L., Zachara E. and Bellocci F. (2003) Cardiac features of Emery-Dreifuss muscular dystrophy caused by lamin A/C gene mutations. *Eur Heart J* **24 (24)**: 2227-36.

Sasseville A. M. and Raymond Y. (1995) Lamin A precursor is localized to intranuclear foci. *J Cell Sci* **108 (Pt 1)**: 273-85.

Schirmer E. C., Florens L., Guan T., Yates J. R., 3rd and Gerace L. (2003) Nuclear membrane proteins with potential disease links found by subtractive proteomics. *Science* **301 (5638)**: 1380-2.

Segura-Totten M., Kowalski A. K., Craigie R. and Wilson K. L. (2002) Barrier-to-autointegration factor: major roles in chromatin decondensation and nuclear assembly. *J Cell Biol* **158 (3)**: 475-85.

Senior A. and Gerace L. (1988) Integral membrane proteins specific to the inner nuclear membrane and associated with the nuclear lamina. *J Cell Biol* **107 (6 Pt 1)**: 2029-36.

Shackleton S., Lloyd D. J., Jackson S. N., Evans R., Niermeijer M. F., Singh B. M., Schmidt H., Brabant G., Kumar S., Durrington P. N., Gregory S., O'Rahilly S. and Trembath R. C. (2000) LMNA, encoding lamin A/C, is mutated in partial lipodystrophy. *Nat Genet* **24 (2)**: 153-6.

Shah S., Tugendreich S. and Forbes D. (1998) Major binding sites for the nuclear import receptor are the internal nucleoporin Nup153 and the adjacent nuclear filament protein Tpr. *J Cell Biol* **141 (1)**: 31-49.

Shimi T., Koujin T., Segura-Totten M., Wilson K. L., Haraguchi T. and Hiraoka Y. (2004) Dynamic interaction between BAF and emerin revealed by FRAP, FLIP, and FRET analyses in living HeLa cells. *J Struct Biol* **147 (1)**: 31-41.

Shumaker D. K., Lee K. K., Tanhehco Y. C., Craigie R. and Wilson K. L. (2001) LAP2 binds to BAF.DNA complexes: requirement for the LEM domain and modulation by variable regions. *Embo J* **20 (7)**: 1754-64.

Simos G. and Georgatos S. D. (1992) The inner nuclear membrane protein p58 associates in vivo with a p58 kinase and the nuclear lamins. *Embo J* **11 (11)**: 4027-36.

Simos G., Maison C. and Georgatos S. D. (1996) Characterization of p18, a component of the lamin B receptor complex and a new integral membrane protein of the avian erythrocyte nuclear envelope. *J Biol Chem* **271 (21)**: 12617-25.

Skare P., Kreivi J. P., Bergstrom A. and Karlsson R. (2003) Profilin I colocalizes with speckles and Cajal bodies: a possible role in pre-mRNA splicing. *Exp Cell Res* **286 (1)**: 12-21.

Small K., Wagener M. and Warren S. T. (1997) Isolation and characterization of the complete mouse emerin gene. *Mamm Genome* **8 (5)**: 337-41.

Smythe C., Jenkins H. E. and Hutchison C. J. (2000) Incorporation of the nuclear pore basket protein nup153 into nuclear pore structures is dependent upon

lamina assembly: evidence from cell-free extracts of Xenopus eggs. *Embo J* **19 (15)**: 3918-31.

Sogin M. L. (1991) Early evolution and the origin of eukaryotes. *Curr Opin Genet Dev* **1 (4)**: 457-63.

Someren J. S., Faber L. E., Klein J. D. and Tumlin J. A. (1999) Heat shock proteins 70 and 90 increase calcineurin activity in vitro through calmodulin-dependent and independent mechanisms. *Biochem Biophys Res Commun* **260 (3)**: 619-25.

Soulham B. and Worman H. (1995) Signals and structural features involved in integral membrane protein targeting to the inner nuclear membrane. *J. Cell Biol.* **130**: 15-27.

Speckman R. A., Garg A., Du F., Bennett L., Veile R., Arioglu E., Taylor S. I., Lovett M. and Bowcock A. M. (2000) Mutational and haplotype analyses of families with familial partial lipodystrophy (Dunnigan variety) reveal recurrent missense mutations in the globular C-terminal domain of lamin A/C. *Am J Hum Genet* **66 (4)**: 1192-8.

Squarzoni S., Sabatelli P., Capanni C., Petrini S., Ognibene A., Toniolo D., Cobianchi F., Zauli G., Bassini A., Baracca A., Guarnieri C., Merlini L. and Maraldi N. M. (2000) Emerin presence in platelets. *Acta Neuropathol (Berl)* **100 (3)**: 291-8.

Starr D. A. and Han M. (2003) ANChors away: an actin based mechanism of nuclear positioning. *J Cell Sci* **116 (Pt 2)**: 211-6.

Starr D. A., Hermann G. J., Malone C. J., Fixsen W., Priess J. R., Horvitz H. R. and Han M. (2001) unc-83 encodes a novel component of the nuclear envelope and is essential for proper nuclear migration. *Development* **128 (24)**: 5039-50.

Stierle V., Couprie J., Ostlund C., Krimm I., Zinn-Justin S., Hossenlopp P., Worman H. J., Courvalin J. C. and Duband-Goulet I. (2003) The carboxyl-terminal region common to lamins A and C contains a DNA binding domain. *Biochemistry* **42 (17)**: 4819-28.

Stoffler D., Feja B., Fahrenkrog B., Walz J., Typke D. and Aebi U. (2003) Cryo-electron tomography provides novel insights into nuclear pore architecture: implications for nucleocytoplasmic transport. *J Mol Biol* **328 (1)**: 119-30.

Stuurman N., Heins S. and Aebi U. (1998) Nuclear lamins: their structure, assembly, and interactions. *J Struct Biol* **122 (1-2)**: 42-66.

Sullivan K. M., Busa W. B. and Wilson K. L. (1993) Calcium mobilization is required for nuclear vesicle fusion in vitro: implications for membrane traffic and IP3 receptor function. *Cell* **73 (7)**: 1411-22.

Sullivan T., Escalante-Alcalde D., Bhatt H., Anver M., Bhat N., Nagashima K., Stewart C. L. and Burke B. (1999) Loss of A-type lamin expression compromises nuclear envelope integrity leading to muscular dystrophy. *J Cell Biol* **147 (5)**: 913-20.

Takamoto K., Hirose K., Uono M. and Nonaka I. (1984) A genetic variant of Emery-Dreifuss disease. Muscular dystrophy with humeropelvic distribution, early joint contracture, and permanent atrial paralysis. *Arch Neurol* **41 (12)**: 1292-3.

Takemura M. (2001) Poxviruses and the origin of the eukaryotic nucleus. *J Mol Evol* **52 (5)**: 419-25.

Talkop U. A., Talvik I., Sonajalg M., Sibul H., Kolk A., Piirsoo A., Warzok R., Wulff K., Wehnert M. S. and Talvik T. (2002) Early onset of cardiomyopathy

in two brothers with X-linked Emery-Dreifuss muscular dystrophy. *Neuromuscul Disord* **12 (9)**: 878-81.

Taylor J., Sewry C. A., Dubowitz V. and Muntoni F. (1998) Early onset, autosomal recessive muscular dystrophy with Emery-Dreifuss phenotype and normal emerin expression. *Neurology* **51 (4)**: 1116-20.

Terasaki M., Campagnola P., Rolls M. M., Stein P. A., Ellenberg J., Hinkle B. and Slepchenko B. (2001) A new model for nuclear envelope breakdown. *Mol Biol Cell* **12 (2)**: 503-10.

Tews D. S. (1999) Emerin. *Int J Biochem Cell Biol* **31 (9)**: 891-4.

Toniolo D. and Minetti C. (1999) Muscular dystrophies: alterations in a limited number of cellular pathways? *Curr Opin Gen & Dev* **9**: 275-82.

Toniolo D., Bione S. and Arahata K. (1999) Emery-Dreifuss muscular dystrophy In: *Neuromuscular Disorders: Clinical and molecular genetics* Wiley Press

Tsuchiya Y., Hase A., Ogawa M., Yorifuji H. and Arahata K. (1999) Distinct regions specify the nuclear membrane targeting of emerin, the responsible protein for Emery-Dreifuss muscular dystrophy. *Eur J Biochem* **259 (3)**: 859-65.

Usuda N., Arai H., Sasaki H., Hanai T., Nagata T., Muramatsu T., Kincaid R. L. and Higuchi S. (1996) Differential subcellular localization of neural isoforms of the catalytic subunit of calmodulin-dependent protein phosphatase (calcineurin) in central nervous system neurons: immunohistochemistry on formalin-fixed paraffin sections employing antigen retrieval by microwave irradiation. *J Histochem Cytochem* **44 (1)**: 13-8.

Van der Kooi A., Ledderhof M., De Voogt W. G., Res C. J., Bouwsma G., Troost D., Busch H. F., Becker A. E. and De Visser M. (1996) A newly recognised autosomal dominant limb-girdle muscular dystrophy with cardiac involvement. *Ann Neurol* **39**: 636-642.

Vaughan A., Alvarez-Reyes M., Bridger J. M., Broers J. L., Ramaekers F. C., Wehnert M., Morris G. E., Whitfield W. G. F. and Hutchison C. J. (2001) Both emerin and lamin C depend on lamin A for localization at the nuclear envelope. *J Cell Sci* **114 (Pt 14)**: 2577-90.

Vellai T., Takacs K. and Vida G. (1998) A new aspect to the origin and evolution of eukaryotes. *J Mol Evol* **46 (5)**: 499-507.

Vergnes L., Peterfy M., Bergo M. O., Young S. G. and Reue K. (2004) Lamin B1 is required for mouse development and nuclear integrity. *Proc Natl Acad Sci U S A* **101 (28)**: 10428-33.

Vigers G. P. A. and Lohka M. J. (1991) A distinct vesicle population targets membranes and pore complexes to the nuclear envelope in Xenopus eggs. *J Cell Biol* **112 (4)**: 545-56.

Vigers G. P. A. and Lohka M. J. (1992) Regulation of nuclear envelope precursor functions during cell division. *J Cell Sci* **102**: 273-284.

Vlcek S., Korbei B. and Foisner R. (2002) Distinct functions of the unique C terminus of LAP2alpha in cell proliferation and nuclear assembly. *J Biol Chem* **277 (21)**: 18898-907.

Vohanka S., Vytopil M., Bednarik J., Lukas Z., Kadanka Z., Schildberger J., Ricotti R., Bione S. and Toniolo D. (2001) A mutation in the X-linked Emery-Dreifuss muscular dystrophy gene in a patient affected with conduction cardiomyopathy. *Neuromuscul Disord* **11 (4)**: 411-3.

Vorburger K., Kitten G. T. and Nigg E. A. (1989) Modification of nuclear lamin proteins by a mevalonic acid derivative occurs in reticulocyte lysates and

requires the cysteine residue of the C-terminal CXXM motif. *Embo J* **8 (13)**: 4007-13.

Vytopil M., Vohanka S., Vlasinova J., Toman J., Novak M., Toniolo D., Ricotti R. and Lukas Z. (2004) The screening for X-linked Emery-Dreifuss muscular dystrophy amongst young patients with idiopathic heart conduction system disease treated by a pacemaker implant. *Eur J Neurol* **11 (8)**: 531-4.

Wagner N., Schmitt J. and Krohne G. (2004) Two novel LEM-domain proteins are splice products of the annotated Drosophila melanogaster gene CG9424 (Bocksbeutel). *Eur J Cell Biol* **82 (12)**: 605-16.

Walss-Bass C., Xu K., David S., Fellous A. and Luduena R. F. (2002) Occurrence of nuclear beta(II)-tubulin in cultured cells. *Cell Tissue Res* **308 (2)**: 215-23.

Walss C., Kreisberg J. I. and Luduena R. F. (1999) Presence of the betaII isotype of tubulin in the nuclei of cultured mesangial cells from rat kidney. *Cell Motil Cytoskeleton* **42 (4)**: 274-84.

Walter M. C., Witt T. N., Weigel B. S., Reilich P., Richard P., Pongratz D., Bonne G., Wehnert M. S. and Lochmuller H. (2005) Deletion of the LMNA initiator codon leading to a neurogenic variant of autosomal dominant Emery-Dreifuss muscular dystrophy. *Neuromuscul Disord* **15 (1)**: 40-4.

Walther T. C., Alves A., Pickersgill H., Galy V., Hulsman B. B., Kocher T., Wilm M., Allen R. T., Mattaj I. W. and Doye V. (2003) The conserved Nup107-160 complex is critical for nuclear pore complex assembly. *Cell* **113**: 195-206.

Wiese C., Goldberg M. W., Allen T. D. and Wilson K. L. (1997) Nuclear envelope assembly in Xenopus extracts visualized by scanning EM reveals a transport-dependent 'envelope smoothing' event. *J Cell Sci* **110 (Pt 13)**: 1489-502.

Wiese C. and Wilson K. L. (1993) Nuclear membrane dynamics. *Curr Opin Cell Biol* **5 (3)**: 387-94.

Wilkinson F. L., Holaska J. M., Zhang Z., Sharma A., Manilal S., Holt I., Stamm S., Wilson K. L. and Morris G. E. (2003) Emerin interacts in vitro with the splicing-associated factor, YT521-B. *Eur J Biochem* **270 (11)**: 2459-66.

Wilson K. L. (2000) The nuclear envelope, muscular dystrophy and gene expression. *Trends Cell Biol* **10 (4)**: 125-9.

Wilson K. L. and Newport J. (1988) A trypsin-sensitive receptor on membrane vesicles is required for nuclear envelope formation in vitro. *J Cell Biol* **107**: 57-68.

Wilson K. L., Zastrow M. S. and Lee K. K. (2001) Lamins and disease: insights into nuclear infrastructure. *Cell* **104 (5)**: 647-50.

Wischnitzer S. (1958) An electron microscope study of the nuclear envelope of amphibian oocytes. *J Ultrastruct Res* **1 (3)**: 201-22.

Wolff N., Gilquin B., Courchay K., Callebaut I., Worman H. J. and Zinn-Justin S. (2001) Structural analysis of emerin, an inner nuclear membrane protein mutated in X-linked Emery-Dreifuss muscular dystrophy. *FEBS Lett* **501 (2-3)**: 171-6.

Wood Z. A., Schroder E., Robin Harris J. and Poole L. B. (2003) Structure, mechanism and regulation of peroxiredoxins. *Trends Biochem Sci* **28 (1)**: 32-40.

Worman H. J. and Courvalin J. C. (2000) The inner nuclear membrane. *J Membr Biol* **177 (1)**: 1-11.

Worman H. J., Yuan J., Blobel G. and Georgatos S. D. (1988) A lamin B receptor in the nuclear envelope. *Proc Natl Acad Sci U S A* **85 (22)**: 8531-4.

Wu J., Matunis M. J., Kraemer D., Blobel G. and Coutavas E. (1995) Nup358, a cytoplasmically exposed nucleoporin with peptide repeats, Ran-GTP binding sites, zinc fingers, a cyclophilin A homologous domain, and a leucine-rich region. *J Biol Chem* **270 (23)**: 14209-13.

Yakel J. L. (1997) Calcineurin regulation of synaptic function: from ion channels to transmitter release and gene transcription. *Trends Pharmacol Sci* **18 (4)**: 124-34.

Yang L., Guan T. and Gerace L. (1997) Integral membrane proteins of the nuclear envelope are dispersed throughout the endoplasmic reticulum during mitosis. *J Cell Biol* **137 (6)**: 1199-210.

Yang L., Guan T. and Gerace L. (1997) Lamin-binding fragment of LAP2 inhibits increase in nuclear volume during the cell cycle and progression into S phase. *J Cell Biol* **139 (5)**: 1077-87.

Yates J. R., Bagshaw J., Aksmanovic V. M., Coomber E., McMahon R., Whittaker J. L., Morrison P. J., Kendrick-Jones J. and Ellis J. A. (1999) Genotype-phenotype analysis in X-linked Emery-Dreifuss muscular dystrophy and identification of a missense mutation associated with a milder phenotype. *Neuromuscul Disord* **9 (3)**: 159-65.

Yates J. R. and Wehnert M. (1999) The Emery-Dreifuss Muscular Dystrophy Mutation Database. *Neuromuscul Disord* **9 (3)**: 199.

Ye Q. and Worman H. J. (1994) Primary structure analysis and lamin B and DNA binding of human LBR, an integral protein of the nuclear envelope inner membrane. *J Biol Chem* **269 (15)**: 11306-11.

Ye Q. and Worman H. J. (1996) Interaction between an integral protein of the nuclear envelope inner membrane and human chromodomain proteins homologous to Drosophila HP1. *J Biol Chem* **271 (25)**: 14653-6.

Yorifuji H., Tadano Y., Tsuchiya Y., Ogawa M., Goto K., Umetani A., Asaka Y. and Arahata K. (1997) Emerin, deficiency of which causes Emery-Dreifuss muscular dystrophy, is localized at the inner nuclear membrane. *Neurogenetics* **1 (2)**: 135-40.

Young J. C., Agashe V. R., Siegers K. and Hartl F. U. (2004) Pathways of chaperone-mediated protein folding in the cytosol. *Nat Rev Mol Cell Biol* **5 (10)**: 781-91.

Zhang Q., Ragnauth C. D., Skepper J. N., Worth N. F., Warren D. T., Roberts R. G., Weissberg P. L., Ellis J. A. and Shanahan C. M. (2005) Nesprin-2 is a multi-isomeric protein that binds lamin and emerin at the nuclear envelope and forms a subcellular network in skeletal muscle. *J Cell Sci* **118 (Pt 4)**: 673-87.

Zhang Q., Ragnauth C., Greener M. J., Shanahan C. M. and Roberts R. G. (2002) The nesprins are giant actin-binding proteins, orthologous to Drosophila melanogaster muscle protein MSP-300. *Genomics* **80 (5)**: 473-81.

Zhang Q., Skepper J. N., Yang F., Davies J. D., Hegyi L., Roberts R. G., Weissberg P. L., Ellis J. A. and Shanahan C. M. (2001) Nesprins: a novel family of spectrin-repeat-containing proteins that localize to the nuclear membrane in multiple tissues. *J Cell Sci* **114 (Pt 24)**: 4485-98.

Zhen Y. Y., Libotte T., Munck M., Noegel A. A. and Korenbaum E. (2002) NUANCE, a giant protein connecting the nucleus and actin cytoskeleton. *J Cell Sci* **115 (Pt 15)**: 3207-22.

Zillig W., Palm P., Reiter W. D., Gropp F., Puhler G. and Klenk H. P. (1988) Comparative evaluation of gene expression in archaebacteria. *Eur J Biochem* **173 (3)**: 473-82.